

2012

# $\alpha$ 2-ADRENOCEPTOR AND 5-HT<sub>3</sub> SEROTONIN RECEPTOR LIGANDS AS POTENTIAL ANALGESIC ADJUVANTS

Genevieve Alley

*Virginia Commonwealth University*

Follow this and additional works at: <http://scholarscompass.vcu.edu/etd>

 Part of the [Pharmacy and Pharmaceutical Sciences Commons](#)

© The Author

---

Downloaded from

<http://scholarscompass.vcu.edu/etd/2867>

This Dissertation is brought to you for free and open access by the Graduate School at VCU Scholars Compass. It has been accepted for inclusion in Theses and Dissertations by an authorized administrator of VCU Scholars Compass. For more information, please contact [libcompass@vcu.edu](mailto:libcompass@vcu.edu).

© Genevieve Sirles Alley 2012

All Rights Reserved

$\alpha_2$ -ADRENOCEPTOR AND 5-HT<sub>3</sub> SEROTONIN RECEPTOR LIGANDS AS  
POTENTIAL ANALGESIC ADJUVANTS

A dissertation submitted in partial fulfillment of the requirements for the degree of Doctor  
of Philosophy at Virginia Commonwealth University.

by

Genevieve Sirles Alley  
Bachelor of Science in Biology, Virginia Commonwealth University 2005

Director: Małgorzata Dukat, Ph.D.  
Associate Professor, Department of Medicinal Chemistry

Virginia Commonwealth University  
Richmond, Virginia  
August 2012

## ACKNOWLEDGMENT

First, I would like to thank Dr. Małgorzata Dukat for her continued assistance and advice throughout my studies. This guidance has helped me better understand and appreciate medicinal chemistry. Also, a special thanks is given to both Dr. Dukat and Dr. Richard A. Glennon for their constant quizzing during group meetings, which not only helped me recongnize what I did not already understand, but also, improved my ability to devise potential solutions for future research problems. Furthermore, I could not have successfully completed this dissertation work without the help of Dr. Jin-Sung Kim as my synthetic chemistry trainer, Dr. Phil Mosier as my molecular modeling trainer and Dr. Richard Young and Shawquia Young as mentors and instructors for the behavioral animal studies. These trainers provided me with much guidance and leadership, which helped me remain optimistic and patient through the various research problems that occurred. Furthermore, I would like to thank Virginia Commonwealth University and the School of Pharmacy for giving me this opportunity as well as providing me with financial assistance for the graduate school award for dissertation writing. These studies were supported by the Jeffress Memorial Trust RG-J-778 and the A. D. Williams Trust Fund awarded to Dr. Dukat.

And last but certainly not least, I would like to thank my husband, Stuart Alley, and my parents, Scott and Louisa Sirles, for their constant support and patience throughout my studies at VCU. A special thanks is given to my graduate school colleagues, Jessica Worsham, Kendra Haney and Rossana Ferrera, who provided support, motivation and confidence even when I was filled with frustration and defeat. I could not have successfully completed my graduate work without all of these people in the lab and at home.

## TABLE OF CONTENTS

List of Tables .....	ix
List of Figures .....	xi
List of Schemes .....	xxiv
List of Abbreviations .....	xxv
Abstract .....	xxviii
I. Introduction .....	1
II. Background .....	7
A. Current therapy for cancer pain .....	7
1. Nonopioid therapies.....	8
2. Opioid therapies .....	9
3. Adjuvant therapies.....	10
4. Pain pathways and pain control theories .....	10
B. Adrenoceptors .....	11
1. Classification .....	11
2. $\alpha_2$ -Adrenoceptors.....	13
a) Structure and distribution .....	13
b) Adrenoceptor agonists .....	16

1) Pharmacology and clinical relevance.....	16
2) Structure-affinity relationships (SAFIRs) .....	17
c) Adrenoceptor antagonists .....	21
1) Pharmacology and clinical relevance.....	21
2) Structure-affinity relationships (SAFIRs) .....	21
d) Binding mode of $\alpha_2$ -adrenoceptor agonists .....	24
e) Descending control of pain.....	25
C. Serotonin receptors .....	26
1. Classification .....	26
2. 5-HT <sub>3</sub> receptors .....	29
a) Structure and distribution .....	29
b) 5-HT <sub>3</sub> receptor agonists .....	31
c) 5-HT <sub>3</sub> receptor antagonists .....	34
d) Descending control of pain.....	35
D. MD-354 ( <b>21</b> ) .....	39
1. Binding affinity .....	39
2. In vitro functional activity.....	40
3. In vivo functional activity .....	41
a) MD-354 ( <b>21</b> ) administered alone.....	41
b) MD-354 ( <b>21</b> ) administered in combination with clonidine ( <b>7</b> ).....	42
III. Specific aims and rationale .....	49

A. To further investigate the mechanism of action of the analgesia-potentiating effect of clonidine ( <b>7</b> ) by MD-354 ( <b>21</b> ) .....	49
B. Exploration of conformationally-constrained rotamers of MD-354 ( <b>21</b> ).....	56
C. MD-354 ( <b>21</b> ) binding mode at $\alpha_2$ -adrenoceptors .....	61
IV. Results and discussion .....	65
A. Pharmacological studies: Nociceptive and locomotor activity animal models and binding assays.....	65
1. Ondansetron ( <b>23</b> ) .....	69
2. <i>meta</i> -Chlorophenylbiguanide ( <b>20</b> ; <i>m</i> CPBG) .....	72
a) Tail-flick assay .....	72
b) Hot-plate assay.....	78
c) Locomotor activity assay .....	81
d) Summary.....	83
3. SR57227A ( <b>22</b> ).....	84
a) Tail-flick assay .....	84
b) Hot-plate assay .....	89
c) Locomotor activity assay .....	91
d) Summary.....	93
4. TDIQ ( <b>6</b> ).....	94
a) Tail-flick assay .....	94
b) Hot-plate assay .....	103

c) Locomotor activity assay .....	106
d) Summary.....	108
5. Binding assays .....	111
6. Discussion .....	115
B. Synthesis.....	135
1. <i>meta</i> -Chlorophenylbiguanide Hydrochloride ( <b>20</b> ; <i>m</i> CPBG) .....	135
2. 2-Amino-7-chloroquinoline Hydrochloride ( <b>28</b> ) .....	136
3. 2-Amino-7-chloro-1,2,3,4-tetrahydroquinoline Hydrochloride ( <b>31</b> ) .....	139
4. 3-Amino-6-chloroisoquinoline Hydrochloride ( <b>29</b> ).....	144
5. 3-Amino-6-chloro-1,2,3,4-tetrahydroisoquinoline Hydrochloride ( <b>32</b> ) .....	146
6. 2-Amino-7-chloronaphthalene Hydrochloride ( <b>30</b> ).....	147
7. 2-Amino-7-chlorotetralin Hydrochloride ( <b>33</b> ).....	149
8. 2-Amino-5-chlorotetralin Hydrochloride ( <b>65</b> ).....	151
9. 2-Amino-5,7-dichloro-3,4-dihydroquinazoline Hydrochloride ( <b>38</b> ).....	151
10. 2-Amino-3,4-dihydroquinazoline Hydrochloride ( <b>39</b> ).....	153
C. Molecular modeling .....	154
1. MD-354 ( <b>21</b> ) rotamers .....	156
2. $\alpha_{2A}$ -Adrenoceptor 3D models.....	158
3. $\alpha_{2B}$ -Adrenoceptor 3D models.....	172
4. $\alpha_{2C}$ -Adrenoceptor 3D models.....	177
5. Discussion .....	179



V. Conclusions .....	185
VI. Experimental .....	194
A. Pharmacological studies.....	194
1. Animals.....	194
2. Drugs.....	194
3. Behavioral assays .....	195
a) Tail-flick assay .....	195
b) Hot-plate assay.....	196
c) Locomotor activity assay.....	197
4. Statistical analysis .....	198
5. Isobolographic analysis .....	198
B. Synthesis .....	199
<i>meta</i> -Chlorophenylbiguanide Hydrochloride ( <b>20</b> ) .....	199
2-Amino-7-chloroquinoline Hydrochloride ( <b>28</b> ) .....	200
3-Amino-6-chloroisoquinoline ( <b>29</b> ).....	201
2-Amino-7-chloronaphthalene Hydrochloride ( <b>30</b> ).....	201
2-Amino-7-chlorotetralin Hydrochloride ( <b>33</b> ).....	202
2-Amino-5,7-dichloro-3,4-dihydroquinazoline Hydrochloride ( <b>38</b> ).....	203
2-Amino-3,4-dihydroquinazoline Hydrochloride ( <b>39</b> ).....	204
<i>meta</i> -Chloroaniline Hydrochloride ( <b>41</b> ).....	205
[2-(4-Chloro-2-nitrophenyl)vinyl]dimethylamine ( <b>43</b> ).....	206

4-Chloro-2-nitrobenzaldehyde ( <b>44</b> ).....	206
3-(4-Chloro-2-nitrophenyl)acrylonitrile ( <b>45</b> ).....	207
( <i>E</i> )-3-(2-Amino-4-chlorophenyl)acrylonitrile ( <b>46</b> ).....	207
7-Chloro-2-acetamidoquinoline ( <b>49</b> ).....	208
4-Chloro-2-cyanomethylbenzotrile ( <b>52</b> ).....	208
3-Amino-1-bromo-6-chloroisoquinoline ( <b>53</b> ).....	209
3,6-Dinitro-1,8-naphthalic anhydride ( <b>57</b> ).....	210
2,7-Dinitronaphthalene ( <b>58</b> ).....	210
2-Amino-7-nitronaphthalene ( <b>59</b> ).....	211
7-Chloro-2-nitronaphthalene ( <b>60</b> ).....	211
3-Chlorophenylacetyl chloride ( <b>62</b> ).....	212
7-Chloro- $\beta$ -tetralone ( <b>63</b> ) and 5-chloro- $\beta$ -tetralone ( <b>64</b> ).....	212
2-Amino-5-chlorotetralin Hydrochloride ( <b>65</b> ).....	213
4,6-Dichloroisatoic anhydride ( <b>67</b> ).....	214
2-Amino-5,7-dichloroquinazolin-4(3 <i>H</i> )-one ( <b>68</b> ).....	215
2-Aminoquinazolin-4(3 <i>H</i> )-one ( <b>70</b> ).....	216
C. Molecular modeling.....	217
References.....	219
Vita.....	251

## List of Tables

Table 1: Affinity of norepinephrine ( <b>1</b> ) at $\alpha_{2A}$ -, $\alpha_{2B}$ -, and $\alpha_{2C}$ -ARs; radioligand binding data ( $[^3\text{H}]\text{RX821002}$ ) are reported as $K_i$ values (nM) at human cloned $\alpha_2$ -ARs expressed in Chinese hamster ovary (CHO) cells. ....	19
Table 2: Binding profile of the imidazoline class of $\alpha_2$ -AR agonists at $\alpha_{2A}$ -, $\alpha_{2B}$ -, and $\alpha_{2C}$ -ARs; radioligand binding ( $[^3\text{H}]\text{RX821002}$ ) are reported as $K_i$ values (nM) at human cloned $\alpha_2$ -ARs expressed in Chinese hamster ovary (CHO) cells. ....	20
Table 3: Summary of the secondary messenger systems involved in 5-HT receptors. .	28
Table 4: Summary of the analgesic activity of 5-HT <sub>3</sub> receptor ligands in nociceptive animal models (routes of administrations: i.t., intrathecal; i.p., intraperitoneal; s.c., subcutaneous; i.c.v., intracerebroventricular). ....	38
Table 5: MD-354 ( <b>21</b> ) binding profile. ....	40
Table 6: Literature summary of the ability of <i>m</i> CPBG ( <b>20</b> ) to cross the BBB. ....	52
Table 7: Receptor affinity ( $K_i$ , nM) for MD-354 ( <b>21</b> ) and conformationally-constrained MD-354 ( <b>21</b> ) analogs <b>26</b> and <b>27</b> . ....	57
Table 8: Summary of the pharmacological assays; the dose of clonidine ( <b>7</b> ; where employed) in allcombination studies is 0.25 mg/kg. ....	110

Table 9: Characterization of [<sup>35</sup>S]GTPγS binding to CHO cell membranes expressing human α<sub>2A</sub>-, α<sub>2B</sub>-, or α<sub>2C</sub>-ARs in low salt conditions. Potency is represented as EC<sub>50</sub> values (nM) with the 95% CI in parenthesis. Efficacy (or maximal stimulation over basal) is expressed as intrinsic activity (IA) compared to (-)NE (**1**; Pohjanoksa and Scheinin, unpublished data). .....113

Table 10: Competitive binding affinity at human α<sub>2</sub>-ARs expressed in CHO cells employing [ethyl-<sup>3</sup>H]RS-79948-197 radioligand (α<sub>2</sub>-AR antagonist). Binding affinity is expressed as K<sub>i</sub> values (nM) with the 95% CI in parenthesis (Pohjanoksa and Scheinin, unpublished data). .....114

Table 11: Competitive binding affinity at human α<sub>2</sub>-ARs expressed in CHO cells employing [<sup>3</sup>H]clonidine radioligand (α<sub>2</sub>-AR agonist). Binding affinity is expressed as K<sub>i</sub> values ± S.E.M. (nM; unpublished data). .....114

Table 12: Summary of the previously reported mechanistic studies associated with the analgesic potentiation of clonidine (**7**; 0.25 mg/kg) by MD-354 (**21**; 0.3-10 mg/kg). ...116

Table 13: Interactions between α<sub>2</sub>-ARs and catecholamines. ....163

Table 14: Distances (Å) of favorable HB and ionic interactions observed in proposed binding mode between ligands and the (a) active and (b) inactive α<sub>2A</sub>-ARs. ....167

Table 15: Distances (Å) of favorable HB and ionic interactions observed in proposed binding mode between ligands and the (a) active and (b) inactive α<sub>2B</sub>-ARs. ....174

## List of Figures

Figure 1: Structures of adrenergic neurotransmitters: norepinephrine (1) and epinephrine (2). .....	12
Figure 2: Classification of adrenoceptors. ....	12
Figure 3: A generalized representation of the structure of GPCRs. ....	14
Figure 4: Extracellular view of the structure of GPCRs. ....	14
Figure 5: Structures of representative adrenoceptor ligands from the phenylethylamine class: the $\beta$ -AR-selective ligand isoproterenol (3), $\alpha$ -AR-selective ligand methylnorepinephrine (4), $\alpha$ -AR-selective ligand phenylephrine (5) and the $\alpha_2$ -AR-selective ligand TDIQ (6; $K_i$ : $\alpha_{2A} = 75$ , $\alpha_{2B} = 97$ , $\alpha_{2C} = 65$ nM). ....	18
Figure 6: Structures of $\alpha_2$ -AR antagonists; $\alpha_{2A/2B/2C}$ -AR binding affinity reported as $K_i$ values (nM). ....	23
Figure 7: Structure of the neurotransmitter serotonin (16). ....	27
Figure 8: Representation of the structure of ligand-gated ion channels: (a) receptor subunit containing four transmembrane spanning helices and (b) pentameric structure of the receptor with M2 (shaded) lining the ion channel. ....	30

Figure 9: Structures of 5-HT <sub>3</sub> receptor agonists: (a) serotonin ( <b>16</b> ) and analogs ( <b>17</b> , <b>18</b> ) and (b) arylbiguanides ( <b>19</b> , <b>20</b> ) and an arylguanidine ( <b>21</b> ); 5-HT <sub>3</sub> receptor binding affinity reported as $K_i$ values (nM). .....	32
Figure 10: Structure of the 5-HT <sub>3</sub> receptor agonist SR57227A ( <b>22</b> ); 5-HT <sub>3</sub> receptor binding affinity reported as a $K_i$ value (nM). .....	33
Figure 11: Structures of some representative 5-HT <sub>3</sub> receptor antagonists ( <b>23-25</b> ); 5-HT <sub>3</sub> receptor binding affinity reported as $K_i$ values (nM). .....	35
Figure 12: Potentiation of the antinociceptive effect ( $\pm$ S.E.M.) of clonidine ( <b>7</b> ; 0.25 mg/kg) by MD-354 ( <b>21</b> ; 0.3-30 mg/kg) in the mouse tail-flick assay. Asterisks denote a significant difference compared to the control group [clonidine ( <b>7</b> ) 0.25 mg/kg]; * $P < 0.05$ , ** $P < 0.01$ , one-way ANOVA followed by Dunnett's post hoc test. ....	43
Figure 13: Structures of rotamers of MD-354 ( <b>21</b> ) and related conformationally-constrained analogs <b>26</b> and <b>27</b> (quinazoline numbering indicated in red). .....	57
Figure 14: Structures of MD-354 ( <b>21</b> )-related analogs ( <b>28-30</b> ) and their reduced forms ( <b>31-33</b> ). .....	58
Figure 15: MD-354 ( <b>21</b> ) structure-affinity relationship results; 5-HT <sub>3</sub> receptor binding affinity reported as $K_i$ values (nM). .....	59
Figure 16: Structures of conformationally-constrained MD-354 ( <b>21</b> ) analogs <b>38</b> and <b>39</b> . .....	60

Figure 17: Antinociceptive effect ( $\pm$  S.E.M.) of clonidine (**7**; 0.25-2.0 mg/kg, s.c.) in the mouse tail-flick assay ( $n = 8-24$  mice/treatment). Asterisks denote a significant difference compared to the control group (saline);  $**P < 0.01$ ,  $***P < 0.001$ , one-way ANOVA ( $F_{4,59} = 9.399$ ) followed by Dunnett's post hoc test. .... 66

Figure 18: Antinociceptive effect ( $\pm$  S.E.M.) of clonidine (**7**; 0.25-2.0 mg/kg, s.c.) in the mouse hot-plate assay ( $n = 9-10$  mice/treatment). Asterisks denote a significant difference compared to the control group (saline);  $**P < 0.01$ ,  $***P < 0.001$ , one-way ANOVA ( $F_{4,42} = 11.94$ ) followed by Dunnett's post hoc test. .... 67

Figure 19: Effect ( $\pm$  S.E.M.) of s.c. administered clonidine (**7**; pre-injection time: 5 min, 0.25 mg/kg) on (a) total movement episodes, (b) total movement time, (c) total movement distance, and (d) vertical entries with a 15-min recording time in the mouse locomotor activity assay ( $n = 8-10$  mice/treatment). Asterisks denote a significant difference compared to the control group (saline);  $**P < 0.01$ ,  $***P < 0.001$ , Student's t-test. .... 68

Figure 20: Effect ( $\pm$  S.E.M.) of ondansetron (**23**; 0.01-1.0 mg/kg, s.c.) on the antinociceptive action of the MD-354 (**21**; 1.0 mg/kg, s.c.)/clonidine (**7**; 0.25 mg/kg, s.c.) combination in the mouse tail-flick assay ( $n = 8-23$  mice/treatment). No significant difference ( $P > 0.05$ ) compared to the control group [MD-354/clonidine (**21/7**) combination] was detected; one-way ANOVA ( $F_{3,43} = 0.1831$ ) followed by Dunnett's post hoc test. .... 70

Figure 21: Effect ( $\pm$  S.E.M.) of ondansetron (**23**; 0.01-1.0 mg/kg, s.c.) on the antinociceptive action of the MD-354 (**21**; 6.0 mg/kg, s.c.)/clonidine (**7**; 0.25 mg/kg, s.c.) combination in the mouse tail-flick assay ( $n = 8-19$  mice/treatment). No significant difference ( $P > 0.05$ ) compared to the control group [MD-354/clonidine (**21/7**)

combination] was detected; one-way ANOVA ( $F_{3,39} = 1.381$ ) followed by Dunnett's post hoc test. .... 71

Figure 22: Antinociceptive effect ( $\pm$  S.E.M.) of *m*CPBG [**20**; 0.3-10 mg/kg, s.c., 20-min (orange squares) or 45-min (green triangles) pre-injection times] in the mouse tail-flick assay ( $n = 7-9$  mice/treatment). No significant difference ( $P > 0.05$ ) compared to the control group (saline) was detected; one-way ANOVA ( $F_{5,41} = 1.079$  and  $F_{5,44} = 0.6228$ , respectively) followed by Dunnett's post hoc test. Saline data not shown. .... 72

Figure 23: (a) Antinociceptive effect ( $\pm$  S.E.M.) of *m*CPBG (**20**; 0.3-10 mg/kg, s.c., 45-min pre-injection time) in combination with clonidine (**7**; 0.25 mg/kg, s.c.) in the mouse tail-flick assay ( $n = 8-24$  mice/treatment). Asterisks denote a significant difference compared to the control group (0.25 mg/kg dose of clonidine; **7**); \*\* $P < 0.01$ , \*\*\* $P < 0.001$ , one-way ANOVA ( $F_{5,88} = 5.002$ ) followed by Dunnett's post hoc test. (b) Antinociceptive effect ( $\pm$  S.E.M.) of *m*CPBG (**20**; 10 mg/kg) in combination with clonidine (**7**; 0.25 mg/kg) at variable *m*CPBG (**20**) pre-injection times (20-120 min) in the mouse tail-flick assay ( $n = 8-17$  mice/treatment). .... 74

Figure 24: Effect ( $\pm$  S.E.M.) of ondansetron (**23**; 0.00001-2.0 mg/kg, s.c.) on the antinociceptive action of the *m*CPBG (**20**; 6.0 mg/kg, s.c.)/clonidine (**7**; 0.25 mg/kg, s.c.) combination in the mouse tail-flick assay ( $n = 8-16$  mice/treatment). No significant difference ( $P > 0.05$ ) compared to the control group [*m*CPBG/clonidine (**20/7**) combination] was detected; one-way ANOVA ( $F_{7,66} = 0.3224$ ) followed by Dunnett's post hoc test. .... 75

Figure 25: Effect ( $\pm$  S.E.M.) of tropisetron (**25**; 0.00001-0.1 mg/kg, s.c.) on the antinociceptive action of the *m*CPBG (**20**; 6.0 mg/kg, s.c.)/clonidine (**7**; 0.25 mg/kg, s.c.) combination in the mouse tail-flick assay ( $n = 8-16$  mice/treatment). Asterisks denote a significant difference compared to the control group [*m*CPBG/clonidine (**20/7**)



combination]; \* $P < 0.05$ , one-way ANOVA ( $F_{5,50} = 2.866$ ) followed by Dunnett's post hoc test. .... 76

Figure 26: Effect ( $\pm$  S.E.M.) of tropisetron methiodide (0.00001-0.1 mg/kg, s.c.) on the antinociceptive action of the *m*CPBG (**20**; 6.0 mg/kg, s.c.)/clonidine (**7**; 0.25 mg/kg, s.c.) combination in the mouse tail-flick assay ( $n = 8-17$  mice/treatment). No significant difference ( $P > 0.05$ ) compared to the control group [*m*CPBG/clonidine (**20/7**) combination] was detected; one-way ANOVA ( $F_{3,45} = 0.9382$ ) followed by Dunnett's post hoc test. .... 77

Figure 27: Effect ( $\pm$  S.E.M.) of  $\alpha_2$ -AR antagonist yohimbine (**11**; 0.01-6.0 mg/kg, s.c.) on the antinociceptive action of the *m*CPBG (**20**; 6.0 mg/kg, s.c.) and clonidine (**7**; 0.25 mg/kg, s.c.) combination in the mouse tail-flick assay ( $n = 8-16$  mice/treatment). Asterisks denote a significant difference compared to the control group [*m*CPBG/clonidine (**20/7**) combination]; \* $P < 0.05$ , \*\* $P < 0.01$ , \*\*\* $P < 0.001$ , one-way ANOVA ( $F_{6,62} = 6.525$ ) followed by Dunnett's post hoc test. .... 78

Figure 28: Antinociceptive effect ( $\pm$  S.E.M.) of *m*CPBG (**20**; 0.3-10 mg/kg, s.c.) in the mouse hot-plate assay ( $n = 8$  mice/treatment). No significant difference ( $P > 0.05$ ) compared to the control group (saline) was detected; one-way ANOVA ( $F_{5,42} = 1.212$ ) followed by Dunnett's post hoc test. .... 79

Figure 29: Antinociceptive effect ( $\pm$  S.E.M.) of *m*CPBG (**20**; 0.3-10 mg/kg, s.c.) in combination with clonidine (**7**; 1.0 mg/kg, s.c.) in the mouse hot-plate assay ( $n = 8-10$  mice/treatment). Asterisks denote a significant difference compared to the control group (1.0 mg/kg dose of clonidine; **7**); \*\* $P < 0.01$ , one-way ANOVA ( $F_{4,45} = 2.844$ ) followed by Dunnett's post hoc test. .... 80

Figure 30: Effect ( $\pm$  S.E.M.) of the co-administration of *m*CPBG (**20**; 6.0 mg/kg, s.c., pre-injection time: 30 min) and clonidine (**7**; 0.25 mg/kg, s.c., pre-injection time: 5 min) on (a) total movement episodes, (b) total movement time, (c) total movement distance, and (d) vertical entries with a 15-min recording time in the mouse locomotor activity assay ( $n = 10$  mice/treatment). No significant difference ( $P > 0.05$ ) compared to the control group [clonidine (**7**) 0.25 mg/kg] was detected; Student's t-test. .... 82

Figure 31: Antinociceptive effect ( $\pm$  S.E.M.) of SR57227A (**22**; 0.3-30 mg/kg, s.c.) in the mouse tail-flick assay ( $n = 8$  mice/treatment). Asterisks denote a significant difference compared to the control group (saline);  $*P < 0.05$ , one-way ANOVA ( $F_{6,49} = 4.344$ ) followed by Dunnett's post hoc test. .... 85

Figure 32: Antinociceptive effect ( $\pm$  S.E.M.) of SR57227A (**22**; 0.3-30 mg/kg, s.c.) in the mouse tail-flick assay ( $n = 8$  mice/treatment). No significant difference ( $P > 0.05$ ) compared to the control group (saline) was detected; one-way ANOVA ( $F_{6,49} = 4.574$ ) followed by Dunnett's post hoc test. .... 86

Figure 33: Hyperalgesic effect ( $\pm$  S.E.M.) of SR57227A (**22**; 1.0-10 mg/kg, s.c.) in the modified mouse tail-flick assay ( $n = 6-8$  mice/treatment). For each treatment group, bars on the left depict the pre-treatment tail-flick latency. Asterisks denote a significant difference compared to the control group (pre-treatment tail-flick latency);  $***P < 0.001$ , Student's t-test. .... 87

Figure 34: Antinociceptive effect ( $\pm$  S.E.M.) of SR57227A (**22**; 0.3-10 mg/kg, s.c.) in combination with clonidine (**7**; 0.25 mg/kg, s.c.) in the mouse tail-flick assay ( $n = 8-24$  mice/treatment). No significant difference ( $P > 0.05$ ) compared to the control group [0.25 mg/kg dose of clonidine (**7**)] was detected; one-way ANOVA ( $F_{5,58} = 0.6047$ ) followed by Dunnett's post hoc test. .... 88

Figure 35: Antinociceptive effect ( $\pm$  S.E.M.) of SR57227A (**22**; 0.3-10 mg/kg, s.c.) in combination with clonidine (**7**; 0.5 mg/kg, s.c.) in the mouse tail-flick assay ( $n = 8-24$  mice/treatment). No significant difference ( $P > 0.05$ ) compared to the control group [0.5 mg/kg dose of clonidine (**7**)] was detected; one-way ANOVA ( $F_{5,66} = 0.4993$ ) followed by Dunnett's post hoc test. .... 89

Figure 36: Antinociceptive effect ( $\pm$  S.E.M.) of SR57227A (**22**; 0.3-30 mg/kg, s.c.) in the mouse hot-plate assay ( $n = 8-9$  mice/treatment). Asterisks denote a significant difference compared to the control group (saline);  $***P < 0.001$ , one-way ANOVA ( $F_{5,47} = 5.322$ ) followed by Dunnett's post hoc test. .... 90

Figure 37: Antinociceptive effect ( $\pm$  S.E.M.) of SR57227A (**22**; 0.3-10 mg/kg, s.c.) in combination with clonidine (**7**; 1.0 mg/kg, s.c.) in the mouse hot-plate assay ( $n = 9-20$  mice/treatment). No significant difference ( $P > 0.05$ ) compared to the control group [SR57227A/clonidine (**22/7**) combination] was detected; one-way ANOVA ( $F_{4,53} = 0.4547$ ) followed by Dunnett's post hoc test. .... 91

Figure 38: Effect ( $\pm$  S.E.M.) of SR57227A (**22**; 30 mg/kg, s.c., pre-injection time: 0 min) on (a) total movement episodes, (b) total movement time, (c) total movement distance, and (d) vertical entries with a 45-min recording time in the mouse locomotor activity assay ( $n = 8$  mice/treatment). Asterisks denote a significant difference compared to the control group (saline);  $**P < 0.01$ ,  $***P < 0.001$ , Student's t-test. .... 92

Figure 39: Antinociceptive effect ( $\pm$  S.E.M.) of TDIQ (**6**; 0.3-10 mg/kg, s.c.) in the mouse tail-flick assay ( $n = 8$  mice/treatment). No significant difference ( $P > 0.05$ ) compared to the control group (saline) was detected; one-way ANOVA ( $F_{4,35} = 0.6850$ ) followed by Dunnett's post hoc test. .... 95

Figure 40: Antinociceptive effect ( $\pm$  S.E.M.) of TDIQ (**6**; 0.3-3.0 mg/kg, s.c.) in combination with clonidine (**7**; 0.25 mg/kg, s.c.) in the mouse tail-flick assay ( $n = 8-24$  mice/treatment). Asterisks denote a significant difference compared to the control group (0.25 mg/kg dose of clonidine; **7**); \* $P < 0.05$ , \*\* $P < 0.01$ , one-way ANOVA ( $F_{3,51} = 10.19$ ) followed by Dunnett's post hoc test. .... 95

Figure 41: Antinociceptive effect ( $\pm$  S.E.M.) of TDIQ (**6**; 0.3-10 mg/kg, s.c.) in combination with clonidine (**7**; 0.1 mg/kg, s.c.) in the mouse tail-flick assay ( $n = 8-16$  mice/treatment). No significant difference ( $P > 0.05$ ) compared to the control group [0.1 mg/kg dose of clonidine (**7**)] was detected; one-way ANOVA ( $F_{4,51} = 1.579$ ) followed by Dunnett's post hoc test. .... 96

Figure 42: Effect ( $\pm$  S.E.M.) of BRL44408 (**15**; 0.03-3.0 mg/kg, s.c.) on the antinociceptive action of the TDIQ (**6**; 3.0 mg/kg, s.c.)/clonidine (**7**; 0.25 mg/kg, s.c.) combination in the mouse tail-flick assay ( $n = 8-15$  mice/treatment). Asterisks denote a significant difference compared to the control group [TDIQ/clonidine (**6/7**) combination]; \* $P < 0.05$ , \*\*\* $P < 0.001$ , one-way ANOVA ( $F_{6,59} = 9.751$ ) followed by Dunnett's post hoc test. ....97

Figure 43: Effect ( $\pm$  S.E.M.) of imiloxan (**12**; 0.1-3.0 mg/kg, s.c.) on the antinociceptive action of the TDIQ (**6**; 3.0 mg/kg, s.c.)/clonidine (**7**; 0.25 mg/kg, s.c.) combination in the mouse tail-flick assay ( $n = 8-15$  mice/treatment). Asterisks denote a significant difference compared to the control group [TDIQ/clonidine (**6/7**) combination]; \* $P < 0.05$ , one-way ANOVA ( $F_{4,45} = 3.223$ ) followed by Dunnett's post hoc test. ....98

Figure 44: Effect ( $\pm$  S.E.M.) of ARC-239 (**14**; 0.3-10 mg/kg, s.c.) on the antinociceptive action of the TDIQ (**6**; 3.0 mg/kg, s.c.)/clonidine (**7**; 0.25 mg/kg, s.c.) combination in the mouse tail-flick assay ( $n = 8-15$  mice/treatment). Asterisks denote a significant difference compared to the control group [TDIQ/clonidine (**6/7**) combination]; \* $P < 0.05$ ,

\*\* $P < 0.01$ , \*\*\* $P < 0.001$ , one-way ANOVA ( $F_{4,44} = 7.435$ ) followed by Dunnett's post hoc test. ....99

Figure 45: Dose-response lines determined by regression analysis for clonidine (**7**) alone (red squares) and the co-administration of TDIQ (**6**) and clonidine (**7**) given in a 3:1 (green circles) and 12:1 (blue triangles) fixed-ratio in the mouse tail-flick assay ( $n = 8-24$  mice/treatment), plotted as log clonidine (**7**) dose. ....100

Figure 46: Dose-response lines determined by regression analysis for clonidine (**7**) alone (red squares) and co-administration of TDIQ (**6**) and clonidine (**7**) given in a 3:1 (green circles) and 12:1 (blue triangles) fixed-ratio in the mouse tail-flick assay ( $n = 8-24$  mice/treatment), plotted as log total administered dose. ....101

Figure 47: The isobologram shows the line of additivity (broken gray line),  $ED_{50mix}$  for the 3:1 (green circles) and 12:1 (blue triangles) fixed-ratios of TDIQ (**6**) and clonidine (**7**), and  $ED_{50add}$  (red squares) from the mouse tail-flick results ( $n = 8-24$  mice/treatment). Asterisks denote a significant difference compared to the control ( $ED_{50add}$  values); \* $P < 0.05$ , \*\* $P < 0.01$ , Student's t-test. ....102

Figure 48: Antinociceptive effect ( $\pm$  S.E.M.) of TDIQ (**6**; 0.3-10 mg/kg, s.c.) in the mouse hot-plate assay ( $n = 8-10$  mice/treatment). No significant difference ( $P > 0.05$ ) compared to the control group (saline) was detected; one-way ANOVA ( $F_{4,41} = 0.2881$ ) followed by Dunnett's post hoc test. ....103

Figure 49: Antinociceptive effect ( $\pm$  S.E.M.) of TDIQ (**6**; 0.3-10 mg/kg, s.c.) in combination with clonidine (**7**; 0.25 mg/kg, s.c.) in the mouse hot-plate assay ( $n = 8-28$  mice/treatment). No significant difference ( $P > 0.05$ ) compared to the control group [0.25 mg/kg dose of clonidine (**7**)] was detected; one-way ANOVA ( $F_{4,56} = 2.191$ ) followed by Dunnett's post hoc test. ....104

Figure 50: Antinociceptive effect ( $\pm$  S.E.M.) of TDIQ (**6**; 0.3-10 mg/kg, s.c.) in combination with clonidine (**7**; 1.0 mg/kg, s.c.) in the mouse hot-plate assay ( $n = 9-20$  mice/treatment). Asterisks denote a significant difference compared to the control group (1.0 mg/kg dose of clonidine; **7**); \* $P < 0.05$ , \*\* $P < 0.01$ , one-way ANOVA ( $F_{4,53} = 3.927$ ) followed by Dunnett's post hoc test. ....105

Figure 51: Antinociceptive effect ( $\pm$  S.E.M.) of TDIQ (**6**; 0.3-10 mg/kg, s.c.) in combination with clonidine (**7**; 2.0 mg/kg, s.c.) in the mouse hot-plate assay ( $n = 11-19$  mice/treatment). Asterisks denote a significant difference compared to the control group (2.0 mg/kg dose of clonidine; **7**); \* $P < 0.05$ , \*\* $P < 0.01$ , one-way ANOVA ( $F_{4,58} = 4.954$ ) followed by Dunnett's post hoc test. ....106

Figure 52: Effect ( $\pm$  S.E.M.) of TDIQ (**6**; 0.3-3.0 mg/kg) alone and in combination with clonidine (**7**; 0.25 mg/kg) on (a) total movement episodes and (b) total movement time with a 45-min recording time in the mouse locomotor activity assay ( $n = 8$  mice/treatment). No significant difference ( $P > 0.05$ ) compared to the control group [saline and clonidine (**7**; 0.25 mg/kg), respectively] was detected; one-way ANOVA ( $F_{3,22} = 0.4039$  and  $F_{3,20} = 0.3899$ ) followed by Dunnett's post hoc test. ....107

Figure 53: Effects of  $\alpha_2$ -AR agents [a) (-)NE (**1**), b) TDIQ (**6**), c) clonidine (**7**), and d) MD-354 (**21**)] on [ $^{35}$ S]GTP $\gamma$ S binding (incubation buffer containing low Na $^+$  and GDP concentrations) in CHO cell membranes expressing human  $\alpha_2$ -ARs ( $\alpha_{2A}$ : ●;  $\alpha_{2B}$ : ■;  $\alpha_{2C}$ : ▲). Data points represent the mean  $\pm$  S.E.M. (each dose examined in triplicate). ...112

Figure 54: X-ray crystal structure of  $\beta_2$ -AR (2RH1): TM1 (red), TM2 (orange), TM3 (yellow), TM4 (green), TM5 (cyan), TM6 (blue), TM7 (magenta), intra- and extra-cellular loops (tan) and inverse agonist (carazolol; gray). ....155

Figure 55: (a) Energy associated with the various torsion angles of the rotatable bond in MD-354 (**21**) (red: TFF; blue: AM1); (b) the four lowest-energy rotamers of MD-354 (**21**); +/- synclinal (*sc*) and +/- anticlinal (*ac*). .....157

Figure 56: Amino acid sequence alignment of 6 GPCRs (human muscarinic acetylcholine receptor M1, human vasopressin V1a receptor, human dopamine D3 receptor, human  $\beta_2$  adrenoceptor, human delta-type opioid receptor and bovine rhodopsin receptor) and human  $\alpha_{2A}$ -AR (ADA2A\_HUMAN); the 7 transmembrane helices are highlighted in yellow and highly conserved amino acids amongst GPCRs are highlighted in cyan. ....159

Figure 57: A Ramachandran plot of the active  $\alpha_{2A}$ -AR homology model (generated by PROCHECK; Sybyl 8.1). .....161

Figure 58: Proposed binding mode of (*R*)-epinephrine (**2**) in the active  $\alpha_{2A}$ -AR model. Amino acids within 4 Å are shown as capped sticks (grey) and distances (Å) of favorable ionic and HB interactions are shown in orange. ....165

Figure 59: Proposed binding mode of -*ac*- (magenta) and +*sc*- (orange) MD-354 (**21**) in the active  $\alpha_{2A}$ -AR model. Amino acids within 4 Å are shown in capped sticks (grey) and distances (Å) of favorable HB or ionic interactions are shown in orange.....168

Figure 60: Proposed binding mode of +*sc*-MD-354 (**21**) in the active  $\alpha_{2A}$ -AR model; close-up of the interaction between the guanidine-D3.32 hydrogen bond network with the aryl ring of F7.39. D3.32 and F7.39 are shown in capped sticks (grey) and distances (Å) of favorable HB interactions are shown in orange whereas the centroid-to-centroid distance between the aryl ring of F7.39 and the 6-membered ring formed between the guanidine and D3.32 are shown by the black arrow. ....169

Figure 61: Proposed binding mode of +sc-MD-354 (**21**) in the inactive  $\alpha_{2A}$ -AR model. Amino acids within 4 Å are shown in capped sticks (grey) and distances (Å) of favorable HB or ionic interactions are shown in orange. ....170

Figure 62: Proposed binding mode of +sc-MD-354 (**21**) in the inactive  $\alpha_{2A}$ -AR model; close-up of the interaction between the guanidine-D3.32 hydrogen bond network with the aryl ring of F7.39. D3.32 and F7.39 are shown in capped sticks (grey) and distances (Å) of favorable HB interactions are shown in orange whereas the centroid-to-centroid distance between the aryl ring of F7.39 and the 6-membered ring formed between the guanidine and D3.32 are shown by the black arrow. ....171

Figure 63: Proposed binding mode of -ac- (magenta) and +sc- (orange) MD-354 (**21**) in the active  $\alpha_{2B}$ -AR model. Amino acids within 4 Å are shown in capped sticks and distances (Å) of favorable HB or ionic interactions are shown in orange. ....175

Figure 64: Proposed binding mode of -sc- (green), +ac (magenta), and +sc- (orange) MD-354 (**21**) in the inactive  $\alpha_{2B}$ -AR model. Amino acids within 4 Å are shown in capped sticks and distances (Å) of favorable HB or ionic interactions are shown in orange. ..176

Figure 65: Proposed binding mode of -ac- (purple) and +sc- (orange) MD-354 (**21**) in the active  $\alpha_{2C}$ -AR model. Amino acids within 4 Å are shown in capped sticks (grey) and distances (Å) of favorable HB or ionic interactions are shown in orange .....178

Figure 66: Proposed binding mode of (*R*)-Epinephrine (**2**) (magenta), -ac- (orange) and +sc- (green) MD-354 (**21**) in the active  $\alpha_{2A}$ -AR model. Key amino acids of  $\alpha_{2A}$ -ARs are shown in capped sticks (grey). ....180



## List of Schemes

Scheme 1: Synthesis of compound <b>20</b> . .....	136
Scheme 2: Synthesis of compound <b>28</b> . .....	137
Scheme 3: Synthesis of compounds <b>28</b> and <b>46</b> . .....	138
Scheme 4: Synthesis of compound <b>31</b> . .....	140
Scheme 5: Synthesis of compound <b>48</b> . .....	142
Scheme 6: Synthesis of compound <b>31</b> . .....	143
Scheme 7: Synthesis of compound <b>29</b> . .....	145
Scheme 8: Synthesis of compound <b>32</b> . .....	147
Scheme 9: Synthesis of compound <b>30</b> . .....	148
Scheme 10: Synthesis of compound <b>33</b> . .....	149
Scheme 11: Synthesis of compounds <b>63</b> and <b>64</b> . .....	150
Scheme 12: Synthesis of compound <b>65</b> . .....	151
Scheme 13: Synthesis of compound <b>38</b> . .....	152
Scheme 14: Synthesis of compound <b>39</b> . .....	153

## List of Abbreviations

5-HT	5-hydroxytryptamine or serotonin
5-HTQ	<i>N,N,N</i> -trimethyl-5-HT
ANOVA	analysis of variance
AR	adrenoceptor
BBB	blood-brain barrier
CI	confidence interval
CHO	Chinese hamster ovary
CNS	central nervous system
COX-2	cyclooxygenase type 2
ED	effective dose
EL	extracellular loop
EPI	epinephrine
GABA	gamma-aminobutyric acid
GPCR	G protein-coupled receptor
G proteins	GTP-binding protein

HPLC	high performance liquid chromatography
IA	intrinsic activity
i.c.v.	intracerebroventricular
IL	intracellular loop
i.p.	intraperitoneal
i.t.	intrathecal
LGIC	ligand-gated ion channel
<i>m</i> CPBG	<i>meta</i> -chlorophenylbiguanide
MD-354	<i>meta</i> -chlorophenylguanidine or <i>m</i> CPG
MPE	maximal possible effect
NE	norepinephrine
N <sub>2</sub> O	nitrous oxide
NSAID	nonsteroidal anti-inflammatory drug
PBG	phenylbiguanide
SAFIR	structure-affinity relationship
SAR	structure-activity relationship
s.c.	subcutaneous
S.E.M.	standard error of the mean

SR57227A	1-(6-chloro-2-pyridyl)-4-piperidinylamine
TDIQ	5,6,7,8-tetrahydro-1,3-dioxolo[4,5-g]isoquinoline
TM	transmembrane
WHO	World Health Organization

## ABSTRACT

### $\alpha_2$ -ADRENOCEPTOR AND 5-HT<sub>3</sub> SEROTONIN RECEPTOR LIGANDS AS POTENTIAL ANALGESIC ADJUVANTS

By Genevieve Sirles Alley, Ph.D.

A dissertation submitted in partial fulfillment of the requirements for the degree of Doctor of Philosophy at Virginia Commonwealth University.

Virginia Commonwealth University, 2012.

Major Director: Małgorzata Dukat, Ph.D.  
Associate Professor, Department of Medicinal Chemistry

There continues to be a need for more effective analgesics. The  $\alpha_2$ -adrenoceptor (AR) agonist clonidine is an analgesic whose use is severely limited by undesirable side effects. *meta*-Chlorophenylguanidine (MD-354), an agent developed in our laboratory, selectively potentiates the antinociceptive effects of clonidine in a biphasic manner. Mechanistic studies suggest that both 5-HT<sub>3</sub> receptor and  $\alpha_2$ -AR mechanisms are involved.

To further evaluate mechanisms underlying the analgesia-potentiating effect of clonidine by MD-354, pharmacological studies using more established 5-HT<sub>3</sub> receptor agonists: *meta*-chlorophenylbiguanide (*m*CPBG) and centrally-acting SR57227A, and non-selective  $\alpha_2$ -adrenoceptor ligand TDIQ, administered alone and in combination with

clonidine, were conducted in mouse antinociceptive assays. None of the examined analogs produced an antinociceptive effect when administered alone. Nevertheless, *m*CPBG potentiated the antinociceptive actions of clonidine in a monophasic manner and the effect was antagonized by the 5-HT<sub>3</sub> receptor antagonist tropisetron but not by tropisetron methiodide, suggesting that potentiation is, at least in part, due to a central 5-HT<sub>3</sub> receptor mechanism. SR57227A did not alter the antinociceptive actions of clonidine. TDIQ was found to potentiate the analgesic actions of clonidine in a synergistic manner (as determined by an isobolographic analysis) and the effect was blocked by  $\alpha_2$ -AR antagonists (BRL-44408, imiloxan, ARC-239;  $\alpha_{2A}$ -,  $\alpha_{2B}$ -, and  $\alpha_{2C}$ -AR antagonists, respectively). This supports the hypothesis that MD-354 could be potentiating the analgesic actions of clonidine via an  $\alpha_2$ -AR agonist mechanism.

In order to explore the role of the ring nitrogen atoms and the chloro substituent of conformationally-constrained rotamers of MD-354, analogs of 2-amino-7-chloro-3,4-dihydroquinazoline, with a varying number of nitrogen atoms in the ring were synthesized. Preliminary binding affinity results indicated that the ring nitrogen atoms are essential for 5-HT<sub>3</sub> receptor binding.

In attempt to explain the varied binding and functional activity of MD-354 at  $\alpha_2$ -ARs, 3D homology models of  $\alpha_{2A}$ -,  $\alpha_{2B}$ - and  $\alpha_{2C}$ -AR were generated and docking studies of the low-energy rotamers of MD-354 were conducted.

The present studies support a role for the involvement of 5-HT<sub>3</sub> receptors and  $\alpha_2$ -ARs in antinociception. Analgesic adjuvants with a dual mechanism of action such as MD-354 might represent a promising avenue to pain treatment.

## I. Introduction

Cancer, which is one of the most deadly diseases among Americans, is commonly associated with various types of pain with various degrees of intensity and duration due to multiple sources.<sup>1,2</sup> In general, cancer pain is due to (a) direct invasion of tumor into bones, soft tissue, nerves, tendons, or connective tissue, (b) metastases, and/or (c) cancer-related treatments such as surgery, radiation and chemotherapy.<sup>2</sup>

The World Health Organization (WHO) developed a three-step analgesic ladder that communicated guidelines for cancer pain management.<sup>3</sup> The first line of therapy for cancer pain therapy is administration of nonopioids such as nonsteroidal anti-inflammatory drugs (NSAIDs) or acetaminophen.<sup>2-4</sup> However, NSAIDs that nonspecifically inhibit cyclooxygenases type 1 and 2 can cause undesirable effects such as renal and gastrointestinal effects (e.g., ulceration and bleeding).<sup>5,6</sup> Although NSAIDs that are selective for cyclooxygenase type 2 are devoid of these side effects, recent studies indicate that these agents increase the risk of stroke and heart attack.<sup>5,6</sup> In the second line of therapy, WHO recommends adding opioids to the treatment.<sup>2-4</sup> Although opioids have been found to be very effective analgesics, physicians and patients have concerns that physical dependence and tolerance will result from opioid treatments and, furthermore, adverse effects of such agents include respiratory depression, nausea and sedation.<sup>7,8</sup>

Adjuvant analgesics might be a solution for individual patients due to their particular symptoms of cancer-related pain and/or their sensitivity to certain adverse effects.<sup>7</sup> For example, the  $\alpha_2$ -adrenoceptor (AR) agonist clonidine is used to relieve severe cancer pain.<sup>9</sup>

Behavioral, neurochemical, and electrophysiological studies indicate an adrenoceptor role in antinociception via spinal administration of norepinephrine (NE; **1**) or electrical stimulation of cerebral AR cell nuclei.<sup>10-15</sup> The descending pathway is influenced by NE (**1**), which is receptor-dependent and affects the nociceptive threshold.<sup>16</sup> Regarding the receptor subtypes of  $\alpha_2$ -ARs ( $\alpha_{2A}$ -,  $\alpha_{2B}$ - and  $\alpha_{2C}$ -ARs), there are knockout mouse studies as well as pharmacological studies such as systemic/spinal administration of selective  $\alpha_{2A}$ -AR agonists and antagonists that indicate an  $\alpha_{2A}$ -AR role in analgesia, but an antinociceptive role for  $\alpha_{2B}$ - and  $\alpha_{2C}$ -ARs is unclear.<sup>16-18</sup>

Additionally, serotonin receptors seem to modulate mechanisms of descending inhibition and descending facilitation in the dorsal horn.<sup>16</sup> Leading to both pronociceptive and antinociceptive actions, various studies such as electrical brain stimulation, morphine-induced antinociception, and direct administration of serotonin (5-HT) into the spinal cord suggest that descending serotonergic pathways exert opposing nociceptive effects (modulation of descending and facilitating inhibitory pathways).<sup>19,20</sup> These varying effects produced by the endogenous ligand 5-HT could be due to the multiple subtypes of 5-HT receptors (i.e., it is the receptor, rather than the neurotransmitter, that is responsible for the excitatory or inhibitory action) and/or the localization of specific 5-HT receptors.



With regard to the 5-HT<sub>3</sub> receptor subtype, most of the current studies indicate an excitatory role in neuronal activity; specifically, phospholipase C activity is enhanced by activation of 5-HT<sub>3</sub> receptors, which, in turn, influences neuronal activity.<sup>21-24</sup> However, to date, the mechanism of pronociception is unclear, possibly due to incomplete characterization of 5-HT<sub>3</sub> receptors (e.g., 5-HT<sub>3A</sub> vs. 5-HT<sub>3AB</sub> receptors), and more research is necessary to fully understand 5-HT<sub>3</sub> receptors' role in the descending control of pain,.

In vivo pharmacological results are also, ambiguous; for example, the analgesic action of phenylbiguanide seems to be dependent on the nociceptive animal model, as it produces an antinociceptive effect in the rat hot-plate assay, whereas it shows saline-like effects in the rat tail-flick assay.<sup>25</sup> Furthermore, different analgesic effects observed in the tail-flick assay are seemingly due to species; 5-HT<sub>3</sub> receptor agonists (e.g., phenylbiguanide and *meta*-chlorophenylbiguanide) produce saline-like effects in the rat tail-flick assay, but show antinociceptive effects in the mouse model.<sup>25-28</sup> Although there are a few exceptions, in general, 5-HT<sub>3</sub> receptor antagonists (e.g., tropisetron and zacopride) produce saline-like effects in antinociceptive animal models.<sup>29</sup>

In view of the roles of  $\alpha_2$ -ARs and 5-HT<sub>3</sub> receptors in pain, *meta*-chlorophenylguanidine (MD-354), which was identified in our laboratory, was found to possess a rather selective binding profile. MD-354 was shown to display high affinity to the ligand-gated ion channel 5-HT<sub>3</sub> receptors ( $K_i = 35$  nM), and to the low- and high-affinity states of the G protein-coupled  $\alpha_2$ -adrenoceptors ( $K_i$ :  $\alpha_{2A}$ -AR, 110 and 825 nM;  $\alpha_{2B}$ -AR, 220 and 25 nM;  $\alpha_{2C}$ -AR, 4,700 and 140 nM, respectively).<sup>30-33</sup> In vitro functional assays ([<sup>35</sup>S]GTP $\gamma$ S assay) indicated that MD-354 behaves as a weak partial agonist at

$\alpha_{2A}$ -ARs, but at high concentrations MD-354 nonselectively antagonizes the agonist effect of NE at all three receptor subtypes.<sup>31</sup>

As MD-354 has an interesting binding profile with regards to antinociception, its functional activity in the mouse tail-flick and hot-plate assays have been investigated. However, in both assays, MD-354 failed to produce a statistically significant antinociceptive effect.<sup>33</sup> Although MD-354 produced saline-like effects in the mouse tail-flick and hot-plate assays, it was found to potentiate the antinociceptive effect of an “inactive” dose of clonidine (an  $\alpha_2$ -AR agonist) in the mouse tail-flick assay in a biphasic manner.<sup>33</sup> That is, as MD-354 doses increased, the antinociceptive properties of clonidine were potentiated by MD-354 in a biphasic manner (dose-response curve displays two peaks at 1.0 and 10.0 mg/kg doses of MD-354). Clonidine, one of the few non-opioid FDA-approved treatments for cancer pain, is a potent analgesic agent, but also produces undesirable side effects including sedation. However, MD-354 displayed selective potentiation of clonidine; specifically, MD-354 potentiated the analgesic properties of clonidine in the mouse tail-flick assay, but did not potentiate the adverse sedative effect of clonidine in the mouse locomotor activity assay, which could have substantial clinical ramifications for the treatment of cancer-related pain.<sup>29,33</sup>

The potentiating effect could be due to different mechanisms; for example, the low-dose potentiating effect might be caused by activation of 5-HT<sub>3</sub> receptors, whereas the high-dose potentiating effect might be due to action at one or more of the  $\alpha_2$ -ARs. In fact, mechanistic studies suggest that the low-dose potentiation of clonidine by MD-354 may be due, at least in part, to a 5-HT<sub>3</sub> receptor agonist mechanism.<sup>34</sup> However, when 5-HT<sub>3</sub> receptor antagonists (e.g., zacopride and tropisetron) were co-administered with

the clonidine/MD-354 (high dose) combination, neither potentiation nor attenuation of the antinociceptive effect occurred, which indicates that the high-dose potentiation is unlikely due to the 5-HT<sub>3</sub> receptor character of MD-354.<sup>29</sup> Due to MD-354's binding affinity at  $\alpha_2$ -ARs, various  $\alpha_2$ -ARs antagonists with different binding selectivity were examined for their antinociceptive properties both alone and in combination with low- and high doses of MD-354 and clonidine. However, difficulty arises in such mechanistic studies because of a lack of highly selective ligands at the three subtypes of  $\alpha_2$ -ARs. The mouse tail-flick assay results incorporating various  $\alpha_2$ -AR antagonists such as the non-selective  $\alpha_2$ -AR antagonist yohimbine, the moderately selective  $\alpha_{2B}$ - and  $\alpha_{2A}$ -AR antagonists imiloxan and BRL44408, respectively, in combination with clonidine suggest that  $\alpha_{2B}$ -AR antagonists can potentiate the action of clonidine.<sup>31,33</sup> In other words, if MD-354 behaves as an  $\alpha_{2B}$ -AR antagonist, then it might be potentiating the antinociceptive effect of clonidine (either the low-dose or high-dose peak) via an  $\alpha_{2B}$ -AR antagonist mechanism of action. Nevertheless, a possible  $\alpha_{2A}$ - and/or  $\alpha_{2C}$ -AR mechanism cannot be ruled out. When the abovementioned  $\alpha_2$ -AR antagonists were co-administered with the clonidine/MD-354 combination (low dose), attenuation of the antinociceptive effect occurred.<sup>31</sup> Because, by definition, antagonists block the effect of agonists, these observations suggest an  $\alpha_2$ -AR agonist mechanism in the actions associated with the potentiation of clonidine by a low dose of MD-354. Therefore, from the abovementioned mechanistic studies, MD-354 seems to potentiate the antinociceptive actions of an inactive dose of clonidine, at least in part, via a 5-HT<sub>3</sub> receptor and an  $\alpha_2$ -AR mechanism.

Such results lead to the current project objectives. The first main goal is to determine the mechanism of action of the analgesia-potentiating effect of clonidine by MD-354. In the present investigation, this mechanism of action will be evaluated by studying the more established 5-HT<sub>3</sub> receptor agonist *meta*-chlorophenylbiguanide, the known centrally-acting 5-HT<sub>3</sub> receptor agonist SR57227A, and the non-selective  $\alpha_2$ -AR ligand TDIQ. Second, an objective of this study is to explore the conformationally-constrained rotamers of MD-354 as such conformational constraint might enlighten the manner in which MD-354 binds to 5-HT<sub>3</sub> receptors. Furthermore, the role of the ring nitrogen atoms and the chloro substituent in 5-HT<sub>3</sub> receptor binding will be evaluated by synthesizing conformationally-constrained analogs of MD-354 (analogs which lack one or more nitrogen atoms or chloro substituents as compared to MD-354). Also, as MD-354 has high binding affinity at all three subtypes of  $\alpha_2$ -ARs, docking studies of MD-354 at the low- and high-affinity states of  $\alpha_{2A}$ -,  $\alpha_{2B}$ - and  $\alpha_{2C}$ -AR homology models will be performed in order to better explain the binding affinity and functional activity of MD-354.

## II. Background

### A. Current therapy for cancer pain

After heart disease, cancer is the most deadly disease among Americans.<sup>1</sup> In 2010, approximately 1.5 million new cancer cases were expected to be diagnosed in the United States alone and 0.5 million Americans were expected to die from cancer.<sup>1</sup> Many cancer patients deal with various types of pain throughout their treatment program. Statistical data suggest a high incidence of cancer-related pain in patients specifically affecting 9 million people each year.<sup>35</sup>

Cancer-related pain is multifaceted; there are multiple types of pain with various degrees of intensity and duration due to multiple sources.<sup>2</sup> Cancer pain is a result of: (a) direct invasion of tumor into bones, soft tissue, nerves, tendons, or connective tissue, (b) metastases, and/or (c) cancer-related treatments including surgery, radiation and chemotherapy.<sup>2</sup>

The three main physiological types of pain associated with cancer are nociceptive/somatic, visceral, and neuropathic pain, which are caused by the disease, itself and by side effects of various cancer treatments.<sup>2</sup> Nociceptive pain (similar to somatic pain) is due to nociceptor activation, which results from tissue injury from surgery or from the tumor, itself.<sup>2</sup> Cancer patients may also develop pain that originates from the organs within the abdomen, pelvis or thorax, which is comprehensively called

visceral pain.<sup>2</sup> And, finally, neuropathic pain results from injury to the central or peripheral nervous system and, specifically in cancer patients, it arises due to cancer treatments such as surgery, radiation, and chemotherapy.<sup>2</sup>

In 1986, the WHO developed a three-step analgesic ladder that described guidelines for the management of cancer pain.<sup>3</sup> The general guidelines describe steps that progressively increase the strength of required analgesic agents.<sup>2-4</sup> It suggests that cancer patients dealing with pain start with nonopioid therapies such as NSAIDs or acetaminophen (with or without adjuvant agents).<sup>2-4</sup> If the pain persists or the intensity increases, physicians are recommended to administer combination products, which include weak opioid and nonopioid analgesics (e.g., acetaminophen or acetylsalicylic acid plus codeine, hydrocodone, or oxycodone).<sup>2-4</sup> And, finally, if pain continues to persist, step 3 of the WHO cancer pain ladder proposes the use of stronger opioids such as morphine.<sup>2-4</sup>

## **1. Nonopioid therapies**

As suggested by the WHO guidelines for cancer pain therapy, the first line of therapy is administration of nonopioids.<sup>2-4</sup> Traditional NSAIDs, selective cyclooxygenase type 2 (COX-2) inhibitors, and acetylsalicylic acid reduce inflammatory pain by blocking prostanoid production.<sup>36</sup> NSAIDs that nonspecifically inhibit both types of cyclooxygenases (type 1 and 2) can cause renal and gastrointestinal side effects including ulceration and bleeding.<sup>5,6</sup> Even though selective COX-2 inhibitors are devoid of this gastric side effect while maintaining analgesic properties, these agents have

been recently shown to increase the risk of stroke and heart attack when administered in high doses.<sup>5,6</sup> Although NSAIDs have been found to effectively control cancer pain,<sup>7</sup> these side-effect concerns have resulted in product discontinuation or black box warnings.<sup>5,6</sup> Acetaminophen, which displays analgesic and antipyretic properties, is also used for mild to moderate pain in cancer patients.<sup>2</sup> The main concern with the administration of high doses of acetaminophen is an increased risk of hepatotoxicity.<sup>2</sup>

## **2. Opioid therapies**

Based on the cancer pain step ladder developed by the WHO, various opioids are added to the treatment starting in the second step.<sup>2-4</sup> Whether the agent is a full agonist, partial agonist, or mixed agonist-antagonist, most opioid drugs act at mu opioid receptors, but some are non-selective and, therefore, also bind to kappa and delta opioid receptors.<sup>2</sup> In addition to continued use of acetaminophen or acetylsalicylic acid, mild opioids such as codeine, hydrocodone, or oxycodone are used in the second step of cancer pain treatment.<sup>2</sup> If pain persists after step 2, stronger opioids (e.g., morphine, hydromorphone, fentanyl) replace the milder agents.<sup>2</sup> Although these stronger opioid agents are typically very effective as analgesics, physicians and patients have concerns that opioids will result in physical dependence and tolerance.<sup>7,8</sup> Additional adverse effects of opioids include respiratory depression, nausea, constipation, and sedation.<sup>7</sup>

### **3. Adjuvant therapies**

Cancer pain is multifaceted; thus, it is difficult to control. Adjuvant analgesics are drugs that were originally developed for a different indication; many of these agents have no effect when administered alone, but enhance the antinociceptive properties of a known analgesic.<sup>37</sup> Adjuvant analgesics are a promising solution for individual patients due to their particular symptoms of cancer-related pain and/or their sensitivity to certain adverse effects.<sup>7</sup> The main groups of adjuvant therapies for cancer pain are corticosteroids (e.g., dexamethasone), antidepressants (e.g., tricyclic antidepressants), and anticonvulsants (e.g., gabapentin).<sup>5-8</sup> An additional adjuvant analgesic, clonidine, which is an  $\alpha_2$ -AR agonist, is used to relieve severe cancer pain especially in neuropathic pain.<sup>9</sup>

### **4. Pain pathways and pain control theories**

In the mid-17th century, the reflex theory was developed by René Descartes in an attempt to describe pain.<sup>38</sup> The reflex theory stated that pain messages were sent from pain receptors in the skin to pain centers in the brain through a specific pain pathway.<sup>39</sup> The reflex theory was used both for the pain pathway and the treatment of pain for more than 300 years. It was thought that if the reflex theory was correct, then alleviation of pain could result from disconnection of the pain pathway.<sup>39</sup> This theory was not refuted until 1965 with Melzack and Wall's gate theory.<sup>40</sup> The gate theory suggested that the dorsal horn of the spinal cord acts as a gate, which can open (or



close) to allow (or block) pain messages to travel to the brain and back to the site of pain.<sup>40</sup>

Two pain pathways describe the chain of nerve fibers along which impulses can travel: (a) afferent or ascending pathways transmit impulses from the periphery to the brain and (b) efferent or descending pathways transmit impulses from the brain to the spinal cord.<sup>16</sup> In general, serotonergic and adrenergic neurons have been found to play a role in the descending pathway of pain perception in the raphe nuclei and locus coeruleus, respectively.<sup>41,42</sup> These descending neurons transmit pain signals from the brain into the dorsal horn where they display inhibitory actions that can hinder the perception of pain stimuli.<sup>16</sup>

## **B. Adrenoceptors**

### **1. Classification**

Norepinephrine (**1**; NE; noradrenaline) and epinephrine (**2**; EPI; adrenaline) (Figure 1) are endogenous neurotransmitters that produce various functional effects such as hypotension, sedation, and analgesia via ARs.<sup>43</sup> In 1948, Alquist proposed two classes of ARs;  $\alpha$ -ARs, which produce excitatory effects and  $\beta$ -ARs, which produce inhibitory effects.<sup>44</sup> About 25 years later,  $\alpha$ -ARs were divided into  $\alpha_1$ - and  $\alpha_2$ -AR subpopulations based on in vitro experiments that suggested  $\alpha_1$ -ARs were located postsynaptically, whereas  $\alpha_2$ -ARs were presynaptic receptors.<sup>45</sup> Although this theory was

later negated, the same nomenclature of  $\alpha$ -ARs ( $\alpha_1$ - and  $\alpha_2$ -ARs) was subsequently proposed due to the relative affinities of various agonists and antagonists.<sup>46</sup>

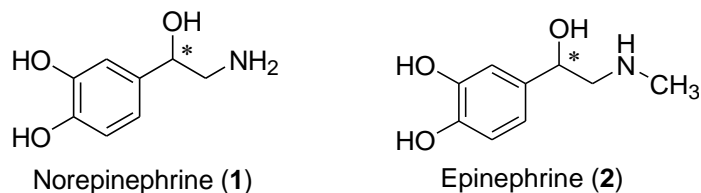


**Figure 1.** Structures of adrenergic neurotransmitters: norepinephrine (1) and epinephrine (2).

The  $\alpha_1$ - and  $\alpha_2$ -ARs were later differentiated into six subpopulations ( $\alpha_{1A}$ -,  $\alpha_{1B}$ -,  $\alpha_{1D}$ -,  $\alpha_{2A}$ -,  $\alpha_{2B}$ -, and  $\alpha_{2C}$ -ARs) based on radioligand binding studies<sup>47,48</sup> and molecular cloning studies.<sup>48-51</sup> Similar studies discovered subpopulations of the  $\beta$ -ARs and eventually Bylund and co-workers<sup>54</sup> identified a total of nine types of adrenoceptors by molecular cloning and proposed the following nomenclature:  $\alpha_1$ -,  $\alpha_2$ -, and  $\beta$ -ARs, that were subdivided into  $\alpha_{1A}$ -,  $\alpha_{1B}$ -,  $\alpha_{1D}$ -,  $\alpha_{2A}$ -,  $\alpha_{2B}$ -,  $\alpha_{2C}$ -,  $\beta_1$ -,  $\beta_2$ -, and  $\beta_3$ -AR subclasses (Figure 2).

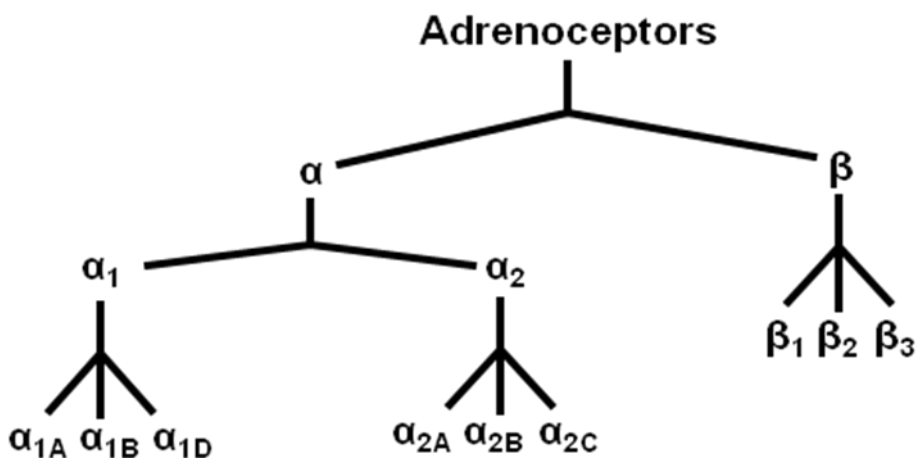


**Figure 2.** Classification of adrenoceptors.<sup>54</sup>

There is a hole in the current adrenoceptor nomenclature because there is not an  $\alpha_{1C}$ -AR subtype. This subtype was initially proposed but was later determined to be incorrectly identified.<sup>53</sup>

## **2. $\alpha_2$ -Adrenoceptors**

### **a) Structure and distribution**

All three subtypes of  $\alpha_2$ -ARs are members of the G protein-coupled receptor (GPCR) family, which are integral membrane proteins structurally characterized by 7  $\alpha$ -helical transmembrane-spanning domains (TM1-TM7) connected by three intracellular loops (IL1-IL3), three extracellular loops (EL1-EL3), an extracellular amino-terminal domain, and an intracellular carboxyl-terminal domain (Figures 3 and 4)<sup>53</sup> Interaction of the receptor with an agonist supposedly induces a conformational change in the receptor which allows it to associate with a G protein and this, in turn, initiates a signaling cascade that produces an effect.<sup>43,53</sup>

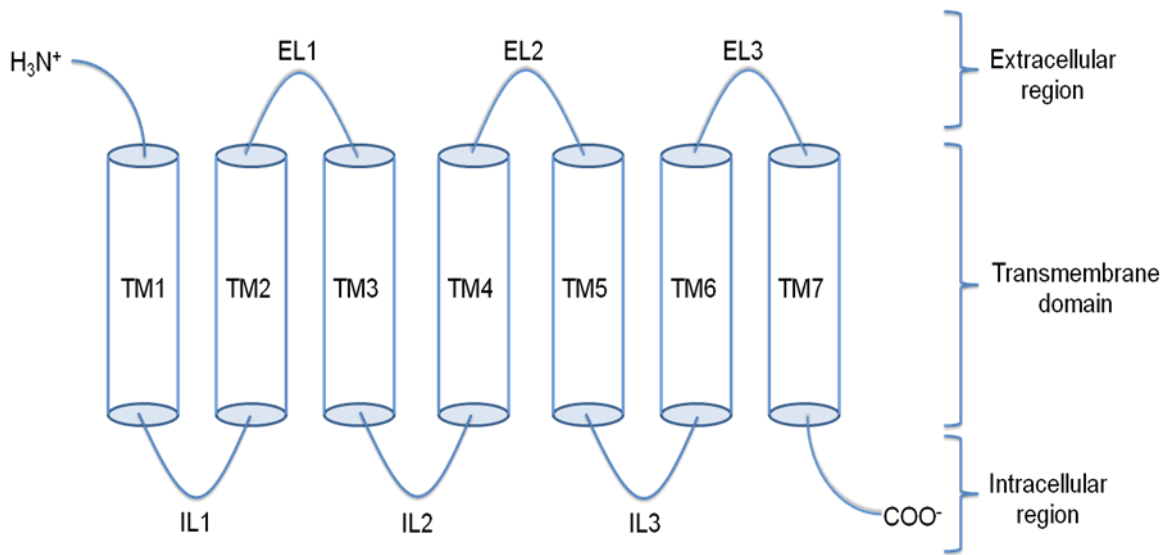


**Figure 3.** A generalized representation of the structure of a GPCR.

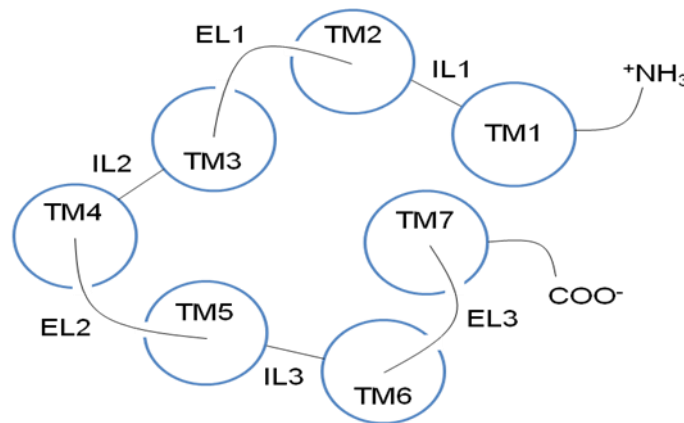


**Figure 4.** Extracellular view of the structure of GPCRs.

In the past decade, the structure and function of GPCRs have been studied progressively due to an increase in the availability of crystal structure data of various receptors such as bovine rhodopsin, human  $\beta_2$ -AR, turkey  $\beta_1$ -AR, and human  $A_{2A}$  adenosine receptors.<sup>55-59</sup> There are two main mechanisms of GPCR activation, that incorporate highly conserved residues amongst most GPCRs. The *ionic lock* is

represented by an interaction between an arginine (R) residue in the conserved TM3 DRY motif and a negatively-charged residue (either D or E) in TM6 of bovine rhodopsin, that seems to hold the intracellular ends of TM3 and TM6 together to, thereby, restrain the receptor in an inactive state.<sup>55</sup> The ionic lock has been associated with the constitutive activity of the receptor.<sup>60</sup> Although this locking mechanism has been postulated for many GPCRs, there is evidence that it does not exist in all receptors including turkey  $\beta_1$ -ARs, human  $\beta_2$ -ARs, human  $A_{2A}$  adenosine receptors, and human histamine  $H_4$  receptors.<sup>60</sup>

The **rotameric switch**, which is thought to be associated with the *global toggle switch*, involves the highly conserved CWxP motif in TM6.<sup>61</sup> Although current crystal structures do not show torsion angle changes of tryptophan (W), spectroscopic studies suggest that the conserved W of the CWxP motif exchanges between rotameric states (*g+* and *trans*). This change in W's rotameric state appears to be associated with a TM6 conformational change during activation.<sup>62,63</sup> The active conformation of W can interact with the aromatic ring of a highly conserved phenylalanine (F) moiety in TM5. In addition, it has been recently found that site-directed mutations at the conserved W eliminates constitutive activity.<sup>64</sup> Although there is no crystal structure of inactive or active conformations of the  $\alpha_2$ -ARs, there is a relatively high homology between the sequence of  $\alpha_{2A/2B/2C}$ -ARs and  $\beta_2$ -ARs, as well as with other GPCRs, especially within conserved residues and/or motifs.

Although the receptor densities of the three subtypes of  $\alpha_2$ -ARs are dissimilar in humans, all three  $\alpha_2$ -adrenoceptors are generally found throughout peripheral tissues and in many neuronal populations within the central nervous system (CNS).<sup>65</sup> Gene

expression studies in rat brain show a high density of mRNA encoding  $\alpha_{2A}$ -ARs in the locus coeruleus,<sup>66</sup> as well as in the brain stem, cerebral cortex, dorsal horn, and hypothalamus.<sup>67</sup> In addition to wide distribution throughout the CNS,  $\alpha_{2A}$ -AR mRNA has been found both pre- and post-synaptically in rat brain.<sup>68</sup> Though the other two subtypes were found in lower expression levels compared to  $\alpha_{2A}$ -ARs throughout the brain, mRNA encoding  $\alpha_{2C}$ -ARs was found mainly in the rat hippocampus, olfactory system, dorsal horn, striatum, and cerebral cortex, while that for the  $\alpha_{2B}$ -ARs was mainly expressed in the thalamus.<sup>66</sup>

## **b) Adrenoceptor agonists**

### **1) Pharmacology and clinical relevance**

NE (1) and EPI (2), both of which are endogenous adrenoceptor agonists, bind to ARs and are believed to induce a conformational change in the receptor that leads to activation of heterotrimeric GTP-binding proteins (G proteins). The specific intracellular signal is dependent on the type of G protein associated with the receptor.<sup>69</sup> Three of the known signal transduction pathways of  $\alpha_2$ -AR agonists are: (a) activation of  $G_i$  proteins, which leads to the inhibition of adenylyl cyclase, thereby inhibiting the production of cyclic adenosine monophosphate, (b) suppression of voltage-activated calcium channels, which decreases extracellular  $Ca^{2+}$  flow into target cells, via  $G_o$  proteins, and (c) stimulation of  $K^+$  channels via  $G_i$  proteins.<sup>69</sup>

Studies with genetically modified  $\alpha_2$ -AR knockout mice have provided insight on subtype specific functions.<sup>17</sup> For example, knockout mouse studies indicate that  $\alpha_{2A}$ -ARs are mainly implicated in adrenoceptor functions such as hypotension, sedation, and analgesia, whereas  $\alpha_{2B}$ -ARs seem to play a role in NO-induced analgesia and salt-induced hypertension.<sup>18,70</sup> Studies from knockout mice suggest that CNS effects, such as locomotion and stress response, are due to the  $\alpha_{2C}$ -AR subtype.<sup>70,71</sup>

## 2) Structure-affinity relationships (SAFIRs)

The two main classes of  $\alpha_2$ -AR agonists are phenylethylamines and imidazolines.<sup>70</sup> The phenylethylamines, such as the endogenous agonists NE (**1**) and EPI (**2**; Figure 1), in general, contain an aromatic ring and a two-carbon chain with a  $\beta$ -hydroxy group and a terminal amine. *R*-Enantiomers are the *eutomers* and, therefore, have greater affinity at  $\alpha_2$ -ARs than agents with the *S*-configuration of the  $\beta$ -OH group.<sup>53</sup> Affinity at  $\alpha_2$ -ARs is maximal when the amine is *N*-methyl-substituted, but dramatically decreases as the size of the *N*-substituent increases.<sup>53</sup> For example, EPI (**2**) has greater affinity than NE (**1**), but less than the  $\beta$ -AR-selective ligand isoproterenol (**3**; Figure 1), where the *N*-substituent is an isopropyl group (Table 1).<sup>53</sup> A methyl substituent at the  $\alpha$ -position (e.g.,  $\alpha$ -methylnorepinephrine, **4**) is tolerated but not the ethyl homolog (e.g., ethylnorepinephrine), which has diminished  $\alpha$ -AR binding, thereby producing a  $\beta$ -AR-selective ligand.<sup>53</sup> The dihydroxy groups found in the endogenous agonists (or other catechol-containing compounds) provide binding activity at all  $\alpha$ - and

$\beta$ -AR subtypes, but if the *p*-OH group is removed  $\beta$ -AR affinity is abolished while  $\alpha$ -AR affinity is only reduced (e.g., phenylephrine; **5**; Figure 5).<sup>53</sup>

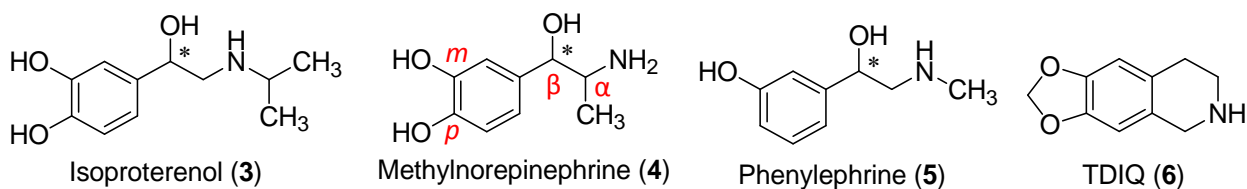


**Figure 5.** Structures of representative adrenoceptor ligands from the phenylethylamine class: the  $\beta$ -AR-selective ligand isoproterenol (**3**), the  $\alpha$ -AR-selective ligand methylnorepinephrine (**4**), the  $\alpha$ -AR-selective ligand phenylephrine (**5**), and the  $\alpha_2$ -AR-selective ligand TDIQ (**6**;  $K_i$ :  $\alpha_{2A}$  = 75,  $\alpha_{2B}$  = 97,  $\alpha_{2C}$  = 65 nM, which is nonselective amongst the three  $\alpha_{2A}$ -adrenoceptors).<sup>53</sup>

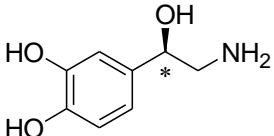
Described structurally as a conformationally-restricted phenylalkylamine, TDIQ (**6**; 5,6,7,8-tetrahydro-1,3-dioxolo[4,5-*g*]isoquinoline; Figure 5), synthesized in our laboratory, is an agent that binds rather non-selectively at all three  $\alpha_2$ -AR subtypes ( $K_i$ :  $\alpha_{2A}$  = 75,  $\alpha_{2B}$  = 97, and  $\alpha_{2C}$  = 65 nM), but possesses little affinity for other neurotransmitter receptors.<sup>72</sup> In fact, amongst 31 receptors and transporters examined, TDIQ (**6**) only had modest affinity at two receptors ( $K_i$ : dopamine  $D_3$  = 1,440 nM and serotonin 5-HT<sub>7</sub> = 1,750 nM).<sup>72</sup>

The second class of  $\alpha_2$ -AR agonists is the imidazolines, that includes the FDA-approved antihypertensive and analgesic agent clonidine (**7**).<sup>73,74</sup> Clonidine (**7**) behaves as a partial agonist at all three  $\alpha_2$ -AR subtypes, but also shows some activity at  $\alpha_1$ -ARs and imidazoline receptors.<sup>53,75</sup> Extensive SAFIR studies indicate the following: (a) binding affinity at  $\alpha_2$ -ARs decreases when the *o*-position is modified: Cl > Br > CF<sub>3</sub> >> F, but is unaffected when modified to a methyl group, (b) clonidine-constrained

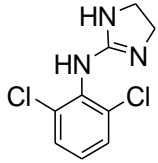
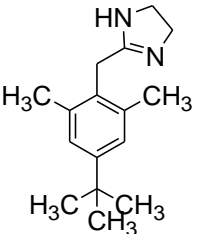
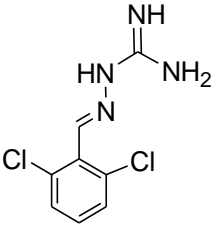
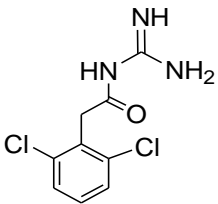


analogs indicate that the anti-periplanar orientation of the imidazoline/aromatic ring is the preferred conformation of these ligands, (c) the aniline NH is not required for binding affinity (e.g., oxymetazoline; **8**), and (d) the guanidine moiety could be changed by opening the imidazoline ring [e.g., guanabenz (**9**) and guanfacine (**10**)] without reducing activity, but changing the binding affinities (Table 2).<sup>53,70,76</sup>

**Table 1.** Affinity of norepinephrine (**1**) at  $\alpha_{2A}$ -,  $\alpha_{2B}$ -, and  $\alpha_{2C}$ -ARs; radioligand binding data ( $[^3\text{H}]\text{RX821002}$ ) are reported as  $K_i$  values (nM) at human cloned  $\alpha_2$ -ARs expressed in Chinese hamster ovary (CHO) cells.<sup>76</sup>

Compound	$K_i$ (nM)		
	$\alpha_{2A}$ -AR	$\alpha_{2B}$ -AR	$\alpha_{2C}$ -AR
 (R)-Norepinephrine ( <b>1</b> )	195	182	98

**Table 2.** Binding profile of the imidazoline class of  $\alpha_2$ -AR agonists at  $\alpha_{2A}$ -,  $\alpha_{2B}$ -, and  $\alpha_{2C}$ -ARs; radioligand binding ( $[^3\text{H}]\text{RX821002}$ ) are reported as  $K_i$  values (nM) at human cloned  $\alpha_2$ -ARs expressed in Chinese hamster ovary (CHO) cells.<sup>76</sup>

Compound	$K_i$ (nM)		
	$\alpha_{2A}$ -AR	$\alpha_{2B}$ -AR	$\alpha_{2C}$ -AR
 Clonidine ( <b>7</b> )	16	36	59
 Oxymetazoline ( <b>8</b> )	3	>1,000	107
 Guanabenz ( <b>9</b> )	5	112	200
 Guanfacine ( <b>10</b> )	25	309	>1,000

Guanabenz (**9**) and guanfacine (**10**) are FDA-approved agents for the treatment of hypertension and attention deficit hyperactivity disorder, respectively.<sup>77,78</sup> Both of these agents display increased selectivity for  $\alpha_2$ -ARs over  $\alpha_1$ -ARs in comparison with clonidine (**7**), but they still cause adverse effects such as hypotension, bradycardia, and sedation.<sup>70</sup>

### **c) Adrenoceptor antagonists**

#### **1) Pharmacology and clinical relevance**

By definition,  $\alpha_2$ -AR antagonists block the actions produced by  $\alpha_2$ -AR agonists, which, in general, include activation of  $G_{i/o}$  proteins. Therefore, pharmacologically,  $\alpha_2$ -AR antagonists have affinity but no efficacy at  $\alpha_2$ -ARs. Antagonists can either bind at the orthosteric site (i.e., the binding site for the endogenous agonist – norepinephrine) or an allosteric site; these agents will directly or indirectly inhibit agonist binding, respectively.

#### **2) Structure-affinity relationships (SAFIRs)**

There is a wide variety of structural diversity amongst  $\alpha_2$ -AR antagonists, but these agents display little selectivity amongst the three  $\alpha_2$ -AR subtypes. On one hand, these antagonists can be, structurally, much larger than the typical agonist, while, on the other hand, they can be analogous to the structure of an agonist with only a minor

chemical modification.<sup>70</sup> Their lack of selectivity limits their ability to function as pharmacological tools, which is one of the reasons that the biological function of each subtype is unclear.

The most common non-selective  $\alpha_2$ -AR antagonist is yohimbine (**11**; Figure 6), an alkaloid derived from *Pausinystlia yohimbe* bark and *Rauwolfia* root.<sup>53</sup> Yohimbine (**11**) was historically used as an aphrodisiac in Africa.<sup>79</sup> It is now used for the treatment of erectile dysfunction, but its efficacy has not been adequately confirmed and, therefore, it is not commonly used.<sup>79</sup> The main therapeutic uses of  $\alpha_2$ -AR antagonists revolve around the treatment of depression and diabetes.<sup>70,80</sup> Yohimbine (**11**) has a high affinity for  $\alpha_2$ -ARs (Figure 6), but also has moderate affinity and antagonistic behavior at  $\alpha_1$ -ARs ( $K_i$ :  $\alpha_{1A}$  = 200,  $\alpha_{1B}$  = 158, and  $\alpha_{1D}$  = 158 nM), 5-HT<sub>1A</sub> ( $K_i$  = 50 nM), 5-HT<sub>1D</sub> ( $K_i$  = 25 nM), and dopamine D<sub>2</sub> ( $K_i$  = 398 nM) receptors.<sup>53,81</sup>

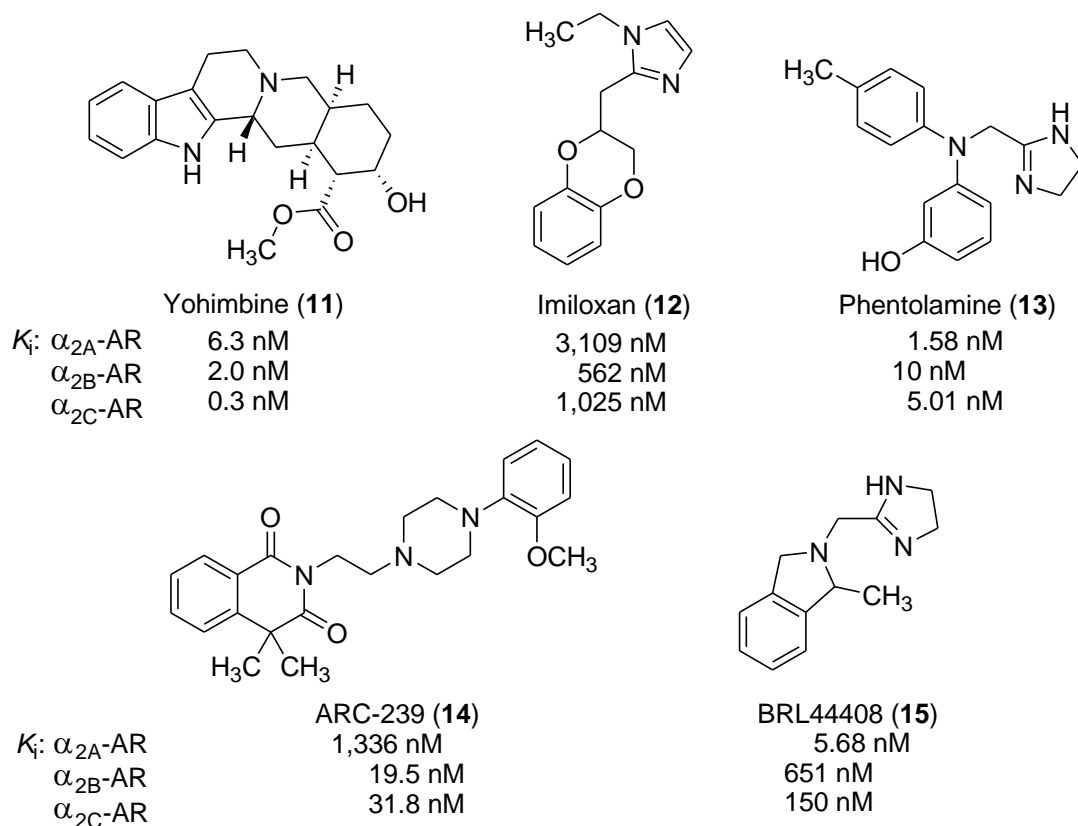


**Figure 6.** Structures of  $\alpha_2$ -AR antagonists;  $\alpha_{2A/2B/2C}$ -AR binding affinity reported as  $K_i$  values (nM).<sup>31,53,70,81,82</sup>

Due to yohimbine's (11) non-selective binding profile, other  $\alpha_2$ -AR antagonists have been developed as pharmacological tools such as imiloxan (12) and phentolamine (13; Figure 6).<sup>31,70,81</sup> Recently, there have been some small improvements on receptor subtype selectivity. For example, ARC-239 (14) displays 50-fold selectivity for  $\alpha_{2B/2C}$ - over  $\alpha_{2A}$ -AR, while BRL44408 (15) has selectivity for  $\alpha_{2A}$ -ARs amongst the three  $\alpha_2$ -AR subtypes (Figure 6).<sup>82</sup>

#### d) Binding mode of $\alpha_2$ -adrenoceptor agonists

The Easson-Stedman hypothesis<sup>83,84</sup> suggests a three-point interaction between adrenoceptors and catecholamines [e.g., NE (**1**) and EPI (**2**): (a) the protonated aliphatic amine, (b) the catecholic hydroxyl groups, and (c) the  $\beta$ -hydroxyl group. The introduction of a chiral center at the  $\beta$ -position of these ligands extended the hypothesis to suggest the following relative potencies:  $R(-) > S(+)$  = desoxy, which was later verified by their binding affinities at all  $\alpha$ -ARs.<sup>83,84</sup>

Molecular modeling studies, in some cases combined with site-directed mutagenesis data, support the Easson-Stedman hypothesis. These studies predicted the following interactions between  $\alpha_2$ -ARs and catecholamines: (a) an ionic interaction between the highly conserved D3.32 aspartate moiety and the charged nitrogen atom of the catecholamine, (b) a hydrogen bond interaction between two serines (S5.42 and S5.46) and the *meta*- and *para*-hydroxyl groups of the catecholamine, respectively, and (c) a possible hydrogen bond interaction between either S2.61 or Y6.55 and the  $\beta$ -hydroxyl group.<sup>70,85,86</sup> These amino acid residues are common in all three subtypes of  $\alpha_2$ -ARs.

The numbering of the amino acid residues is based on Ballesteros-Weinstein nomenclature.<sup>87</sup> Each transmembrane amino acid is assigned two numbers separated by a period: the first number corresponds to the transmembrane number (TM1-7) and the second number corresponds to the distance from the most highly conserved residue in each transmembrane amongst all GPCRs.<sup>87</sup> This highly conserved amino acid is arbitrarily given a value of 50 and any amino acid in the same transmembrane segment

that is closer to the carboxy-terminus is given a value >50, while those amino acids that are closer to the amino-terminus are given a value of <50.<sup>87</sup> For example, the amino acid D3.32 is an aspartate residue located in TM3 and is 17 amino acids closer to the amino-terminus in comparison to the most highly conserved amino acid of all GPCRs in TM3 (3.50).

### **e) Descending control of pain**

Behavioral, neurochemical, and electrophysiological studies indicate an adrenoceptor role in antinociception via spinal administration of NE (1) or electrical stimulation of cerebral AR cell nuclei.<sup>10-15</sup> There is overwhelming evidence of post-synaptic mechanisms involved in the analgesic properties of NE (1) and only preliminary and less-compelling data to suggest a pre-synaptic mechanism.<sup>12,88</sup> In addition, NE (1) affects the descending pathway associated with the serotonergic pathway from the nucleus raphae magnus to the dorsal horn.<sup>16</sup> The nucleus raphae magnus contains a high concentration of pre- and post-synaptic, inhibitory  $\alpha_2$ -ARs.<sup>16</sup>

The descending pathway is influenced by NE (1), which is receptor-dependent and affects the nociceptive threshold.<sup>16</sup> As for the  $\alpha_{2A}$ -AR subtype, density and distribution in the dorsal horn seem to correlate with its role in antinociception.<sup>67</sup> An  $\alpha_{2A}$ -AR role in analgesia is supported by systemic and spinal administration of selective  $\alpha_{2A}$ -AR agonists and antagonists as well as by studies using  $\alpha_{2A}$ -AR knockout mice.<sup>16-18</sup>

There are some data that suggest an antinociceptive role for  $\alpha_{2B}$ - and  $\alpha_{2C}$ -ARs in the descending pathway, but these are unclear; lack of  $\alpha_2$ -AR subtype-selective agents

magnifies this ambiguous hypothesis. For example,  $\alpha_{2B}$ -AR knockout mice failed to exhibit antinociceptive effects to nitrous oxide ( $N_2O$ ), a known anesthetic and analgesic agent.<sup>89</sup> Unfortunately, this is difficult to explain neurochemically because of the density and distribution of  $\alpha_{2B}$ -ARs (e.g., low concentration of  $\alpha_{2B}$ -ARs in the spinal cord).<sup>66</sup> On the other hand,  $\alpha_{2C}$ -ARs seem to play a pro-nociceptive role in the dorsal horn via excitatory effects of the descending noradrenergic pathway, but just like the  $\alpha_{2B}$ -ARs, the  $\alpha_{2C}$ -AR subtype is poorly expressed in the human dorsal horn.<sup>12</sup>

## C. Serotonin receptors

### 1. Classification

Serotonin (5-hydroxytryptamine or 5-HT; **16**, Figure 7) is a monoamine neurotransmitter that has been implicated in various disease states such as depression, anxiety, migraine, pain, and schizophrenia.<sup>90</sup> Serotonin (**16**) binds to 5-HT receptors, which are all GPCRs except for the ligand-gated ion channel (LGIC) 5-HT<sub>3</sub> receptors.<sup>90</sup> Theories have been proposed and modified throughout the long history since the discovery of serotonin receptors, which have, in turn, often enhanced 5-HT receptor nomenclature.<sup>91</sup>



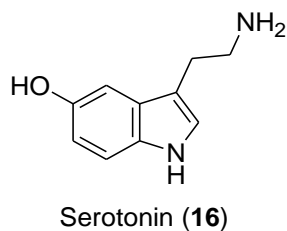


**Figure 7.** Structure of the neurotransmitter serotonin (**16**).

The criteria for the classification of 5-HT receptors began with functional data only, but over time it became more robust with additional experimental evidence including operational, structural, and transductional verification.<sup>92</sup> For example, 5-HT<sub>1C</sub> receptors were later renamed 5-HT<sub>2C</sub> receptors due to their high sequence homology with other 5-HT<sub>2</sub> receptors and their common phosphoinositol second messenger system as opposed to the adenylate cyclase second messenger system associated with 5-HT<sub>1</sub> receptors.<sup>90,93</sup> The second messenger systems of the serotonin receptors include coupling to adenylate cyclase (AC) or phospholipase C (PLC); this is summarized in Table 3.

**Table 3.** Summary of the second messenger systems involved in 5-HT receptor transduction.<sup>94,95</sup>

Receptor subpopulation	Transducer	Effector
5-HT <sub>1A</sub>	G <sub>i</sub> /G <sub>o</sub>	AC inhibition
5-HT <sub>1B</sub>	G <sub>i</sub> /G <sub>o</sub>	AC inhibition
5-HT <sub>1D</sub>	G <sub>i</sub> /G <sub>o</sub>	AC inhibition
5-ht <sub>1e</sub>	G <sub>i</sub> /G <sub>o</sub>	AC inhibition
5-HT <sub>1F</sub>	G <sub>i</sub> /G <sub>o</sub>	AC inhibition
5-HT <sub>2A</sub>	G <sub>i</sub> /G <sub>o</sub> , G <sub>q</sub> /G <sub>11</sub>	AC inhibition, PLC stimulation
5-HT <sub>2B</sub>	G <sub>q</sub> /G <sub>11</sub>	PLC stimulation
5-HT <sub>2C</sub>	G <sub>i</sub> /G <sub>o</sub> , G <sub>q</sub> /G <sub>11</sub>	AC inhibition, PLC stimulation
5-HT <sub>3A</sub>	N/A	Cation channel
5-HT <sub>3AB</sub>	N/A	Cation channel
5-HT <sub>4</sub>	G <sub>s</sub>	AC stimulation
5-ht <sub>5a</sub>	G <sub>i</sub> /G <sub>o</sub> , G <sub>q</sub> /G <sub>11</sub>	AC inhibition, PLC stimulation
5-HT <sub>6</sub>	G <sub>s</sub> , G <sub>q</sub> /G <sub>11</sub>	AC stimulation, PLC stimulation
5-HT <sub>7</sub>	G <sub>s</sub>	AC stimulation

The Nomenclature Committee of the International Union of Pharmacology currently classifies 5-HT receptors as: 5-HT<sub>1A</sub>, 5-HT<sub>1B</sub>, 5-HT<sub>1D</sub>, 5-ht<sub>1e</sub>, 5-HT<sub>1F</sub>, 5-HT<sub>2A</sub>, 5-HT<sub>2B</sub>, 5-HT<sub>2C</sub>, 5-HT<sub>3A</sub>, 5-HT<sub>3AB</sub>, 5-HT<sub>4</sub>, 5-ht<sub>5a</sub>, 5-HT<sub>6</sub>, and 5-HT<sub>7</sub>.<sup>94,95</sup> This receptor classification was based on the following criteria: operational or drug-binding characteristics, transductional or receptor-effector coupling, and structural or nucleotide/ amino acid sequence of the gene/receptor.<sup>90,93</sup> Lower case receptor nomenclature (e.g., 5-ht<sub>1e</sub> and 5-ht<sub>5a</sub>) is used until all the receptor population criteria have been met.<sup>93</sup>

## 2. 5-HT<sub>3</sub> receptors

### a) Structure and distribution

In contrast to the other G protein-coupled serotonin receptors, 5-HT<sub>3</sub> receptors are LGIC receptors. These receptors are cation-selective and part of the Cys-loop superfamily of LGICs, which include similar proteins such as nicotinic acetylcholine and gamma-aminobutyric acid (GABA<sub>A/C</sub>) receptors.<sup>96</sup> 5-HT<sub>3</sub> receptors are composed of 5 subunits (pentamers) that surround a central core that forms an ion channel (Figure 8).<sup>97</sup> Each subunit is composed of a large extracellular amine terminus, four transmembrane-spanning domains (M1-M4) connected by intracellular and extracellular loops, and an extracellular carboxyl terminus (Figure 8a).<sup>97</sup> The M2 transmembrane domain lines the ion channel (Figure 8b).<sup>97</sup>

Five human 5-HT<sub>3</sub> receptor subunits have been cloned and termed 5-HT3A, 5-HT3B, 5-HT3C, 5-HT3D, and 5-HT3E subunits, but current data suggest that a 5-HT3A subunit is required for receptor function.<sup>96</sup> 5-HT3A, but not 5-HT3B, subunits have been shown to assemble into functional homopentamers via expression in *Xenopus laevis* oocytes.<sup>21,97-99</sup> Co-expression of 5-HT3A and 5-HT3B subunits provides evidence for a functional heteromeric receptor<sup>97-100</sup> and atomic-force microscopy studies indicate that the 5-HT<sub>3</sub>AB receptor has two 5-HT3A and three 5-HT3B subunits in the following subunit arrangement: B-B-A-B-A.<sup>101</sup> To date, the role of the 5-HT3C, 5-HT3D, and 5-HT3E subunits in receptor function is unclear.

Although the two known functional 5-HT<sub>3</sub> receptors (5-HT<sub>3</sub>A and 5-HT<sub>3</sub>AB) seem to be very similar; there is a slight difference in ion selectivity. Both receptors have monovalent cation permeability (e.g., Na<sup>+</sup> and K<sup>+</sup>) and negligible anion permeability, whereas the homomeric 5-HT<sub>3</sub>A receptors are also permeable to divalent cations such as Ca<sup>2+</sup>.<sup>97,102-104</sup> This difference in cation selectivity seems to be due to differences in transmembrane M2 residues that line the channel.<sup>103</sup>

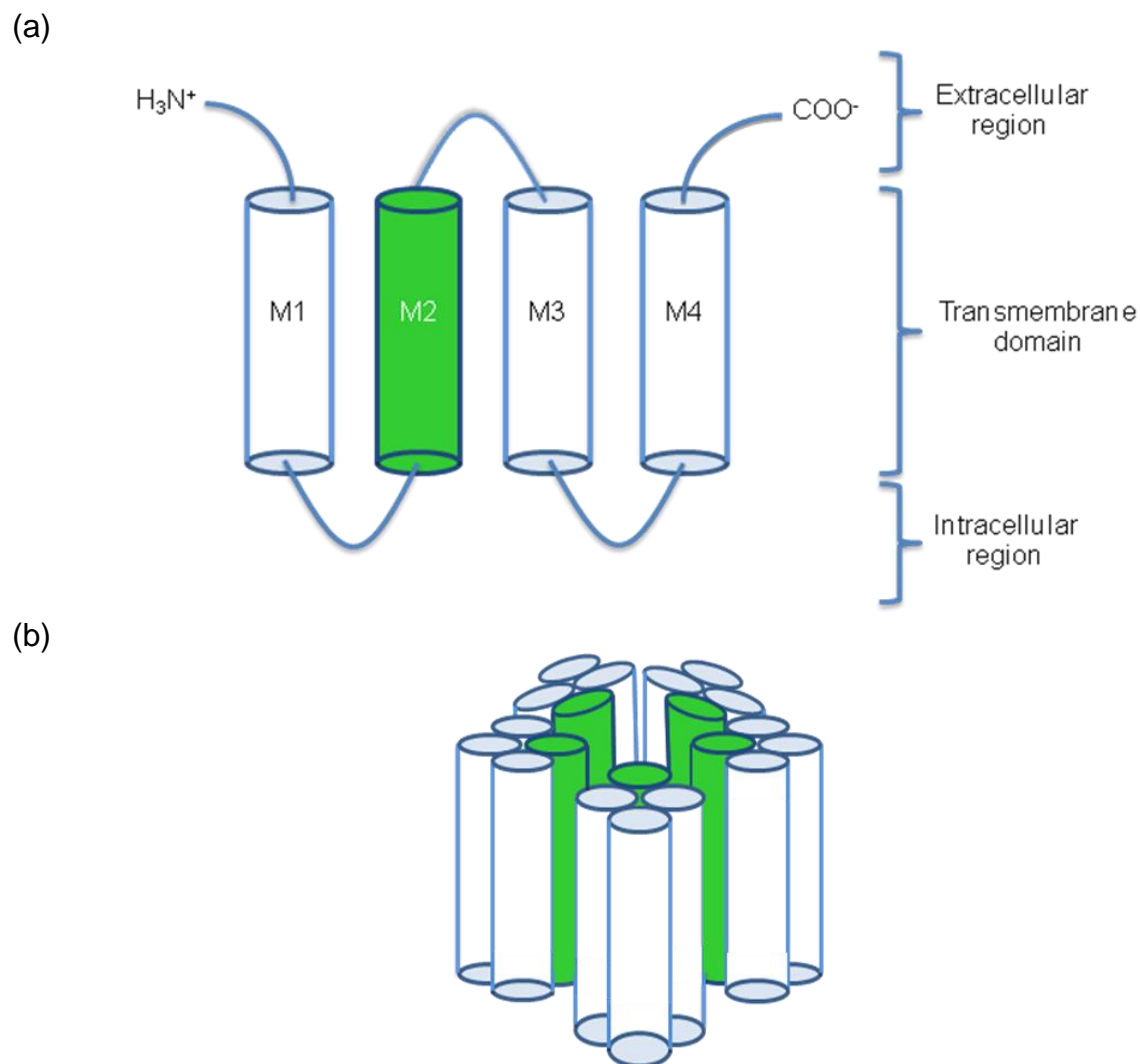


**Figure 8.** Representation of the structure of ligand-gated ion channels: (a) receptor subunit containing four transmembrane spanning helices and (b) a pentameric structure of the receptor with M2 (shaded) lining the ion channel.<sup>97</sup>

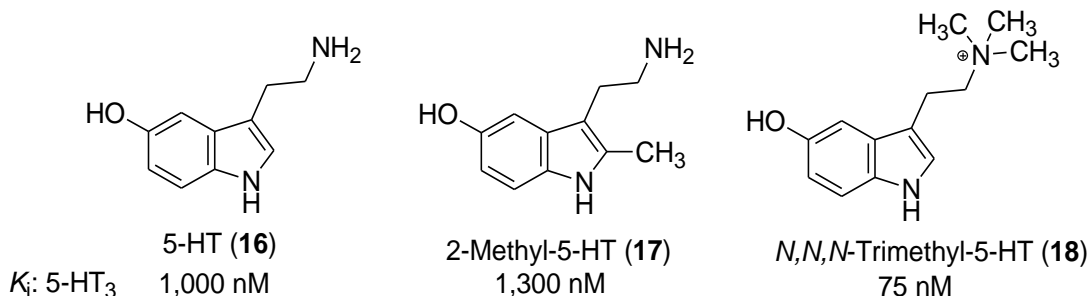
Although 5-HT<sub>3</sub> receptors (originally referred to as 5-HT-M receptors due to their sensitivity to morphine) were first found in the peripheral nervous system, their highest densities are in the CNS.<sup>105,106</sup> Within the CNS, autoradiographical studies indicate highest levels in the brainstem including the area postrema, the dorsal motor nucleus of the vagus nerve, and the nucleus tractus solitarius and lower levels in the forebrain.<sup>107-</sup><sup>109</sup> In addition to their various CNS distribution, 5-HT<sub>3</sub> receptors can be found both pre- and post-synaptically.<sup>105</sup> Presynaptic 5-HT<sub>3</sub> receptors seem to modulate neurotransmitter (e.g., dopamine, GABA, and acetylcholine) release following Ca<sup>2+</sup> influx.<sup>105</sup>

#### **b) 5-HT<sub>3</sub> receptor agonists**

There are various types of chemical structures that bind to 5-HT<sub>3</sub> receptors and that behave as partial or full agonists. The endogenous neurotransmitter, 5-HT (**16**), binds in a non-selective manner to human 5-HT<sub>3</sub> receptors with modest affinity ( $K_i = 1,000$  nM) and, although its 2-methyl analog (i.e., **17**, 2-methyl-5-HT) has slightly lower affinity ( $K_i = 1,300$  nM) and reduced agonistic activity, it has increased selectivity for 5-HT<sub>3</sub> receptors (Figure 9).<sup>110,111</sup> Due to its greater selectivity, 2-methyl-5-HT (**17**) was used in early 5-HT<sub>3</sub> receptor research, but, unfortunately, more recently it has been found to also bind to 5-HT<sub>6</sub> receptors.<sup>112</sup> Another analog of 5-HT (**16**), *N,N,N*-trimethyl-5-HT (**18**; 5-HTQ), was found to have greater selectivity and affinity at 5-HT<sub>3</sub> receptors in comparison to 5-HT (**16**), but systemic administration of the quaternary amine **18**

might not readily penetrate the blood-brain barrier (BBB) minimizing its central effect (Figure 9).<sup>111</sup>

(a)



(b)

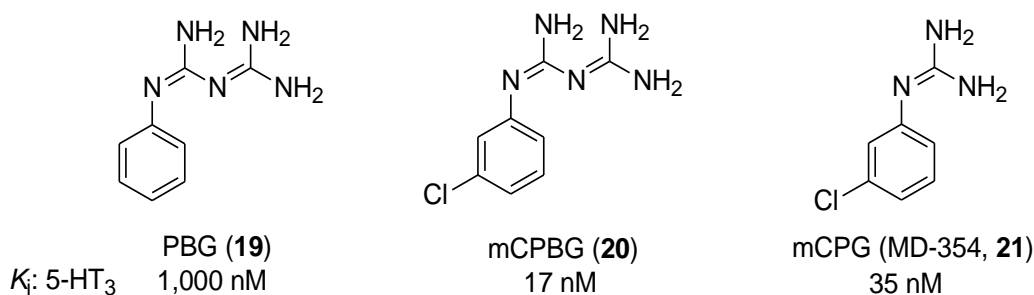


**Figure 9.** Structures of 5-HT<sub>3</sub> receptor agonists: (a) serotonin (**16**) and analogs (**17**, **18**) and (b) arylbiguanides (**19**, **20**) and an arylguanidine (**21**); 5-HT<sub>3</sub> receptor binding affinity is reported as  $K_i$  values (nM).<sup>110,111,113</sup>

Structurally different than 5-HT (**16**), phenylbiguanide (**19**, PBG) has modest 5-HT<sub>3</sub> receptor affinity ( $K_i = 1,000$  nM) and behaves as an agonist (Figure 9).<sup>111</sup> Structural modifications of **19** have led to many agonists with greater affinity. For example, the *meta*-chloro analog (**20**, *m*CPBG) has 60-fold increased affinity at human 5-HT<sub>3</sub> receptors ( $K_i = 17$  nM; Figure 9).<sup>111</sup> Aryl substitution of **19** with chloro group(s) at various positions (e.g., 2-chloro-PBG and 3,4,5-trichloro-PBG) showed decreased  $K_i$  values to the low nanomolar range in comparison to PBG (**19**).<sup>32,114</sup> Affinity was

retained when the biguanide moiety of *m*CPBG (**20**) was deconstructed to a guanidine as in *meta*-chlorophenylguanidine (**21**, *m*CPG, MD-354;  $K_i = 35$  nM; Figure 9).<sup>111,113</sup> Just like the arylbiguanides, the arylguanidines have improved affinity with the addition of chloro groups to the phenyl ring.<sup>111,113</sup>

SR57227A (**22**; 1-(6-chloropyrid-2-yl)-4-piperidinylamine; Figure 10) is a selective 5-HT<sub>3</sub> receptor agonist ( $K_i = 103$  nM), which can penetrate the BBB.<sup>115</sup> This agent (i.e., **22**) has been found to behave as an agonist both at central and peripheral 5-HT<sub>3</sub> receptors, which makes it a powerful pharmacological tool for detection of CNS effects mediated by 5-HT<sub>3</sub> receptors.<sup>115</sup>

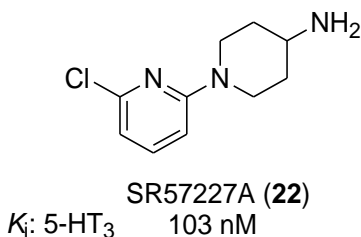


**Figure 10.** Structure of the 5-HT<sub>3</sub> receptor agonist SR57227A (**22**); 5-HT<sub>3</sub> receptor binding affinity reported as a  $K_i$  value (nM).<sup>115</sup>

Although there are no current high-resolution structural data for the 5-HT<sub>3</sub> receptor, homology models have been generated based on the similar acetylcholine binding protein crystal structure.<sup>116-118</sup> In addition to these 5-HT<sub>3</sub> receptor homology models, site-directed mutagenesis studies indicate an agonist and, therefore, a competitive antagonist, extracellular binding site at the interface of two subunits of the 5-HT<sub>3</sub> receptor.<sup>119,120</sup>

### c) 5-HT<sub>3</sub> receptor antagonists

Various 5-HT<sub>3</sub> receptor antagonists such as ondansetron (**23**; trade name: Zofran; Figure 11) and granisetron (trade name: Kytril) are used clinically to treat chemotherapy-induced nausea and vomiting.<sup>121</sup> Also, zacopride (**24**; Figure 11), a 5-HT<sub>3</sub> receptor antagonist and 5-HT<sub>4</sub> receptor agonist, has been shown to be a useful antiemetic agent for cancer patients.<sup>121</sup> In addition, preliminary results suggest that 5-HT<sub>3</sub> receptor antagonists influence the reward pathway (e.g., they reduce drug-induced self-administration of drugs such as ethanol or amphetamine), regulate food intake, produce anxiolytic effects, and attenuate chronic neuropathic pain.<sup>91,121</sup>

Antagonists at 5-HT<sub>3</sub> receptors were first discovered by modifying the chemical structure of cocaine, which was found to be a weak antagonist at 5-HT-M receptors.<sup>90,122</sup> Modifications led to the first selective 5-HT<sub>3</sub> receptor antagonists, bemisetron (MDL 72222) and tropisetron (**25**; Figure 11).<sup>90,123,124</sup> In fact, the centrally acting 5-HT<sub>3</sub> receptor antagonist, tropisetron (**25**; Figure 11), has become a valuable pharmacological tool because its quaternary amine analog, tropisetron methiodide, retains 5-HT<sub>3</sub> receptor antagonist activity but only at peripheral receptors due to its inability to cross the BBB.<sup>113</sup> Numerous similar compounds, which were classified as keto compounds, were synthesized. This class typically contains a carbonyl-containing linker between an aromatic/heteroaromatic ring and a basic amine.<sup>91,124</sup> Most of these ligands are selective for 5-HT<sub>3</sub> receptors, but some have affinity at 5-HT<sub>1P</sub> and/or 5-HT<sub>4</sub> receptors.<sup>91</sup>



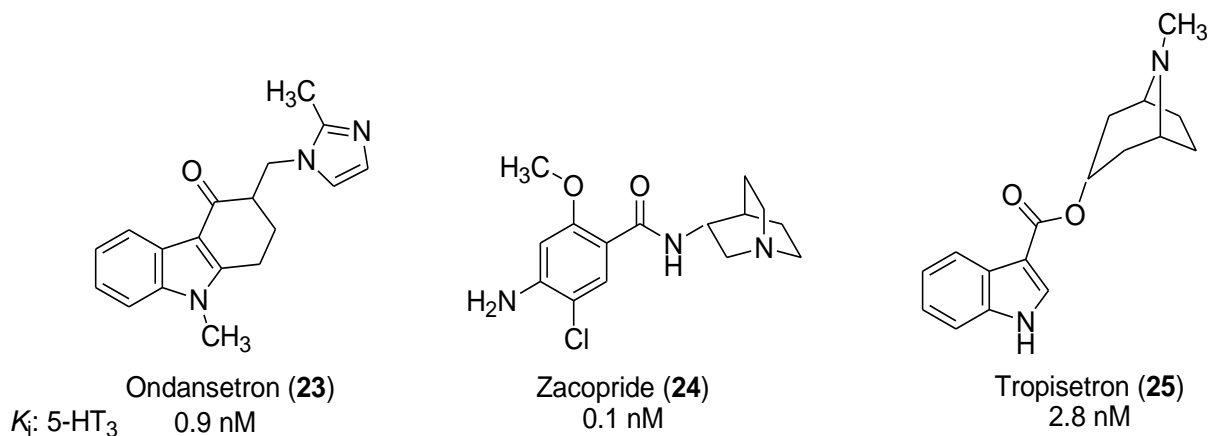


**Figure 11.** Structures of some representative 5-HT<sub>3</sub> receptor antagonists (**23-25**); 5-HT<sub>3</sub> receptor binding affinity reported as  $K_i$  values (nM).<sup>125,126</sup>

In general, the basic aliphatic amine can tolerate small substituents; specifically, a methyl substituent is optimal as in tropisetron (**25**).<sup>91,124</sup> Binding affinity at 5-HT<sub>3</sub> receptors seems to be favorable when the aromatic/heteroaromatic ring is a fused 6,5-ring system (e.g., an indole in **23** and **25**).<sup>91,124</sup> Also, the carbonyl group is typically coplanar with the aromatic system.<sup>91,124</sup> Extensive structure-affinity relationships of 5-HT<sub>3</sub> receptor antagonists have provided selective and high-affinity ligands.<sup>90,91</sup>

#### d) Descending control of pain

Serotonin receptors seem to modulate mechanisms of descending inhibition and descending facilitation in the dorsal horn.<sup>16</sup> Serotonergic input is involved with primary afferent fibers, projection neurons, and inhibitory interneurons and, therefore, 5-HT (**16**) is associated with conveying information from tissues and organs into the CNS and transmitting signals from the CNS to the effector cells.<sup>16</sup>

It was first thought that 5-HT (**16**) reduced nociceptive transmission in the dorsal horn, but there is a plethora of contradicting studies.<sup>19</sup> Various studies such as electrical brain stimulation, morphine-induced antinociception, and direct administration of 5-HT (**16**) into the spinal cord suggest that descending serotonergic pathways exert opposing nociceptive processing effects in the dorsal horn: modulation of descending and facilitating inhibitory pathways.<sup>19,20</sup> This leads to both pronociceptive and antinociceptive actions; there are two possible reasons for these contradictory actions from one neurotransmitter. Varying effects could be due to: (a) the multiple subtypes of 5-HT receptors (i.e., it is the receptor, rather than the neurotransmitter, that is responsible for the excitatory or inhibitory action) and/or (b) the localization of specific 5-HT receptors.

Focusing on the 5-HT<sub>3</sub> receptor subtype, most of the current data indicate an excitatory role in neuronal activity. Upon activation of 5-HT<sub>3</sub> receptors, phospholipase C activity is enhanced which, in turn, causes a cytosolic calcium influx leading to a cascade of intracellular changes and activity.<sup>21-24</sup> In conjunction with behavioral studies suggesting a pronociceptive role of 5-HT<sub>3</sub> receptors, it has been reported that they potentiate the release of the pronociceptive transmitter substance P in the dorsal horn.<sup>20,24</sup> In addition to an unclear mechanism, there are some contradictory data suggesting a suppression in substance P release.<sup>16</sup> Although, to date, it is clear that more research is necessary to fully understand 5-HT<sub>3</sub> receptors' role in the descending control of pain, it is possible that the ambiguous data are due to incomplete characterization of 5-HT<sub>3</sub> receptors (e.g., 5-HT<sub>3A</sub> vs. 5-HT<sub>3AB</sub> receptors).

Previously reported in vivo studies present contradictory analgesic effects of 5-HT<sub>3</sub> receptor agents in nociceptive animal studies (summarized in Table 4). Similar to the pharmacological profile of various 5-HT<sub>3</sub> receptor antagonists, 5-HT<sub>3</sub> receptor agonists can display anti- or pronociceptive effects. This might be due to the species, the animal model, or the route of drug administration. For example, the analgesic action of PBG (**19**) seems to be dependent on the nociceptive animal model; PBG (**19**, i.t.) produces an antinociceptive effect in the rat hot-plate assay, whereas it shows saline-like effects in the rat tail-flick assay.<sup>25</sup> Likewise, the more potent 5-HT<sub>3</sub> receptor agonist *m*CPBG (**20**; i.t.) displayed analgesic effects in the rat formalin and paw pressure assay, but no effect was observed in the rat tail-flick assay.<sup>26,127,128</sup> Different analgesic effects observed in the tail-flick assay are seemingly due to species; 5-HT<sub>3</sub> receptor agonists produce saline-like effects in the rat tail-flick assay, but show antinociceptive effects in the mouse model.<sup>25-28</sup>

**Table 4.** Summary of the analgesic activity of 5-HT<sub>3</sub> receptor ligands in nociceptive animal models (routes of administrations: i.t., intrathecal; i.p., intraperitoneal; s.c., subcutaneous; i.c.v, intracerebroventricular).

<b>Animal Model</b>	<b>Agent</b>	<b>Agonist or antagonist</b>	<b>Species</b>	<b>Admin route</b>	<b>Analgesic activity</b>	<b>Ref</b>
Tail-flick	mCPBG	agonist	rat	i.t.	no	26
	PBG	agonist	rat	i.t.	no	25
	2-Me-5-HT	agonist	mouse	i.t.	yes, blocked by tropisetron & zacopride	28
	SR57227A	agonist	mouse	i.p.	yes, blocked by bemisetron & zacopride	27
	tropisetron	antagonist	rat	i.t.	no	26
			rat	s.c.	no	129
			mouse	s.c.	no	29
	zacopride	antagonist	rat	i.t.	no	30
			mouse	i.p.	no	29
			mouse	s.c.	no	29
	ondansetron	antagonist	mouse	s.c.	no	29
			mouse	s.c.		
Hot-plate	PBG	agonist	rat	i.t.	yes	25
	2-Me-5-HT	agonist	rat	i.t.	yes	130
	tropisetron	antagonist	rat	s.c.	no	129
	ondansetron	antagonist	rat	i.t.	no	129
Paw pressure	5-HT	agonist	rat	i.t.	yes, blocked by granisetron & tropisetron	127, 128
					no	128
	2-Me-5-HT	agonist	rat	i.t.	yes, blocked by tropisetron & granisetron	127, 128, 131
					yes	132
	tropisetron	antagonist	rat	i.t.	no	127, 128,
			rat	i.p.	yes	132
	ondansetron	antagonist	rat	i.t.	no	131
			rat	i.t.	no	128, 131
Formalin	mCPBG	agonist	rat	i.t.	yes	133
	tropisetron	antagonist	rat	s.c.	yes	129
	ondansetron	antagonist	rat	i.t.	no	129, 133

In general, administration of 5-HT<sub>3</sub> receptor antagonists produces saline-like effects in antinociceptive animal models, but there are some exceptions. For example, s.c. administration of tropisetron (**25**) showed analgesic actions in the rat formalin test.<sup>129</sup> Also, ondansetron (**23**) showed antinociceptive effects upon i.p. administration in a mechanical nociceptive animal model (rat paw pressure assay).<sup>132</sup> Thus far, these contradictory observations are inadequately understood.

#### **D. MD-354 (21)**

##### **1. Binding affinity**

The 5-HT<sub>3</sub> receptor ligand MD-354 (**21**) was identified in our laboratory in 1996.<sup>32</sup> Radioligand binding assays at 30 different aminergic receptors indicated that MD-354 (**21**) possesses a rather selective binding profile. The receptors for which MD-354 (**21**) displays high affinity include the ligand-gated ion channel serotonin 5-HT<sub>3</sub> receptors (Table 5).<sup>32</sup> Subsequently, MD-354 (**21**) was found to bind to the low- and high-affinity states of the G protein-coupled  $\alpha_2$ -adrenoceptors as determined using the antagonist radioligand ([ethyl-<sup>3</sup>H]RS-79948-197) and the agonist radioligand ([<sup>125</sup>I]clonidine), respectively (Table 5).<sup>31,33</sup> It is thought that radiolabeled agonists label the high-affinity state of the receptor, whereas radiolabeled antagonists label both high- and low-affinity states of the receptor.<sup>134</sup>

**Table 5.** MD-354 (**21**) binding profile.<sup>31-33</sup>

Receptor population	$K_i$ (nM)
5-HT <sub>3</sub>	35 <sup>a</sup>
$\alpha_{2A}$ -ARs	110 <sup>b</sup> , 825 <sup>c</sup>
$\alpha_{2B}$ -ARs	220 <sup>b</sup> , 25 <sup>c</sup>
$\alpha_{2C}$ -ARs	4,700 <sup>b</sup> , 140 <sup>c</sup>

Radioligands used in binding assays: <sup>a</sup>[<sup>3</sup>H]GR65630 (a 5-HT<sub>3</sub> receptor antagonist), <sup>b</sup>[ethyl-<sup>3</sup>H]RS-79948-197 (an adrenoceptor antagonist) and <sup>c</sup>[<sup>125</sup>I]clonidine (an adrenoceptor agonist).

Additionally, MD-354 (**21**) has very modest affinity for 5-HT<sub>1A</sub> ( $K_i = 4,100$  nM), 5-HT<sub>5A</sub> ( $K_i = 4,160$  nM), and 5-HT<sub>7</sub> ( $K_i = 680$  nM) receptors as well as  $\alpha_{1A}$ - ( $K_i = 300$  nM) and  $\alpha_{1B}$ - ( $K_i = 1,900$  nM) ARs, but no affinity (i.e.,  $K_i > 10,000$  nM) at the remaining serotonin receptor and adrenoceptor subtypes, dopamine D<sub>1</sub>-D<sub>5</sub> receptors, mu and kappa opioid receptors, m<sub>1</sub>-m<sub>5</sub> muscarinic receptors, rat H<sub>1</sub> histamine receptors, phencyclidine receptors, NMDA receptors, benzodiazepine receptors, and the aminergic transporters (serotonin, dopamine, and norepinephrine).<sup>33</sup>

## 2. In vitro functional activity

Functional [<sup>35</sup>S]GTP $\gamma$ S assays were performed with two types of buffer conditions: low and high concentrations of NaCl. Experimental conditions with low salt concentrations have been found optimal for the detection of partial agonist activity.<sup>134</sup> As concluded by these assays, MD-354 (**21**) behaves as a weak partial agonist at  $\alpha_{2A}$ -

ARs in low and high salt conditions ( $EC_{50} = 0.83$  and  $1.4 \mu\text{M}$ , respectively).<sup>31</sup> At high concentrations ( $>100 \mu\text{M}$ ), MD-354 (**21**) nonselectively antagonized the agonist effect of norepinephrine (**1**; NE) at all three receptor subtypes.<sup>31</sup>

### 3. In vivo functional activity

#### a) MD-354 (**21**) administered alone

Numerous in vivo pharmacological studies involving 5-HT<sub>3</sub> receptor agents, such as MD-354 (**21**), have been reported. Initial MD-354 (**21**) functional studies included the rat von Bezold-Jarisch assay, which examined reflex bradycardia, and the rabbit bladder assay.<sup>32</sup> Although MD-354 (**21**) behaved as an agonist in both of these assays, it showed reduced potency in comparison to the biguanide analog *m*CPBG (**20**).<sup>32</sup> Low doses (e.g., 10 mg/kg, i.p.) of MD-354 (**21**) also were shown to reduce cisplatin-induced emesis, whereas higher doses (40 mg/kg, i.p.) elicited an emetic effect in the shrew.<sup>113</sup> MD-354 (**21**) has been used as a training drug in drug discrimination studies. The discriminative stimulus effects of MD-354 (**21**) in rats (training dose = 2.0 mg/kg) seems to be a central 5-HT<sub>3</sub> receptor-mediated effect because it is usually only centrally-acting agents that serve as discriminative stimuli, and because the stimulus effects of MD-354 (**21**) were antagonized by the 5-HT<sub>3</sub> receptor antagonists zacopride (**24**) and tropisetron (**25**), but not by tropisetron methiodide.<sup>113,135</sup> This quaternary analog (tropisetron methiodide) retains the antagonist properties of tropisetron (**25**) but is not able to readily cross the BBB.<sup>113,135</sup>

Since 5-HT<sub>3</sub> receptors and α<sub>2</sub>-ARs both have been implicated in pain, MD-354 (**21**) was examined in mouse tail-flick and hot-plate assays. In the mouse tail-flick assay, MD-354 (**21**; doses: 1.0-30 mg/kg, s.c.) showed saline-like effects using various pretreatment times.<sup>33</sup> Similarly, MD-354 (**21**) failed to produce a statistically significant antinociceptive effect (in comparison to saline control) at various doses (3.0-30 mg/kg, s.c.) and pretreatment times in the mouse hot-plate assay.<sup>33</sup> And, finally, the spontaneous activity of MD-354 (**21**) was examined and MD-354 (**21**) was found to produce saline-like effects in mice indicating it is neither a CNS stimulant nor a CNS depressant.<sup>31,33,135</sup> Another possible conclusion is that MD-354 (**21**) is unable to penetrate the BBB to produce its effect(s).

#### **b) MD-354 (**21**) administered in combination with clonidine (**7**)**

Although MD-354 (**21**; 1.0-30 mg/kg) produced no analgesic effects when administered alone, it potentiated the antinociceptive effect of an “inactive” dose of clonidine (**7**) in the mouse tail-flick assay [MD-354 (**21**) doses 1.0-30 mg/kg], but didn't significantly potentiate or attenuate the effect of clonidine (**7**) in the mouse hot-plate assay [MD-354 (**21**) doses 10-30 mg/kg].<sup>33</sup> Moreover, in the mouse tail-flick assay the analgesic effect of the MD-354/clonidine (**21/7**) combination appeared to be biphasic (Figure 12).<sup>34</sup> The antinociceptive properties of clonidine (**7**) were potentiated by MD-354 (**21**) as depicted by both peaks [Peaks A and B at 1.0 and 10 mg/kg doses of MD-354 (**21**), respectively] of the biphasic dose-response curve (Figure 12). The potentiating effect of MD-354 (**21**) in combination with clonidine (**7**) illustrated by Peaks



A and B could be due to different mechanisms such as: (a) 5-HT<sub>3</sub> receptor agonism or antagonism, (b) action at one or more  $\alpha_2$ -ARs ( $\alpha_{2A}$ -,  $\alpha_{2B}$ -, and/or  $\alpha_{2C}$ -ARs), or (c) action at neither 5-HT<sub>3</sub> receptors nor  $\alpha_2$ -ARs.<sup>34</sup> Alternatively, the biphasic actions of the combination might be due to a combination of these mechanisms. For example, the low-dose potentiating effect (i.e., effect illustrated by Peak A) might be caused by activation of 5-HT<sub>3</sub> receptors, whereas the potentiating effect produced by a higher dose of MD-354 (**21**; 10 mg/kg; Peak B) might be due to action at one or more of the  $\alpha_2$ -ARs ( $\alpha_{2A}$ -,  $\alpha_{2B}$ -, and/or  $\alpha_{2C}$ -ARs).<sup>34</sup>

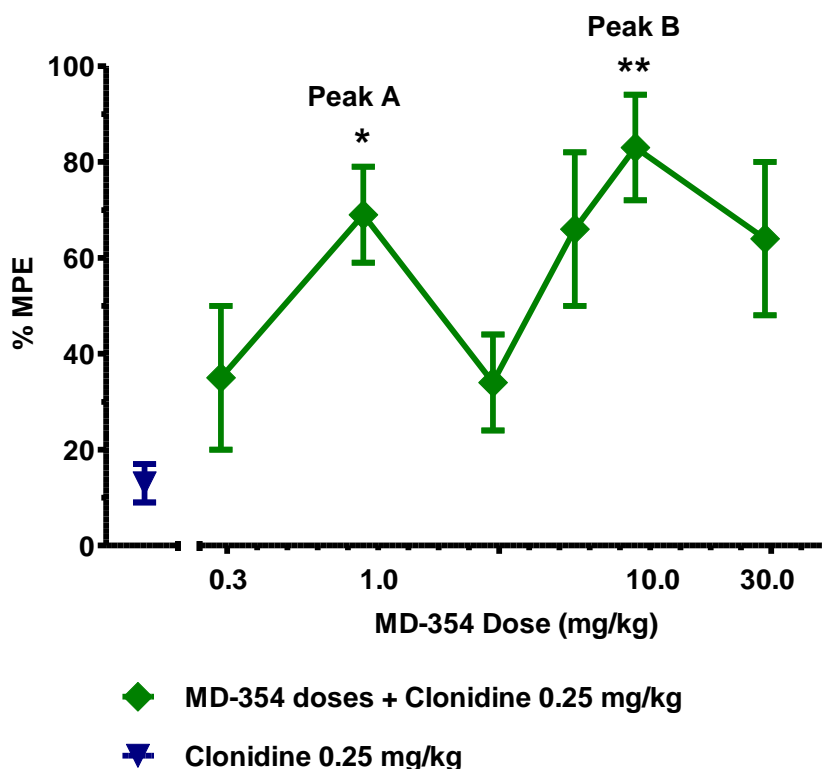


**Figure 12.** Potentiation of the antinociceptive effect ( $\pm$  S.E.M.) of an “inactive” antinociceptive dose of clonidine (**7**; 0.25 mg/kg) by MD-354 (**21**; 0.3-30 mg/kg) in the mouse tail-flick assay. Asterisks denote a significant difference compared to the control group [clonidine (**7**) 0.25 mg/kg]; \* $P < 0.05$ , \*\* $P < 0.01$ , one-way ANOVA followed by Dunnett’s post hoc test.<sup>34</sup>

*The role of 5-HT<sub>3</sub> receptors in the potentiation of clonidine (7)-induced antinociception by MD-354 (21) depicted by Peaks A and B (Figure 12).* Since MD-354 (21) is a 5-HT<sub>3</sub> receptor partial agonist, it is possible that its potentiating effect on clonidine (7) antinociception is due to either 5-HT<sub>3</sub> receptor agonism or antagonism. The role of 5-HT<sub>3</sub> receptors in the potentiation of clonidine (7) antinociception by a low- and high dose of MD-354 (21) illustrated by Peaks A and B (Figure 12), respectively, was examined by co-administration of 5-HT<sub>3</sub> receptor antagonists with: (a) clonidine (7) alone and (b) the combination of MD-354 (21; 1.0 or 6.0 mg/kg) and clonidine (7; 0.25 mg/kg).

When administered alone via the s.c. route, three 5-HT<sub>3</sub> receptor antagonists [ondansetron (23; 0.02-2.0 mg/kg), zacopride (24; 0.0001-2.0 mg/kg), and tropisetron (25; 0.0001-1.0 mg/kg)] showed saline-like effects in the mouse tail-flick assay, but significantly potentiated the antinociceptive effect of an “inactive” dose of clonidine (7; 0.25 mg/kg).<sup>29</sup> This potentiating effect suggests that blockade of 5-HT<sub>3</sub> receptors can augment the analgesic properties of clonidine (7). Therefore, it is possible that 5-HT<sub>3</sub> receptor antagonism could be implicated in the mechanism underlying Peak A and/or B.

Tropisetron (25) attenuated the antinociceptive effect observed in Peak A [i.e., the effect produced by the co-administration of MD-354 (21; 1.0 mg/kg) and clonidine (7; 0.25 mg/kg)].<sup>34</sup> This observation supports a 5-HT<sub>3</sub> receptor agonist mechanism for MD-354 (21) in Peak A.

The role of 5-HT<sub>3</sub> receptors in Peak B was examined by mechanistic studies involving 5-HT<sub>3</sub> receptor antagonists. For example, the 5-HT<sub>3</sub> receptor antagonist zacopride (24) failed to potentiate the antinociceptive effect of MD-354 (21) in the

mouse tail-flick assay; that is, co-administration of zacopride (**24**) and MD-354 (**21**) produced saline-like effects.<sup>29</sup> Also, the potentiation of clonidine (**7**; 0.25 mg/kg) by a high dose of MD-354 (**21**; 6.0 mg/kg) was neither potentiated nor attenuated by zacopride (**24**).<sup>29,33</sup> This suggests that the effect represented by Peak B is not due to 5-HT<sub>3</sub> receptor agonist action.

Additional mechanistic studies were conducted. In the mouse tail-flick assay, the more selective 5-HT<sub>3</sub> receptor antagonist tropisetron (**25**; 0.0001-1.0 mg/kg) in comparison to zacopride (**24**; acts at both 5-HT<sub>3</sub> and 5-HT<sub>4</sub> receptors) was also found to neither potentiate nor attenuate the antinociceptive effect of the MD-354/clonidine (**21/7**) combination when a high dose of MD-354 (**21**; 6 mg/kg) was administered.<sup>29</sup> These combined results indicated a 5-HT<sub>3</sub> receptor agonist mechanism associated with Peak A only.

It seems rather unlikely that the potentiating effect associated with Peak B is due to the 5-HT<sub>3</sub> receptor agonist character of MD-354 (**21**) because two structurally diverse 5-HT<sub>3</sub> receptor antagonists [zacopride (**24**) and tropisetron (**25**)] failed to block the antinociceptive effect of the MD-354/clonidine (**21/7**) combination (Peak B).<sup>29</sup> Alternatively, it is possible that the potentiation of the antinociceptive effect of clonidine (**7**) by a high dose (6.0 mg/kg) of MD-354 (**21**) might be due to 5-HT<sub>3</sub> receptor antagonism. This hypothesis was supported by the potentiating action of 5-HT<sub>3</sub> receptor antagonists [e.g., zacopride (**24**), tropisetron (**25**), and ondansetron (**23**)] co-administered with clonidine (**7**) in the mouse tail-flick assay.<sup>29</sup>

*The role of  $\alpha_2$ -ARs in the potentiation of clonidine (**7**)-induced antinociception by MD-354 (**21**) depicted by Peaks A and B (Figure 12). Various  $\alpha_2$ -AR antagonists with*

different binding selectivity were examined for their antinociceptive properties both alone and in combination with low and high doses (1.0 or 6.0 mg/kg, respectively) of MD-354 (**21**) and 0.25 mg/kg of clonidine (**7**). One difficulty in mechanistic studies involving the three subtypes of  $\alpha_2$ -ARs is the lack of highly selective ligands. Only preferentially adrenoceptor-selective antagonists are known; for example, imiloxan (**12**) and BRL44408 (**15**) have modest selectivity at  $\alpha_{2B}$ - and  $\alpha_{2A}$ -ARs, respectively (see Figure 6 for  $\alpha_2$ -AR binding affinities).<sup>82,136,137</sup>

The non-selective  $\alpha_2$ -AR antagonist yohimbine (**11**; 0.1-1.0 mg/kg) and the moderately selective  $\alpha_{2B}$ - and  $\alpha_{2A}$ -AR antagonists imiloxan (**12**; 0.1-1.0 mg/kg) and BRL44408 (**15**; 0.3-10 mg/kg), respectively, showed no antinociceptive effects when administered alone.<sup>31,33</sup> Yohimbine (**11**) and BRL44408 (**15**) failed to affect the analgesic properties of an “inactive” dose of clonidine (**7**; 0.25 mg/kg); that is, the co-administration of yohimbine (**11**) and clonidine (**7**), as well as BRL44408 (**15**) and clonidine (**7**), produced saline-like effects in the tail-flick assay.<sup>31</sup> Conversely, imiloxan (**12**; 0.1-3.0 mg/kg) significantly potentiated the antinociceptive effect of a saline-like dose of clonidine (**7**; 0.25 mg/kg).<sup>31</sup> Although this does not rule out a possible  $\alpha_{2A}$ - or  $\alpha_{2C}$ -AR mechanism, the results obtained with imiloxan (**12**) suggest that  $\alpha_{2B}$ -AR antagonists can potentiate the action of clonidine (**7**). In other words, if MD-354 (**21**) behaves as an  $\alpha_{2B}$ -AR antagonist, then it might be potentiating the antinociceptive effect of clonidine (**7**; Peak A and/or B) via an  $\alpha_{2B}$ -AR antagonist mechanism of action.

In the mouse tail-flick assay, the non-selective  $\alpha_2$ -AR antagonist yohimbine (**11**) blocked the analgesic effect of Peak A [1.0 mg/kg dose of MD-354 (**21**) + 0.25 mg/kg dose of clonidine (**7**)] in a dose-dependent manner ( $AD_{50} = 0.33$  mg/kg), which suggests

that at least one of the  $\alpha_2$ -AR subtypes is involved in the action.<sup>31</sup> Next, preferentially selective agents were studied; imiloxan (**12**) and BRL44408 (**15**) both attenuated the antinociceptive effect of the co-administration of MD-354 (**21**; 1.0 mg/kg) and clonidine (**7**; 0.25 mg/kg) in a dose-dependent fashion ( $AD_{50}$  = 0.17 and 2.1 mg/kg, respectively).<sup>31</sup> Because, by definition, antagonists block the effect of agonists, these observations suggest an  $\alpha_2$ -AR agonist mechanism in the actions associated with Peak A.

Thus far, imiloxan (**12**) is the only  $\alpha_2$ -AR agent that has been examined in mechanistic studies of Peak B. And, although imiloxan (**12**) was found to attenuate the effect of a lower dose of MD-354 (**21**; 1 mg/kg) in combination with clonidine (**7**; 0.25 mg/kg) illustrated by Peak A, it failed to alter the enhanced antinociception produced by administration of a 6 mg/kg dose of MD-354 (**21**) in combination with clonidine (**7**; 0.25 mg/kg) depicted by Peak B.<sup>31,33</sup> These results suggest that the antinociceptive effect produced by co-administration of a lower dose (1.0 mg/kg) of MD-354 (**21**) and 0.25 mg/kg dose of clonidine (**7**) is mediated by an  $\alpha_{2B}$ -AR agonist mechanism (i.e., an  $\alpha_{2B}$ -AR agonist mechanism seems to play a role in the effect associated with Peak A, but not Peak B; Figure 12).

Initial binding data for imiloxan (**12**) at cloned human  $\alpha_2$ -ARs ( $K_i$ :  $\alpha_{2A}$  = 1584,  $\alpha_{2B}$  = 126,  $\alpha_{2C}$  = 1000 nM)<sup>136</sup> suggested  $\alpha_{2B}$ -AR preferential selectivity, but later studies showed reduced binding selectivity ( $K_i$ :  $\alpha_{2A}$  = 3,109,  $\alpha_{2B}$  = 562, and  $\alpha_{2C}$  = 1,025 nM), as well as functional activity ([<sup>35</sup>S] GTP $\gamma$ S assay;  $K_i$ :  $\alpha_{2A}$  = 316,  $\alpha_{2B}$  = 68,  $\alpha_{2C}$  = 151 nM).<sup>31,137</sup> The latter studies showed very modest selectivity with an  $\alpha_{2B}$ -AR activity of only five- and two-times greater than that for  $\alpha_{2A}$ -AR and  $\alpha_{2C}$ -AR activity, respectively.

Due to possible low  $\alpha_2$ -AR subtype selectivity, it is difficult to rule out an  $\alpha_{2B}$ -AR involvement in the action for Peak B.

To date, MD-354 (**21**) seems to potentiate the antinociceptive effect of clonidine (**7**), at least in part, via a 5-HT<sub>3</sub> receptor and an  $\alpha_2$ -AR mechanism.<sup>31,29</sup> It is unclear which AR subtypes are specifically involved;  $\alpha_{2A}$ - and  $\alpha_{2B}$ -ARs seem to play a role due to attenuation of the effect of the MD-354/clonidine (**21/7**) combination by the reasonably selective antagonists BRL44408 (**15**) and imiloxan (**12**), respectively, but an  $\alpha_{2C}$ -AR mechanism cannot be ruled out because imiloxan (**12**) has moderate affinity and activity at  $\alpha_{2C}$ -ARs.<sup>31</sup>

### III. Specific aims and rationale

#### A. To further investigate the mechanism of action of the analgesia-potentiating effect of clonidine (**7**) by MD-354 (**21**)

Epidural administration of clonidine (**7**), an  $\alpha_2$ -AR agonist, is one of the few non-opioid FDA-approved treatments of cancer pain. Although clonidine (**7**) is a potent analgesic agent, it produces undesirable side effects, including sedation and hypotension, limiting its use to clinical settings.<sup>70,73,74</sup> One of the main goals of our laboratory is to develop adjuvant agents to minimize the side effects of clonidine (**7**) while retaining its analgesic action. It has been previously shown by our laboratory that MD-354 (**21**) is a 5-HT<sub>3</sub> receptor/ $\alpha_2$ -AR ligand. Although MD-354 (**21**) is inactive when administered alone, it selectively potentiates the antinociceptive actions of an “inactive” analgesic dose of clonidine (**7**).<sup>29,33</sup> This seems to be a selective effect because MD-354 (**21**) did not potentiate the sedative effect of clonidine (**7**).<sup>29,33</sup> In other words, MD-354 (**21**) potentiates the desired analgesic, but not the adverse sedative effects of clonidine (**7**). This could have substantial clinical ramifications for the treatment of cancer-related pain.

More specifically, when MD-354 (**21**; 0.3-30 mg/kg) and a sub-threshold (i.e., an “inactive”) analgesic dose of clonidine (**7**; 0.25 mg/kg) were co-administered, a biphasic analgesic effect was observed (Figure 12).<sup>34</sup> Analgesic potentiation of clonidine (**7**)-

induced antinociception produced by MD-354 (**21**), illustrated by Peaks A and B (Figure 12), might be due to different mechanisms (e.g., 5-HT<sub>3</sub> receptor agonism/antagonism,  $\alpha_{2A}$ -,  $\alpha_{2B}$ -, or  $\alpha_{2C}$ -AR action, or a combination of these mechanisms). Mechanistic studies have determined that this analgesic potentiation is due, at least in part, to a 5-HT<sub>3</sub> receptor and an  $\alpha_2$ -adrenoceptor mechanism.<sup>29,33</sup>

Since mechanistic studies of Peak A indicate potentiation by 5-HT<sub>3</sub> receptor agonism, then the more established 5-HT<sub>3</sub> receptor agonist *meta*-chlorophenylbiguanide (**20**; *m*CPBG) should produce a similar effect in combination with clonidine (**7**). In previous *in vivo* studies, *i.t.* administration of *m*CPBG (**20**) produced antinociceptive effects in some animal models (e.g., rat paw pressure and formalin test; Table 4).<sup>127-133</sup> However, in the rat tail-flick assay, *m*CPBG (**20**; *i.t.*) failed to produce a significant effect.<sup>26</sup> But, *m*CPBG (**20**) has not been examined in this assay via *s.c.* administration. Similarly, *i.t.* administered PBG [**19**; a much lower-affinity 5-HT<sub>3</sub> receptor agonist, the des-chloro analog of *m*CPBG (**20**)], produced saline-like effects in the tail-flick assay but, in contrast, showed antinociceptive effects in the hot-plate assay when administered by an *i.t.* route.<sup>25</sup> To the best of our knowledge, examination of the antinociceptive effect of *m*CPBG (**20**) in the hot-plate assay has not been reported.

In this study, we will determine the antinociceptive actions of *m*CPBG (**20**) when administered alone in mice via *s.c.* administration. Since, *m*CPBG (**20**) has not been previously examined in the mouse tail-flick assay via a *s.c.* route of administration, a time-course study will be undertaken to determine optimal pre-injection times. Then, combination studies [co-administration of *m*CPBG (**20**) and clonidine (**7**)] will be evaluated to determine if *m*CPBG (**20**) behaves in a manner similar to MD-354 (**21**) in



the tail-flick assay [i.e., to determine if it potentiates the antinociceptive actions of clonidine (**7**)]. If an ED<sub>50</sub> dose (a dose that produces 50% MPE or 50% maximal possible effect) of clonidine (**7**) is administered in combination with *m*CPBG (**20**), it will be possible to detect either attenuation or potentiation of the effect. If potentiation by *m*CPBG (**20**) is observed, 5-HT<sub>3</sub> antagonists [e.g., ondansetron (**23**) and tropisetron (**25**)] will be examined to assess *m*CPBG's (**20**) mechanism of action. If a 5-HT<sub>3</sub> receptor antagonist blocks the antinociceptive effect of the *m*CPBG/clonidine (**20/7**) combination, this will provide evidence for a 5-HT<sub>3</sub> receptor agonist-mediated mechanism of action.

Literature data concerning *m*CPBG (**20**) and related compounds acting as central agents is unclear and limited. Contradictory data describing the ability of *m*CPBG (**20**) to cross the BBB is presented in Table 6. There seems to be a species-related difference; *m*CPBG (**20**) appears to cross the BBB in rat but, perhaps, not in mice.<sup>115,138,139</sup> Also, there is a discrepancy in the log P value depending on the experimental method employed. A log P value for *m*CPBG of -0.38 has been reported using the shake-flask method, whereas our laboratory has shown *m*CPBG (**20**) to be more lipophilic (log P = 1.70) using an HPLC (high performance liquid chromatography) technique.<sup>118,140</sup> In general, drugs with log P values ranging from 1.5 to 2.5 can penetrate the BBB.<sup>141</sup> Therefore, the log P value obtained from the shake-flask method indicates negligible BBB penetration, whereas data from the HPLC method suggests that *m*CPBG (**20**) should cross the BBB. However, it should be noted that the study with *m*CPBG (**20**) and MD-354 (**21**) in the shake-flask method employed their water soluble salts (hydrochloride and nitrate salts, respectively).

**Table 6.** Literature summary of the ability of *m*CPBG (**20**) to cross the BBB.

<i>m</i> CPBG ( <b>20</b> ) does cross the BBB	<i>m</i> CPBG ( <b>20</b> ) does <u>not</u> cross the BBB
<ul style="list-style-type: none"><li>• <i>m</i>CPBG (<b>20</b>) displaced [<sup>3</sup>H]GR67330 in rat entorhinal cortex.<sup>139</sup></li><li>• [<sup>3</sup>H]<i>m</i>CPBG labeled 5-HT<sub>3</sub> receptor recognition sites in rat brain.<sup>138</sup></li><li>• Relative retention times using HPLC: <i>m</i>CPBG (<b>20</b>) log P = 1.70<sup>118</sup></li></ul>	<ul style="list-style-type: none"><li>• <i>m</i>CPBG (<b>20</b>) did not displace [<sup>3</sup>H] granisetron in mouse cortical membranes.<sup>115</sup></li><li>• Shake-flask method: <i>m</i>CPBG (<b>20</b>) log P = -0.38<sup>140</sup></li><li>• <i>m</i>CPBG (<b>20</b>) showed hypothermic effects [blocked by ondansetron (<b>23</b>)] by i.c.v., but not i.p., routes in mice.<sup>142</sup></li></ul>

There is evidence that *m*CPBG (**20**) does not penetrate the BBB (Table 6). This might also be a species related effect. Therefore, in addition to receptor mechanism studies, central versus peripheral activity will be evaluated. If *m*CPBG (**20**) is acting via a centrally-mediated 5-HT<sub>3</sub> receptor agonist mechanism, it should be possible to antagonize the effect with the centrally-acting 5-HT<sub>3</sub> receptor antagonist tropisetron (**25**). The quaternary amine analog of tropisetron (**25**), tropisetron methiodide, behaves as a 5-HT<sub>3</sub> receptor antagonist that does not readily penetrate the BBB. Therefore, tropisetron methiodide can be utilized as a control because it should only produce a peripheral antagonist effect.

If a 5-HT<sub>3</sub> receptor mechanism is supported in the above studies, the role of this mechanism in clonidine's (**7**) potentiation by MD-354 (**21**) will be further evaluated by examining a centrally-acting 5-HT<sub>3</sub> receptor agonist. Unlike *m*CPBG (**20**), there is compelling evidence that SR57227A (**22**; 1-(6-chloropyrid-2-yl)-4-piperidinylamine; Figure 10) behaves as an agonist at central 5-HT<sub>3</sub> receptors.<sup>115</sup> SR57227A (**22**)

displays affinity at 5-HT<sub>3</sub> receptors ( $K_i = 103$  nM) but lacks an  $\alpha_2$ -AR component.<sup>115</sup> In fact, i.p. administration of SR57227A (**22**; 1.0-20 mg/kg) has been previously shown to produce antinociceptive effects in the mouse tail-flick assay.<sup>27</sup> Due to these functional properties, the effect of SR57227A (**22**; s.c.) will be studied when administered alone and in combination with clonidine (**7**) in mouse thermal antinociceptive assays. A s.c. route of administration will be used because our previous studies employed s.c. injections and SR57227A (**22**) can penetrate the BBB and, therefore, should produce peripheral and/or central effects via the s.c. route. Just as in the case of *m*CPBG (**20**), a time course study is critical in determining optimal pre-injection times. If MD-354 (**21**) potentiates the antinociceptive effect of clonidine (**7**) via a central 5-HT<sub>3</sub> receptor agonist mechanism, the centrally-acting 5-HT<sub>3</sub> receptor agonist SR57227A (**22**) should also potentiate the effect of an “inactive” dose of clonidine (**7**). In fact, it is expected that an additive antinociceptive effect will be displayed due to the analgesic actions of SR57227A (**22**) and clonidine (**7**) when administered alone.<sup>27,33</sup> Analgesic potentiation of clonidine (**7**) by SR57227A (**22**) will give additional support for a central 5-HT<sub>3</sub> receptor agonist mechanism for Peak A ( Figure 12).

Since mechanistic studies of the analgesia-potentiating effect of clonidine (**7**) by MD-354 (**21**) have also suggested a role for  $\alpha_2$ -ARs (e.g., an  $\alpha_2$ -AR agonist mechanism in Peak A), TDIQ (**6**; 5,6,7,8-tetrahydro-1,3-dioxolo[4,5-*g*]isoquinoline; Figure 5) will be examined in mouse antinociceptive assays. TDIQ (**6**), an agent developed in our laboratory, binds to all three  $\alpha_2$ -AR subtypes ( $K_i$ :  $\alpha_{2A} = 75$ ,  $\alpha_{2B} = 97$ , and  $\alpha_{2C} = 65$  nM) but possesses no affinity for 5-HT<sub>3</sub> receptors.<sup>72</sup> Since TDIQ (**6**) and clonidine (**7**) have similar binding profiles (i.e., they bind nonselectively to  $\alpha_2$ -ARs), it is expected that TDIQ

(6) will display antinociceptive effects in the tail-flick assay. The goal of this study includes the examination of the analgesic effect of TDIQ (6) alone and in combination with clonidine (7), as well as mechanistic studies involving selected  $\alpha_2$ -AR antagonists. That is, if TDIQ (6) augments the antinociceptive effect of clonidine (7), then selective  $\alpha_2$ -AR antagonists [e.g., imiloxan (12), ARC-239 (14), and BRL44408 (15)] will be co-administered with the TDIQ/clonidine (6/7) combination to help explain the mechanism of action. In addition to mechanistic studies, if TDIQ (6) is found to potentiate the antinociceptive actions of clonidine (7), an isobolographic analysis will be conducted to determine the nature of the potentiation because, due to its similar binding profile, TDIQ (6) might simply be another clonidine (7)-like agent. In this case, the effect should be additive. More specifically, an isobolographic analysis will assess if the biological effect produced by a combination of TDIQ (6) and clonidine (7) is greater than, equal to, or smaller than, the sum of the individual effects of the component drugs.

Furthermore, if antinociception is observed with the above agents [*m*CPBG (20), SR57227A (22), and TDIQ (6)] in the tail-flick assay, then analgesic actions will be analyzed in a second nociceptive mouse model, the hot-plate assay. Both of these assays model acute thermal pain, but hot-plate latencies are thought to reflect supraspinal responses, whereas tail-flick latencies generally reflect spinal responses.<sup>143</sup> The reflexes produced in the tail-flick assay may not always be entirely due to spinal responses; they may be affected by supraspinal structures, too.<sup>143</sup> In addition, it is possible that there is a learned response related to both of these animal models (i.e., reiteration of the test can lead to false antinociceptive observations).<sup>143</sup> Therefore, it is important to subject the animals to the assay conditions sparingly. Drugs examined in

the hot-plate assay will include *m*CPBG (**20**), SR57227A (**22**), and TDIQ (**6**) alone and in combination with clonidine (**7**). These combined results should provide information related to possible novel mechanisms for pain therapy.

And, lastly, a mouse locomotor activity assay is often conducted to evaluate the sedative/locomotor properties of antinociceptive agents. If it is found that an agent (or combination of agents) produces a hypolocomotor (or depressant) or a hyperlocomotor (or stimulant) action, it is difficult to interpret antinociceptive assay results. Moreover, data are easier to interpret when it is known that the antinociceptive effect is not associated with sedation or general behavioral depression (or stimulation), as these adverse effects could alter the behavioral interpretation of the mouse assay in a way that would emulate analgesic actions. For example, the hot-plate assay measures the time it takes a mouse to jump from a heated surface (or another behavioral response). If an agent produces decreased motor activity (i.e., depressed locomotor action), then increased jump latency could be erroneously interpreted as an antinociceptive effect.<sup>144</sup> In addition, clonidine (**7**) produces sedative effects, so it is important to determine if potentiation of clonidine's (**7**) antinociceptive actions by *m*CPBG (**20**) is a selective effect. That is, does a potential adjuvant analgesic [e.g., *m*CPBG (**20**), SR57227A (**22**) or TDIQ (**6**)] selectively potentiate the antinociceptive effects of clonidine (**7**) or does it non-selectively potentiate the antinociceptive and sedative effects of clonidine (**7**)? For these reasons, it will be valuable to examine the locomotor properties of agents that produce an analgesia-potentiating effect in combination with clonidine (**7**).

## B. Exploration of conformationally-constrained rotamers of MD-354 (**21**)

Another objective of this study is to further investigate the role of 5-HT<sub>3</sub> receptors in analgesia by developing agents that retain 5-HT<sub>3</sub> receptor character with reduced  $\alpha_2$ -AR properties. As already mentioned, the conformational requirements for the interaction of imidazolines [e.g., clonidine (**7**)] with  $\alpha_2$ -ARs calls for a nearly perpendicular plane between the aromatic rings and the imidazoline-containing moiety.<sup>70</sup> Therefore, if MD-354 (**21**) mimics the binding mode of clonidine (**7**), conformational constraint, as with **26** (Figure 13), should result in retention of 5-HT<sub>3</sub> receptor affinity but in a reduction of  $\alpha_2$ -AR affinity.

Because MD-354 (**21**) possesses a rotatable bond (bond between C<sup>1</sup> and the aniline N atom), it exists as an indefinite number of rotamers. Thus, introduction of conformational constraint might enlighten the manner in which MD-354 (**21**) interacts with 5-HT<sub>3</sub> receptors. When MD-354 (**21**) is constrained into a quinazoline ring [e.g., 2-amino-7-chloro-3,4-dihydroquinazoline (**26**) and 2-amino-5-chloro-3,4-dihydroquinazoline (**27**)], two extreme rotamers are represented as illustrated in Figure 13.

And, indeed, it was determined in initial competitive binding assays that **26**, not **27**, has comparable binding affinity to MD-354 (**21**); **27** has decreased binding affinity at 5-HT<sub>3</sub> receptors relative to **26** (Table 7).<sup>140,145</sup> Due to these initial results, **26** seems to be the conformationally-constrained analog that best mimics MD-354 (**21**) and, therefore, will be used as the parent compound in subsequent structure-affinity relationship studies.

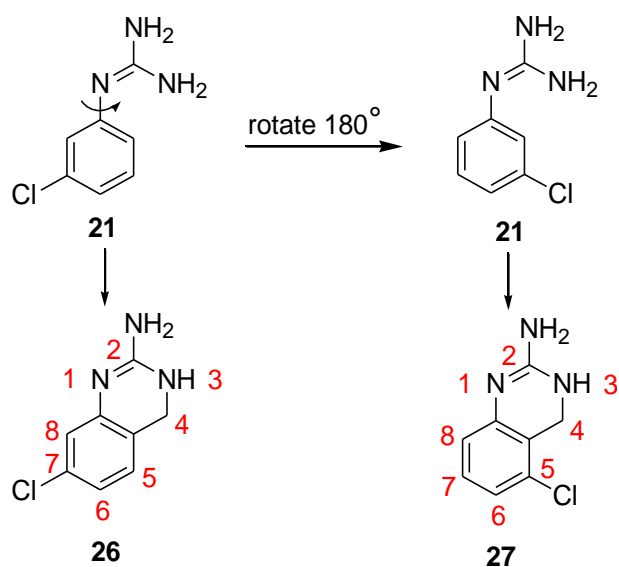


**Figure 13.** Structures of rotamers of MD-354 (**21**) and related conformationally-constrained analogs **26** and **27** (quinazoline numbering indicated in red).

**Table 7.** Receptor affinity ( $K_i$ , nM) for MD-354 (**21**) and conformationally-constrained MD-354 (**21**) analogs **26** and **27**.

	$K_i$ (nM)			
	5-HT <sub>3</sub>	$\alpha_{2A}$ -AR	$\alpha_{2B}$ -AR	$\alpha_{2C}$ -AR
MD-354 ( <b>21</b> )	35 <sup>a</sup>	825 <sup>d</sup>	25 <sup>d</sup>	140 <sup>d</sup>
MKD-65 ( <b>26</b> )	34 <sup>b</sup>	1384 <sup>c</sup>	555 <sup>c</sup>	1328 <sup>c</sup>
SY-70 ( <b>27</b> )	1021 <sup>c</sup>	1305 <sup>c</sup>	984 <sup>c</sup>	2270 <sup>c</sup>

<sup>a</sup>Ref. 32, <sup>b</sup>Ref. 140, <sup>c</sup>Ref. 145, and <sup>d</sup>Ref. 33.

*Role of the ring nitrogen atoms.* In order to determine the role of quinazoline ring nitrogen atoms in the binding at 5-HT<sub>3</sub> receptors, des-nitrogen analogs of **26** will be prepared and evaluated (Figure 14). In other words, nitrogen atoms of **26** will be

systematically replaced one by one with an  $sp^2$  hybridized carbon atom [e.g., 2-amino-7-chloroquinoline (**28**), 3-amino-6-chloroisoquinoline (**29**), and 2-amino-7-chloronaphthalene (**30**); Figure 14]. For example, compound **28** does not contain the 3-position nitrogen atom of **26**, and **29** lacks the 1-position N atom found in **26**. Compound **30** lacks both of these N atoms. Compounds **31-33** will evaluate the role of saturation/unsaturation on the binding of **28-30** at 5-HT<sub>3</sub> receptors.

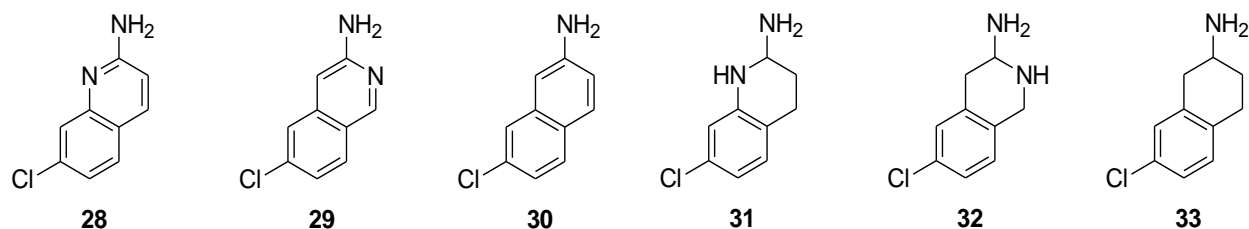


**Figure 14.** Structures of MD-354 (**21**)-related analogs **28-30** and their reduced forms (**31-33**).

Structure-affinity relationship studies of arylguanidines, such as MD-354 (**21**), have been previously conducted.<sup>32,114</sup> It was found that if one of the terminal amine nitrogen atoms of MD-354 (**21**) was replaced by a carbonyl group or H atom (e.g., **34** and **35**), 5-HT<sub>3</sub> receptor affinity was abolished (i.e.,  $K_i > 10,000$  nM; Figure 15).<sup>32</sup> But, **34** is no longer basic. Furthermore, it might not be the lack of the N atom that accounts for the decreased affinity of **35**; rather it might be a lack of electrons associated with the amine. Hence, it would be difficult to predict the affinity of **28** *a priori*. Nevertheless, based on these studies, if **26** has the same binding mode as MD-354 (**21**), as 5-HT<sub>3</sub> receptor binding affinity seems to indicate, then **28** might have little to no affinity at 5-HT<sub>3</sub> receptors. When the aniline nitrogen atom of MD-354 (**21**) was replaced with an  $sp^3$  C atom in the arylguanidine SAFIR studies, 5-HT<sub>3</sub> receptor affinity was reduced by



approximately 35-fold (**36**; Figure 15).<sup>32</sup> Compound **37** also lacked affinity. But, here too, the electronic character of the chain has been altered. Compounds **28-30** will be prepared and evaluated to address this issue.

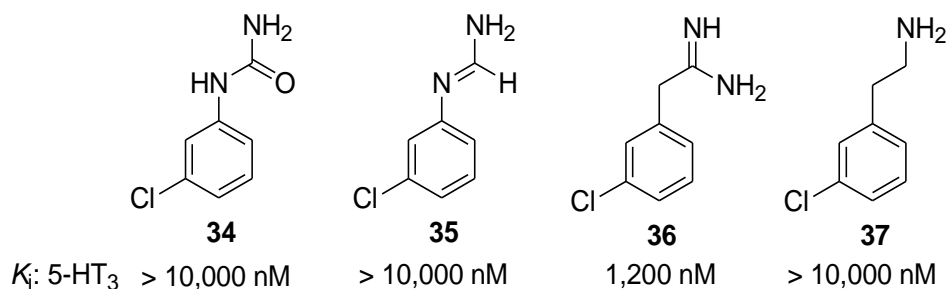


**Figure 15.** MD-354 (**21**) structure-affinity relationship results; 5-HT<sub>3</sub> receptor binding affinity reported as K<sub>i</sub> values (nM).<sup>32</sup>

In addition to MD-354 (**21**) analogs **28-30**, the reduced form of each, will be synthesized to give 2-amino-7-chloro-1,2,3,4-tetrahydroquinoline (**31**), 3-amino-6-chloro-1,2,3,4-tetrahydroisoquinoline (**32**), and 2-amino-7-chlorotetralin (**33**), respectively (Figure 14). This will, in effect, modulate the basicities of the amine functions in question. Although it is unknown if these novel agents will retain affinity for 5-HT<sub>3</sub> receptors, it is difficult to predict the trend. If these nitrogen atoms are directly implicated in interactions with the receptor (e.g., ionic or H-bond interactions between the ligand and the receptor), then the increased basic property of compounds **31-33** will be expected to increase 5-HT<sub>3</sub> receptor affinity in comparison to compounds **28-30**. For example, compound **30** and **33** contain an aniline versus an aliphatic sp<sup>3</sup> hybridized amine moiety, which have approximate pK<sub>a</sub> values of 4.6 and 10.6, respectively.<sup>148</sup> Therefore, compound **33** has increased basic character that may improve the strength of the interactions with 5-HT<sub>3</sub> receptors in comparison with **30**. That is, if the strength of

the interactions between the ligand and receptor is enhanced, receptor binding affinity will increase (or produce a lower  $K_i$  value). In the case of the modification of **32** to **29**, as well as **31** to **28**, the  $s$  character of the ring nitrogen atom ( $sp^3$  to  $sp^2$  hybridization) is increased, which localizes the nitrogen lone electron pair closer to the nitrogen nucleus and, therefore, reduces its ability to donate an electron pair (or, in other words, reduces its Lewis basicity). This principle is supported by  $pK_a$  values for piperidine (11.3) and pyridine (5.2).<sup>146</sup>

*Role of the chloro substituent.* It is proposed to prepare the dichloro- and unsubstituted analogs, 2-amino-5,7-dichloro-3,4-dihydroquinazoline (**38**) and 2-amino-3,4-dihydroquinazoline (**39**), respectively (Figure 16).

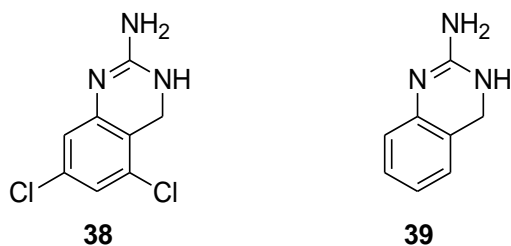


**Figure 16.** Structures of conformationally-constrained MD-354 (**21**) analogs **38** and **39**.

In addition to SAFIR studies involving modification to the guanidine moiety of MD-354 (**21**)-related compounds, extensive aryl substitution was also evaluated. For example, the des-chloro analog of MD-354 (**21**) had reduced 5-HT<sub>3</sub> receptor binding affinity (phenylguanidine:  $K_i = 2,340$  nM) by approximately 70-fold.<sup>32</sup> Also, although *m*-chlorophenylguanidine [MD-354 (**21**):  $K_i = 35$  nM] possessed the highest binding affinity of all the monochlorinated aryl guanidines (e.g., *o*-chlorophenylguanidine and *p*-chlorophenylguanidine:  $K_i = 190$  and 320 nM, respectively), the 3,4-dichloro ( $K_i = 3.1$

nM) analog of MD-354 (**21**) displayed an even higher 5-HT<sub>3</sub> receptor binding affinity.<sup>32,114</sup> Therefore, if it is assumed that the MD-354 (**21**) conformationally-constrained analogs bind in a similar manner to MD-354 (**21**), it might be expected that **38** and **39** will possess increased and decreased 5-HT<sub>3</sub> receptor binding affinity, respectively, in comparison to the parent compound, **26**.

### C. MD-354 (**21**) binding mode at $\alpha_2$ -adrenoceptors

MD-354 (**21**), an agent that binds with varied affinity at all three  $\alpha_2$ -ARs, has been found to potentiate the antinociceptive effects of clonidine (**7**) due, at least in part, to an  $\alpha_2$ -AR mechanism.<sup>31</sup> In fact, competitive binding studies indicated that MD-354 (**21**) binds at the low-affinity states of  $\alpha_{2A/2B/2C}$ -ARs ( $K_i$  = 110, 220, and 4,700 nM, respectively) and at the high-affinity states of  $\alpha_{2A/2B/2C}$ -ARs ( $K_i$  = 825, 25, and 140 nM, respectively).<sup>31,34</sup> Furthermore, functional assays show that MD-354 (**21**) is a weak partial agonist at  $\alpha_{2A}$ -ARs, but an antagonist at  $\alpha_{2B/2C}$ -ARs.<sup>31</sup>

A goal of the current studies is to explain the binding affinity and functional activity of MD-354 (**21**) via examination of its binding mode to graphic receptor models of low- and high-affinity states for  $\alpha_{2A}$ -,  $\alpha_{2B}$ -, and  $\alpha_{2C}$ -ARs. Since there are no current high-resolution structures available for  $\alpha_2$ -ARs, a model of each subtype of the  $\alpha_2$ -ARs will be generated using the inactive  $\beta_2$ -AR crystal structure as a template (pdb = 2RH1; Sybyl 8.1).<sup>57</sup> These three models of  $\alpha_{2A/2B/2C}$ -ARs mimic the low-affinity state because an inverse agonist is bound to the  $\beta_2$ -AR in the crystal structure (i.e., an inverse agonist binds preferentially to the inactive conformation of the receptor).<sup>57</sup>

There are also no high-resolution structures of the active state of  $\alpha_2$ -ARs or the similar  $\beta_2$ -ARs. Therefore, the active or high-affinity state of the  $\alpha_2$ -ARs will be modeled by modifying the low-affinity state models. The main modifications include: (a) rotation of TM6, (b) tilting the TM5 extracellular portion into the binding pocket, and (c) “turning on” the *toggle switch* by modifying the  $\chi_1$  rotameric state of C6.47, W6.48, and F6.52. These modifications will be made and will be assumed to simulate an active state because they have been observed in other active-state structures of GPCRs.<sup>61-63</sup> To validate these  $\alpha_2$ -AR models, the endogenous ligands NE (**1**) and EPI (**2**) will be docked (Gold 4.0) and their resulting docked poses will be compared to other homology models reported in the literature as well as considering available site-directed mutagenesis data.

Since MD-354 (**21**) contains rotatable bonds (Figure 13), before docking MD-354 (**21**) a systematic search will be conducted to identify its low-energy rotamers (Sybyl 8.1). These low-energy rotamers will be docked (Gold 4.0) to all six models (i.e., the low- and high-affinity states of  $\alpha_{2A}$ -,  $\alpha_{2B}$ -, and  $\alpha_{2C}$ -AR models) to determine binding modes. Results from this study will provide homology models of all three subtypes of  $\alpha_2$ -ARs in both low- and high-affinity states based on a relatively new  $\beta_2$ -AR crystal structure.<sup>57</sup> Also, more specifically, it will present potential binding modes of MD-354 (**21**) at all three receptors, which, in turn, might explain its variable binding and functional activities at  $\alpha_{2A}$ -,  $\alpha_{2B}$ -, and  $\alpha_{2C}$ -ARs.

Summary of the studies involved in the specific aims:

A. Investigation of the mechanism of action of the analgesia-potential effect of clonidine (**7**) by MD-354 (**21**):

- Examine clonidine (**7**) alone in the tail-flick and hot-plate assays.
- Examine *m*CPBG (**20**) alone in the tail-flick and hot-plate assays.
- Combination #1: examine *m*CPBG (**20**) + clonidine (**7**) in the tail-flick and hot-plate assays.
- Examine the mouse brain-penetrant 5-HT<sub>3</sub> receptor agonist SR57227A (**22**) alone in the tail-flick and hot-plate assays.
- Combination #2: examine SR57227A (**22**) + clonidine (**7**) in the tail-flick and hot-plate assays.
- Examine a non-selective adrenoceptor agent lacking 5-HT<sub>3</sub> receptor properties, TDIQ (**6**), alone in the tail-flick and hot-plate assays.
- Combination #3: examine TDIQ (**6**) + clonidine (**7**) in the tail-flick and hot-plate assays.
- If any of the above treatments produce antinociceptive effects in either assay, sedative effects will be analyzed in the locomotor activity assay.
- If analgesic potentiation is observed in any of the combinations (#1-3), mechanistic studies will be conducted in the same nociceptive assay.
  - For combinations #1 and 2: examine 5-HT<sub>3</sub> receptor antagonists [ondansetron (**23**), tropisetron (**25**), or tropisetron methiodide] + combination.
  - For combinations #1-3: examine  $\alpha_2$ -AR antagonists [yohimbine (**11**), BRL44408 (**15**), imiloxan (**12**), or ARC-239 (**14**)] + combination.

B. Exploration of conformationally-constrained rotamers of MD-354 (**21**):

- To determine the role of the nitrogen atoms of **26**, des-amino analogs (**28-30**) and the corresponding reduced forms (**31-33**) will be synthesized.
- To determine the role of the chloro substituent of conformationally-constrained analogs of MD-354 (**21**), **38** and **39** will be synthesized.

C. Study the MD-354 (**21**) binding mode at  $\alpha_2$ -ARs:

- Construct  $\alpha_{2A}$ -,  $\alpha_{2B}$ -, and  $\alpha_{2C}$ -AR homology models of the inactive state based on the inactive  $\beta_2$ -AR crystal structure template.
- Modify the  $\alpha_{2A}$ -AR inactive model to generate the  $\alpha_{2A}$ -AR active model;  $\alpha_{2B}$ - and  $\alpha_{2C}$ -AR active models will be generated using the  $\alpha_{2A}$ -AR active model as a template.
- Dock endogenous ligands [NE (**1**) and EPI (**2**)] in the 6 models.
- Conduct a low-energy conformational search of MD-354 (**21**).
- Dock low-energy conformers of MD-354 (**21**) in the 6 models.

## IV. Results and discussion

### A. Pharmacological studies: Nociceptive and locomotor activity animal models and binding assays

Pharmacological assays conducted in this project assessed the potential attenuation or potentiation of the antinociceptive effect of the  $\alpha_2$ -AR agonist clonidine (**7**) by prospective adjuvant agents. First, the effects of clonidine (**7**) were evaluated when administered alone in all assays utilized in the succeeding combination studies (mouse tail-flick, hot-plate, and locomotor assays; control: saline). Pre-injection times employed for clonidine (**7**) were those previously determined in our laboratory and, therefore, were not necessary to re-establish.<sup>33,147,148</sup> On the other hand, when evaluating agents in behavioral assays such as tail-flick and hot-plate assays, it is best to keep the environment constant, which includes the animal “handler”. Therefore, it was necessary to repeat these assays with administration of clonidine (**7**) using the predetermined pre-injection times to establish a new dose-response curve for the present studies. The data from these clonidine (**7**) dose-response curves were used to calculate ED<sub>50</sub> values and were utilized in statistical analysis of subsequent combination studies.

In the mouse tail-flick and hot-plate assays, clonidine (**7**) produced antinociceptive effects in a dose-dependent manner (Figures 17 and 18, respectively). A low dose of clonidine (**7**; 0.25 mg/kg) produced saline-like effects, but as the dose

was increased (up to 2.0 mg/kg), the observed antinociceptive effect increased (tail-flick: % MPE = 62-82; ED<sub>50</sub> = 0.4 ± 0.07 mg/kg and hot-plate: % MPE = 27-73; ED<sub>50</sub> = 0.9 ± 0.06 mg/kg) in both assays (Figures 17 and 18, respectively). These ED<sub>50</sub> values are very similar to previously reported values [clonidine (**7**) ED<sub>50</sub> = 0.5 and 0.8 mg/kg for tail-flick and hot-plate assays, respectively].<sup>33</sup>

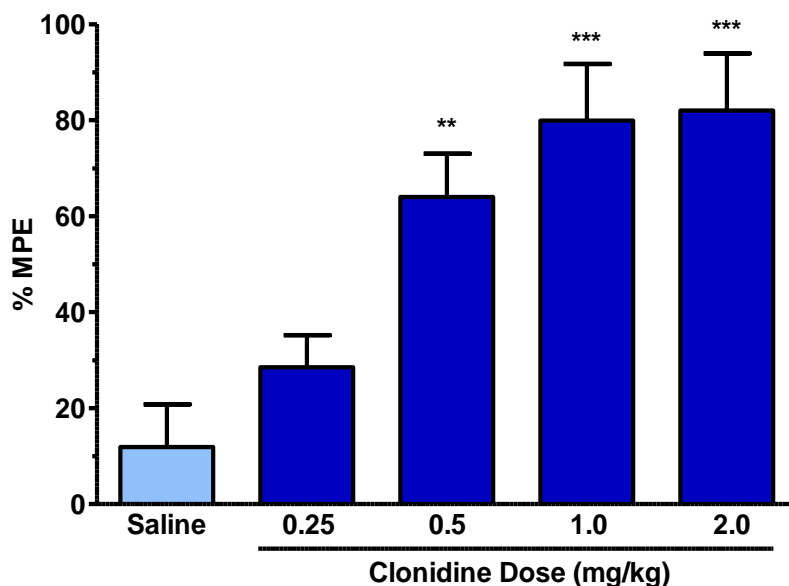


**Figure 17.** Antinociceptive effect ( $\pm$  S.E.M.) of clonidine (**7**; 0.25-2.0 mg/kg, s.c.) in the mouse tail-flick assay ( $n = 8-24$  mice/treatment). Asterisks denote a significant difference compared to the control group (saline); \*\* $P < 0.01$ , \*\*\* $P < 0.001$ , one-way ANOVA ( $F_{4,59} = 9.399$ ) followed by Dunnett's post hoc test.



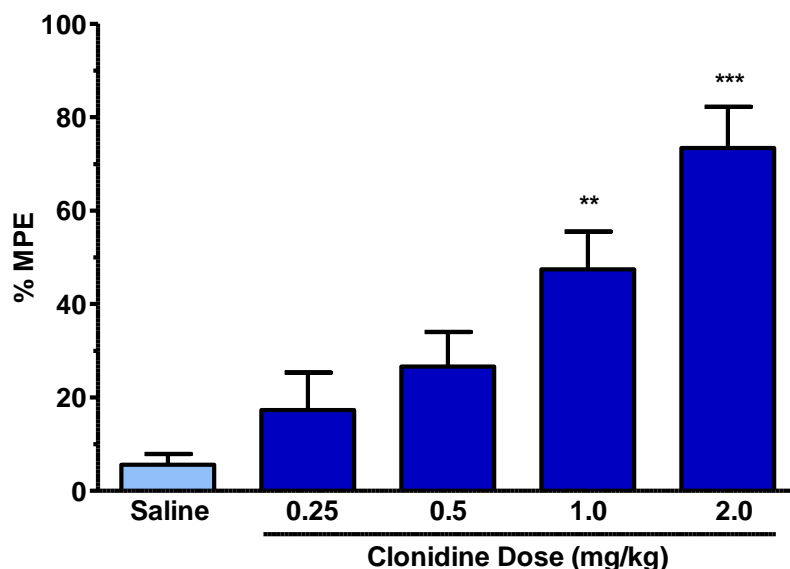


**Figure 18.** Antinociceptive effect ( $\pm$  S.E.M.) of clonidine (**7**; 0.25-2.0 mg/kg, s.c.) in the mouse hot-plate assay ( $n = 9-10$  mice/treatment). Asterisks denote a significant difference compared to the control group (saline); \*\* $P < 0.01$ , \*\*\* $P < 0.001$ , one-way ANOVA ( $F_{4,42} = 11.94$ ) followed by Dunnett's post hoc test.

Since clonidine (**7**) has been previously reported to produce sedative effects, its central depressant properties (e.g., the locomotor actions: movement episodes, movement time, movement distance, and vertical entries) were evaluated in mouse locomotor activity assays (Figure 19).<sup>29</sup> Subcutaneous administration of a 0.25 mg/kg dose of clonidine (**7**) [i.e., a dose of clonidine (**7**) shown to be statistically inactive in the tail-flick and hot-plate assays] was analyzed in the locomotor activity assay because this dose will be used in subsequent combination studies.

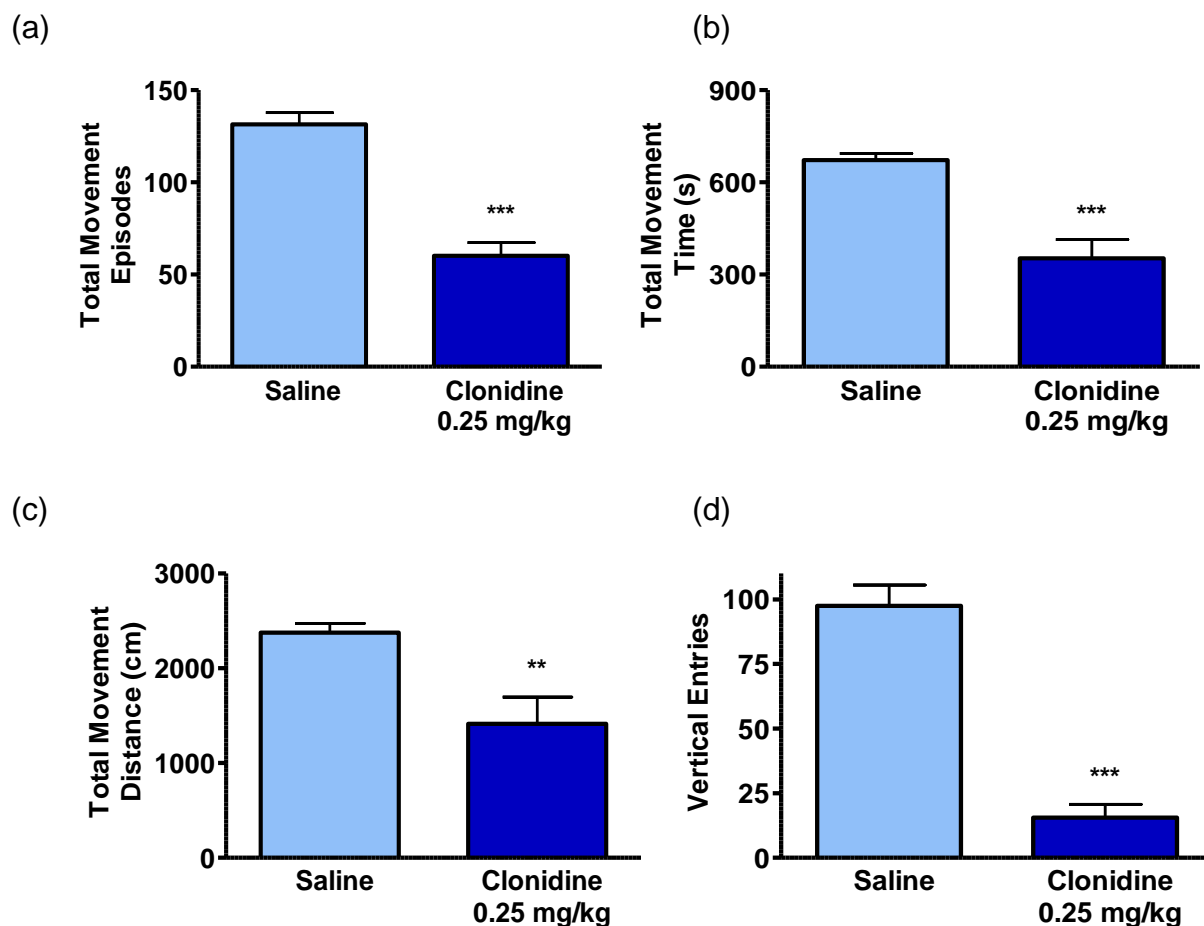


**Figure 19.** Effect ( $\pm$  S.E.M.) of s.c. administered clonidine (**7**; pre-injection time: 5 min, 0.25 mg/kg) on (a) total movement episodes, (b) total movement time, (c) total movement distance, and (d) vertical entries with a 15-min recording time in the mouse locomotor activity assay ( $n = 8-10$  mice/treatment). Asterisks denote a significant difference compared to the control group (saline); \*\* $P < 0.01$ , \*\*\* $P < 0.001$ , Student's t-test.

Results from the locomotor activity assay indicated a general hypolocomoter action of clonidine (**7**). That is, s.c. administration of clonidine (**7**; 0.25 mg/kg) produced a significant reduction in locomotor actions in all four parameters compared to saline vehicle (Figure 19); total movement episodes ( $60.2 \pm 7.1$ ,  $P < 0.001$ ), total movement times ( $352.9 \pm 60.5$  s,  $P < 0.001$ ), total movement distance ( $1,414.7 \pm 280.9$  cm,  $P <$

0.01), and vertical entries ( $15.5 \pm 5.2$ ,  $P < 0.001$ ). This is a clonidine (**7**) dose that produced saline-like effects in both mouse antinociceptive assays (tail-flick and hot-plate: Figures 17 and 18, respectively). Since there was a 5-min pre-injection time for clonidine (**7**), sedative properties were measured for 15 min, which corresponds to the pre-injection time in the antinociceptive assays (20 min).

### 1. Ondansetron (**23**)

In previous MD-354/clonidine (**21/7**) combination studies, the analgesic potentiation (depicted by Peak A; Figure 12) was blocked by a 5-HT<sub>3</sub> receptor antagonist [tropisetron (**25**)]. Due to differences in actions of various 5-HT<sub>3</sub> receptor antagonists, a second agent was studied.<sup>115</sup> Previously, ondansetron (**23**; 0.02-2.0 mg/kg, s.c.) showed no effect in the mouse tail-flick assay (% MPE = 1-4).<sup>29</sup> Ondansetron (**23**; 0.01-1.0 mg/kg) failed to affect the antinociceptive effects of the Peak A MD-354/clonidine (**21**; 1.0 mg/kg + **7**; 0.25 mg/kg) combination (Figure 20). Ondansetron (**23**; 0.01-1.0 mg/kg) was also found to neither attenuate nor potentiate the analgesic actions of the Peak B combination [6.0 mg/kg dose of MD-354 (**21**) + 0.25 mg/kg dose of clonidine (**7**); Figure 21].

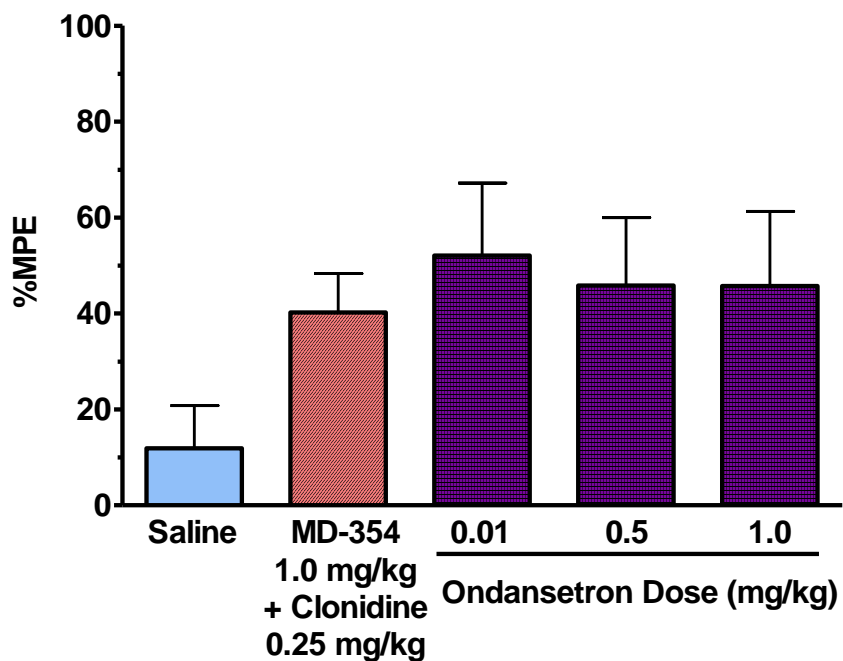


**Figure 20.** Effect ( $\pm$  S.E.M.) of ondansetron (**23**; 0.01-1.0 mg/kg, s.c.) on the antinociceptive action of the MD-354 (**21**; 1.0 mg/kg, s.c.)/clonidine (**7**; 0.25 mg/kg, s.c.) combination in the mouse tail-flick assay ( $n = 8-23$  mice/treatment). No significant difference ( $P > 0.05$ ) compared to the control group [MD-354/clonidine (**21/7**) combination] was detected; one-way ANOVA ( $F_{3,43} = 0.1831$ ) followed by Dunnett's post hoc test.

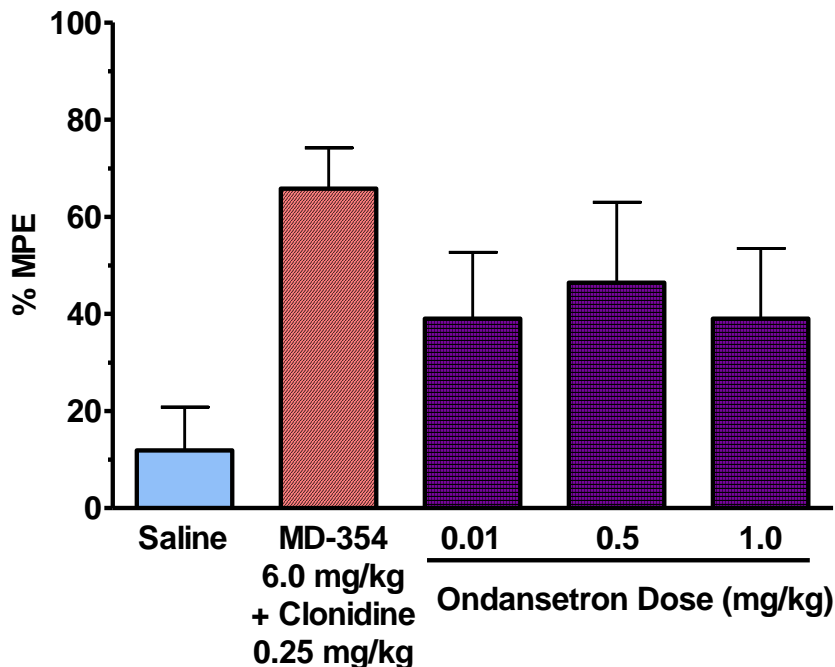


**Figure 21.** Effect ( $\pm$  S.E.M.) of ondansetron (**23**; 0.01-1.0 mg/kg, s.c.) on the antinociceptive action of the MD-354 (**21**; 6.0 mg/kg, s.c.)/clonidine (**7**; 0.25 mg/kg, s.c.) combination in the mouse tail-flick assay ( $n = 8-19$  mice/treatment). No significant difference ( $P > 0.05$ ) compared to the control group [MD-354/clonidine (**21/7**) combination] was detected; one-way ANOVA ( $F_{3,39} = 1.381$ ) followed by Dunnett's post hoc test.

The results presented in Figure 20 differ from the mechanistic studies using tropisetron (**25**), which indicated a 5-HT<sub>3</sub> receptor agonist mechanism for the potentiating activity of a low dose of MD-354 (**21**; 1.0 mg/kg) in combination with an “inactive” dose of clonidine (**7**; 0.25 mg/kg) depicted by Peak A.<sup>34</sup> However, ondansetron's (**23**) failure to attenuate the effect (Figure 21) of the high-dose combination [depicted by Peak B; MD-354 (**21**; 6.0 mg/kg) + clonidine (**7**; 0.25 mg/kg)] is similar to the mechanistic studies with zacopride (**24**) and tropisetron (**25**).<sup>29,33</sup>

## 2. *meta*-Chlorophenylbiguanide (20; *m*CPBG)

### a) Tail-flick assay

In the present study, the more established 5-HT<sub>3</sub> receptor agonist *m*CPBG (20) was evaluated alone and in combination with clonidine (7) to examine its possible potentiation of clonidine (7)-induced analgesia. After comparing antinociceptive effects produced by *m*CPBG (20) with a 20- and 45-min pre-injection time, it was determined that 45 min was optimal (Figure 22). Nevertheless, as illustrated by the dose-response curves, *m*CPBG (20; 0.3-10 mg/kg, s.c.) failed to produce significant antinociception (% MPE < 36) when administered alone (Figure 22).

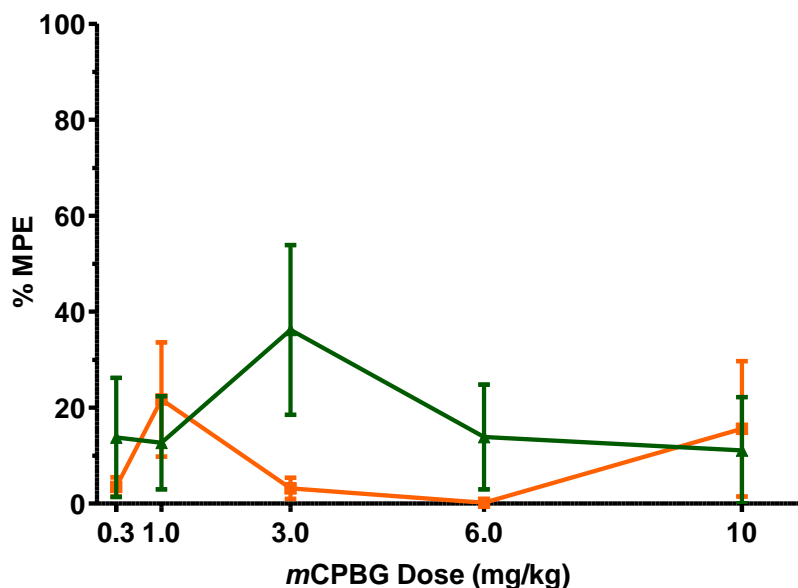
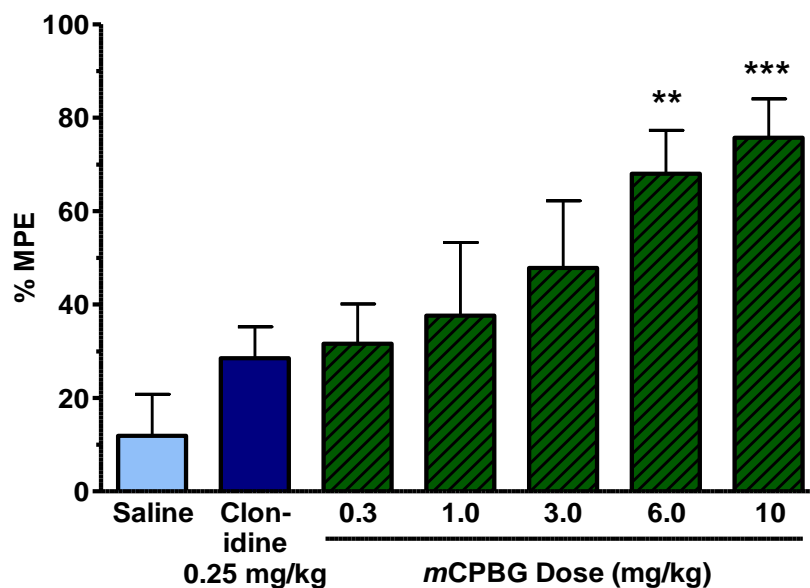


**Figure 22.** Antinociceptive effect ( $\pm$  S.E.M.) of *m*CPBG [20; 0.3-10 mg/kg, s.c., 20-min (orange squares) or 45-min (green triangles) pre-injection times] in the mouse tail-flick assay ( $n = 7-9$  mice/treatment). No significant difference ( $P > 0.05$ ) compared to the control group (saline) was detected; one-way ANOVA ( $F_{5,41} = 1.079$  and  $F_{5,44} = 0.6228$ , respectively) followed by Dunnett's post hoc test. Saline data not shown.

*m*CPBG (**20**; 0.3-10 mg/kg, s.c.), although inactive when administered alone, potentiated an “inactive” dose of clonidine (**7**; 0.25mg/kg, s.c.) dose-dependently in the mouse tail-flick assay ( $ED_{50} = 1.6 \pm 0.14$  mg/kg; Figure 23a). In fact, the potentiating effect observed by the *m*CPBG/clonidine (**20/7**) combination persisted for at least 120 min (Figure 23b).

Since *m*CPBG (**20**) was found to potentiate the antinociceptive effect of an “inactive” dose of clonidine (**7**; Figure 23), the effect of 5-HT<sub>3</sub> receptor and  $\alpha_2$ -AR antagonists on the effect of *m*CPBG (**20**)/clonidine (**7**) was examined.<sup>149</sup> Ondansetron (**23**), which has been used clinically to treat chemotherapy-induced nausea and vomiting, is a 5-HT<sub>3</sub> receptor antagonist. When ondansetron (**23**; 0.00001-2.0 mg/kg) was co-administered with the *m*CPBG/clonidine (**20/7**) combination, neither attenuation nor potentiation was observed in comparison to the effect produced by *m*CPBG (**20**; 6.0 mg/kg) and clonidine (**7**; 0.25 mg/kg) in the tail-flick assay (Figure 24).

(a)



(b)

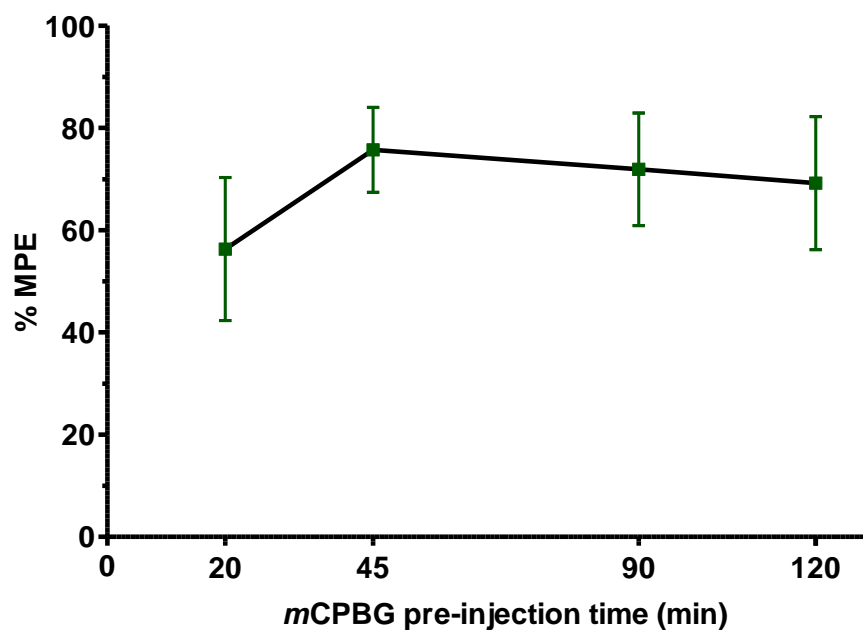


**Figure 23.** (a) Antinociceptive effect ( $\pm$  S.E.M.) of *mCPBG* (**20**; 0.3-10 mg/kg, s.c., 45-min pre-injection time) in combination with clonidine (**7**; 0.25 mg/kg, s.c.) in the mouse tail-flick assay ( $n = 8-24$  mice/treatment). Asterisks denote a significant difference compared to the control group (0.25 mg/kg dose of clonidine; **7**); \*\* $P < 0.01$ , \*\*\* $P < 0.001$ , one-way ANOVA ( $F_{5,88} = 5.002$ ) followed by Dunnett's post hoc test. (b) Antinociceptive effect ( $\pm$  S.E.M.) of *mCPBG* (**20**; 10 mg/kg) in combination with clonidine (**7**; 0.25 mg/kg) at variable *mCPBG* (**20**) pre-injection times (20-120 min) in the mouse tail-flick assay ( $n = 8-17$  mice/treatment).



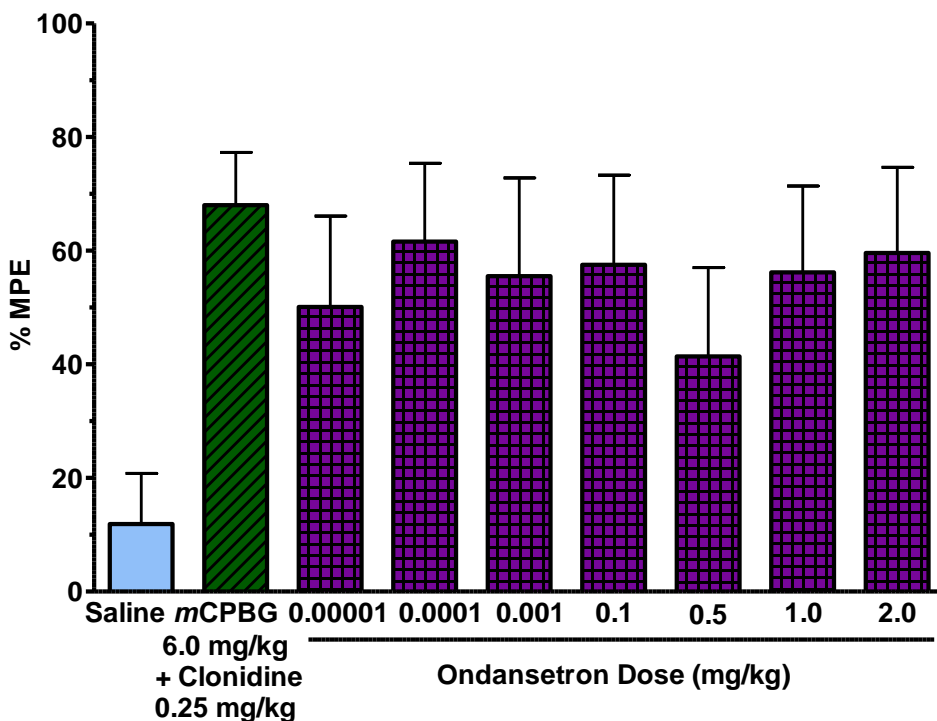


**Figure 24.** Effect ( $\pm$  S.E.M.) of ondansetron (**23**; 0.00001-2.0 mg/kg, s.c.) on the antinociceptive action of the *m*CPBG (**20**; 6.0 mg/kg, s.c.)/clonidine (**7**; 0.25 mg/kg, s.c.) combination in the mouse tail-flick assay ( $n = 8-16$  mice/treatment). No significant difference ( $P > 0.05$ ) compared to the control group [*m*CPBG/clonidine (**20/7**) combination] was detected; one-way ANOVA ( $F_{7,66} = 0.3224$ ) followed by Dunnett's post hoc test.

The second 5-HT<sub>3</sub> receptor antagonist examined was tropisetron (**25**) because previously reported studies have shown opposing effects among 5-HT<sub>3</sub> receptor antagonists [e.g., ondansetron (**23**) and tropisetron (**25**)].<sup>115</sup> Although tropisetron (**25**; 0.0000001-1.0 mg/kg, s.c.) showed no effect when administered alone (% MPE < 10; data not shown), tropisetron (**25**; 0.00001-0.1 mg/kg) attenuated the antinociceptive effect of the *m*CPBG/clonidine (**20/7**) combination as illustrated by a U-shaped dose-response curve (Figure 25).<sup>29,150</sup> The results indicate that a 0.0001 mg/kg dose of

tropisetron (**25**) significantly blocked the potentiating effect of clonidine (**7**) by *m*CPBG (**20**; Figure 25).

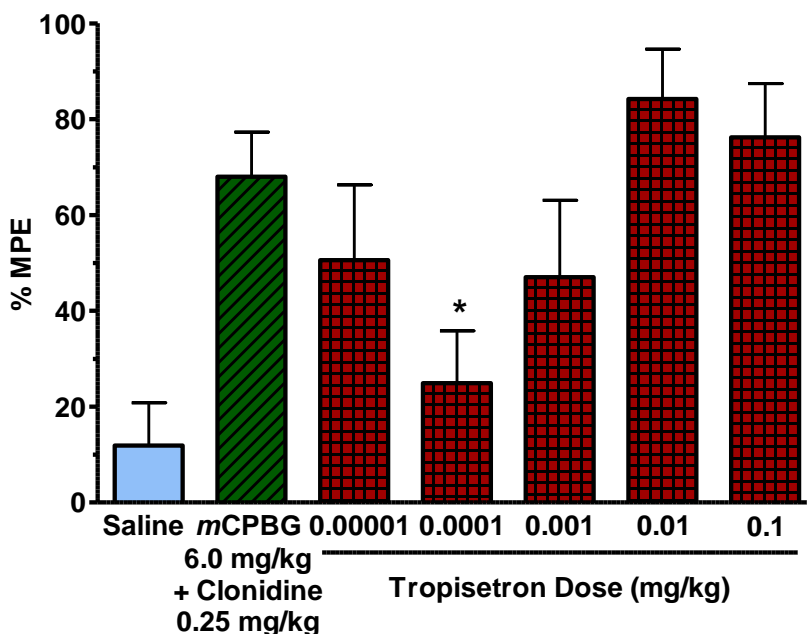


**Figure 25.** Effect ( $\pm$  S.E.M.) of tropisetron (**25**; 0.00001-0.1 mg/kg, s.c.) on the antinociceptive action of the *m*CPBG (**20**; 6.0 mg/kg, s.c.)/clonidine (**7**; 0.25 mg/kg, s.c.) combination in the mouse tail-flick assay ( $n = 8-16$  mice/treatment). Asterisks denote a significant difference compared to the control group [*m*CPBG/clonidine (**20/7**) combination]; \* $P < 0.05$ , one-way ANOVA ( $F_{5,50} = 2.866$ ) followed by Dunnett's post hoc test.

Since tropisetron (**25**) studies indicated involvement of a 5-HT<sub>3</sub> receptor mechanism, the quaternized analog of tropisetron (tropisetron methiodide) was examined in combination studies. Tropisetron methiodide behaves as a 5-HT<sub>3</sub> receptor antagonist, but does not readily cross the BBB.<sup>116</sup> As a result, the analyses of tropisetron (**25**) and tropisetron methiodide not only examine the receptor mechanism, but also can support or refute a centrally-mediated effect. In other words, tropisetron

methiodide acts as a control because it will only produce peripheral effects (if any). Tropisetron methiodide (0.00001-0.1 mg/kg) did not alter the antinociception produced by the combination in the mouse tail-flick assay (Figure 26).

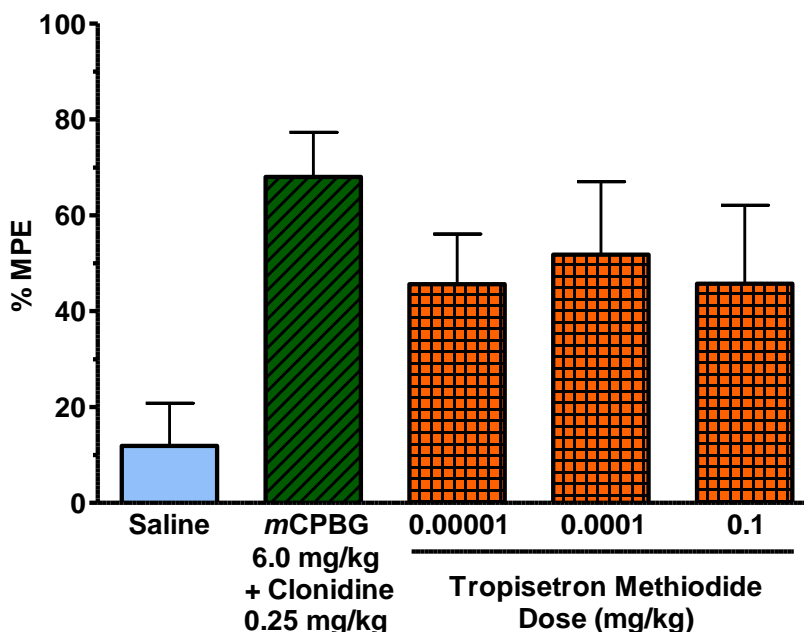


**Figure 26.** Effect ( $\pm$  S.E.M.) of tropisetron methiodide (0.00001-0.1 mg/kg, s.c.) on the antinociceptive action of the *m*CPBG (**20**; 6.0 mg/kg, s.c.)/clonidine (**7**; 0.25 mg/kg, s.c.) combination in the mouse tail-flick assay ( $n = 8-17$  mice/treatment). No significant difference ( $P > 0.05$ ) compared to the control group [*m*CPBG/clonidine (**20/7**) combination] was detected; one-way ANOVA ( $F_{3,45} = 0.9382$ ) followed by Dunnett's post hoc test.

And finally, to determine if there is an  $\alpha_2$ -AR component associated with the potentiation of clonidine (**7**) by *m*CPBG (**20**; Figure 23), the non-selective  $\alpha_2$ -AR antagonist yohimbine (**11**) was examined. When administered alone, yohimbine (**11**; 0.1-1.0 mg/kg, s.c.) produced saline-like effects in the mouse tail-flick assay (% MPE < 1).<sup>31,150</sup>

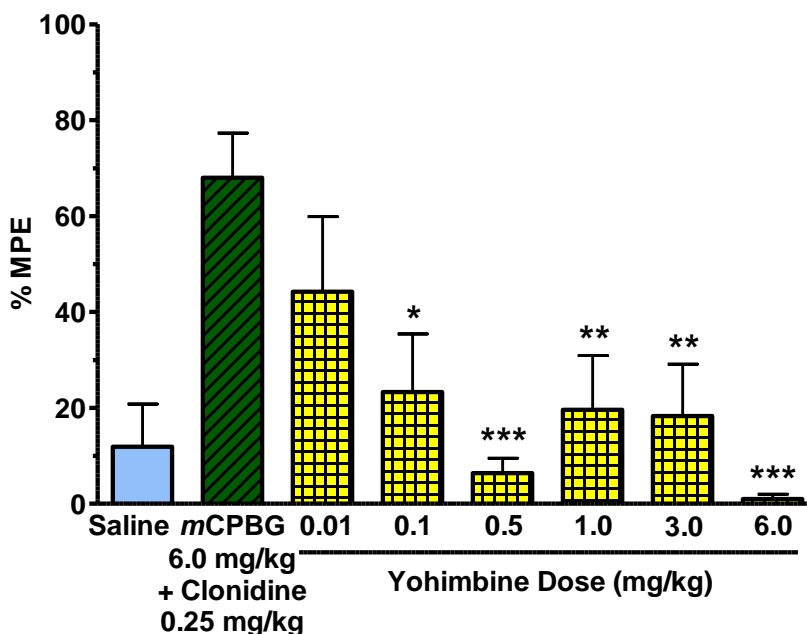


**Figure 27.** Effect ( $\pm$  S.E.M.) of  $\alpha_2$ -AR antagonist yohimbine (**11**; 0.01-6.0 mg/kg, s.c.) on the antinociceptive action of the *m*CPBG (**20**; 6.0 mg/kg, s.c.) and clonidine (**7**; 0.25 mg/kg, s.c.) combination in the mouse tail-flick assay ( $n = 8-16$  mice/treatment). Asterisks denote a significant difference compared to the control group [*m*CPBG/clonidine (**20/7**) combination]; \* $P < 0.05$ , \*\* $P < 0.01$ , \*\*\* $P < 0.001$ , one-way ANOVA ( $F_{6,62} = 6.525$ ) followed by Dunnett's post hoc test.

Yohimbine (**11**; 0.01-6.0 mg/kg), however, attenuated the potentiating effect of the *m*CPBG/clonidine (**20/7**) combination in a dose-dependent manner in the mouse tail-flick assay ( $AD_{50} = 0.04$  mg/kg, 95% CL = 0.006-0.2 mg/kg; Figure 27).

### b) Hot-plate assay

Before any combination studies were conducted, the antinociceptive effect of the agents when administered alone was examined in the mouse hot-plate assay. In prior hot-plate studies, clonidine (**7**) displayed reduced analgesic potency ( $ED_{50} = 0.9$  mg/kg; Figure 18) in comparison to the tail-flick assay ( $ED_{50} = 0.4$  mg/kg; Figure 17). And

similar to the tail-flick results (Figure 22), *m*CPBG (**20**; 0.3-10 mg/kg) failed to produce any significant analgesic effects in the hot-plate assay (% MPE = 3-14; Figure 28).

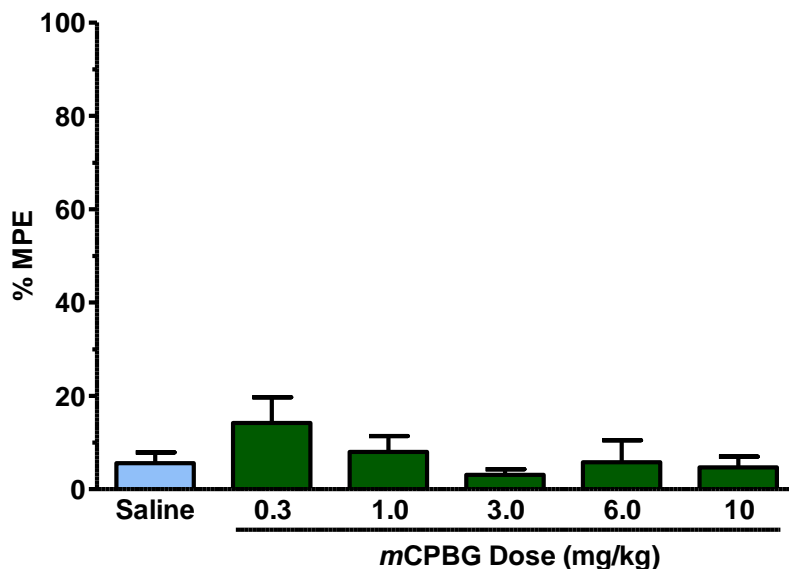


**Figure 28.** Antinociceptive effect ( $\pm$  S.E.M.) of *m*CPBG (**20**; 0.3-10 mg/kg, s.c.) in the mouse hot-plate assay ( $n = 8$  mice/treatment). No significant difference ( $P > 0.05$ ) compared to the control group (saline) was detected; one-way ANOVA ( $F_{5,42} = 1.212$ ) followed by Dunnett's post hoc test.

In the present investigation, clonidine (**7**; 1.0 mg/kg dose, which approximately equals the calculated  $ED_{50}$  dose, and which produced about 50% MPE) was co-administered with *m*CPBG (**20**; 0.3-10 mg/kg, s.c.). And while 0.3-1.0 mg/kg doses of *m*CPBG (**20**) only slightly attenuated (% MPE = 27-32;  $P > 0.05$ ) the antinociceptive effect of clonidine (**7**), significant attenuation (% MPE =  $13.5 \pm 4.9$ ;  $P < 0.01$ ) was observed when 3.0 mg/kg of *m*CPBG (**20**) was co-administered (Figure 29).

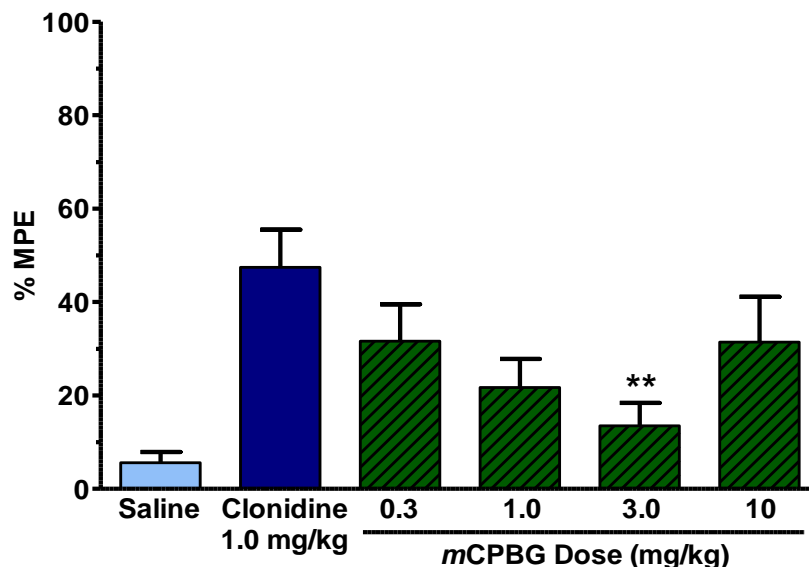


**Figure 29.** Antinociceptive effect ( $\pm$  S.E.M.) of *mCPBG* (**20**; 0.3-10 mg/kg, s.c.) in combination with clonidine (**7**; 1.0 mg/kg, s.c.) in the mouse hot-plate assay ( $n = 8-10$  mice/treatment). Asterisks denote a significant difference compared to the control group (1.0 mg/kg dose of clonidine; **7**); \*\* $P < 0.01$ , one-way ANOVA ( $F_{4,45} = 2.844$ ) followed by Dunnett's post hoc test.

The attenuating effect of clonidine (**7**)-induced antinociception by *mCPBG* (**20**; 0.3-3.0 mg/kg) seemed to be dose-dependent ( $AD_{50} = 0.8$  mg/kg, 95% CL = 0.25-2.6 mg/kg). However, a higher dose of *mCPBG* [(**20**): 10 mg/kg] only slightly antagonized ( $P > 0.05$ ) the effect [i.e., the effect produced by clonidine (**7**; 1.0 mg/kg) alone was not significantly different than that of the co-administration of *mCPBG* (**20**; 10 mg/kg) and clonidine (**7**; 1.0 mg/kg); Figure 29]. It is important to note, there was a rather large standard error in this combination (% MPE =  $31.4 \pm 9.7$ ; Figure 29).

### c) Locomotor activity assay

Analgesic actions were observed when *m*CPBG (**20**) was co-administered with clonidine (**7**; 0.25 mg/kg dose) in the mouse tail-flick assay (Figure 23a). It was necessary to determine if this antinociceptive potentiation was a selective potentiation. In other words, does *m*CPBG (**20**) only potentiate the analgesic actions of clonidine (**7**) and not its sedative properties? Also, because clonidine (**7**) has already been reported to display hypolocomotor effects, the dose used in the tail-flick assay [0.25 mg/kg clonidine (**7**)] should be evaluated in the same species (male ICR mice) and should be used as a control for the combination treatment group.<sup>29</sup> A low dose of clonidine (**7**; 0.25 mg/kg), which showed no analgesic effects in the tail-flick and hot-plate assays, produced hypolocomotor actions (Figure 19).

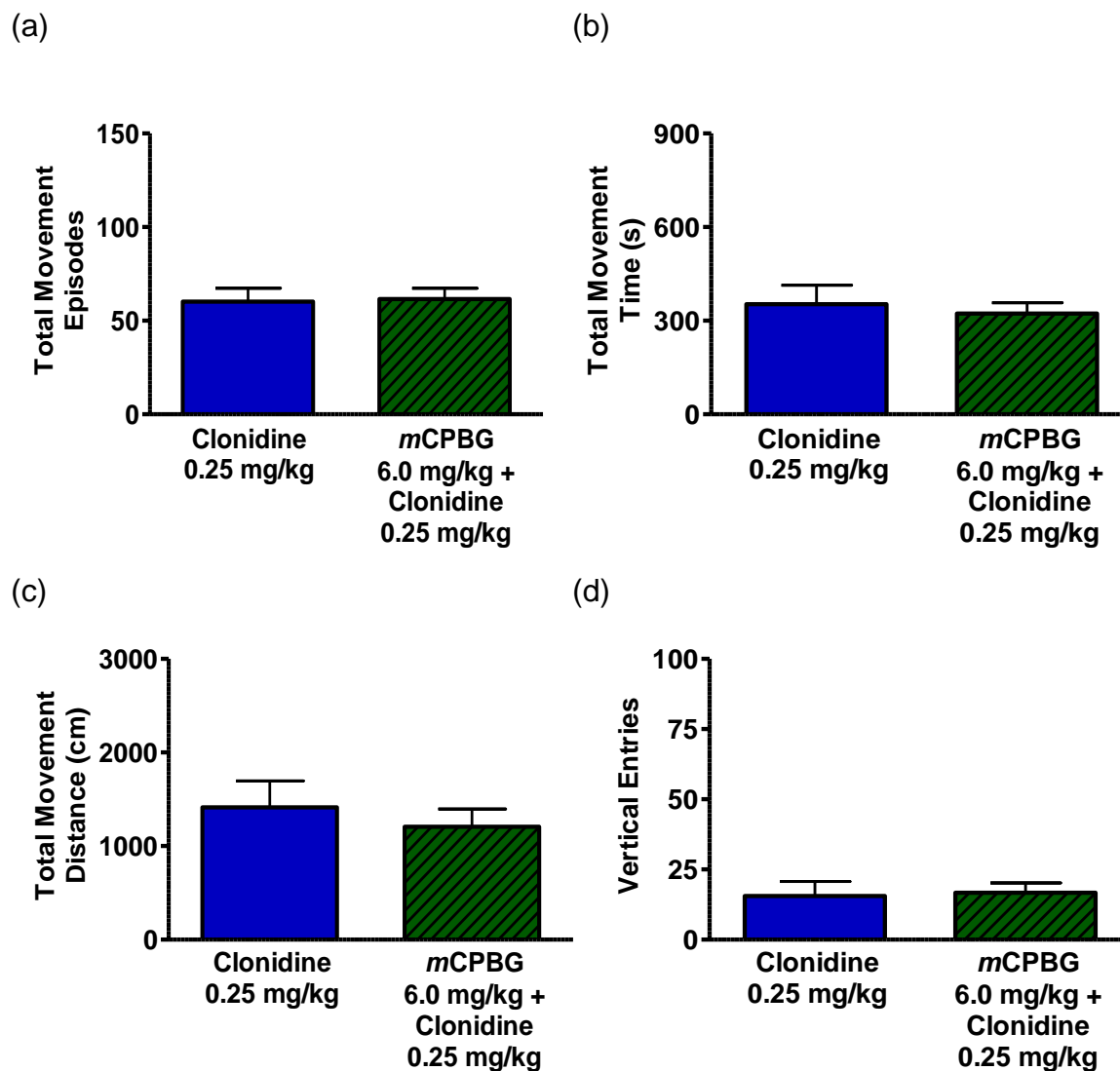


**Figure 30.** Effect ( $\pm$  S.E.M.) of the co-administration of *m*CPBG (**20**; 6.0 mg/kg, s.c., pre-injection time: 30 min) and clonidine (**7**; 0.25 mg/kg, s.c., pre-injection time: 5 min) on (a) total movement episodes, (b) total movement time, (c) total movement distance, and (d) vertical entries with a 15-min recording time in the mouse locomotor activity assay ( $n = 10$  mice/treatment). No significant difference ( $P > 0.05$ ) compared to the control group [clonidine (**7**) 0.25 mg/kg] was detected; Student's t-test.

The doses selected for the locomotor activity combination studies [6.0 mg/kg *m*CPBG (**20**) + 0.25 mg/kg clonidine (**7**)] were those that produced a statistically



significant increase in antinociceptive effects (% MPE =  $68.0 \pm 9.3$ ;  $P < 0.01$ ) in the tail-flick assay (Figure 23a). As illustrated in Figure 30, *m*CPBG (**20**; 6.0 mg/kg) did not alter the locomotor effects of clonidine (**7**; 0.25 mg/kg) in any of the four parameters measured ( $P > 0.05$ ).

#### d) Summary

The antinociceptive effects of the more established and selective 5-HT<sub>3</sub> receptor agonist *m*CPBG (**20**) administered alone and combination with an “inactive” dose of clonidine (**7**) was examined in the mouse tail-flick assay because a structurally similar agent, MD-354 (**21**), has been shown to potentiate the analgesic actions of clonidine (**7**) in a biphasic manner (Figure 12).<sup>34</sup> Previous mechanistic studies suggested that the first potentiation peak (Peak A in Figure 12), which is produced by a low dose of MD-354 (**21**; 1.0 mg/kg) and clonidine (**7**; 0.25 mg/kg) is, at least in part, due to a 5-HT<sub>3</sub> receptor agonist mechanism and involvement of an  $\alpha_2$ -AR mechanism.<sup>34</sup> To date, it is unclear which  $\alpha_2$ -AR subtype is involved.<sup>34</sup> As for the mechanism of action underlying Peak B [6.0 mg/kg MD-354 (**21**) + 0.25 mg/kg clonidine (**7**)], 5-HT<sub>3</sub> receptor antagonism and  $\alpha_2$ -AR involvement seems to play a role.<sup>29,31</sup>

In the present investigation, similar to results obtained with MD-354 (**21**), *m*CPBG (**20**; 0.3-10 mg/kg) displayed no antinociceptive effects when administered alone (Figure 22), but potentiated the analgesic actions of an “inactive” dose of clonidine (**7**; 0.25 mg/kg) in the mouse tail-flick assay (Figure 23a). In fact, this potentiation was observed over the course of 2 hours (Figure 23b). On the other hand,

unlike the biphasic curve observed with the co-administration of MD-354 (**21**) and clonidine (**7**; 0.25 mg/kg), the dose-response curve illustrating the potentiation by *m*CPBG (**20**) was monophasic (Figures 12 and 21a).

In the second nociceptive animal model (hot-plate assay), *m*CPBG (**20**; 0.3-10 mg/kg) also showed no analgesic effects when administered alone (Figure 28), but contrary to the tail-flick assay, *m*CPBG (**20**) dose-dependently attenuated clonidine's (**7**; 1.0 mg/kg) effect (Figure 29). Although it was found to be statistically insignificant, antagonistic behavior was also observed when MD-354 (**21**) was co-administered with clonidine (**7**) in the mouse hot-plate assay.<sup>33</sup>

And lastly, locomotor effects were evaluated in the analgesia producing combination [6.0 mg/kg *m*CPBG (**20**) + 0.25 mg/kg clonidine (**7**); tail-flick assay]. The results indicated that even though *m*CPBG (**20**) potentiated the antinociceptive effects of a low dose of clonidine (**7**) in the mouse tail-flick assay, it did not alter clonidine's (**7**) locomotor properties (Figure 30).

### **3. SR57227A (22)**

#### **a) Tail-flick assay**

Thus far, MD-354 (**21**) and *m*CPBG (**20**) have been examined in combination studies with clonidine (**7**), and analgesic potentiation of an “inactive” dose of clonidine (**7**) was observed with both of these agents. Mechanistically, this potentiation effect seemed to be, at least in part, due to a 5-HT<sub>3</sub> receptor action. There is question as to

whether MD-354 (**21**) and *m*CPBG (**20**) penetrate the mouse BBB. In contrast, SR57227A (**22**) has been demonstrated to be brain penetrant. Therefore, the analgesic properties of the centrally-acting 5-HT<sub>3</sub> receptor agonist SR57227A (**22**) was examined both alone and in combination with clonidine (**7**). If potentiation is observed when SR57227A (**22**) is co-administered with clonidine (**7**), then mechanistic studies involving 5-HT<sub>3</sub> receptor antagonists will be conducted.

In the tail-flick assay, SR57227A (**22**; 0.3-10 mg/kg) showed saline-like effects (i.e., the antinociceptive effect produced by SR57227A (**22**) was not statistically different than saline; Figure 31). At the highest dose (30 mg/kg) evaluated, SR57227A (**22**) produced an increase in antinociception and even though there was a relatively large standard error, statistical analysis (one-way ANOVA followed by Dunnett's post hoc test) verified a difference between the treatment and control group ( $P < 0.05$ ; Figure 31).

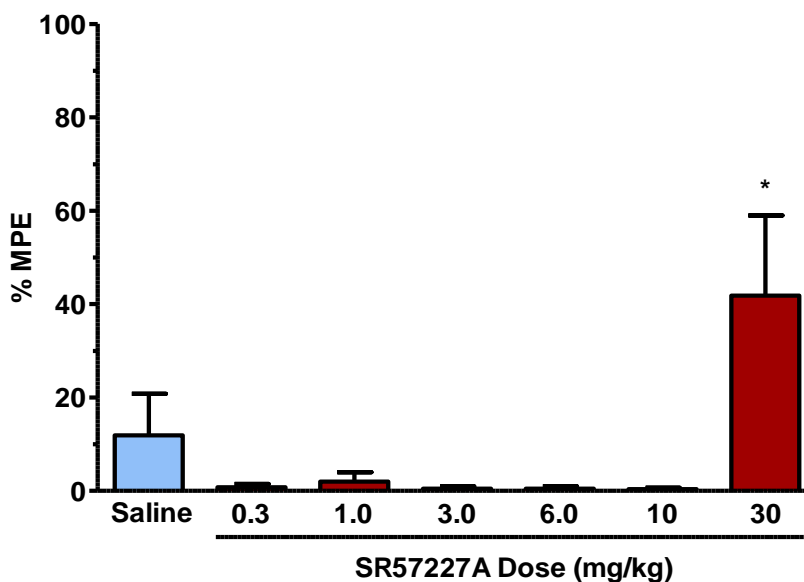


**Figure 31.** Antinociceptive effect ( $\pm$  S.E.M.) of SR57227A (**22**; 0.3-30 mg/kg, s.c.) in the mouse tail-flick assay ( $n = 8$  mice/treatment). Asterisks denote a significant difference compared to the control group (saline);  $*P < 0.05$ , one-way ANOVA ( $F_{6,49} = 4.344$ ) followed by Dunnett's post hoc test.

Tail-flick latency, which is the time delay between the onset of intense light and the tail-flick response, is a second way of measuring tail-flick results. When the results from SR57227A (**22**) administered alone were analyzed in this way, there was no significant difference between the high dose of SR57227A (**22**; 30 mg/kg) and saline in the Dunnett's post hoc test ( $P > 0.05$ ) but, interestingly, it was determined as being significantly different in the Newman-Keuls multiple comparison test ( $P < 0.05$ ; Figure 32).

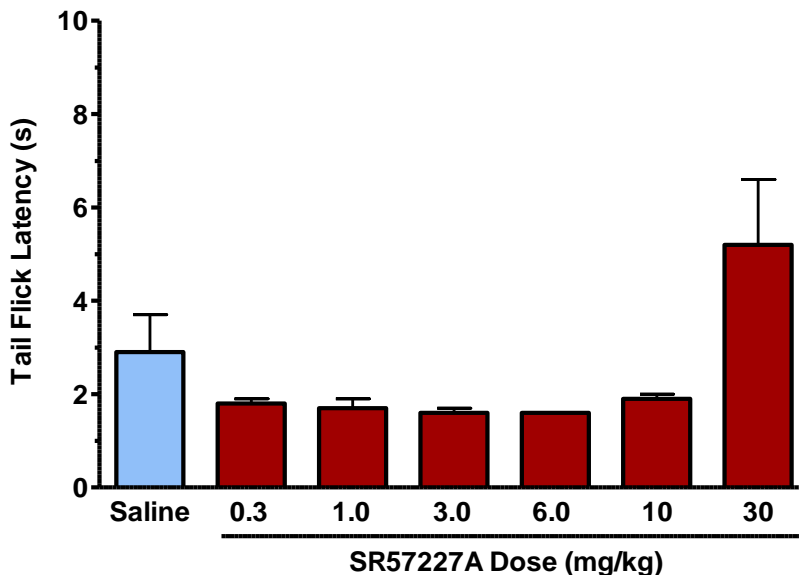


**Figure 32.** Antinociceptive effect ( $\pm$  S.E.M.) of SR57227A (**22**; 0.3-30 mg/kg, s.c.) in the mouse tail-flick assay ( $n = 8$  mice/treatment). No significant difference ( $P > 0.05$ ) compared to the control group (saline) was detected; one-way ANOVA ( $F_{6,49} = 4.574$ ) followed by Dunnett's post hoc test.

Although not significantly different from saline, lower doses of SR57227A (**22**; 0.3-10 mg/kg) showed reduced tail-flick latency (Figures 31 and 32). Therefore, hyperalgesia was examined in a modified tail-flick assay (radiant heat was adjusted so

that pre-treatment tail-flick latencies were 5-7 s). Dose-dependent hyperalgesic effects were observed in the SR57227A (**22**; 1.0-10 mg/kg)-treated mice (Figure 33).

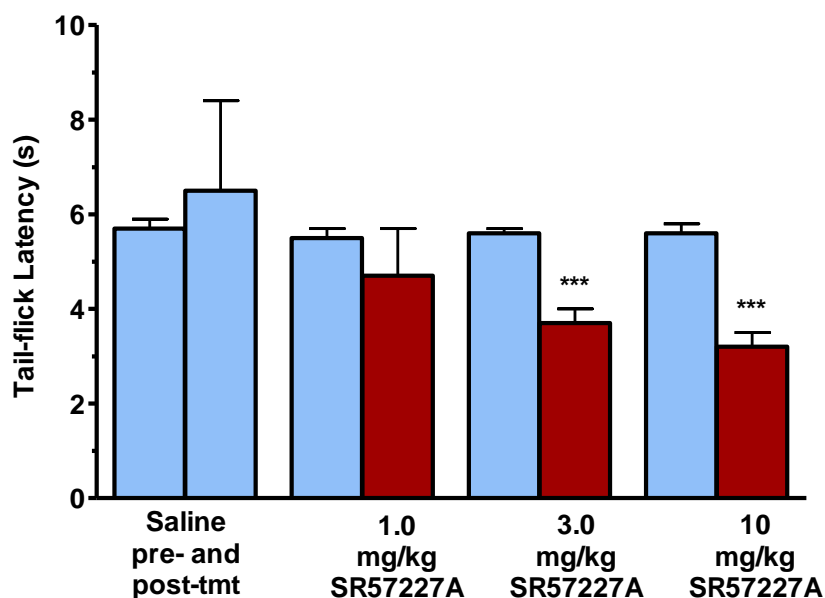


**Figure 33.** Hyperalgesic effect ( $\pm$  S.E.M.) of SR57227A (**22**; 1.0-10 mg/kg, s.c.) in the modified mouse tail-flick assay ( $n = 6-8$  mice/treatment). For each treatment group, bars on the left depict the pre-treatment tail-flick latency. Asterisks denote a significant difference compared to the control group (pre-treatment tail-flick latency); \*\*\* $P < 0.001$ , Student's t-test.

Because MD-354 (**21**) and *m*CPBG (**20**) both potentiated the antinociceptive actions of an “inactive” dose of clonidine (**7**; 0.25 mg/kg), this same dose of clonidine (**7**) was co-administered with the selective 5-HT<sub>3</sub> receptor agonist SR57227A (**22**). In the mouse tail-flick assay, SR57227A (**22**; 0.3-10 mg/kg, s.c.) did not alter the analgesic properties of a saline-like dose of clonidine (**7**; Figure 34).

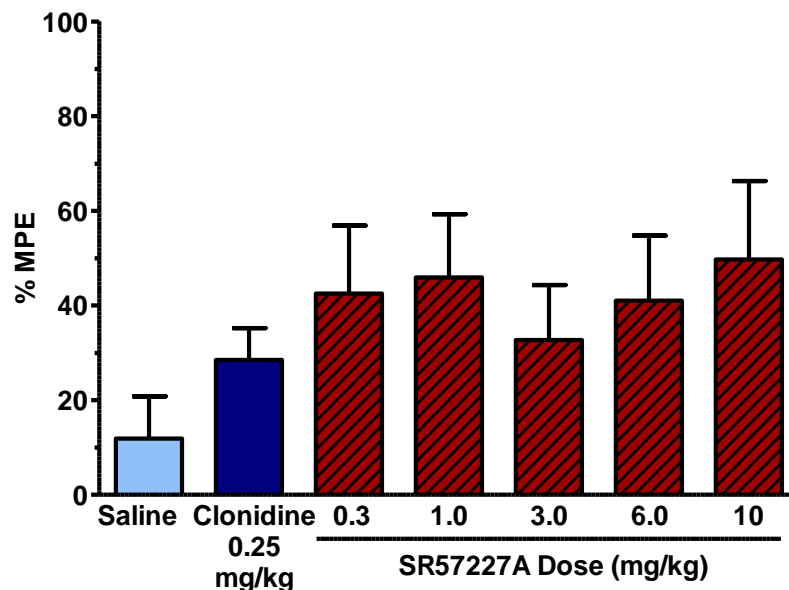


**Figure 34.** Antinociceptive effect ( $\pm$  S.E.M.) of SR57227A (**22**; 0.3-10 mg/kg, s.c.) in combination with clonidine (**7**; 0.25 mg/kg, s.c.) in the mouse tail-flick assay ( $n = 8-24$  mice/treatment). No significant difference ( $P > 0.05$ ) compared to the control group [0.25 mg/kg dose of clonidine (**7**)] was detected; one-way ANOVA ( $F_{5,58} = 0.6047$ ) followed by Dunnett's post hoc test.

Since no potentiation was observed in the previous combination, a higher, more effective dose of clonidine (**7**; calculated  $ED_{50} = 0.5$  mg/kg) was selected to determine if SR57227A (**22**) blocks the antinociceptive effect of clonidine (**7**; Figure 35).

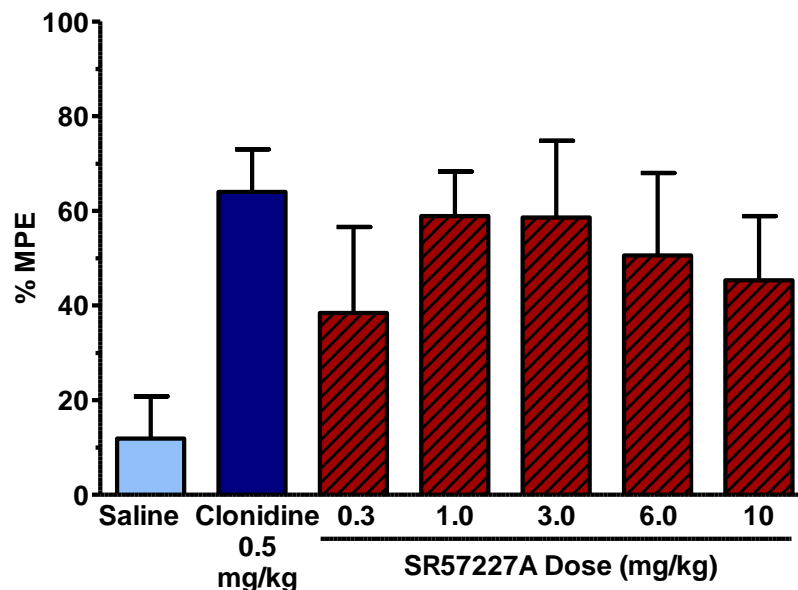


**Figure 35.** Antinociceptive effect ( $\pm$  S.E.M.) of SR57227A (**22**; 0.3-10 mg/kg, s.c.) in combination with clonidine (**7**; 0.5 mg/kg, s.c.) in the mouse tail-flick assay ( $n = 8-24$  mice/treatment). No significant difference ( $P > 0.05$ ) compared to the control group [0.5 mg/kg dose of clonidine (**7**)] was detected; one-way ANOVA ( $F_{5,66} = 0.4993$ ) followed by Dunnett's post hoc test.

Similar to Figure 34, this combination [0.3-10 mg/kg doses of SR57227A (**22**) + 0.5 mg/kg dose of clonidine (**7**)] produced clonidine (**7**)-like effects (Figure 35). That is, the antinociceptive effects of clonidine (**7**) were neither potentiated nor attenuated by SR57227A (**22**).

### b) Hot-plate assay

In the hot-plate assay, s.c. administration of SR57227A (**22**; 0.3-10 mg/kg) produced no antinociception (compared to saline control) but, just as before (i.e., similar to the tail-flick assay results), a higher dose (30 mg/kg) produced analgesic actions

(Figure 36). This high dose of SR57227A (**22**; 30 mg/kg) was significantly different than the saline control ( $P < 0.001$ ; Figure 36).

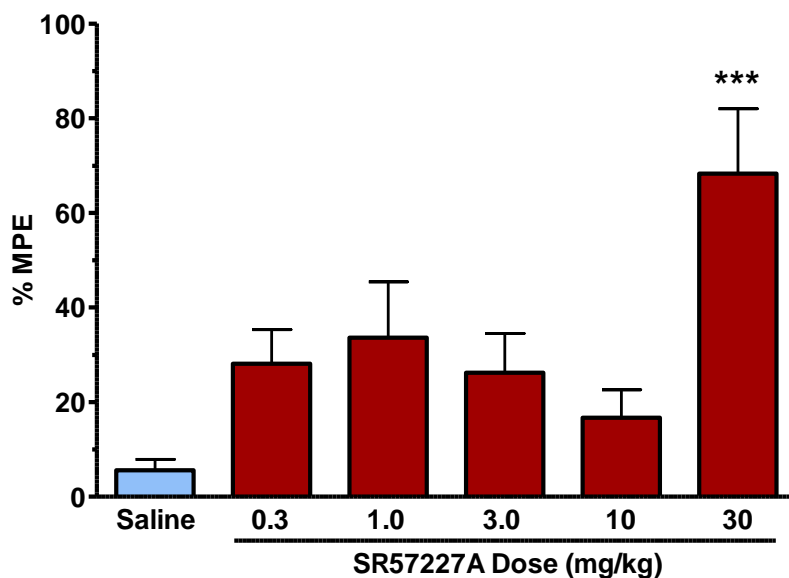


**Figure 36.** Antinociceptive effect ( $\pm$  S.E.M.) of SR57227A (**22**; 0.3-30 mg/kg, s.c.) in the mouse hot-plate assay ( $n = 8-9$  mice/treatment). Asterisks denote a significant difference compared to the control group (saline); \*\*\* $P < 0.001$ , one-way ANOVA ( $F_{5,47} = 5.322$ ) followed by Dunnett's post hoc test.

In combination studies, SR57227A (**22**; 0.3-10 mg/kg) neither potentiated nor attenuated the antinociceptive effect of clonidine (**7**; 1.0 mg/kg; Figure 37).



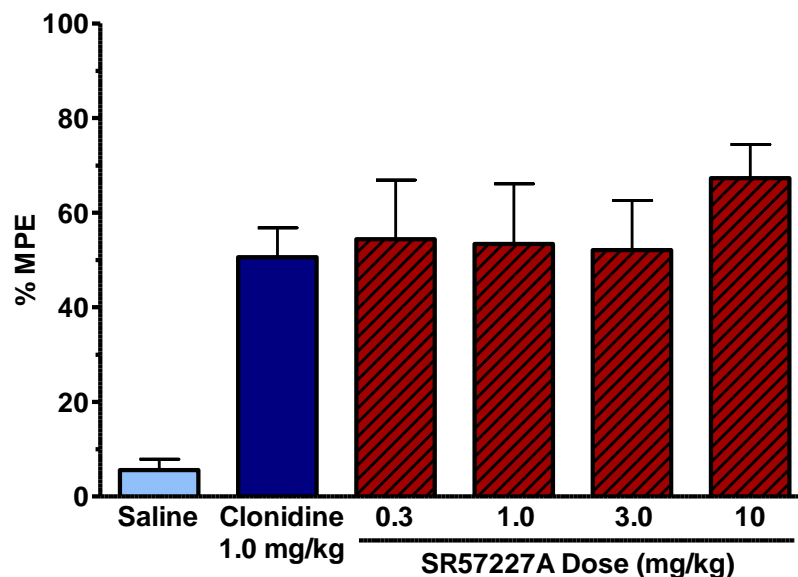


**Figure 37.** Antinociceptive effect ( $\pm$  S.E.M.) of SR57227A (**22**; 0.3-10 mg/kg, s.c.) in combination with clonidine (**7**; 1.0 mg/kg, s.c.) in the mouse hot-plate assay ( $n = 9-20$  mice/treatment). No significant difference ( $P > 0.05$ ) compared to the control group [SR57227A/clonidine (**22/7**) combination] was detected; one-way ANOVA ( $F_{4,53} = 0.4547$ ) followed by Dunnett's post hoc test.

In summary, SR57227A (**22**; 0.3-10 mg/kg) produced no analgesic properties in both examined antinociceptive assays (tail-flick and hot-plate assays) when administered alone and in combination with clonidine (**7**), but a higher dose (30 mg/kg), this 5-HT<sub>3</sub> receptor agonist (**22**) showed augmented antinociceptive effects in the mouse tail-flick and hot-plate assays ( $P < 0.05$  and  $P < 0.001$ , respectively).

### c) Locomotor activity assay

In the mouse locomotor activity assay, a 30 mg/kg dose of SR57227A (**22**; dose that produced antinociceptive effects; Figures 32 and 36) was administered s.c. and compared to a s.c. saline treatment group (Figure 38). Statistical analysis of the

examined locomotor parameters (e.g., total movement episodes, total movement time, total movement distance, and total vertical entries) indicated a significant hypolocomotor action of SR57227A (**22**; 30 mg/kg) in comparison to saline ( $P < 0.01$ ; Figure 38). That is, the only SR57227A (**22**) dose that produced antinociceptive effects in the tail-flick and hot-plate assays, also, produced sedative effects in mice.

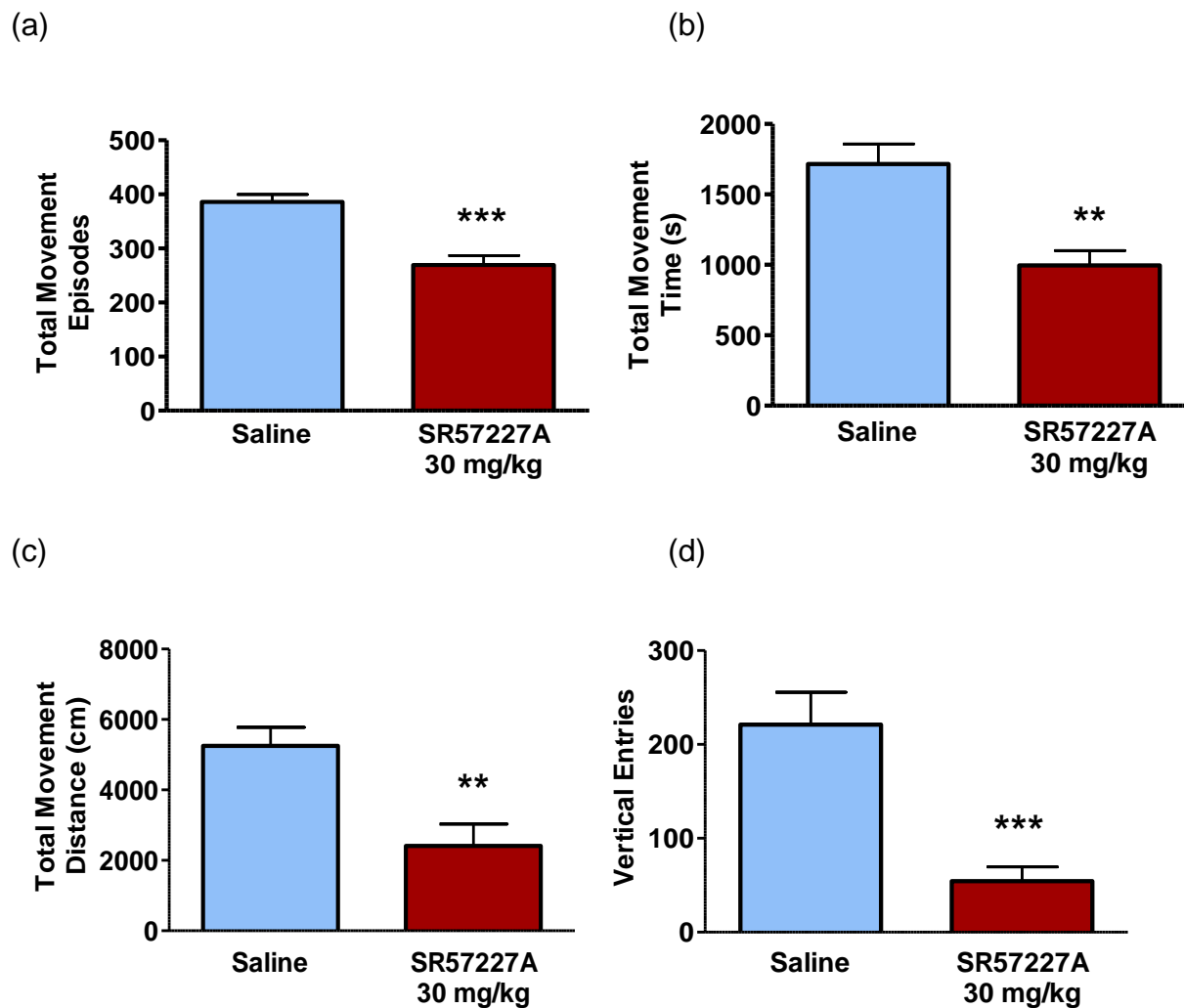


**Figure 38.** Effect ( $\pm$  S.E.M.) of SR57227A (**22**; 30 mg/kg, s.c., pre-injection time: 0 min) on (a) total movement episodes, (b) total movement time, (c) total movement distance, and (d) vertical entries with a 45-min recording time in the mouse locomotor activity assay ( $n = 8$  mice/treatment). Asterisks denote a significant difference compared to the control group (saline); \*\* $P < 0.01$ , \*\*\* $P < 0.001$ , Student's t-test.

Potentialiation of clonidine's (**7**) analgesic properties by SR57227A (**22**) was not observed in either nociceptive animal model (Figures 34, 35 and 37) and therefore, the locomotor activity of the combination was not examined.

#### **d) Summary**

In summary, SR57227A (**22**; 0.3-10 mg/kg, s.c.) produced saline-like effects in both antinociceptive assays ( $P > 0.05$ ; Figures 31 and 34). Conversely, a higher dose (30 mg/kg) of SR57227A (**22**) showed a significant increase in analgesic actions in comparison to saline in the tail-flick and hot-plate assays ( $P < 0.05$  and  $P < 0.001$ , respectively; Figures 31 and 36). However, SR57227A (**22**; 30 mg/kg, s.c.) showed decreased motor activity in all locomotor parameters (movement episodes, movement time, movement distance, and vertical entries) in the mouse locomotor activity assay (Figure 38). Because low doses of SR57227A (**22**; 0.3-10 mg/kg) showed slight analgesic attenuation in the tail-flick assay, a modified tail-flick assay was conducted to detect hyperalgesia. Indeed, SR57227A (**22**) produced hyperalgesic effects ( $P < 0.001$ ) in the modified tail-flick assay (Figure 33).

In the tail-flick combination studies, SR57227A (**22**; 0.3-10 mg/kg, s.c.) neither potentiated nor attenuated the antinociceptive effect of clonidine (**7**; 0.25 or 0.5 mg/kg, s.c.; Figures 34 and 35). Similar to the tail-flick results, SR57227A (**22**; 0.3-10 mg/kg, s.c.) did not alter the antinociception produced by clonidine (**7**; 1.0 mg/kg, s.c.) in the hot-plate assay (Figure 37).

## 4. TDIQ (6)

### a) Tail-flick assay

An  $\alpha_2$ -AR role in the potentiation of clonidine (**7**; 0.25 mg/kg) by MD-354 (**21**) was proposed because previous mechanistic studies showed analgesic attenuation of the MD-354/clonidine (**21/7**) combination by the following  $\alpha_2$ -AR antagonists: yohimbine (**11**; non-selective  $\alpha_2$ -AR antagonist), imiloxan (**12**; preferentially selective  $\alpha_{2B}$ -AR antagonist), and BRL44408 (**15**; preferentially selective  $\alpha_{2A}$ -AR antagonist).<sup>31</sup> Therefore, the  $\alpha_2$ -AR agonist TDIQ (**6**) was selected to further examine the mechanism of action. Although TDIQ (**6**) acts nonselectively at all three subtypes of  $\alpha_2$ -ARs, it is devoid of 5-HT<sub>3</sub> receptor activity.<sup>72</sup>

TDIQ (**6**; 0.3-10 mg/kg), when administered alone in the tail-flick assay, showed no analgesic properties (% MPE = 1-10; Figure 39). However, when TDIQ (**6**; 0.3-3.0 mg/kg) was co-administered with clonidine (**7**; 0.25 mg/kg), potentiation of the antinociceptive effect was observed (ED<sub>50</sub> = 0.6 mg/kg, 95% CL = 0.2-1.3 mg/kg; Figure 40). That is, TDIQ (**6**) potentiated the antinociceptive effect of an “inactive” dose of clonidine (**7**) in a dose-dependent manner (Figure 40).

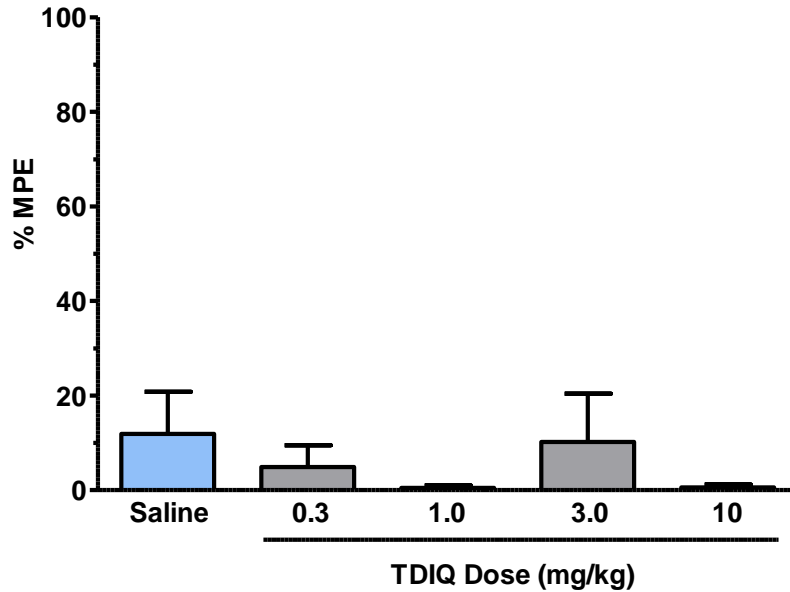


**Figure 39.** Antinociceptive effect ( $\pm$  S.E.M.) of TDIQ (**6**; 0.3-10 mg/kg, s.c.) in the mouse tail-flick assay ( $n = 8$  mice/treatment). No significant difference ( $P > 0.05$ ) compared to the control group (saline) was detected; one-way ANOVA ( $F_{4,35} = 0.6850$ ) followed by Dunnett's post hoc test.

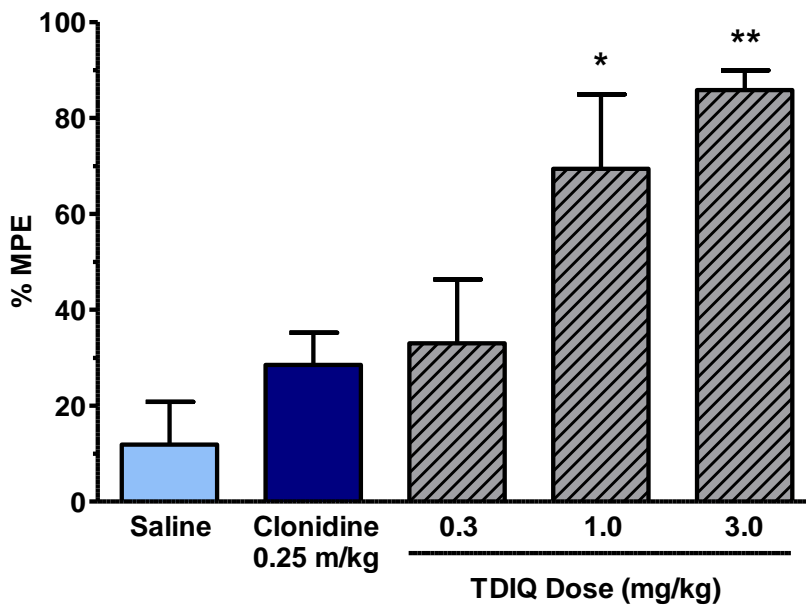


**Figure 40.** Antinociceptive effect ( $\pm$  S.E.M.) of TDIQ (**6**; 0.3-3.0 mg/kg, s.c.) in combination with clonidine (**7**; 0.25 mg/kg, s.c.) in the mouse tail-flick assay ( $n = 8-24$  mice/treatment). Asterisks denote a significant difference compared to the control group (0.25 mg/kg dose of clonidine; **7**); \* $P < 0.05$ , \*\* $P < 0.01$ , one-way ANOVA ( $F_{3,51} = 10.19$ ) followed by Dunnett's post hoc test.

Since 1.0 and 3.0 mg/kg doses of TDIQ (**6**) potentiated the antinociceptive actions of clonidine (**7**; 0.25 mg/kg), TDIQ (**6**) in combination with a lower dose of clonidine (**7**) was investigated. TDIQ (**6**) did not significantly alter the effect of the lower dose (0.1 mg/kg) of clonidine (**7**; Figure 41).

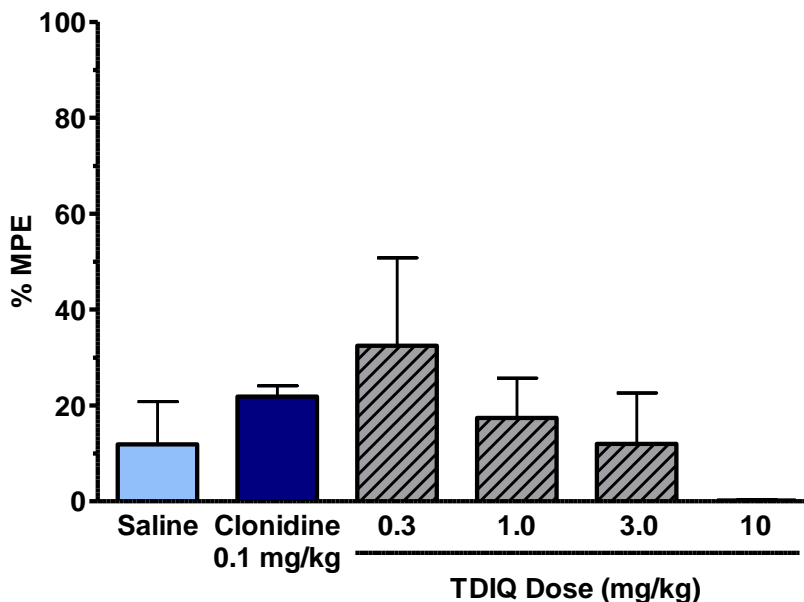


**Figure 41.** Antinociceptive effect ( $\pm$  S.E.M.) of TDIQ (**6**; 0.3-10 mg/kg, s.c.) in combination with clonidine (**7**; 0.1 mg/kg, s.c.) in the mouse tail-flick assay ( $n = 8-16$  mice/treatment). No significant difference ( $P > 0.05$ ) compared to the control group [0.1 mg/kg dose of clonidine (**7**)] was detected; one-way ANOVA ( $F_{4,51} = 1.579$ ) followed by Dunnett's post hoc test.

Since TDIQ (**6**) was found to potentiate the analgesic action of clonidine (**7**; 0.25 mg/kg) in the mouse tail-flick assay (Figure 40), additional combination studies were conducted to investigate the mechanism of action (Figure 40). The following  $\alpha_2$ -AR antagonists were selected for mechanistic studies: BRL44408 (**15**; preferentially selective at  $\alpha_{2A}$ -ARs), imiloxan (**12**; preferentially selective at  $\alpha_{2B}$ -ARs), and ARC-239

(**14**; preferentially selective at  $\alpha_{2B/2C}$ -ARs). All three  $\alpha_2$ -AR antagonists lacked antinociceptive effects when administered alone in the mouse tail-flick assay (% MPE = 0-5).<sup>31,150</sup> When BRL44408 (**15**; 0.03-3.0 mg/kg, s.c.) was co-administered with the combination, attenuation of the antinociceptive effect of the combination [3.0 mg/kg dose of TDIQ (**6**) + 0.25 mg/kg dose of clonidine (**7**)] was observed ( $AD_{50}$  = 0.2 mg/kg, 95% CL = 0.05-0.5 mg/kg; Figure 42).

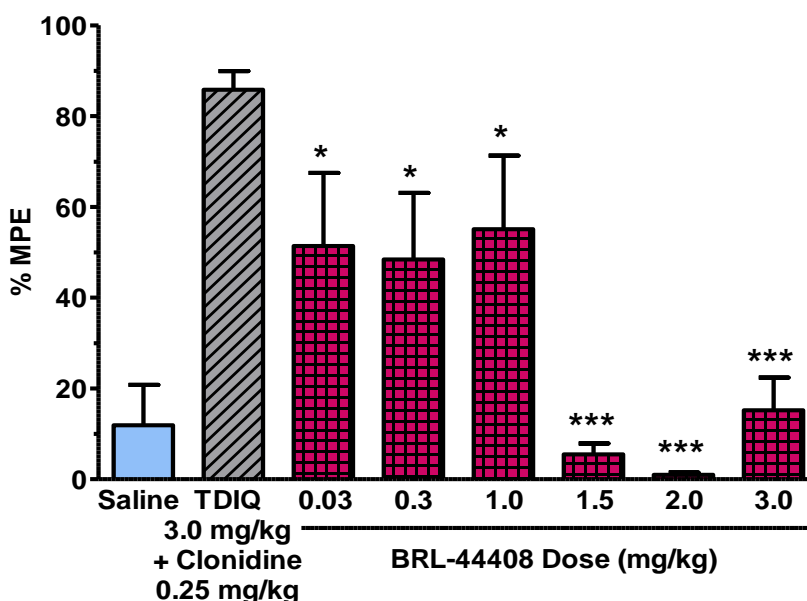


**Figure 42.** Effect ( $\pm$  S.E.M.) of BRL44408 (**15**; 0.03-3.0 mg/kg, s.c.) on the antinociceptive action of the TDIQ (**6**; 3.0 mg/kg, s.c.)/clonidine (**7**; 0.25 mg/kg, s.c.) combination in the mouse tail-flick assay ( $n = 8-15$  mice/treatment). Asterisks denote a significant difference compared to the control group [TDIQ/clonidine (**6/7**) combination]; \* $P < 0.05$ , \*\*\* $P < 0.001$ , one-way ANOVA ( $F_{6,59} = 9.751$ ) followed by Dunnett's post hoc test.

Imiloxan (**12**; 0.1-3.0 mg/kg, s.c.) only attenuated ( $P < 0.05$ ) the analgesic effect of the TDIQ/clonidine (**6/7**) combination at a medium dose (0.3 mg/kg; Figure 43). That is, lower (0.1 mg/kg) and higher (1.0-3.0 mg/kg) doses of imiloxan (**12**) did not alter ( $P >$

0.05) the antinociception produced by the combination [3.0 mg/kg TDIQ (6) + 0.25 mg/kg clonidine (7); Figure 43].

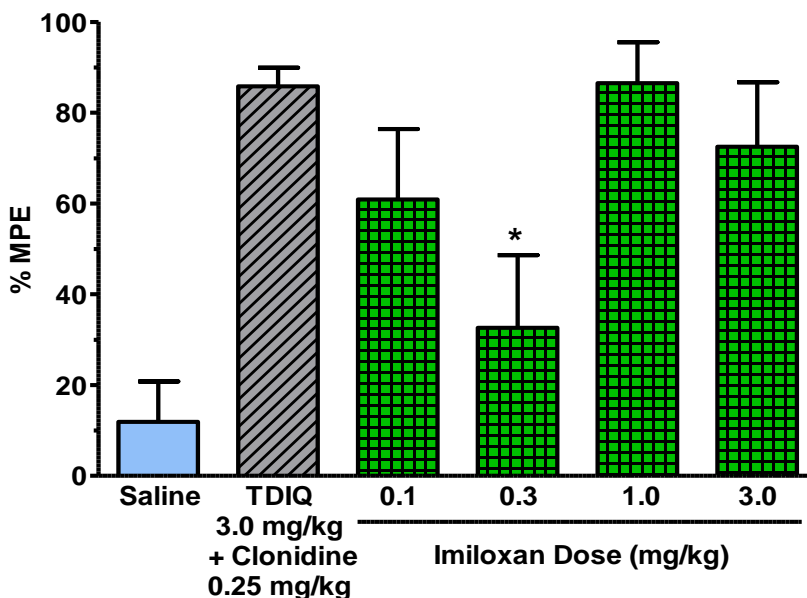


**Figure 43.** Effect ( $\pm$  S.E.M.) of imiloxan (12; 0.1-3.0 mg/kg, s.c.) on the antinociceptive action of the TDIQ (6; 3.0 mg/kg, s.c.)/clonidine (7; 0.25 mg/kg, s.c.) combination in the mouse tail-flick assay ( $n = 8-15$  mice/treatment). Asterisks denote a significant difference compared to the control group [TDIQ/clonidine (6/7) combination];  $*P < 0.05$ , one-way ANOVA ( $F_{4,45} = 3.223$ ) followed by Dunnett's post hoc test.

Finally, the  $\alpha_{2B/2C}$ -AR antagonist ARC-239 (14; 0.3-10 mg/kg, s.c.) blocked the analgesic actions of the TDIQ/clonidine (6/7) combination in a dose-dependent manner ( $AD_{50} = 0.6$  mg/kg, 95% CL = 0.2-2.3 mg/kg; Figure 44).



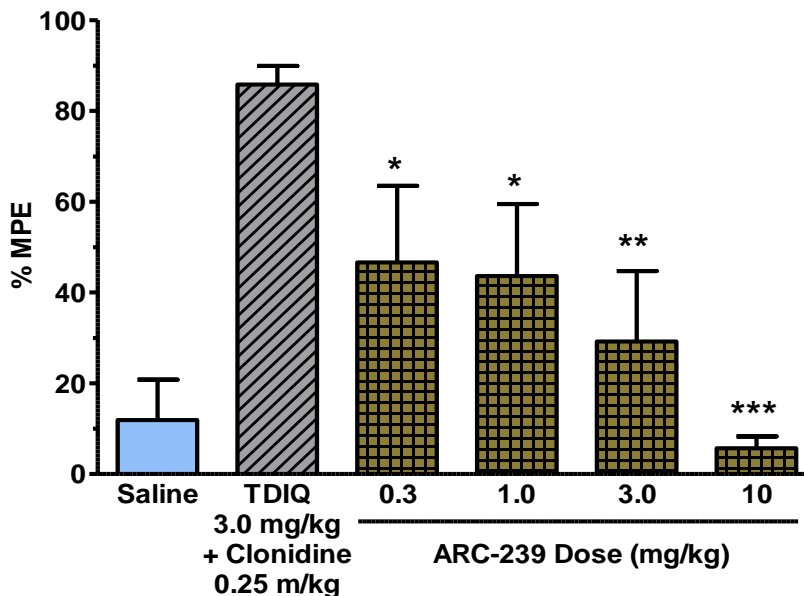


**Figure 44.** Effect ( $\pm$  S.E.M.) of ARC-239 (**14**; 0.3-10 mg/kg, s.c.) on the antinociceptive action of the TDIQ (**6**; 3.0 mg/kg, s.c.)/clonidine (**7**; 0.25 mg/kg, s.c.) combination in the mouse tail-flick assay ( $n = 8-15$  mice/treatment). Asterisks denote a significant difference compared to the control group [TDIQ/clonidine (**6/7**) combination]; \* $P < 0.05$ , \*\* $P < 0.01$ , \*\*\* $P < 0.001$ , one-way ANOVA ( $F_{4,44} = 7.435$ ) followed by Dunnett's post hoc test.

Clearly, TDIQ (**6**) potentiates the antinociceptive action of clonidine (**7**). If both clonidine (**7**) and TDIQ (**6**) are non-selective (among  $\alpha_2$ -ARs)  $\alpha_2$ -AR agonists, TDIQ's (**6**) potentiation of clonidine (**7**)-induced antinociception might simply be an additive effect of the two agents. To further characterize the analgesic potentiation of clonidine (**7**; 0.25 mg/kg) produced by TDIQ (**6**; Figure 40), an isobolographic analysis was conducted. An isobolographic analysis is a method that assesses if a biological effect produced by a combination of drugs is greater than, equal to, or smaller than, the sum of the individual effects of the component drugs. Specifically, does TDIQ (**6**) behave in a synergistic or simply additive manner when co-administered with clonidine (**7**) in the mouse tail-flick assay?

In an isobolographic analysis, synergism is evaluated by comparing the experimental  $ED_{50mix}$  of a fixed-ratio of TDIQ (6) and clonidine (7) to the theoretical  $ED_{50add}$  of a simply additive mixture having the same proportions. Since TDIQ (6) does not produce antinociception when administered alone, the  $ED_{50add}$  will only be dependent on clonidine's (7) effect. First, co-administration of fixed ratios of the TDIQ/clonidine (6/7) combination were examined in the tail-flick assay; the co-administration of the 3:1 and 12:1 fixed-ratios of TDIQ (6) and clonidine (7) resulted in a leftward shift compared to the clonidine (7) dose-response regression line (Figure 45).

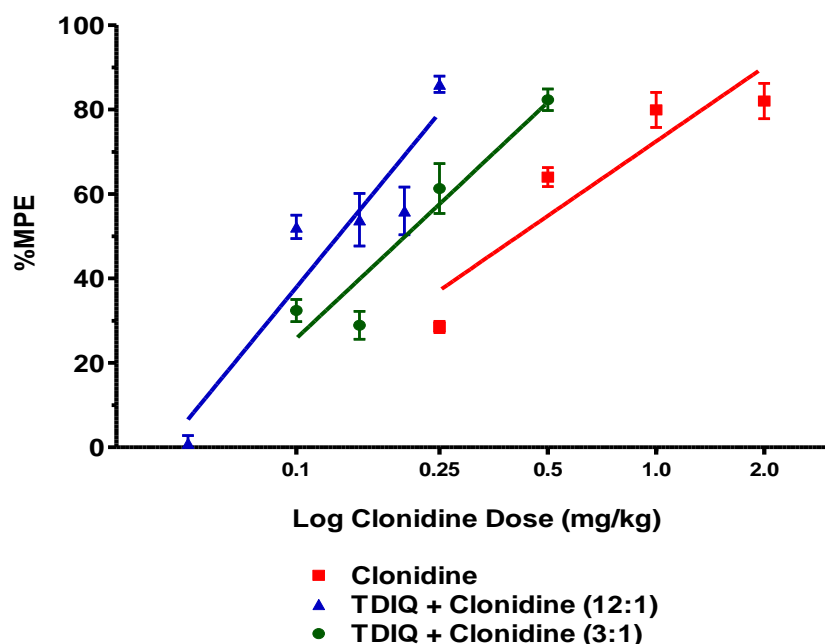


**Figure 45.** Dose-response lines determined by regression analysis for clonidine (7) alone (red squares) and the co-administration of TDIQ (6) and clonidine (7) given in a 3:1 (green circles) and 12:1 (blue triangles) fixed-ratio in the mouse tail-flick assay ( $n = 8-24$  mice/treatment), plotted as log clonidine (7) dose.

Next, a regression analysis of % MPE vs. log total dose graphically presented  $ED_{50\text{clonidine}}$  (0.44 mg/kg),  $ED_{50\text{mix}}$  (0.79 mg/kg) for the 3:1 fixed-ratio, and  $ED_{50\text{mix}}$  (1.64 mg/kg) for the 12:1 fixed-ratio (Figure 46).  $ED_{50\text{add}}$  values for both fixed-ratios can be calculated:  $ED_{50\text{add}} = ED_{50\text{clonidine}}/P = 0.44/(1/4) = 1.76$  mg/kg for the 3:1 fixed ratio and  $ED_{50\text{add}} = ED_{50\text{clonidine}}/P = 0.44/(1/13) = 5.72$  mg/kg for the 12:1 fixed ratio.

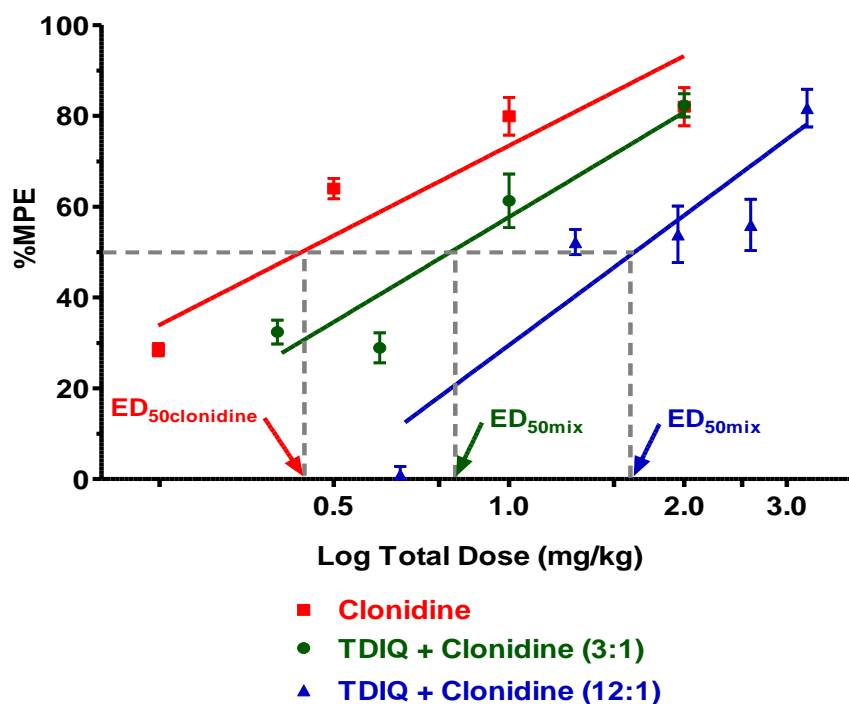


**Figure 46.** Dose-response lines determined by regression analysis for clonidine (7) alone (red squares) and co-administration of TDIQ (6) and clonidine (7) given in a 3:1 (green circles) and 12:1 (blue triangles) fixed-ratio in the mouse tail-flick assay ( $n = 8-24$  mice/treatment), plotted as log total administered dose.

The line of additivity is based solely on  $ED_{50\text{clonidine}}$  because TDIQ (6) was found to be inactive when administered alone in the mouse tail-flick assay (Figure 39). Because both  $ED_{50\text{mix}}$  values are plotted significantly below the line of additivity, the 3:1

and 12:1 fixed ratios of TDIQ (**6**) and clonidine (**7**) behaved in a synergistic manner ( $P < 0.5$  and  $P < 0.01$ , respectively; Figure 47).

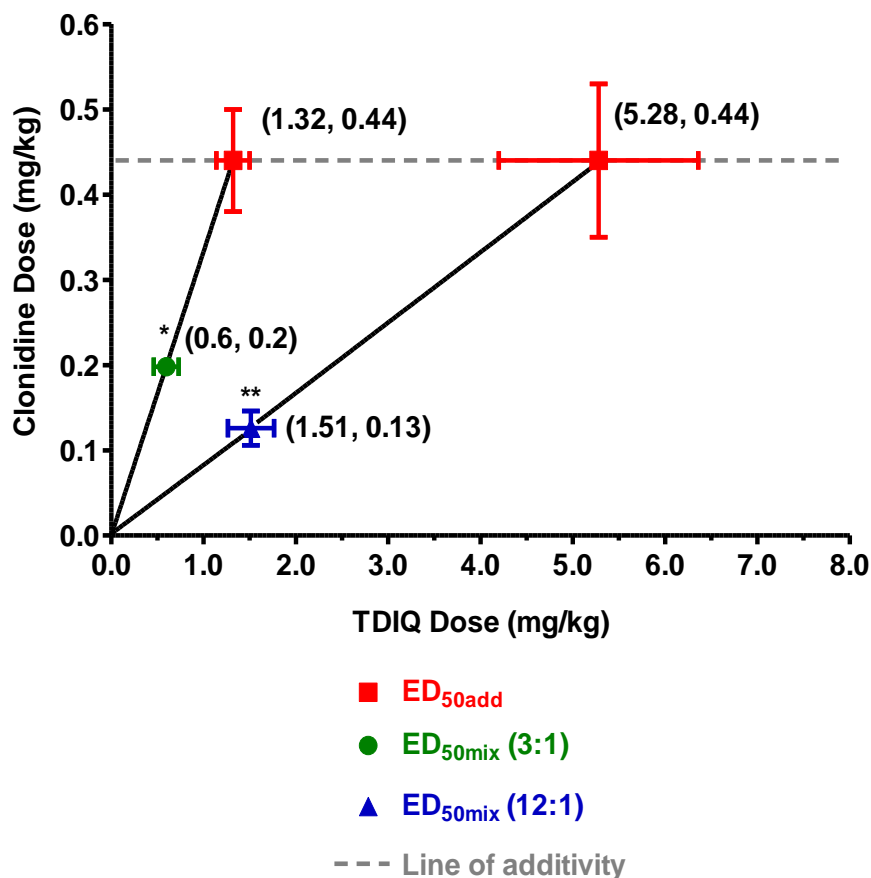


**Figure 47.** The isobologram shows the line of additivity (broken gray line), ED<sub>50mix</sub> for the 3:1 (green circles) and 12:1 (blue triangles) fixed-ratios of TDIQ (**6**) and clonidine (**7**), and ED<sub>50add</sub> (red squares) from the mouse tail-flick results ( $n = 8-24$  mice/treatment). Asterisks denote a significant difference compared to the control (ED<sub>50add</sub> values); \* $P < 0.05$ , \*\* $P < 0.01$ , Student's t-test.

Since the experimental ED<sub>50mix</sub> for a 3:1 and 12:1 fixed-ratio of TDIQ (**6**) and clonidine (**7**) was statistically different than the theoretical ED<sub>50add</sub> of a simply additive mixture having the same proportions, TDIQ (**6**) potentiates the analgesic actions of clonidine (**7**) in a synergistic (or super-additive) manner [i.e., the isobologram (Figure 47) suggests that the biological effect (antinociception) produced by the combination of

TDIQ (6) and clonidine (7) is greater than the sum of the individual effects of the component drugs].

### b) Hot-plate assay

The analgesic properties of TDIQ (6) administered alone and in combination with clonidine (7) in a second nociceptive animal model, the hot-plate assay, were examined. When TDIQ (6) was s.c. administered in mice, no antinociception was observed in the hot-plate assay (Figure 48). This lack of antinociception is similar to the tail-flick results for TDIQ (6; Figure 39).

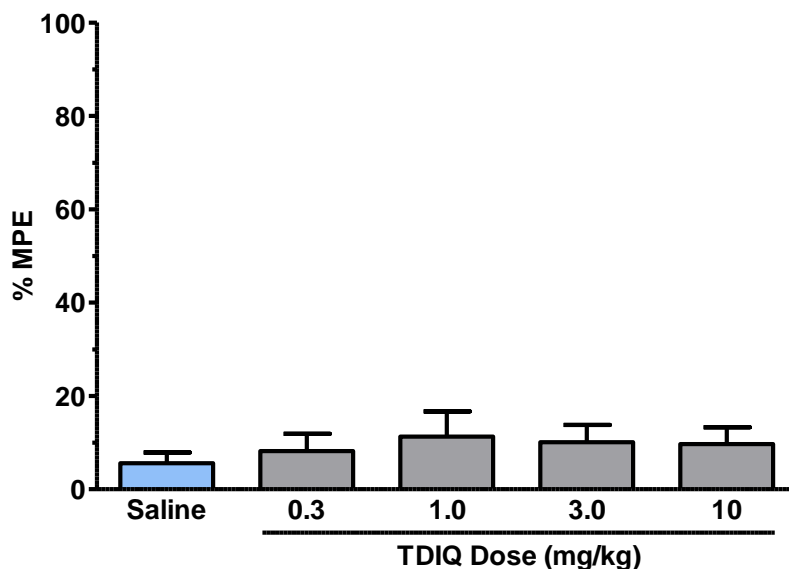


**Figure 48.** Antinociceptive effect ( $\pm$  S.E.M.) of TDIQ (6; 0.3-10 mg/kg, s.c.) in the mouse hot-plate assay ( $n = 8-10$  mice/treatment). No significant difference ( $P > 0.05$ ) compared to the control group (saline) was detected; one-way ANOVA ( $F_{4,41} = 0.2881$ ) followed by Dunnett's post hoc test.

In the tail-flick combination studies, TDIQ (6) potentiated a low, “inactive” dose of clonidine (7; 0.25 mg/kg; Figure 40) and, therefore, the first hot-plate combination study examined the co-administration of a low, “inactive” dose of clonidine (7; 0.25 mg/kg) and TDIQ (6). Unlike in the tail-flick assay, TDIQ (6) did not potentiate the antinociceptive effects of a low dose of clonidine (7) in the mouse hot-plate assay (Figure 49). In fact, there seemed to be a slight attenuation of effect; this observed attenuation was not significantly different from the control.

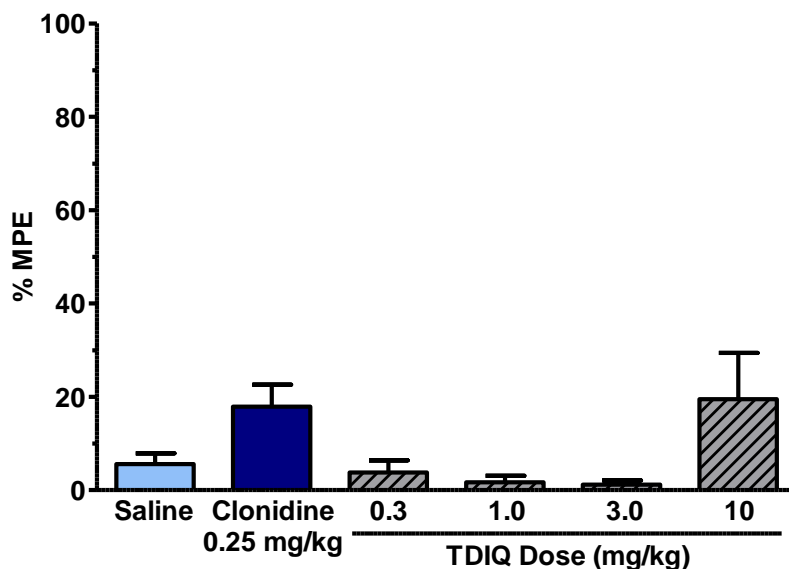


**Figure 49.** Antinociceptive effect ( $\pm$  S.E.M.) of TDIQ (6; 0.3-10 mg/kg, s.c.) in combination with clonidine (7; 0.25 mg/kg, s.c.) in the mouse hot-plate assay ( $n = 8-28$  mice/treatment). No significant difference ( $P > 0.05$ ) compared to the control group [0.25 mg/kg dose of clonidine (7)] was detected; one-way ANOVA ( $F_{4,56} = 2.191$ ) followed by Dunnett's post hoc test.

Due to slight attenuation observed in Figure 49, the dose of clonidine (7) was increased so that significant attenuation by TDIQ (6) might be more readily observed. TDIQ (6; 0.3-10 mg/kg) co-administered with a dose similar to the calculated  $ED_{50}$  (0.9

mg/kg) of clonidine (**7**; 1.0 mg/kg) produced a significant decrease in antinociception ( $AD_{50} = 1.4$  mg/kg, 95% CL = 0.26-7.84 mg/kg) in comparison to clonidine (**7**; 1.0 mg/kg) alone (% MPE =  $50.6 \pm 6.2$ ; Figure 50). A similar analgesic attenuation (% MPE = 32-36) by TDIQ (**6**; 0.3-10 mg/kg) was detected in an even larger dose of clonidine (**7**; 2.0 mg/kg; Figure 51).

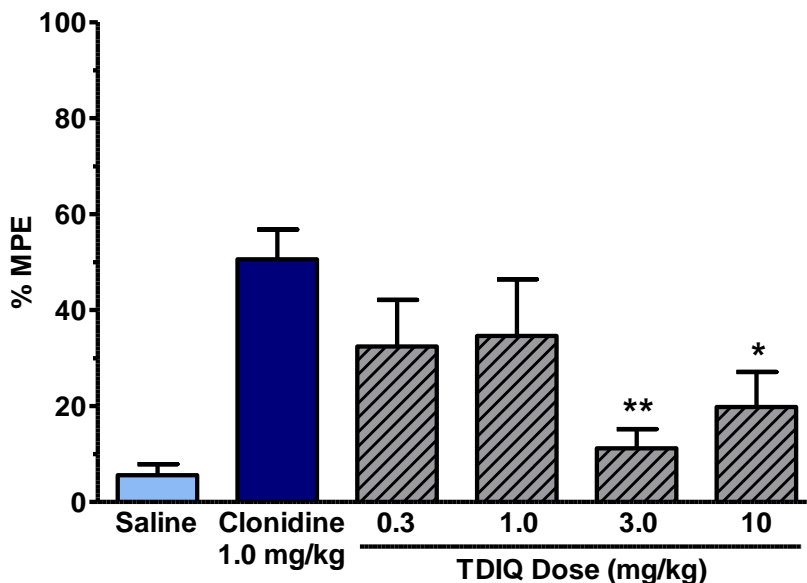


**Figure 50.** Antinociceptive effect ( $\pm$  S.E.M.) of TDIQ (**6**; 0.3-10 mg/kg, s.c.) in combination with clonidine (**7**; 1.0 mg/kg, s.c.) in the mouse hot-plate assay ( $n = 9-20$  mice/treatment). Asterisks denote a significant difference compared to the control group (1.0 mg/kg dose of clonidine; **7**); \* $P < 0.05$ , \*\* $P < 0.01$ , one-way ANOVA ( $F_{4,53} = 3.927$ ) followed by Dunnett's post hoc test.

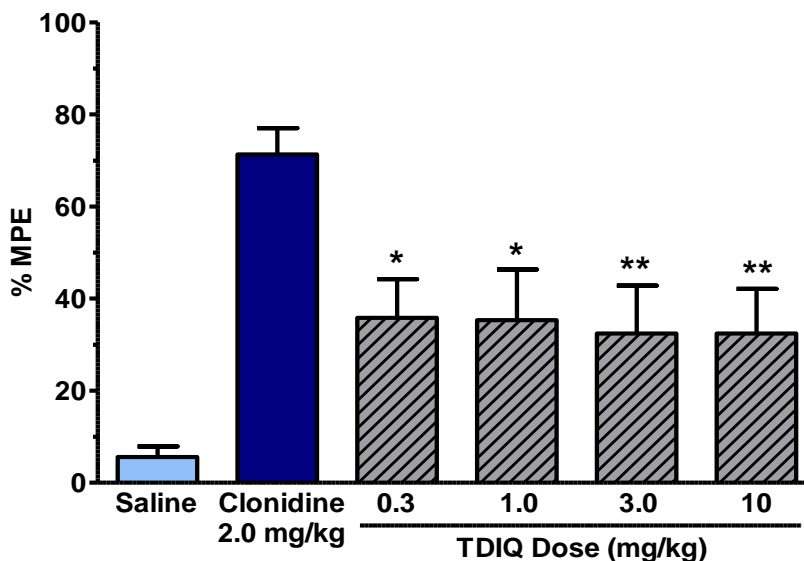


**Figure 51.** Antinociceptive effect ( $\pm$  S.E.M.) of TDIQ (**6**; 0.3-10 mg/kg, s.c.) in combination with clonidine (**7**; 2.0 mg/kg, s.c.) in the mouse hot-plate assay ( $n = 11-19$  mice/treatment). Asterisks denote a significant difference compared to the control group (2.0 mg/kg dose of clonidine; **7**); \* $P < 0.05$ , \*\* $P < 0.01$ , one-way ANOVA ( $F_{4,58} = 4.954$ ) followed by Dunnett's post hoc test.

In the mouse hot-plate assay, the non-selective  $\alpha_2$ -AR agonist TDIQ (**6**; 0.3-10 mg/kg) produced no antinociceptive effects when administered alone (Figure 48) and interestingly, attenuated the analgesic actions of a 1.0 and 2.0 mg/kg dose of clonidine (**7**; Figures 50 and 49, respectively). This attenuating effect produced by TDIQ (**6**) differs from that observed in the tail-flick assay (Figure 40).

### c) Locomotor activity assay

Locomotor activity of TDIQ (**6**; 0.3-3.0 mg/kg, s.c.) alone and in combination with clonidine (**7**; 0.25 mg/kg, s.c.) has been previously examined in our laboratory.<sup>151</sup> TDIQ (**6**; 0.3-3.0 mg/kg, s.c.) did not significantly differ from saline in the mouse locomotor



activity assay in all four stimulant parameters ( $P > 0.05$ ) with one exception (Figure 52). A 3.0 mg/kg dose of TDIQ (**6**) did show decreased vertical entries ( $P < 0.05$ ; data not shown).

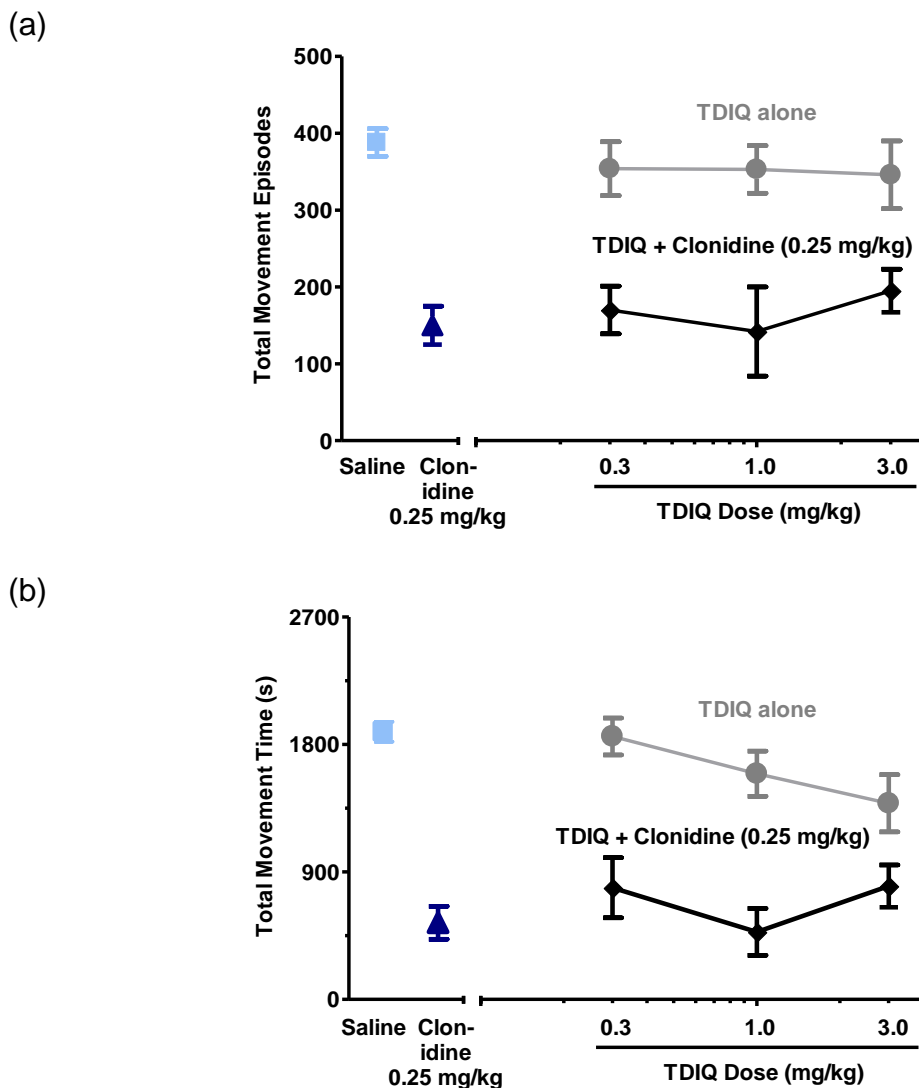


**Figure 52.** Effect ( $\pm$  S.E.M.) of TDIQ (**6**; 0.3-3.0 mg/kg) alone and in combination with clonidine (**7**; 0.25 mg/kg) on (a) total movement episodes and (b) total movement time with a 45-min recording time in the mouse locomotor activity assay ( $n = 8$  mice/treatment). No significant difference ( $P > 0.05$ ) compared to the control group [saline and clonidine (**7**; 0.25 mg/kg), respectively] was detected; one-way ANOVA ( $F_{3,22} = 0.4039$  and  $F_{3,20} = 0.3899$ ) followed by Dunnett's post hoc test.<sup>151</sup>

In the combination studies, co-administration of TDIQ (**6**; 0.3-3.0 mg/kg) and clonidine (**7**; 0.25 mg/kg) produced locomotor activity similar to the effect observed by the s.c. administration of clonidine (**7**; 0.25 mg/kg) alone (Figure 52).

#### **d) Summary**

Briefly, when TDIQ (**6**) was administered alone, it produced no antinociceptive effects in the tail-flick (Figure 39) and hot-plate (Figure 48) assays. And since MD-354 (**21**) potentiated clonidine's (**7**) antinociceptive effect, at least in part, by an  $\alpha_2$ -AR mechanism, the effect of the co-administration of the  $\alpha_2$ -AR agonist TDIQ (**6**) and clonidine (**7**) was also examined. Indeed, TDIQ (**6**) potentiated the analgesic effect of an "inactive" dose of clonidine (**7**; 0.25 mg/kg) in the mouse tail-flick assay (Figure 40). In contrast, although statistically non-significant, TDIQ (**6**) slightly attenuated the effect of an even lower dose (0.1 mg/kg) of clonidine (**7**; Figure 41). To further characterize the analgesic potentiation observed in Figure 40, an isobolographic analysis was conducted. These studies indicated that 3:1 and 12:1 fixed ratios of TDIQ (**6**) and clonidine (**7**) behave synergistically in the mouse tail-flick assay (Figure 47).

To investigate the mechanism of action,  $\alpha_2$ -AR antagonists were co-administered with the TDIQ/clonidine (**6/7**) combination. More specifically, the preferentially selective  $\alpha_{2A}$ -AR antagonist BRL44408 (**15**; 0.03-3.0 mg/kg),  $\alpha_{2B}$ -AR antagonist imiloxan (**12**; 0.1-3.0 mg/kg), and  $\alpha_{2B/2C}$ -AR antagonist ARC-239 (**14**; 0.3-10 mg/kg) significantly attenuated the analgesic potentiation of clonidine (**7**; 0.25 mg/kg) produced by TDIQ (**6**) in the mouse tail-flick assay (Figures 42, 43, and 44, respectively).

In the hot-plate assays, TDIQ (**6**) initially seemed to have no effect on the antinociceptive actions of clonidine (**7**; 0.25 mg/kg; Figure 49), but the effect of higher doses (1.0 and 2.0 mg/kg) of clonidine (**7**) was significantly attenuated by TDIQ (**6**; Figures 50 and 49, respectively).

In the final pharmacological studies, the locomotor activity of TDIQ (**6**) alone and in combination with clonidine (**7**) was assessed. In the mouse locomotor activity assay, s.c. administration of TDIQ (**6**; 0.3-3.0 mg/kg) produced saline-like effects (Figure 52). But more importantly, the TDIQ/clonidine (**6/7**) combinations that produced enhanced antinociceptive effects in the tail-flick assay (Figure 40) were examined in the mouse locomotor activity assay; results indicated that the co-administration of TDIQ (**6**; 0.3-3.0 mg/kg) and clonidine (**7**; 0.25 mg/kg) was not statistically different than control [clonidine (**7**); Figure 52].

**Table 8.** Summary of the pharmacological assays; the dose of clonidine (**7**; where employed) in all combination studies is 0.25 mg/kg.

<b>Treatment</b>	<b>Mouse tail-flick assay</b>	<b>Mouse hot-plate</b>
MD-354 ( <b>21</b> ; up to a 30 mg/kg dose)	inactive <sup>33</sup>	inactive <sup>33</sup>
Clonidine ( <b>7</b> )	ED <sub>50</sub> = 0.4 mg/kg	ED <sub>50</sub> = 0.9 mg/kg
+ MD-354 ( <b>21</b> )	biphasic potentiation <sup>34</sup>	no potentiation <sup>33</sup>
MD-354 ( <b>21</b> ; 1.0 mg/kg) + clonidine ( <b>7</b> )		
+ ondansetron ( <b>23</b> )	failed to attenuate	
+ tropisetron ( <b>25</b> )	AD <sub>50</sub> = 0.00047 mg/kg <sup>34</sup>	
+ yohimbine ( <b>11</b> )	AD <sub>50</sub> = 0.33 mg/kg <sup>31</sup>	
+ BRL44408 ( <b>15</b> )	AD <sub>50</sub> = 2.1 mg/kg <sup>31</sup>	
+ imiloxan ( <b>12</b> )	AD <sub>50</sub> = 0.17 mg/kg <sup>31</sup>	
MD-354 ( <b>21</b> ; 6.0 mg/kg) + clonidine ( <b>7</b> )		
+ ondansetron ( <b>23</b> )	failed to attenuate	
+ zacopride ( <b>24</b> )	failed to attenuate <sup>33,29</sup>	
+ tropisetron ( <b>25</b> )	failed to attenuate <sup>29</sup>	
+ yohimbine ( <b>11</b> )	AD <sub>50</sub> = 2.3 mg/kg	
+ imiloxan ( <b>12</b> )	attenuated (s.c.)	
+ imiloxan ( <b>12</b> )	failed to attenuate (i.p.) <sup>33</sup>	
mCPBG ( <b>20</b> ; up to a 10 mg/kg dose)	inactive	inactive
mCPBG ( <b>20</b> ) + clonidine ( <b>7</b> ; ED <sub>50</sub> dose)		AD <sub>50</sub> = 0.8 mg/kg
mCPBG ( <b>20</b> ) + clonidine ( <b>7</b> )	ED <sub>50</sub> = 1.6 mg/kg	
+ ondansetron ( <b>23</b> )	failed to attenuate	
+ tropisetron ( <b>25</b> )	attenuated	
+ tropisetron methiodide	failed to attenuate	
+ yohimbine ( <b>11</b> )	AD <sub>50</sub> = 0.04 mg/kg	
SR57227A ( <b>22</b> ; 0.3-10 mg/kg)	inactive	inactive
+ clonidine ( <b>7</b> )	failed to potentiate	
+ clonidine ( <b>7</b> ; ED <sub>50</sub> dose)	failed to potentiate/attenuate	failed to potentiate/attenuate
TDIQ ( <b>6</b> ; up to a 10 mg/kg dose)	inactive	inactive
TDIQ ( <b>6</b> ) + clonidine ( <b>7</b> ; ED <sub>50</sub> dose)		attenuated
TDIQ ( <b>6</b> ) + clonidine ( <b>7</b> )	ED <sub>50</sub> = 0.6 mg/kg	failed to potentiate
+ BRL44408 ( <b>15</b> )	AD <sub>50</sub> = 0.2 mg/kg	
+ imiloxan ( <b>12</b> )	AD <sub>50</sub> = 0.2 mg/kg	
+ ARC-239 ( <b>14</b> )	AD <sub>50</sub> = 0.6 mg/kg	

## 5. Binding assays

Various agents [(-)NE (**1**), TDIQ (**6**), clonidine (**7**), and MD-354 (**21**)] were evaluated in  $\alpha_{2A}$ -,  $\alpha_{2B}$ -, and  $\alpha_{2C}$ -AR binding assays: [ $^{35}\text{S}$ ]GTP $\gamma$ S and competitive radioligand binding assays (conducted Dr. Scheinin's Laboratories at University of Turku, Turku, Finland). In the [ $^{35}\text{S}$ ]GTP $\gamma$ S binding assays, activity was analyzed under low salt conditions (i.e., low concentration of NaCl and GDP in the buffer solutions) that favor the detection of partial agonism.<sup>152</sup> In general, partial agonists do not show activity in high salt conditions.

(-)NE (**1**), considered as a full agonist, was analyzed as control [i.e., (-)NE's (**1**) intrinsic activity at each receptor subtype was normalized to 100%]. As depicted in the graph (Figure 53a), (-)NE (**1**) displayed greater efficacy at  $\alpha_{2A}$ - and  $\alpha_{2B}$ -ARs ( $E_{\text{max}} \approx 150\%$  over basal levels) in comparison to  $\alpha_{2C}$ -ARs ( $E_{\text{max}} \approx 75\%$  over basal levels; Pohjanoksa and Scheinin, unpublished data). Similarly, the potency of (-)NE (**1**) is greater at  $\alpha_{2A/2B}$ -ARs ( $EC_{50} = 106$  and  $145$  nM, respectively) than  $\alpha_{2C}$ -ARs ( $EC_{50} = 612$  nM; Pohjanoksa and Scheinin, unpublished data; Table 9).

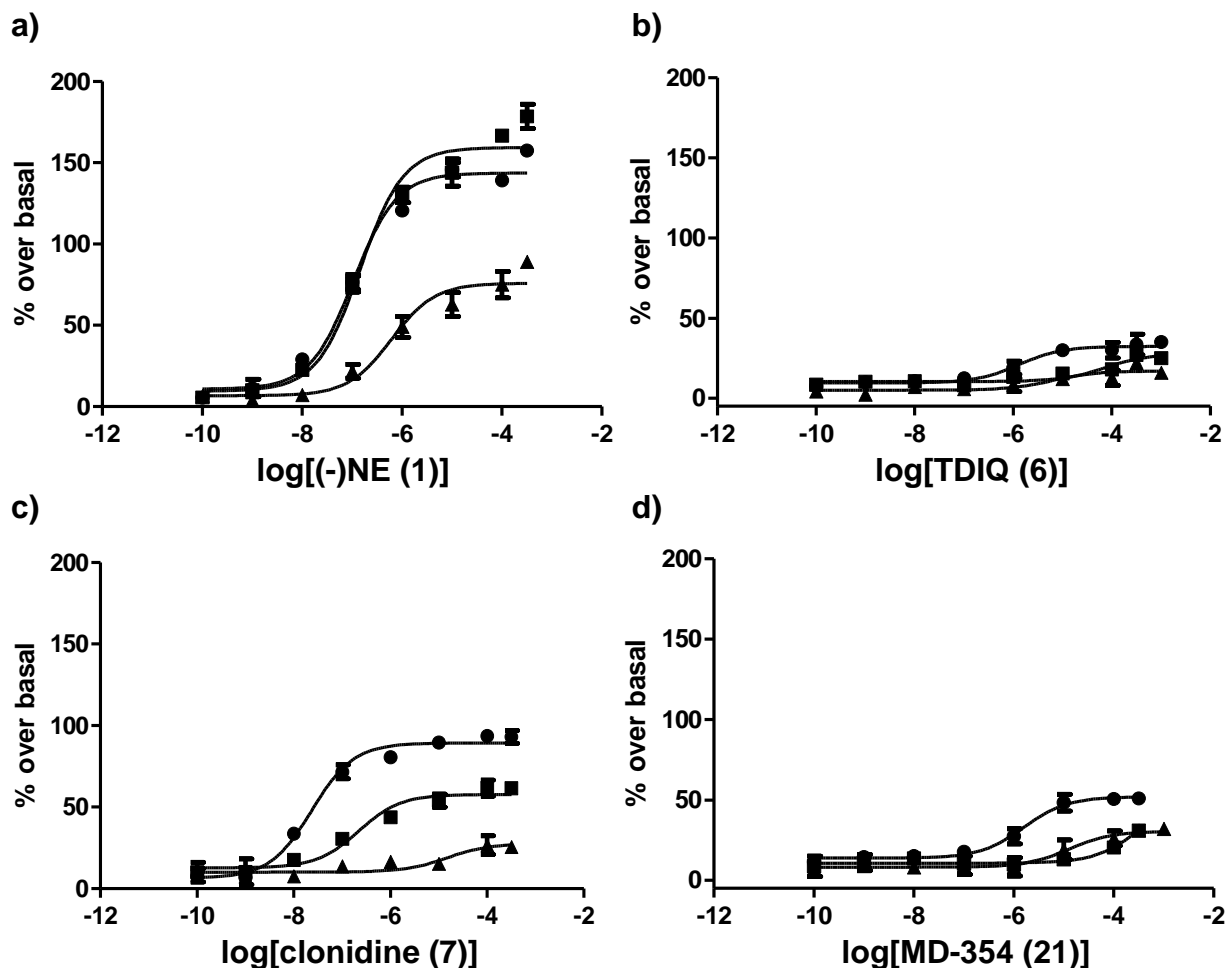


**Figure 53.** Effects of  $\alpha_2$ -AR agents [a) (-)NE (1), b) TDIQ (6), c) clonidine (7), and d) MD-354 (21)] on  $[^{35}\text{S}]\text{GTP}\gamma\text{S}$  binding (incubation buffer containing low  $\text{Na}^+$  and GDP concentrations) in CHO cell membranes expressing human  $\alpha_2$ -ARs ( $\alpha_{2A}$ : ●;  $\alpha_{2B}$ : ■;  $\alpha_{2C}$ : ▲). Data points represent the mean  $\pm$  S.E.M. (each dose examined in triplicate).

TDIQ (6), clonidine (7), and MD-354 (21) were of lower efficacy than the full agonist (-)NE (1; IA = 100%) at all three  $\alpha_2$ -AR subtypes in the  $[^{35}\text{S}]\text{GTP}\gamma\text{S}$  binding assays; that is, intrinsic activity was less than 100% (Figure 53; Pohjanoksa and Scheinin, unpublished data). Table 9 summarizes the potency ( $\text{EC}_{50}$ ) and efficacy [%IA of (-)NE (1)] of the agents examined at  $\alpha_{2A}$ -,  $\alpha_{2B}$ -, and  $\alpha_{2C}$ -ARs (Pohjanoksa and Scheinin, unpublished data).

**Table 9.** Characterization of [<sup>35</sup>S]GTPγS binding to CHO cell membranes expressing human α<sub>2A</sub>-, α<sub>2B</sub>-, or α<sub>2C</sub>-ARs in low salt conditions. Potency is represented as EC<sub>50</sub> values (nM) with the 95% CI in parenthesis. Efficacy (or maximal stimulation over basal) is expressed as intrinsic activity (IA) compared to (-)NE (**1**; Pohjanoksa and Scheinin, unpublished data).

	α <sub>2A</sub>		α <sub>2B</sub>		α <sub>2C</sub>	
	EC <sub>50</sub> (nM)	IA [% of (-)NE ( <b>1</b> )]	EC <sub>50</sub> (nM)	IA [% of (-)NE ( <b>1</b> )]	EC <sub>50</sub> (nM)	IA [% of (-)NE ( <b>1</b> )]
(-)NE ( <b>1</b> )	106 (74-152)	100	145 (94-223)	100	612 (276-1,358)	100
TDIQ ( <b>6</b> )	1,312 (382-4,503)	22	>10,000	18	6,233	22
Clonidine ( <b>7</b> )	23 (16-35)	62	220 (82-587)	36	>10,000	37
MD-354 ( <b>21</b> )	1,588 (757-3,333)	36	>10,000	31	>10,000	41

Affinity at α<sub>2</sub>-AR subtypes (α<sub>2A</sub>, α<sub>2B</sub>, and α<sub>2C</sub>) was examined for the above-mentioned agents via competitive ligand binding assays employing the α<sub>2</sub>-AR antagonist radioligand [ethyl-<sup>3</sup>H]RS-79948-197 (Table 10). The binding affinity for the full agonist (-)NE (**1**) and (as subsequently determined) the partial agonists TDIQ (**6**), clonidine (**7**) and MD-354 (**21**) was measured in CHO cells expressing recombinant human α<sub>2A</sub>-, α<sub>2B</sub>-, and α<sub>2C</sub>-ARs (Table 10, unpublished data). Binding affinity for SR57227A (**22**) at α<sub>2</sub>-AR subtypes was also examined via competitive radioligand binding assays employing the human α<sub>2</sub>-AR agonist radioligand [<sup>3</sup>H]clonidine (Table 11).<sup>145</sup>

**Table 10.** Competitive binding affinity at human  $\alpha_2$ -ARs expressed in CHO cells employing [ethyl- $^3$ H]RS-79948-197 radioligand ( $\alpha_2$ -AR antagonist). Binding affinity is expressed as  $K_i$  values (nM) with the 95% CI in parenthesis (Pohjanoksa and Scheinin, unpublished data).<sup>31</sup>

Ligand	$K_i$ (nM)		
	$\alpha_{2A}$	$\alpha_{2B}$	$\alpha_{2C}$
(-)-NE ( <b>1</b> )	405 (284-578)	579 (421-798)	417 (333-524)
TDIQ ( <b>6</b> )	598 (478-749)	1,183 (904-1,547)	1,782 (1,538-2,065)
Clonidine ( <b>7</b> )	35 (28-45)	98 (81-118)	287 (234-353)
MD-354 ( <b>21</b> )	110 (70-190)	220 (170-280)	4,700 (2,800-7,800)

**Table 11.** Competitive binding affinity at human  $\alpha_2$ -ARs expressed in CHO cells employing [ $^3$ H]clonidine radioligand ( $\alpha_2$ -AR agonist). Binding affinity is expressed as  $K_i$  values  $\pm$  S.E.M. (nM; unpublished data).<sup>145</sup>

Ligand	$K_i$ (nM)		
	$\alpha_{2A}$	$\alpha_{2B}$	$\alpha_{2C}$
SR57227A ( <b>22</b> )	6,653 $\pm$ 665	4,990 $\pm$ 709	8,222 $\pm$ 658

TDIQ (**6**) shows a slight binding preference for  $\alpha_{2A}$ -ARs (2- and 3-fold over  $\alpha_{2B}$ - and  $\alpha_{2C}$ -ARs, respectively) but, in general, has relatively low binding affinity at  $\alpha_2$ -ARs. Similarly, clonidine (**7**) displays higher affinity at  $\alpha_{2A}$ -ARs versus  $\alpha_{2B}$ - and  $\alpha_{2C}$ -ARs (3- and 8-fold difference, respectively). MD-354 (**21**) binds at  $\alpha_{2A}$ - and  $\alpha_{2B}$ -ARs with similar affinity ( $K_i$  = 110 and 220 nM), but with significantly lower binding affinity at  $\alpha_{2C}$ -ARs ( $K_i$  = 4,700 nM). SR57227A (**22**), which has been described in the literature as a selective 5-HT<sub>3</sub> receptor agent, displayed negligible binding affinity at human  $\alpha_{2A}$ -,  $\alpha_{2B}$ -, and  $\alpha_{2C}$ -ARs ( $K_i$  > 1,000 nM; Table 11).<sup>145</sup>



## 6. Discussion

Pharmacological studies were conducted to further characterize the biphasic, analgesic potentiation observed when MD-354 (**21**; 0.3-10 mg/kg) is co-administered with an “inactive” dose of clonidine (**7**; 0.25 mg/kg) in the mouse tail-flick assay (Figure 12).<sup>135</sup> Since MD-354 (**21**) binds to 5-HT<sub>3</sub> receptors and  $\alpha_2$ -ARs (Table 5), it is likely that each peak (Figure 12) depicts a unique mechanism of action. For example, the potentiation depicted by Peak A could be due to 5-HT<sub>3</sub> receptor agonism, whereas Peak B potentiation could be due to  $\alpha_2$ -AR antagonism. In general, the Peak A and/or B potentiating effects could involve: (a) 5-HT<sub>3</sub> receptor agonism or antagonism, (b)  $\alpha_2$ -AR (one or more of the receptor subtypes) agonism or antagonism, (c) a combination of the above, or (d) neither 5-HT<sub>3</sub> receptor nor  $\alpha_2$ -AR action (i.e., that is, some other, yet unidentified, receptor mechanisms might be involved). Previously reported mechanistic studies on MD-354 (**21**) potentiation of the antinociceptive effect of clonidine (**7**) might provide some insight on Peak A and Peak B potentiation (summarized in Table 12).

**Table 12.** Summary of the previously reported mechanistic studies associated with the analgesic potentiation of clonidine (**7**; 0.25 mg/kg) by MD-354 (**21**; 0.3-10 mg/kg).

Mechanistic study results	Comments
<b>Peak A</b>	
<ul style="list-style-type: none"> <li>• Tropicsetron (<b>25</b>) attenuated the antinociceptive effect of the MD-354 (<b>21</b>; 1.0 mg/kg)/clonidine (<b>7</b>; 0.25 mg/kg) combination.<sup>34</sup></li> <li>• Yohimbine (<b>11</b>), imiloxan (<b>12</b>), and BRL44408 (<b>15</b>) attenuated the antinociceptive effect of the MD-354 (<b>21</b>; 1.0 mg/kg)/clonidine (<b>7</b>; 0.25 mg/kg) combination.<sup>31</sup></li> </ul>	<ul style="list-style-type: none"> <li>• This suggests a 5-HT<sub>3</sub> receptor agonist mechanism; but not all 5-HT<sub>3</sub> receptor antagonists [e.g., ondansetron (<b>23</b>)] blocked the effect.</li> <li>• This suggests an <math>\alpha_2</math>-AR agonist mechanism (but, it is unclear which <math>\alpha_2</math>-AR subtype is involved).</li> </ul>
<b>Peak B</b>	
<ul style="list-style-type: none"> <li>• Ondansetron (<b>23</b>), zacopride (<b>24</b>), and tropisetron (<b>25</b>) failed to attenuate the antinociceptive effect of the MD-354 (<b>21</b>; 6.0 mg/kg)/clonidine (<b>7</b>; 0.25 mg/kg) combination.<sup>33,29</sup></li> <li>• Yohimbine (<b>11</b>) and imiloxan (<b>12</b>) attenuated the antinociceptive effect of the MD-354 (<b>21</b>; 6.0 mg/kg)/clonidine (<b>7</b>; 0.25 mg/kg) combination (unpublished data).</li> </ul>	<ul style="list-style-type: none"> <li>• This suggests that 5-HT<sub>3</sub> receptor agonism is not the mechanism of action.</li> <li>• This suggests an <math>\alpha_2</math>-AR agonist mechanism (but, it is unclear which <math>\alpha_2</math>-AR subtype is involved).</li> </ul>
<b>Peak A or B</b>	
<ul style="list-style-type: none"> <li>• Ondansetron (<b>23</b>), zacopride (<b>24</b>), and tropisetron (<b>25</b>) potentiated the antinociceptive effect of clonidine (<b>7</b>; 0.25 mg/kg).<sup>29</sup></li> <li>• Imiloxan (<b>12</b>) potentiated the antinociceptive effects of clonidine (<b>7</b>; 0.25 mg/kg).<sup>31</sup></li> </ul>	<ul style="list-style-type: none"> <li>• This suggests that 5-HT<sub>3</sub> receptor antagonists can potentiate the antinociceptive effects of clonidine (<b>7</b>).</li> <li>• This suggests an <math>\alpha_2</math>-AR antagonist can potentiate the antinociceptive effects of clonidine (<b>7</b>).</li> </ul>

Although numerous mechanistic studies have been conducted, the mechanism of action of the potentiation of clonidine's (7) antinociceptive effect by MD-354 (21) remains elusive. As summarized in Table 12, 5-HT<sub>3</sub> receptors and  $\alpha_2$ -ARs both seem to be involved in both Peak A and B. For example, a low dose of MD-354 (21; 1.0 mg/kg) appears to potentiate the antinociceptive effects of clonidine (7) via a 5-HT<sub>3</sub> receptor agonist mechanism (Peak A), whereas a higher dose of MD-354 (21; 6.0 mg/kg) might be acting as a 5-HT<sub>3</sub> receptor antagonist (Peak B).<sup>29,34</sup> The latter mechanism is speculative; MD-354 (21) shows partial agonist activity at 5-HT<sub>3</sub> receptors and, therefore, can behave functionally as an agonist or antagonist.<sup>113</sup> Also, as shown in our laboratory, three structurally diverse 5-HT<sub>3</sub> receptor antagonists [ondansetron (23), zacopride (24), and tropisetron (25)] enhanced the analgesic actions of an "inactive" dose of clonidine (7) in the tail-flick assay.<sup>29</sup> This observed potentiation is unlikely due to a central depressant effect because co-administration of these 5-HT<sub>3</sub> receptor antagonists [e.g., zacopride (24; 0.01 mg/kg) or tropisetron (25; 0.2 mg/kg)] and the  $\alpha_2$ -AR partial agonist clonidine (7; 0.25 mg/kg) produced results similar to that of control [0.25 mg/kg dose of clonidine (7);  $P > 0.05$ ] in mouse locomotor activity assays.<sup>29</sup> This provides evidence that antagonism at 5-HT<sub>3</sub> receptors augments the antinociceptive effects of clonidine (7), but does not necessarily indicate a 5-HT<sub>3</sub> receptor antagonist role for MD-354 (21) in its analgesic potentiation of clonidine (7) in the mouse tail-flick assay.

In the present investigation, the role of 5-HT<sub>3</sub> receptor involvement in the potentiation of clonidine (7)-induced analgesia was further evaluated. A more established 5-HT<sub>3</sub> receptor agonist, *m*CPBG (20), and a known centrally-acting 5-HT<sub>3</sub>

receptor agonist, SR57227A (**22**), were examined to help clarify the mechanism of action. In the mouse tail-flick assay, no antinociception was observed with s.c. administration of either *m*CPBG (**20**; 0.3-10 mg/kg; Figure 22) or SR57227A (**22**; 0.3-10 mg/kg; Figure 31) alone. However, a high dose (30 mg/kg) of SR57227A (**22**), administered alone, produced a significant effect ( $P < 0.05$ ; Figure 31). Dose-dependent antinociception by SR57227A (**22**, doses of up to 20 mg/kg;  $ED_{50} = 6.5$  mg/kg) has been previously observed in the mouse-tail flick assay but, as opposed to the current study (which employed a s.c. route of administration), SR57227A (**22**) was administered via i.p. injection.<sup>27</sup> It is possible that the observed antinociceptive effect described in the literature is due to route of administration; furthermore, the hypolocomotor effects produced by this dose of SR57227A (**22**), as shown herein, might have interfered with interpretation of its antinociceptive actions. But, two prior studies showed no effect in the mouse locomotor assay when low doses (1.0-10 mg/kg) of SR57227A (**22**) were administered i.p., whereas only a high dose (30 mg/kg) showed hypolocomotor actions.<sup>153,154</sup> This is similar to the results obtained in our laboratory; SR57227A (**22**) elicited saline-like effects when low doses (1.0-10 mg/kg, i.p.) were administered, but sedative-like effects were observed when a high dose of SR57227A (**22**; 30 mg/kg) was administered s.c. in the mouse locomotor activity assay ( $P < 0.01$ ; Figure 38).<sup>155</sup> It is difficult to reconcile differences between the published antinociceptive actions of SR57227A (**22**) with the present investigation, and even more difficult to explain its actions as resulting from sedation, given its lack of effect in locomotor assays (except at a very high dose). But, it might be noted that the single report showing that SR57227A (**22**) possesses antinociceptive action was published

only as an abstract and that various details (e.g., mouse strain and gender, pre-injection times, time of measurement, and apparatus) were not described. Nevertheless, antinociceptive effects have been produced by other 5-HT<sub>3</sub> receptor agonists [5-HT (**16**), 2-methyl-5-HT (**17**), and *m*CPBG (**20**)] in various animal models (tail-flick, paw pressure, and formalin assays; refer to Table 4).<sup>28,127,128,131-133</sup> Therefore, the antinociceptive effects produced by SR57227A (**22**) are plausible, but inconsistent with the present results.

In the combination studies, albeit *m*CPBG (**20**; 0.3-10 mg/kg) augmented the antinociceptive effects of an “inactive” dose of clonidine (**7**; 0.25 mg/kg) in a dose-dependent manner (Figure 23), SR57227A (**22**; 0.3-10 mg/kg) had no effect on clonidine’s (**7**) analgesic properties in the mouse tail-flick assay (Figure 31). It is doubtful that the observed antinociception in the *m*CPBG/clonidine (**20/7**) treatment group is due to the hypolocomotor effects of *m*CPBG (**20**); the analgesia-producing combination [*m*CPBG (**20**; 6.0 mg/kg) + clonidine (**7**; 0.25 mg/kg)] showed clonidine (**7**)-like effects in the mouse locomotor activity assay (Figure 30). In addition, both i.p. and i.c.v. administration of *m*CPBG (**20**), alone, elicited saline-like effects in rat locomotor activity assays.<sup>156,157</sup>

*m*CPBG (**20**) and SR57227A (**22**) have slightly different receptor binding profiles; *m*CPBG (**20**) binds with high affinity at 5-HT<sub>3</sub> receptors ( $K_i = 17$  nM) and with low affinity at  $\alpha_2$ -ARs ( $K_i = 1,445$  or  $3,800$  nM), 5-HT<sub>2A</sub> receptors ( $K_i = 5,700$  nM), and 5-HT<sub>2C</sub> receptors ( $K_i = 1,400$  nM), and according to the current literature, SR57227A (**22**) binds with high affinity only at 5-HT<sub>3</sub> receptors ( $K_i = 103$  nM).<sup>111,115,149,158</sup> It seems that SR57227A (**22**) is relatively selective for 5-HT<sub>3</sub> receptors; however, its affinity for other

receptors was simply reported as >1,000 nM and specific  $K_i$  values were not provided (that is, its affinity for these other receptors might be only slightly greater than 1,000 nM). Bachy and co-workers described SR57227A (**22**) as a highly potent and selective 5-HT<sub>3</sub> receptor agonist; depending on the assay conditions, its  $K_i$  value at 5-HT<sub>3</sub> receptors was approximately 100 nM ( $IC_{50}$  = 199-258 nM).<sup>115</sup> In the same study, SR57227A (**22**) did not bind to other 5-HT receptors (5-HT<sub>1A</sub>, 5-HT<sub>1B</sub>, 5-HT<sub>1C</sub>, 5-HT<sub>1D</sub>, 5-HT<sub>2</sub>, and 5-HT<sub>4</sub>;  $IC_{50}$  > 1,000 nM, exact  $K_i$  values were not reported).<sup>115</sup> Since SR57227A (**22**) binding affinity at  $\alpha_2$ -ARs was ambiguous, our laboratory submitted a sample to the PDSP for binding affinity analysis. Using an  $\alpha_2$ -AR agonist radioligand [<sup>3</sup>H]clonidine, SR57227A (**22**) showed little to no affinity for  $\alpha_2$ -ARs ( $K_i$ :  $\alpha_{2A}$  = 6,653,  $\alpha_{2B}$  = 4,990, and  $\alpha_{2C}$  = 8,222 nM; Roth, unpublished data; refer to Table 11).<sup>145</sup>

In general, both of these agents [*m*CPBG (**20**) and SR57227A (**22**)] bind selectively at 5-HT<sub>3</sub> receptors, but it is possible that the behavioral activity of *m*CPBG (**20**) involves  $\alpha_2$ -ARs and/or 5-HT<sub>2A/2C</sub> receptors. This is unlikely because the affinity of *m*CPBG (**20**) at 5-HT<sub>3</sub> receptors is at least 100 times greater than that for the other receptors. Likewise, the lower-affinity 5-HT<sub>3</sub> receptor agent SR57227A (**22**) binds to other receptors, such as  $\alpha_{2B}$ -ARs, but with very low affinity ( $K_i \approx 5,000$  nM).<sup>145</sup> This binding profile indicates moderate binding selectivity at 5-HT<sub>3</sub> receptors (50-fold difference compared to  $\alpha_{2B}$ -ARs).

The differences observed in the analgesia-potentiating activity of clonidine (**7**) by *m*CPBG (**20**) and SR57227A (**22**) combination studies might be due to species difference. For example, *m*CPBG (**20**) binds at rat 5-HT<sub>3</sub> receptors with 100-times greater affinity than at human 5-HT<sub>3</sub> receptors.<sup>159</sup> Also, the 5-HT<sub>3</sub> receptor efficacy of

*m*CPBG (**20**) is species dependent: ferret (53%), mouse (91%), rat (100%), and human (79-99%).<sup>97,159-162</sup> Most in vitro and in vivo pharmacological assays indicate that *m*CPBG (**20**) is a full 5-HT<sub>3</sub> receptor agonist, however, *m*CPBG (**20**) exhibited partial agonist character in an electrophysiological assay employing NG108-15 cells.<sup>163</sup> More specifically, the *m*CPBG (**20**) response was 54% of the maximal response produced by 5-HT (**16**).<sup>163</sup> Similar to most other pharmacological studies, *m*CPBG (**20**) exhibited a full agonist response in a second electrophysiological study (i.e., utilizing N1E-115 cells).<sup>164</sup> To the best of our knowledge, similar studies have not been conducted with SR57227A (**22**), but it is possible that this agent also has variable binding affinity and/or efficacy at 5-HT<sub>3</sub> receptors in different species.

Another explanation for the analgesic potentiation observed when *m*CPBG (**20**), but not SR57227A (**22**), is co-administered with clonidine (**7**) is its selectivity for 5-HT<sub>3</sub> receptor subpopulations. That is, action at 5-HT<sub>3</sub>AB receptors, but not 5-HT<sub>3</sub>A receptors, might cause a potentiation in clonidine's (**7**) antinociceptive effects. If this is the case, then it is plausible that *m*CPBG (**20**) might act at 5-HT<sub>3</sub>AB receptors whereas SR57227A (**22**) activates 5-HT<sub>3</sub>A receptors. This remains to be investigated.

To the best of our knowledge, binding affinities (under the same conditions) at each human receptor subtype (i.e., 5-HT<sub>3</sub>A vs. 5-HT<sub>3</sub>AB) are unknown for *m*CPBG (**20**) and SR57227A (**22**). As reported in the Background section, *m*CPBG (**20**;  $K_i = 17$  nM) binds at 5-HT<sub>3</sub> receptors (mixture of 5-HT<sub>3</sub>A and 5-HT<sub>3</sub>AB receptors) with higher affinity than SR57227A (**22**;  $K_i = 103$  nM).<sup>111,115</sup> To date, 5-HT<sub>3</sub>A receptor affinity for these two agents have been reported, but the experimental conditions, as well as the species, are different. Ito and co-workers reported binding affinity for 5-HT (**16**;  $K_i = 339$  nM) and

*m*CPBG (**20**;  $K_i = 224$  nM) at cloned human 5-HT<sub>3A</sub> receptors transfected in COS-1 cells employing [<sup>3</sup>H]ramosetron (5-HT<sub>3</sub> receptor antagonist) as a radioligand.<sup>165</sup> Because our laboratory was analyzing the mouse functional activity of SR57227A (**22**), investigation of the binding affinity at 5-HT<sub>3A</sub> receptors was of interest to us. SR57227A's (**22**;  $K_i = 357 \pm 44$  nM) binding affinity at recombinant mouse 5-HT<sub>3A</sub> receptors was evaluated using [<sup>3</sup>H]LY 278,584 (5-HT<sub>3</sub> receptor antagonist; unpublished data).<sup>145</sup> Unfortunately, these values are meaningless without the 5-HT<sub>3AB</sub> binding affinities of both agents. It is also difficult to compare the 5-HT<sub>3A</sub> receptor binding affinities of these two agents due to dissimilar experimental conditions.

Although, binding affinity has not been reported for each receptor subtype, *m*CPBG's (**20**) functional activity has been evaluated both at 5-HT<sub>3A</sub> and 5-HT<sub>3AB</sub> receptors. Two electrophysiological studies were performed and they both suggest that *m*CPBG (**20**) has similar potencies at human 5-HT<sub>3A</sub> and 5-HT<sub>3AB</sub> receptors (e.g., EC<sub>50</sub> = 2.5 and 2.1 μM, respectively).<sup>97,98</sup> But, interestingly, *m*CPBG (**20**) showed greater efficacy at the homomeric 5-HT<sub>3</sub> receptors [5-HT<sub>3A</sub> receptors: 134%, 5-HT<sub>3AB</sub> receptors: 79%; efficacy is expressed as % of 5-HT (**16**) effect].<sup>97</sup> Assuming that this is how *m*CPBG (**20**) behaves in mice, it seems reasonable that *m*CPBG (**20**) produces a greater pharmacological effect via 5-HT<sub>3AB</sub> receptors than at 5-HT<sub>3A</sub> receptors. Therefore, 5-HT<sub>3AB</sub>, rather than 5-HT<sub>3A</sub>, receptor agonism might be responsible for the analgesic potentiation observed in the *m*CPBG/clonidine (**20/7**) combination (Figure 23a). If this is the case, it is possible that the lack of analgesic potentiation of clonidine (**7**) by SR57227A (**22**) is due to negligible 5-HT<sub>3AB</sub> receptor activity.



Both *m*CPBG (**20**) and the structurally-related analog MD-354 (**21**) were inactive (i.e., both agents produced saline-like effects) in the tail-flick assay (Figure 22).<sup>33</sup> On the other hand, the 5-HT<sub>3</sub> receptor agonist SR57227A (**22**) exhibited pronociceptive effects in the mouse tail-flick assay (Figure 33). That is, SR57227A (**22**)-treated mice showed hyperalgesic effects (or increased sensitivity to pain). There are other reports for the hyperalgesic actions of 5-HT<sub>3</sub> receptor agonists. For example, when 5-HT (**16**) or 2-methyl-5-HT (**17**) was applied to human blisters, a hyperalgesic effect resulted.<sup>110</sup> The pain-producing effect evoked by 5-HT (**16**) was inhibited by the 5-HT<sub>3</sub> receptor antagonist tropisetron (**25**).<sup>110</sup> However, a hyperalgesic effect for SR57227A (**22**) has not been previously reported.

Since involvement of  $\alpha_2$ -ARs seems to play a role in the potentiation of the antinociceptive actions of clonidine (**7**) by MD-354 (**21**), it was initially thought that the potentiating effect observed with *m*CPBG (**20**) but not SR57227A (**22**) in the tail-flick assay might be due to the difference in receptor binding selectivity [i.e., *m*CPBG (**20**) may be acting via an  $\alpha_2$ -AR and not a 5-HT<sub>3</sub> receptor mechanism, which would explain why a 5-HT<sub>3</sub> receptor agent such as SR57227A (**22**) that lacks  $\alpha_2$ -AR affinity would not potentiate the antinociceptive effects of clonidine (**7**)]. Hypothetically, if this was correct, a 5-HT<sub>3</sub> receptor antagonist should not attenuate the antinociceptive effects of the *m*CPBG/clonidine (**20/7**) combination. In contrast, the 5-HT<sub>3</sub> receptor antagonist tropisetron (**25**; 0.00001-0.1 mg/kg) attenuated the antinociceptive effect of the *m*CPBG/clonidine (**20/7**) combination, which resulted in a U-shaped dose-response curve (Figure 25). Although it is possible that this type of antagonism (i.e., antagonist effect that produces a U-shaped dose-response curve) is sometimes not detected when

a full range of doses is not examined, U-shaped dose-response curves are observed with many 5-HT<sub>3</sub> receptor antagonists [e.g., ondansetron (**23**)].<sup>166,167</sup> Blockade of the effect of the *m*CPBG/clonidine (**20/7**) combination by the 5-HT<sub>3</sub> receptor antagonist tropisetron (**25**) indicates that *m*CPBG (**20**) may be potentiating clonidine's (**7**) analgesic effects via a 5-HT<sub>3</sub> receptor agonist mechanism.

If a 5-HT<sub>3</sub> receptor agonist mechanism is involved with the potentiating effect of clonidine (**7**) by *m*CPBG (**20**), then it would be expected that a 5-HT<sub>3</sub> receptor antagonist [e.g., ondansetron (**23**)] would block the effect of the combination. Ondansetron (**23**) did not alter the antinociceptive effect of the *m*CPBG/clonidine (**20/7**) combination (Figure 24). It is important to note that previous pharmacological assays involving ondansetron (**23**) and tropisetron (**25**) have produced contradictory results.<sup>168,169</sup> For example, tropisetron (**25**), but not ondansetron (**23**), improved phencyclidine-induced cognitive deficits in mice.<sup>168</sup> And, most analogous to the *m*CPBG (**20**) studies, our laboratory showed analgesic attenuation in the mouse tail-flick assay by tropisetron (**25**), but not by ondansetron (**23**), in the low-dose (1.0 mg/kg) MD-354/clonidine (**21/7**) combination (Figure 20).<sup>34</sup> Therefore, literature precedent suggests that ondansetron's (**23**) lack of effect in our combination studies does not necessarily disprove a 5-HT<sub>3</sub> receptor agonist mechanism proposed from the tropisetron (**25**) results.

Moreover, a locomotor suppressant effect could alter the observed antinociceptive effect in the tail-flick assay. When administered alone, tropisetron (**25**; 0.2 mg/kg, s.c.) and ondansetron (**23**; 0.1-1.0 mg/kg, i.p.) showed saline-like effects in the mouse locomotor activity assay.<sup>29,155,170</sup> Tropisetron (**25**; 0.2 mg/kg) co-

administered with clonidine (**7**; 0.25 mg/kg) showed slightly reduced locomotor activity.<sup>29</sup> However, this attenuation was not statistically different from control [0.25 mg/kg dose of clonidine (**7**)].<sup>29</sup>

To date, it is unknown if *m*CPBG (**20**) crosses the BBB; there is contradictory literature data (summarized in Table 6). Although it is unclear if *m*CPBG (**20**) behaves as a central agent, mechanistic studies suggest that potentiation of the antinociceptive effects of clonidine (**7**) by *m*CPBG (**20**) in the mouse tail-flick assay is due to a central 5-HT<sub>3</sub> receptor agonist mechanism because tropisetron (**25**), but not tropisetron methiodide, attenuated this effect (Figures 24 and 24). Results from this in vivo assay provide an indication that *m*CPBG (**20**) can cross the BBB. Similarly, a 5-HT<sub>3</sub> receptor agonist mechanism was postulated for the analgesic potentiation depicted by Peak A in the MD-354/clonidine (**21/7**) combination studies (Table 12). There is some indication from previous in vivo studies that MD-354 (**21**) acts as a central agent; MD-354 (**21**) neither substituted for nor antagonized, but enhanced the stimulus effects of (+)amphetamine in a rat drug discrimination study.<sup>135</sup> Thus far, although a central mechanism has also been implied in the mouse tail-flick studies, it is unknown if the agonistic behavior of MD-354 (**21**) is due to central or peripheral activation of 5-HT<sub>3</sub> receptors. Additional mechanistic studies are required (e.g., pretreatment with tropisetron methiodide).

In summary, the tail-flick assay results with *m*CPBG (**20**) provide evidence for 5-HT<sub>3</sub> receptor agonist potentiation of an “inactive” dose of clonidine (**7**). This was the same conclusion that was reached from the tail-flick assay results with MD-354 (**21**; Peak A).<sup>34</sup> However, the SR57227A (**22**; 0.3-10 mg/kg) results (Figure 34) indicate that

not all 5-HT<sub>3</sub> receptor agonists augment the analgesic properties of clonidine (**7**). Possible explanations for the lack of potentiation observed upon co-administration of SR57227A (**22**) and clonidine (**7**) include: (a) lower 5-HT<sub>3</sub> receptor binding affinity of SR57227A (**22**;  $K_i = 103$  nM) in comparison to *m*CPBG (**20**;  $K_i = 17$  nM), (b) action at different 5-HT<sub>3</sub> receptor subtypes (e.g., 5-HT<sub>3A</sub> or 5-HT<sub>3AB</sub> receptors), (c) possible offsetting behavioral activity [e.g., pronociceptive effects of SR57227A (**22**)] due to unknown activity at other receptors, (d) species difference, and that (e) unexamined, higher doses of SR57227A (**22**; >10 mg/kg) or temporal parameters might produce/influence potentiating activity. The latter explanation is plausible, but it would be difficult to understand if the analgesic potentiation was due to antinociceptive or sedative effects because a 30 mg/kg dose of SR57227A (**22**) was found to produce hypolocomotor effects in the present investigation (Figure 38). In fact, in a previously reported study, lower i.p. doses of SR57227A (**22**; 3-10 mg/kg) exhibited saline-like effects, whereas a 30 mg/kg dose (i.p.) significantly reduced locomotor activity ( $P < 0.001$ ) in the mouse locomotor activity assay.<sup>154</sup>

The role of 5-HT<sub>3</sub> receptors in potentiating the analgesic effects of clonidine (**7**) was evaluated in a second nociceptive mouse model, the hot-plate assay. Similar to the results in the tail-flick assay, when administered alone, both *m*CPBG (**20**; 0.3-10 mg/kg) and SR57227A (**22**; 0.3-10 mg/kg) showed no antinociceptive effects in the hot-plate assay (Figures 28 and 36, respectively); however, a higher, sedative-producing dose of SR57227A (**22**; 30 mg/kg) showed significant antinociceptive effects in the mouse hot-plate assay (Figure 36). Hence, these “antinociceptive” effects might be attributed to the sedative effect of SR57227A (**22**).

In combination studies, MD-354 (**21**) was found to potentiate the antinociceptive effect of clonidine (**7**) in the tail-flick assay, but not in the hot-plate assay.<sup>33</sup> Reports of contrasting results in tail-flick and hot-plate assays have been documented in the literature; for example, gabapentin attenuated the analgesic actions of the non-selective COX inhibitor metamizol in the mouse tail-flick assay, but did not affect the antinociceptive effects of metamizol in the mouse hot-plate assay.<sup>171</sup> The different effects observed in the tail-flick and hot-plate assays can be explained by different receptor subpopulations (spinal versus supraspinal, respectively) or different receptor mechanisms.<sup>143</sup> In the current study, the ED<sub>50</sub> dose of clonidine (**7**; 1.0 mg/kg) was selected so that potentiation or attenuation could be observed when clonidine (**7**) was co-administered with varying doses of the 5-HT<sub>3</sub> receptor agents *m*CPBG (**20**) and SR57227A (**22**) in the hot-plate assay. *m*CPBG (**20**; 0.3-10 mg/kg) significantly attenuated the antinociceptive effect (AD<sub>50</sub> = 0.8 mg/kg) of clonidine (**7**; Figure 29), but SR57227A (**22**; 0.3-10 mg/kg) failed to potentiate or attenuate the actions of clonidine (**7**; Figure 37) in the hot-plate assay. Different pharmacological effects were observed among these three 5-HT<sub>3</sub> receptor agents; in combination studies with clonidine (**7**; 1.0 mg/kg), the antinociceptive effect was not significantly attenuated (i.e., not statistically significant) by MD-354 (**21**), significantly attenuated by *m*CPBG (**20**), and not affected by SR57227A (**22**).<sup>33</sup>

A high dose of MD-354 (**21**; 30 mg/kg) slightly antagonized the analgesic action of the ED<sub>50</sub> dose of clonidine (**7**) in the hot-plate assay.<sup>33</sup> Therefore, the results in the *m*CPBG [**20**; structurally similar to MD-354 (**21**)]/clonidine (**7**) combination studies were not completely unexpected (Figure 29). MD-354 (**21**) behaves as a partial agonist at 5-

HT<sub>3</sub> receptors and, therefore, could be producing its inhibitory actions via an agonist or antagonist mechanism. In contrast, *m*CPBG (**20**) displays full agonist action at 5-HT<sub>3</sub> receptors (mouse and human).<sup>160</sup> As a result, it is likely that the inhibitory action of clonidine's (**7**) antinociceptive effects by *m*CPBG (**20**) and MD-354 (**21**) in the hot-plate assay is mediated by 5-HT<sub>3</sub> receptor agonism.

If *m*CPBG (**20**) attenuates the analgesic actions of clonidine (**7**) in the mouse hot-plate assay via a 5-HT<sub>3</sub> receptor agonist mechanism, why doesn't administration of SR57227A (**22**) also inhibit the analgesic effect of clonidine (**7**) in the same assay? Even though inhibition by SR57227A (**22**) would further support a 5-HT<sub>3</sub> receptor agonist mechanism, the lack of attenuation by SR57227A (**22**) was not too surprising because, as discussed in the Background section, 5-HT<sub>3</sub> receptor agonists have notoriously produced varying results in nociceptive animal models (Table 4). For example, *m*CPBG (**20**; i.t.) produced saline-like effects, whereas a second 5-HT<sub>3</sub> receptor agonist 2-methyl-5-HT (**17**; i.t.) produced antinociceptive effects in the tail-flick assay.<sup>26,28</sup> The reason for these varying effects among 5-HT<sub>3</sub> receptor agonists remains unclear. It is possible that 5-HT<sub>3</sub> receptor subtype selectivity alters the pharmacological effects of these agents. Two known functional 5-HT<sub>3</sub> receptor types have been identified: homopentameric 5-HT<sub>3A</sub> receptors and heteropentameric 5-HT<sub>3AB</sub> receptors, which are composed of two 5-HT<sub>3A</sub> and three 5-HT<sub>3B</sub> receptor subunits.<sup>21,97-101</sup> Also, there are three other known 5-HT<sub>3</sub> receptor subunits (5-HT<sub>3C</sub>, 5-HT<sub>3D</sub>, and 5-HT<sub>3E</sub>) but, to date, they have unknown function. Unfortunately, the lack of information regarding 5-HT<sub>3</sub> receptors, and the affinity of agents at each of those populations, might lead to ambiguous interpretation of pharmacological results.

Following the combination studies that examined the role of 5-HT<sub>3</sub> receptors in the analgesia potentiation of clonidine (**7**), the role of  $\alpha_2$ -ARs was investigated. It was already determined in mechanistic studies that *m*CPBG (**20**)-potentiation of the antinociceptive effect of an “inactive” dose of clonidine (**7**) in the tail-flick assay, at least in part, involves a 5-HT<sub>3</sub> receptor agonist mechanism. Next, mechanistic studies involving  $\alpha_2$ -AR antagonists were conducted in the mouse tail-flick assay. The non-selective  $\alpha_2$ -AR antagonist yohimbine (**11**; 0.01-6.0 mg/kg) blocked the antinociceptive potentiation of clonidine (**7**) by *m*CPBG (**20**) in a dose-dependent manner (Figure 27). This suggests that the combination is not only acting via a central 5-HT<sub>3</sub> receptor agonist mechanism, but also affects the analgesic properties of clonidine (**7**) via  $\alpha_2$ -ARs.

$\alpha_2$ -AR involvement was also observed in the potentiation of clonidine (**7**) by MD-354 (**21**); the non-selective,  $\alpha_{2A}$ -, and  $\alpha_{2B}$ -AR preferential antagonists [yohimbine (**11**), BRL44408 (**15**), and imiloxan (**12**), respectively] blocked the analgesia-potentiating effect produced by MD-354 (**21**).<sup>31</sup> MD-354 (**21**) binds to all three  $\alpha_2$ -AR subtypes with variable affinity ( $K_i$  = 25-4,700 nM; refer to Table 5) and functionally behaves as a partial agonist at  $\alpha_{2A}$ -ARs [IA = 36% of NE (**1**) activity; EC<sub>50</sub> = 1,588 nM].<sup>31</sup> Additionally, MD-354 (**21**) seems to behave as a partial agonist at  $\alpha_{2B}$ - and  $\alpha_{2C}$ -ARs [IA = 31 and 41% of NE (**1**) activity, respectively], but its potency is very low (EC<sub>50</sub> > 10,000 nM for both subtypes).<sup>31</sup> On the other hand, although subtype selectivity was not examined, *m*CPBG (**20**) has low affinity at  $\alpha_2$ -ARs ( $K_i$  = 1,445 nM) and seems to behave as an  $\alpha_2$ -AR antagonist.<sup>149</sup> In this study, *m*CPBG (**20**) binding affinity was based on rat brain cortex homogenates and the functional data was based on ex vivo mouse studies, in which *m*CPBG (**20**) facilitated NE (**1**) release in mouse cerebral cortex.<sup>149</sup> Although

*m*CPBG (**20**) did produce  $\alpha_2$ -AR antagonist actions at high doses, its potency was rather low compared to the yohimbine (**11**) stereoisomer rauwolscine (i.e., rauwolscine had 340-fold greater potency than *m*CPBG (**20**)).<sup>149</sup>

There are two possible ways of interpreting the mechanistic studies involving  $\alpha_2$ -AR antagonists co-administered with the MD-354/clonidine (**21/7**) combination. The analgesic attenuation could be due to blocking the effect of clonidine (**7**) or MD-354 (**21**). Conversely, since *m*CPBG (**20**) seems to behave as an  $\alpha_2$ -AR antagonist, the analgesic attenuation observed in mechanistic studies utilizing the non-selective  $\alpha_2$ -AR antagonist yohimbine (**11**) in combination with *m*CPBG (**20**) and clonidine (**7**) is most likely due to blocking the effect of clonidine (**7**). *m*CPBG (**20**) might potentiate the antinociceptive effect of clonidine (**7**) in the hot-plate assay if clonidine (**7**) is able to act at  $\alpha_2$ -ARs (i.e., it is essential for clonidine (**7**) to act at  $\alpha_2$ -ARs). In addition, because *m*CPBG (**20**) has low binding affinity for  $\alpha_2$ -ARs ( $K_i = 1,445$  nM) compared to its affinity for 5-HT<sub>3</sub> receptors ( $K_i = 17$  nM), it is unlikely that the pharmacological effects of *m*CPBG (**20**) are due to interaction at  $\alpha_2$ -ARs. Nevertheless, it is important to note that, to the best of our knowledge, the binding affinity and functional activity of *m*CPBG (**20**) at the three  $\alpha_2$ -AR subtypes have not been examined. It is possible that the low affinity data obtained from rat brain cortex homogenates does not depict the affinity of *m*CPBG (**20**) at all  $\alpha_2$ -AR subtypes (e.g., it is possible that *m*CPBG (**20**) displays high affinity at  $\alpha_{2A}$ -AR, but not  $\alpha_{2B}$ - or  $\alpha_{2C}$ -ARs).<sup>149</sup>

Previous literature indicates that the antinociceptive effects of clonidine (**7**) are due to an  $\alpha_{2A}$ -AR agonist mechanism.<sup>172,173</sup> And although clonidine (**7**) binds to all three subtypes of  $\alpha_2$ -ARs with similar affinity (refer to Table 2), it behaves as a partial agonist



at  $\alpha_{2A}$ -ARs and as a very weak partial agonist at  $\alpha_{2B}$ - and  $\alpha_{2C}$ -ARs [%E<sub>max</sub> = 62, 36, and 37% of NE (1) activity; EC<sub>50</sub> = 23, 220, and >10,000 nM, respectively; Pohjanoksa and Scheinin, unpublished data].

The non-selective  $\alpha_2$ -AR agonist TDIQ (6), which is devoid of 5-HT<sub>3</sub> receptor affinity, was evaluated in the mouse tail-flick assay. This agent produced no antinociceptive effects when administered alone, but dose-dependently potentiated the analgesic effect of an “inactive” dose of clonidine (7; Figures 39 and 38, respectively). In fact, an isobolographic analysis of a 3:1 and 12:1 fixed ratio dose of TDIQ (6) and clonidine (7) indicated a synergistic potentiation of the antinociceptive effect (Figure 47). Activation of one receptor mechanism presumably produces a simply additive effect (i.e., the co-administration of the combination should produce the theoretical effect based on the individual potencies of the two drugs).<sup>174,175</sup> Most reports conclude synergy is due to multiple mechanisms (i.e., two drugs acting via different sites, whether that is different anatomical sites or different receptors); a recent study indicated that clonidine (7) and dexmedetomidine produced antinociceptive synergy in mice via a dual receptor mechanism (agonist action at  $\alpha_{2A}$ - and  $\alpha_{2C}$ -ARs).<sup>176</sup> Therefore, the supra-additive effect (or synergistic effect) produced by TDIQ (6) in combination with clonidine (7) suggests multiple mechanisms. For example, the analgesic synergy produced by TDIQ (6) and clonidine (7) could be mediated by an  $\alpha_{2A}$ -AR agonism as well as either a  $\alpha_{2B}$ - or  $\alpha_{2C}$ -AR agonism.

One therapeutic advantage to synergistic drug effects is a decrease in drug doses. This reduced drug dose(s) can theoretically produce efficacy of the desired effect, but reduce efficacy in producing side effects. In the abovementioned

combination studies [e.g., TDIQ (**6**) and clonidine (**7**)], a desired antinociceptive effect occurred without affecting clonidine's (**7**) sedative side effect. That is, a reduced dose of clonidine (**7**; 0.25 mg/kg) in combination with TDIQ (**6**) produced analgesic actions without influencing locomotor activity.

To further understand the mechanism(s) underlying these actions, combination studies were conducted. The mechanistic studies with TDIQ (**6**) produced similar results compared to MD-354 (**21**); that is, the  $\alpha_{2A}$ -,  $\alpha_{2B}$ -, and  $\alpha_{2B/2C}$ -AR preferential antagonists [BRL44408 (**15**), imiloxan (**12**), and ARC-239 (**14**), respectively] significantly blocked the analgesia-potentiating effect of an "inactive" dose of clonidine (**7**) by TDIQ (**6**) in the tail-flick assay (Figures 42, 43, and 44, respectively). In [ $^{35}$ S]GTP $\gamma$ S binding studies, TDIQ (**6**) behaved as a weak partial agonist at  $\alpha_{2A}$ -,  $\alpha_{2B}$ -, and  $\alpha_{2C}$ -ARs [IA = 22%, 18%, and 22% of NE (**1**) activity; EC<sub>50</sub> = 1,300, >10,000, and 6,230 nM, respectively; Pohjanoksa and Scheinin, unpublished data]. Although TDIQ (**6**) produces partial agonist action at all three subtypes of  $\alpha_2$ -ARs, its efficacy (or intrinsic activity) is lower than that of clonidine [**7**; IA = 62%, 36%, and 37% of NE (**1**) activity at  $\alpha_{2A}$ -,  $\alpha_{2B}$ -, and  $\alpha_{2C}$ -ARs; Pohjanoksa and Scheinin, unpublished]. Due to its lower intrinsic activity, TDIQ (**6**) may behave as an  $\alpha_2$ -AR antagonist when co-administered with clonidine (**7**). In fact, previous imiloxan (**12**) studies suggest that  $\alpha_{2B}$ -AR antagonism might account for the potentiation of the antinociceptive effects of clonidine (**7**) in the mouse tail-flick assay (refer to Table 12).<sup>31</sup>

Based on these in vivo results, it is difficult to determine which  $\alpha_2$ -AR subtype is responsible for the analgesic potentiation observed in the TDIQ/clonidine (**6/7**) combination. At this time, none of the  $\alpha_2$ -AR subtypes can be ruled out. It is possible

that one or more of the receptor subtypes plays a role in this potentiating effect. The results are difficult to interpret because the available  $\alpha_2$ -AR antagonists, to date, are only preferentially selective. For example, BRL44408 (**15**) binds to all three  $\alpha_2$ -AR subtypes ( $K_i$ :  $\alpha_{2A} = 5.7$ ,  $\alpha_{2B} = 651$ , and  $\alpha_{2C} = 150$  nM). Even though BRL44408 (**15**) shows preferential binding affinity at  $\alpha_{2A}$ -ARs (e.g., 26-fold over  $\alpha_{2C}$ -ARs), it is possible that BRL44408 (**15**) behaves as an  $\alpha_{2C}$ -AR antagonist at the doses evaluated and, therefore, is able to block the effect of an  $\alpha_{2C}$ -AR agonist.

Similar to the results obtained in the tail-flick study (Figure 39), TDIQ (**6**) produced saline-like effects in the hot-plate assay when administered alone (Figure 48). However, unlike the potentiating effect observed in the tail-flick assay (Figure 40), when TDIQ (**6**) was co-administered with clonidine (**7**; 1.0 and 2.0 mg/kg doses), analgesic attenuation occurred (Figures 50 and 51). In summary, TDIQ (**6**) potentiated the antinociceptive actions of clonidine (**7**) in the mouse tail-flick assay, but blocked clonidine's (**7**) effect in the hot-plate assay.

Opposing results in antinociceptive animal models have been previously described; for example, gabapentin augmented the antinociceptive effects of morphine in the hot-plate assay, but attenuated morphine's effect in the tail-flick assay.<sup>171</sup> As discussed earlier, these contrasting results could be due to spinal versus supraspinal receptor activation. It is generally thought that the tail-flick response is due to a spinal response, whereas antinociceptive effects produced in the hot-plate assay are mostly due to a supraspinal response.<sup>143</sup> Therefore, it is possible that TDIQ (**6**) might attenuate the antinociceptive effect of clonidine (**7**) in the mouse hot-plate assay via a supraspinal mechanism, but its analgesia-potentiating effect in the tail-flick assay is mediated by

spinal receptors. Conversely, there is some controversial data suggesting that this is not the case (i.e., tail-flick responses may be due to both spinal and supraspinal activation).<sup>143</sup>

*m*CPBG (**20**) and TDIQ (**6**) showed similar pharmacological effects in the two thermal nociceptive animal models: analgesic potentiation of an inactive dose of clonidine (**7**; 0.25 mg/kg) in the tail-flick assay and analgesic attenuation of the ED<sub>50</sub> dose of clonidine (**7**; 1.0 mg/kg) in the hot-plate assay. It seems unlikely that *m*CPBG (**20**) and TDIQ (**6**) share the exact same mechanism of action because of a dissimilar binding profile; *m*CPBG (**20**) binds with high affinity at 5-HT<sub>3</sub> receptors ( $K_i = 17$  nM), whereas TDIQ (**6**) binds with high affinity at  $\alpha_2$ -ARs ( $K_i$ :  $\alpha_{2A} = 75$ ,  $\alpha_{2B} = 97$ ,  $\alpha_{2C} = 65$  nM).<sup>53,111,113</sup> On the other hand, the non-selective  $\alpha_2$ -AR antagonist yohimbine (**11**) blocked the analgesic potentiation of clonidine (**7**) by *m*CPBG (**20**) which indicates  $\alpha_2$ -AR involvement in the tail-flick assay (Figure 27).

In previously published hot-plate studies, clonidine's (**7**) antinociceptive actions were augmented by the  $\alpha_2$ -AR agonist guanabenz (**9**; s.c.) in rats and blocked by the  $\alpha_2$ -AR antagonist idazoxan (i.p., i.c.v., or i.t) in mice.<sup>177,178</sup> Therefore, it seems reasonable that TDIQ (**6**) may be attenuating clonidine's (**7**) analgesic actions in the hot-plate assay via an  $\alpha_2$ -AR antagonist mechanism.

In summary, combination studies with clonidine (**7**) and various agents [MD-354 (**21**), *m*CPBG (**20**), SR57227A (**22**), and TDIQ (**6**)] have provided evidence of novel pain mechanisms. Clonidine (**7**), which is a potent analgesic agent, also produces undesired side effects such as sedation. Three of the four agents mentioned above [MD-354 (**21**), *m*CPBG (**20**) and TDIQ (**6**), but not SR57227A (**22**)] were able to potentiate the

antinociceptive effects of an “inactive” dose (i.e., a dose that does not produce antinociceptive effects when administered alone) of clonidine (**7**) in the mouse tail-flick assay. Furthermore, this analgesia-potentiating effect seems to be selective because all three combinations failed to alter the sedative properties of clonidine (**7**). Specifically, the locomotor “action” of the combinations was similar to that of clonidine (**7**; 0.25 mg/kg) when administered alone. Not only does this provide support for a selective potentiating effect, but it also indicates that the analgesic potentiation by MD-354 (**21**), *m*CPBG (**20**) or TDIQ (**6**) is unlikely due to a central depressant effect. When reviewing the mechanistic studies of all three agents, it seems that 5-HT<sub>3</sub> receptor and  $\alpha_2$ -AR agonism can potentiate the analgesic effects of clonidine (**7**) without affecting its sedative properties. To date, it is unclear which  $\alpha_2$ -AR subtype(s) is involved in this potentiating effect. One major disadvantage of studying  $\alpha_2$ -AR agents is the lack of subtype-selective agents; advancement in this area should enhance our current understanding of  $\alpha_2$ -AR pharmacology.

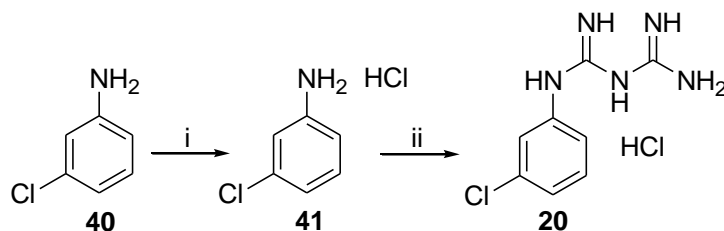
## **B. Synthesis**

### **1. *meta*-Chlorophenylbiguanide Hydrochloride (**20**)**

The hydrochloride salt of *m*CPBG (**20**) was synthesized according to a previously published procedure (Scheme 1).<sup>179</sup> The free base of *meta*-chloroaniline (**40**) was dissolved in absolute EtOH and the hydrochloride salt (**41**) precipitated upon addition of a 35 M solution of HCl/Et<sub>2</sub>O. Compound **41** was purified by recrystallization from

acetone (3x); mp (compared to lit<sup>180</sup> mp) and tlc analysis with an authentic sample supported its identity and purity. Cyanoguanidine and *m*-chloroaniline hydrochloride (**41**) were allowed to stir at reflux for 4 h and then cooled to 10 °C. The resulting precipitate was collected by filtration, washed with Et<sub>2</sub>O, and recrystallized twice from H<sub>2</sub>O to afford *m*CPBG hydrochloride (**20**). Product characterization of **20** (mp, <sup>1</sup>H NMR, and IR) corresponded to previously reported data.<sup>181</sup>

**Scheme 1.**<sup>a</sup>



<sup>a</sup>Reagents and conditions: i) HCl/Et<sub>2</sub>O, absolute EtOH, -10 °C; ii) cyanoguanidine, H<sub>2</sub>O, reflux for 4 h, 10 °C for 24 h.

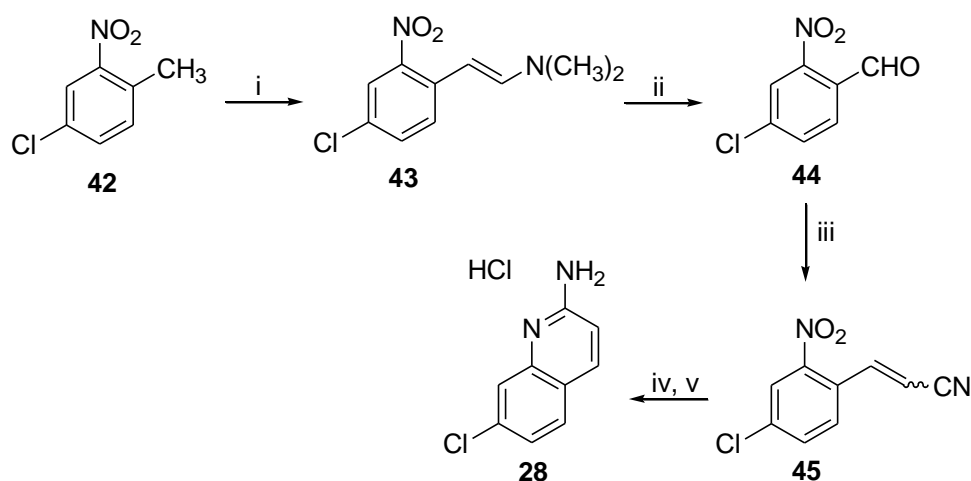
The prepared hydrochloride salt of *m*CPBG (**20**) was used in the abovementioned pharmacological assays (tail-flick, hot-plate, and locomotor activity assays).

## 2. 2-Amino-7-chloroquinoline Hydrochloride (**28**)

Compound **28** was prepared in a five-step synthesis starting with the commercially available toluene analog **42** (Scheme 2). Partial dissociation of DMF-DMA occurred in DMF and deprotonation of **42** occurred in the presence of pyrrolidine;

the resulting *N,N*-dimethylimmonium ion and toluene (**42**) anion reacted and upon elimination of a molecule of methanol, **43** was produced in quantitative yield. Oxidative hydrolysis of enamine **43** using  $\text{NaIO}_4$  led to the formation of benzaldehyde **44**. Compound **44** was converted to **45** upon addition of  $\text{NaH}$ , diethyl cyanomethylphosponate and anhydrous DMF. In the last step, **45** was cyclized with  $\text{SnCl}_2 \cdot 2\text{H}_2\text{O}$  in refluxing absolute EtOH; the resulting free base (**28**) was converted to a hydrochloride salt.

**Scheme 2.**<sup>a</sup>

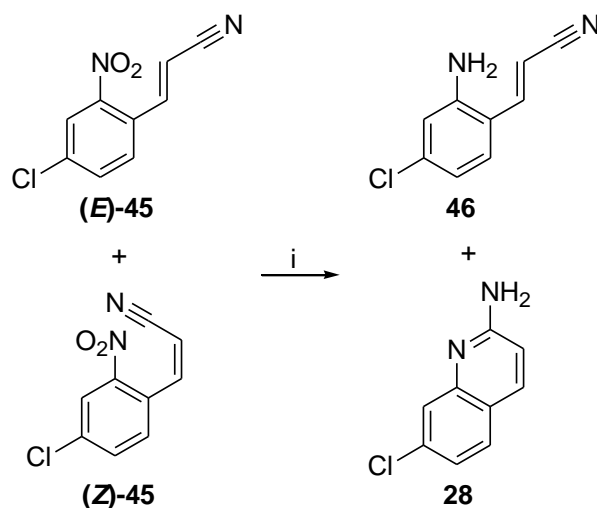


<sup>a</sup>Reagents and conditions: i) DMF·DMA, pyrrolidine, DMF,  $\text{N}_2$ , 110 °C for 1 h; ii)  $\text{NaIO}_4$ ,  $\text{H}_2\text{O}$ , DMF, rt for 1.5 h; iii) diethyl cyanomethylphosponate, anhydrous DMF, 0 °C for 5 min; iv)  $\text{SnCl}_2 \cdot 2\text{H}_2\text{O}$ , absolute EtOH, reflux for 2.5 h; v)  $\text{HCl}/\text{Et}_2\text{O}$ , MeOH.

In the third step of Scheme 2, the isomers of **45** were not separated and purified (i.e., the mixture of (*E/Z*)-**45** was used in the final step without further purification). The reaction (step iv; Scheme 2) was monitored by tlc analysis and once the starting material disappeared, the reaction was worked-up. The resulting crude product

consisted of two compounds ( $R_f = 0.5$  and  $0.9$ ; eluent:  $\text{CH}_2\text{Cl}_2/\text{CH}_3\text{OH}/\text{NH}_4\text{OH} = 9:1:0.1$ ). Following column chromatography, both compounds were fully characterized. Based on  $^1\text{H}$  NMR and IR analyses, only (*Z*)-**45** cyclized to form the free base of **28** ( $R_f = 0.5$ ) as depicted in Scheme 3. Addition of  $\text{Sn}_2\text{Cl}_2 \cdot 2\text{H}_2\text{O}$  to (*E*)-**45** simply reduced the nitro group to an amine, which resulted in the formation of compound **46** ( $R_f = 0.9$ ) as a light-brown solid (Scheme 3).

**Scheme 3.**<sup>a</sup>



<sup>a</sup>Reagents and conditions: i)  $\text{SnCl}_2 \cdot 2\text{H}_2\text{O}$ , absolute EtOH, reflux for 2.5 h.

Although it was easy to separate **28** and **46** by column chromatography and to subsequently characterize each compound, further analysis was necessary to explain the reaction mechanism. In the first attempt to clarify the results, compound (*E/Z*)-**45** was reacted with  $\text{SnCl}_2 \cdot 2\text{H}_2\text{O}$  in absolute EtOH at room temperature, rather than at reflux. It was thought that at the reduced temperature, (*E/Z*)-**45** would be simply



reduced into (*E/Z*)-3-(2-amino-4-chlorophenyl)acrylonitrile (**46**) isomers. However, based on TLC analysis, the same two compounds were produced (i.e., compounds that fluoresced under UV light at  $R_f = 0.5$  and  $0.9$ , which corresponded to **28** and **46**, respectively). Also, time did not seem to play a role in the reaction because the reaction mixture was allowed to stir for 1 week at room temperature followed by 2 days at reflux and the TLC remained the same.

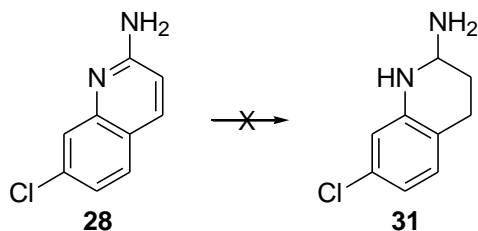
Since it was speculated that one isomer was reduced to an amine while the other isomer was reduced and then cyclized, the mixture of **45** isomers were separated via combi-flash chromatography (eluent: hexanes/EtOAc = 1:0 to 1:1 over 20 min). Unfortunately, only the *Z*-isomer (**45**) was completely purified. In a small-scale reaction, (*Z*)-**45** reacted with  $\text{SnCl}_2 \cdot 2\text{H}_2\text{O}$  at room temperature to afford only one product ( $R_f = 0.5$ ). That is, the *Z*-isomer was reduced and subsequently cyclized to form compound **28**. Since two products (**46** and **28**) were formed when (*E/Z*)-**45** was added to the reaction, the *E*-isomer (compound **46**) must be unable to cyclize under the experimental conditions. IR analysis aided in the structural characterization; compounds **45** and **46** indicated a nitrile moiety (peak at  $2215 \text{ cm}^{-1}$ ) whereas compound **28** showed only a baseline signal in the general nitrile region ( $2200\text{-}2300 \text{ cm}^{-1}$ ).

### 3. 2-Amino-7-chloro-1,2,3,4-tetrahydroquinoline Hydrochloride (**31**)

When planning the synthesis of compound **31**, it was thought that it could be prepared from **28** via catalytic hydrogenation (Scheme 4). Careful attention was given to the selection of catalyst because of the concern of dehalogenation of the 7-position

chloro group. For example, palladium and nickel catalysts have previously been used for the partial hydrogenation of quinolines to 1,2,3,4-tetrahydroquinolines.<sup>182,183</sup> However, these catalysts have also been involved with dehalogenation of aryl halides,<sup>184,185</sup> such as the 7-chloro group in **28**. Due to these concerns, platinum oxide was chosen for the catalytic hydrogenation reaction (Scheme 4). In fact, the chemical literature reported catalytic hydrogenation (conditions: PtO<sub>2</sub>, AcOH, H<sub>2</sub>, rt) of a similar compound (5,6-dichloro-2-methylquinoline).<sup>186</sup> Therefore, dehalogenation of **28** should not occur under these experimental conditions (attempt #1; Scheme 4).

**Scheme 4.**<sup>a</sup>



<sup>a</sup>Reagents and conditions for attempts #1-3: 1) PtO<sub>2</sub>, AcOH, H<sub>2</sub>, 15 psi (18 h); 30 psi (24 h); 45 psi (24 h); 60 psi (24 h); 2) PtO<sub>2</sub>, AcOH, HOCl<sub>4</sub>, H<sub>2</sub>, 60 psi (24 h); 3) Rh/Al<sub>2</sub>O<sub>3</sub>, MeOH, H<sub>2</sub>, 50 psi (24 h).

The experimental procedure reported by Ishikawa and co-workers was first employed in a trial reaction before attempting to hydrogenate **28**.<sup>186</sup> In the model reaction, a solution of isoquinoline in AcOH was partially hydrogenated with PtO<sub>2</sub> under H<sub>2</sub> (50 psi) to afford 1,2,3,4-tetrahydroisoquinoline. Both of these agents (starting material and product) were available in our laboratory and therefore, the reaction was monitored by tlc; tlc analysis suggested complete conversion within 18 h (i.e., UV light detected only the product). Although other laboratories have successfully reduced the

pyridine ring of heterocyclic systems (e.g., quinoline and isoquinoline analogs) with these conditions, attempts to reduce **28** to **31** were unsuccessful.

In the first attempt, **28** was subjected to H<sub>2</sub> under atmospheric pressure ( $\approx$  14.7 psi) for 18 h and no reaction occurred (i.e., tlc analysis indicated only starting material). Subsequently, the pressure was altered to determine if it affected the reaction; increased H<sub>2</sub> pressure (30, 45, and 60 psi) on the Parr hydrogenator for 24 h also resulted in no reaction.

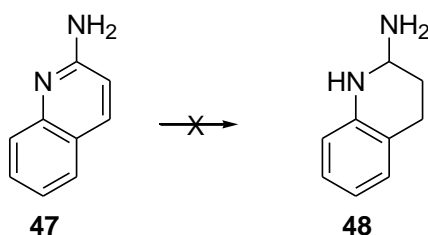
Since time and pressure seemed to have no effect on the reaction, modifying the reagents was considered. In the second attempt, a trace amount of perchloric acid was added to the reaction mixture because strong protic acids can act as promoters (substance that increases catalytic activity).<sup>187</sup> The addition of perchloric acid had no effect on the reaction (attempt #2; Scheme 4).

In the third attempt to reduce the pyridine ring of **28**, the catalyst was changed to Rh/Al<sub>2</sub>O<sub>3</sub>, which was based on a published experimental procedure for the selective hydrogenation (i.e., selective reduction of the pyridine and not the benzene ring) of 6-bromoquinoline as well as 2-substituted quinoline analogs such as 2-methylquinoline with catalyst Rh/Al<sub>2</sub>O<sub>3</sub> and solvent MeOH in the presence of H<sub>2</sub> under increased pressure (50 bar;  $\approx$  725 psi).<sup>188</sup> These analogs were interesting cases because the reaction worked in the presence of a halogen substituent and a substituent at the 2-position of quinoline. It is important to note, that conversion of 2-methylquinoline to 1,2,3,4-tetrahydro-2-methylquinoline was only 40% in 22 h whereas after 1 h, 6-bromoquinoline was consumed.<sup>188</sup> Although there was 100% conversion observed in the 6-bromoquinoline reaction, two products were formed: the desired product 6-bromo-

1,2,3,4-tetrahydroquinoline (82%) and the debrominated product 1,2,3,4-tetrahydroquinoline (18%).<sup>188</sup> In our reaction, **28** was subjected to similar conditions (Rh/Al<sub>2</sub>O<sub>3</sub>, MeOH, H<sub>2</sub>, 50 psi) for 24 hours, but only starting material was detected. It is possible that **28** would undergo hydrogenation at increased pressure (e.g., 50 bar as in the literature procedure), but unfortunately we do not have that capability in our laboratory.

In addition to the PtO<sub>2</sub> experimental (attempt #1; Scheme 4), Ishikawa and co-workers described the partial hydrogenation of the quinoline analog, 6-fluoro-2-methyl-5-(4-methyl-1-piperiziny)quinoline, with 5% platinum on carbon under atmospheric H<sub>2</sub> in high yield (91%).<sup>186</sup> Since **28** was prepared in small quantity, trial reactions were first done with the commercially available dechlorinated starting material (**47**; 2-aminoquinoline). Unfortunately, when **47** was exposed to the same conditions, only starting material fluoresced under UV light (attempt #1; Scheme 5).

#### Scheme 5.<sup>a</sup>



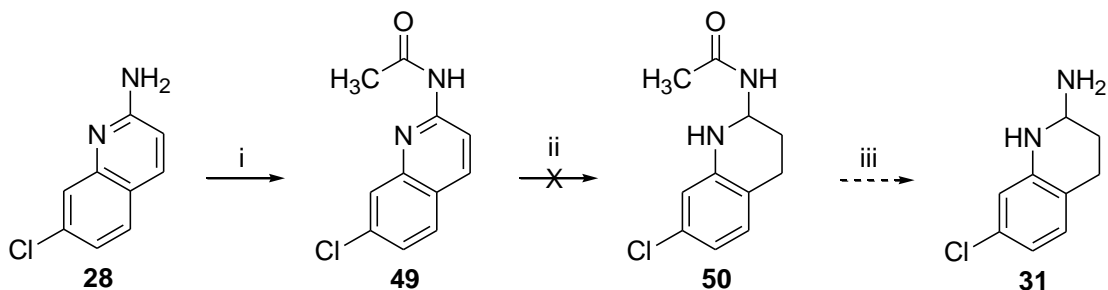
<sup>a</sup>Reagents and conditions for attempts #1 and 2: 1) 5% Pt/C, AcOH, H<sub>2</sub>, 15 psi (24 h); 2) NaCNBH<sub>3</sub>, BF<sub>3</sub>·OEt<sub>2</sub>, MeOH, reflux.

There is another interesting hydrogenation reaction reported in the literature which used NaCNBH<sub>3</sub> in the presence of boron trifluoride etherate in refluxing MeOH to

selectively reduce the nitrogen-containing ring in quinoline derivatives.<sup>189</sup> In a last attempt to convert 2-aminoquinoline (**47**) to 2-amino-1,2,3,4-tetrahydroquinoline (**48**), the same conditions were applied to **47**, but over the course of 9 h no appreciable product formed (reaction monitored by tlc analysis: no products fluoresced under UV light and only a very faint spot near the baseline appeared, but over time this spot did not increase in intensity).

To our knowledge, there is no reported reactions involving the reduction of a 2-aminoquinoline analog to its 1,2,3,4-tetrahydro derivative. However, Moon and Hsi tried to directly hydrogenate 3-aminoquinoline.<sup>190</sup> Although it is stated that the direct hydrogenation of 3-aminoquinoline to 3-amino-1,2,3,4-tetrahydroquinoline was unsuccessful, no details of the reaction conditions (e.g., reagents, time, temperature, etc.) were provided.<sup>190</sup> On the other hand, they were able to selectively reduce the pyridine ring following acylation of the amine in the 3-position.<sup>190</sup> Subsequently, the crude amide was hydrolyzed to afford 3-amino-1,2,3,4-tetrahydroquinoline.<sup>190</sup> Due to these results, attempts were made to reduce 7-chloro-2-formamidoquinoline (**49**) in the same manner (Scheme 6).

**Scheme 6.**<sup>a</sup>



<sup>a</sup>Reagents and conditions: i)  $\text{Ac}_2\text{O}$ ,  $\text{AcOH}$ ,  $\text{THF}$ ,  $\text{N}_2$ ; ii)  $\text{PtO}_2$ ,  $\text{AcOH}$  or  $\text{MeOH}$ ,  $\text{H}_2$ , 50 psi (24-60 h); iii)  $\text{HCl/EtOH}$ ,  $70^\circ\text{C}$ .

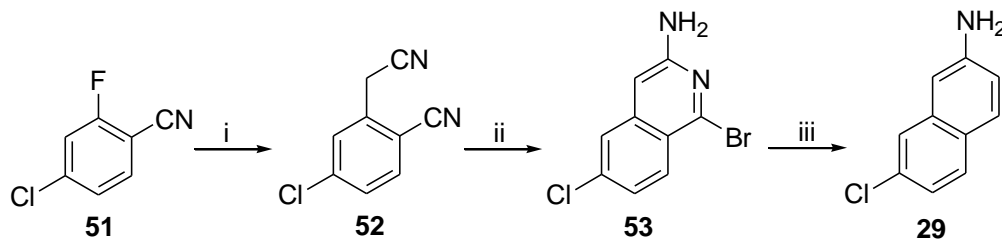
Compound **49** was synthesized by acylating **28** with acetic anhydride (Scheme 6). Unlike the reported results with the 3-formamido derivative, **49** did not reduce to **50**. Various experimental conditions were modified to determine if any affected the reaction (e.g., solvents: AcOH and MeOH, time, and pressure). Though most experimental modifications did not seem to change the reaction progress as monitored by tlc analysis (i.e., only starting material was detected), time appeared to alter the tlc. For example, after 3 d on the Parr hydrogenator (50 psi), there were two faint product spots detected on tlc [eluent: EtOAc/MeOH = 20:1; starting material **49** ( $R_f = 0.5$ ) and products ( $R_f = 0.3$  and  $0.8$ )], but these spots did not increase in intensity and the starting material did not decrease in intensity after an additional 4 d on the Parr hydrogenator. Therefore, the reaction was stopped after a total of 7 d and the two minor products were purified by preparative tlc (eluent: EtOAc/MeOH = 20:1). An insufficient amount was collected by preparative tlc to characterize these compounds. The reaction was repeated on a larger scale, but no products were formed. Synthesis of **31** was abandoned.

#### 4. 3-Amino-6-chloroisoquinoline Hydrochloride (**29**)

Compound **29** was prepared in a three-step synthesis. First, a nucleophilic aromatic substitution of the commercially available starting material 4-chloro-2-fluorobenzonitrile (**51**) occurred resulting in a substitution of the aryl halide with a benzylic nitrile. Specifically, the sodium anion of ethyl cyanoacetate reacted with the 2-fluoro group of **51** to produce an ester intermediate and upon refluxing the ester in water, decarboxylation occurred to yield compound **52**. The di-nitrile product was

purified by recrystallization from Et<sub>2</sub>O (identical mp compared to lit.<sup>191</sup> mp). Cyclization of **52** was achieved by adding a solution of HBr in AcOH, allowing the reaction mixture to stir for 1 h and precipitating compound **53** with Et<sub>2</sub>O. The resulting crude product was neutralized, dried and purified via column chromatography.

**Scheme 7.**<sup>a</sup>



<sup>a</sup>Reagents and conditions: i) ethylcyanoacetate, NaH, DMSO, 0 °C to rt, 30 min., 90 °C for 90 h, water, reflux, 8 h; ii) HBr, AcOH, Et<sub>2</sub>O; iii) n-BuLi in hexanes, anhydrous THF, N<sub>2</sub>, -70 °C, 30 min, absolute EtOH.

In the last step of Scheme 7, selective debromination in the 1-position was attempted; such selective debromination has been previously done on a similar compound, 3-amino-1,6-dibromoisoquinoline.<sup>192</sup> However, when a mixture of 3-amino-1-bromo-6-chloroisoquinoline, ammonium formate, tetrakis(triphenyl phosphine) palladium and DMF was heated to 50 °C in a sealed tube, the TLC analysis after only 8 hours (literature procedure reported 48 hour reaction) displayed a very faint product spot and approximately 8 additional spots. It was apparent that purification of each product would be very difficult.

Therefore, in a second attempt, a known catalyst-free reaction was used to try to synthesize **29**. In this literature reported procedure, selective debromination of both 1-bromo-3-chlorobenzene and 1-bromo-4-chlorobenzene occurred in high yield (approximately 98%).<sup>193</sup> Nevertheless, when **53** was reacted with LiAlH<sub>4</sub> in the

presence of DME for 18 hours (submerged in a ultrasound cleaner), no reaction occurred (only starting material fluoresced on the tlc plate and  $^1\text{H}$  NMR indicated starting material only).

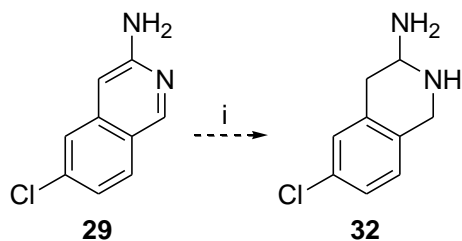
In the last attempt to selectively debrominate, compound **53** was reacted with *n*-butyllithium (2.5 M in hexanes) under a  $\text{N}_2$  atmosphere and followed by ethanolic quenching. This reaction scheme was successfully used to selectively debrominate the 1-position bromo group of 1,3-dibromoisoquinoline.<sup>194</sup> Successful synthesis of the debrominated product **29** occurred when using the procedure of Muchowski et al.,<sup>194</sup> but the product was not without impurities. The tlc analysis showed two products; the major spot was **29** and the minor spot was presumably the *des*-chloro analog of the the product or the *des*-chloro analog of the starting material (i.e., either 3-aminoisoquinoline or 3-amino-1-bromoisoquinoline, respectively). Upon recrystallization from benzene, pure product **29** as a free base was obtained (mp 232-234 °C) and confirmed by elemental analysis. An attempt was made to convert the free base to an HCl salt, however elemental analysis indicated that it was not a pure HCl salt of **29**.

### 5. 3-Amino-6-chloro-1,2,3,4-tetrahydroisoquinoline hydrochloride (**32**)

Similar to the synthesis of **31**, attempts to partially hydrogenate **32** were unsuccessful.



**Scheme 8.<sup>a</sup>**



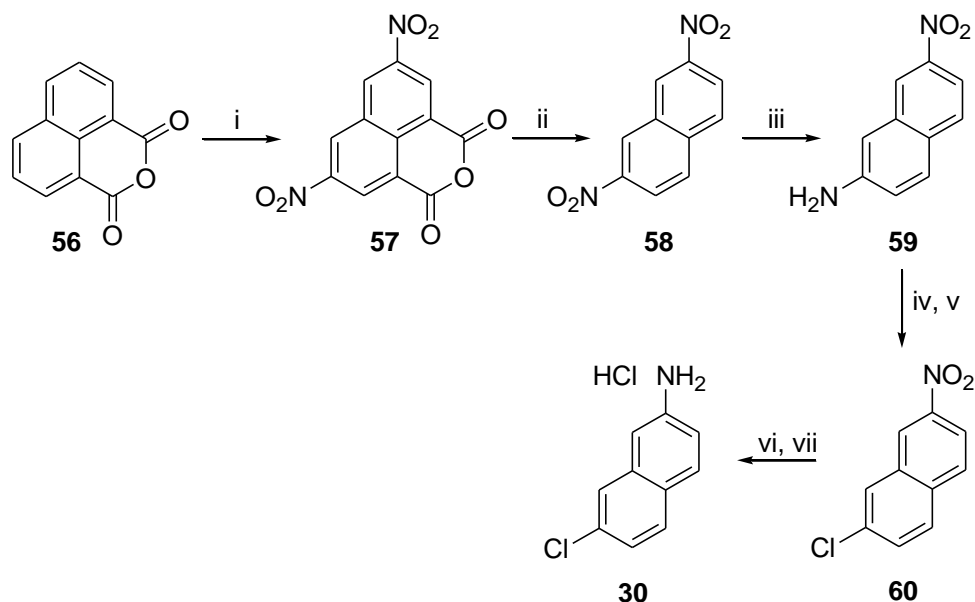
<sup>a</sup>Reagents and conditions: i) PtO<sub>2</sub>, MeOH, H<sub>2</sub>, 50 psi.

Even after reacting **29** with H<sub>2</sub> (50 psi) in the presence of a platinum catalyst for 3 days, only starting material was detected in the reaction mixture based on tlc and <sup>1</sup>H NMR analyses. The route was abandoned.

## 6. 2-Amino-7-chloronaphthalene Hydrochloride (**30**)

Compound **30** was prepared according to literature procedures for similar compounds (Scheme 9).<sup>195-199</sup>

**Scheme 9.<sup>a</sup>**



<sup>a</sup>Reagents and conditions: i)  $\text{H}_2\text{SO}_4$ ,  $\text{HNO}_3$ , 20 °C to 60 °C; ii)  $\text{Cu}$ , quinoline, reflux; iii)  $\text{MeOH}$ , reflux,  $\text{NaSH}$ ,  $\text{MeOH}/\text{H}_2\text{O}$  (1:2), reflux; iv)  $\text{NaNO}_2$ ,  $\text{H}_2\text{SO}_4$ ,  $\text{AcOH}$ , 0 °C; v)  $\text{Cu(I)Cl}$ ,  $\text{HCl}$ , 0 °C; vi)  $\text{PtO}_2$ ,  $\text{H}_2$ , absolute  $\text{EtOH}$ , rt; vii) absolute  $\text{EtOH}$ ,  $\text{HCl}$  (g), 0 °C.

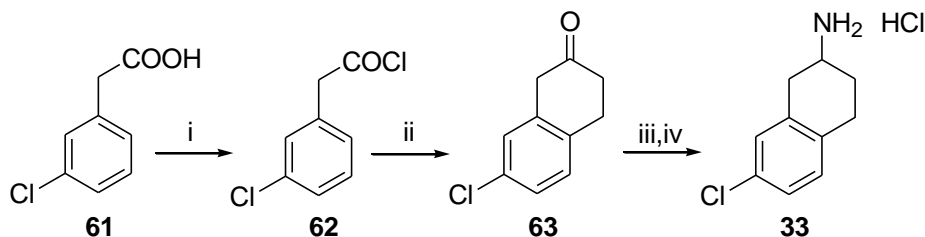
Addition of nitric acid selectively nitrated the starting material **56** at the meta positions to afford 3,6-dinitro-1,8-naphthalic anhydride (**57**). Decarboxylation of the anhydride moiety in a quinoline solution with copper powder, as in step ii, was first described by Shepard et al. in 1930.<sup>200</sup> Although the mechanism is not completely understood, the literature suggests that quinoline's basicity and high boiling point facilitates carboxylate anion formation by withdrawing d-electrons from the copper catalyst.<sup>201,202</sup> In the current case, the decarboxylated product **58** was partially reduced to 2-amino-7-nitronaphthalene (**59**) by the addition of approximately one equivalent of sodium hydrosulfide. In the fourth and fifth step of Scheme 9, the aryl amine was converted to the aryl chloride via a Sandmeyer reaction. In the last step, reduction of **60** to 2-amino-7-chloronaphthalene (**30**) occurred under mild conditions ( $\text{PtO}_2$ , rt,

atmospheric H<sub>2</sub>) in order to reduce the possibility of dehalogenation; subsequently the free base was converted to a hydrochloride salt via the addition of HCl gas to an ethanolic solution.

## 7. 2-Amino-7-chlorotetralin Hydrochloride (33)

Compound **33** was prepared according to a literature procedure for similar compounds (Scheme 10).<sup>203,204,206</sup>

**Scheme 10.**<sup>a</sup>

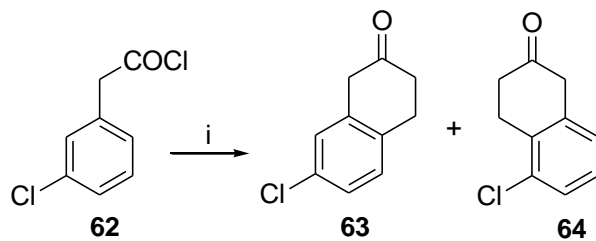


<sup>a</sup>Reagents and conditions: i) SOCl<sub>2</sub>, CH<sub>2</sub>Cl<sub>2</sub>, reflux; ii) CH<sub>2</sub>Cl<sub>2</sub>, AlCl<sub>3</sub>, C<sub>2</sub>H<sub>4</sub> (g), -10 °C to 0 °C, H<sub>2</sub>O; iii) NaBH<sub>3</sub>CN, NH<sub>4</sub>OAc, MeOH, rt; iv) absolute EtOH, HCl/EtOH, 0 °C.

The commercially available phenylacetic acid **61** was converted to the corresponding acid chloride **62** upon the addition of thionyl chloride and was subsequently purified under reduced pressure distillation (0.5 Torr, bp 97-103 °C). In the second step (Friedel-Crafts acylation-cycloaddition reaction<sup>207</sup>), purification of AlCl<sub>3</sub> via *prior* sublimation improved the yield of the reaction. A methylene chloride solution of compound **62** was added to a suspension of AlCl<sub>3</sub> in CH<sub>2</sub>Cl<sub>2</sub> at -10 to 0 °C under inert conditions (Scheme 10, step ii); ethylene gas was bubbled into the reaction mixture for

30 min, which caused the reaction temperature to slightly increase to 5-10 °C. Although no starting material remained, two products were formed due to two possible cyclization reactions (Scheme 11).

**Scheme 11.**<sup>a</sup>



<sup>a</sup>Reagents and conditions: i) CH<sub>2</sub>Cl<sub>2</sub>, AlCl<sub>3</sub>, C<sub>2</sub>H<sub>4</sub> (g), -10 °C to 0 °C, H<sub>2</sub>O.

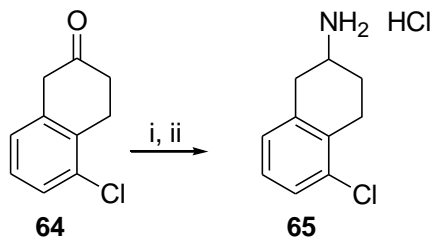
Column chromatography was performed to separate the two tetralones: 5-chloro-β-tetralone (**64**; 15%) and 7-chloro-β-tetralone (**63**; 10%); tlc eluent hexanes/EtOAc = 5:1 (R<sub>f</sub> = 0.6, purple tlc stain and R<sub>f</sub> = 0.5, beige tlc stain, respectively). There were other minor differences between the two products such as 5-chloro-β-tetralone (**64**) was an oil whereas 7-chloro-β-tetralone (**63**) was a low melting point solid (mp 37-38 °C). Structural characterization of the two products was determined by H<sup>1</sup> NMR. Although both products showed three aromatic protons in the H<sup>1</sup> NMR spectrum, there were differences in the chemical shifts and splitting patterns.

To synthesize the desired target compound, **63** was converted to **33** via reductive amination followed by hydrochloride salt formation (Scheme 10).

## 8. 2-Amino-5-chlorotetralin Hydrochloride (65)

Compound **65** was prepared via the same synthetic route as **33** (Scheme 12).

### Scheme 12.<sup>a</sup>



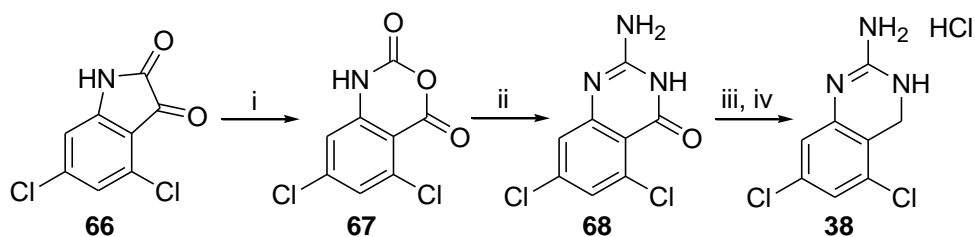
<sup>a</sup>Reagents and conditions: i) NaBH<sub>3</sub>CN, NH<sub>4</sub>OAc, MeOH, rt; ii) absolute EtOH, HCl/EtOH, 0 °C.

The starting material **64** was synthesized from the previous reactions (Schemes 10 and 11). And similar to the preparation of 2-amino-7-chlorotetralin (**33**), reductive amination of  $\beta$ -tetralone **64** produced 2-amino-5-chlorotetralin hydrochloride (**65**; Scheme 12).

## 9. 2-Amino-5,7-dichloro-3,4-dihydroquinazoline Hydrochloride (38)

Compound **38** was prepared according to a literature procedure for similar compounds (Scheme 13).<sup>208-210</sup>

### Scheme 13.<sup>a</sup>



<sup>a</sup>Reagents and conditions: i)  $\text{CrO}_3$ , gl. AcOH,  $\text{Ac}_2\text{O}$ , 90 °C; ii) *S*-methylthioisourea sulfate,  $\text{Na}_2\text{CO}_3$ , aq. MeCN (80%), reflux to rt,  $\text{H}_2\text{O}$ ; iii)  $\text{BH}_3\cdot\text{THF}$  (1M),  $\text{N}_2$ , reflux; iv) absolute EtOH, HCl/EtOH, 0 °C.

The first step was based on a literature procedure,<sup>208</sup> but unlike what was suggested in the literature, the reaction did not go to completion and therefore, starting material **66** and product **67** remained in the reaction mixture. Perhaps due to similar chemical properties, purification via recrystallization (MeOH, isopropanol, or AcOH) and/or chromatography (column or flash) of isatin **66** and isatoic anhydride **67** was not successful. A second oxidation method was attempted in which a suspension of 4,6-dichloroisatin (**66**) in glacial AcOH and concentrated  $\text{H}_2\text{SO}_4$  was heated to 30 °C and then an aqueous solution of  $\text{H}_2\text{O}_2$  was added. However, this reaction did not go to completion as well.

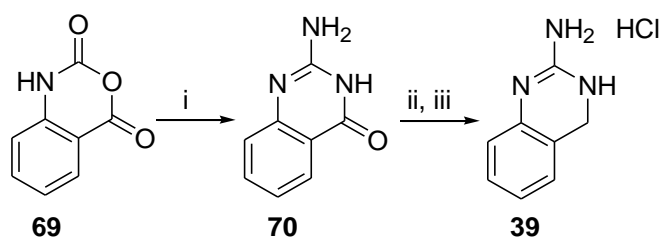
Therefore, the next step was attempted without further purification of **67** because it was thought that it should be easy to purify the product by acid-base extraction. Compound **68** (2-amino-5,7-dichloroquinazolin-4(3H)-one) was prepared by reacting crude isatoic anhydride **67** with *S*-methylthioisourea sulfate (Scheme 13). An acid-base extraction was used to purify the product **68** and recover the starting material (**66**) from

the first step. Reduction of the amide with borane resulted in final compound **38** (Scheme 13). The free base was converted to a hydrochloride salt.

### 10. 2-Amino-3,4-dihydroquinazoline Hydrochloride (**39**)

The des-chloro analog of **38**, 2-amino-3,4-dihydroquinazoline (**39**), was synthesized by the same procedure as described above (Scheme 14).

**Scheme 14.**<sup>a</sup>



<sup>a</sup>Reagents and conditions: i) S-methylthioisourea sulfate, Na<sub>2</sub>CO<sub>3</sub>, aq. MeCN (80%), reflux to rt, H<sub>2</sub>O; ii) BH<sub>3</sub>·THF (1M), N<sub>2</sub>, reflux; iii) absolute EtOH, HCl/EtOH, 0 °C.

Commercially available isatoic anhydride **69** resulted in omission of the first step described in the synthesis of **38**.

Summary: compounds **20**, **28**, **29** (free base), **30**, **33**, **38**, **39**, and **65** were successfully synthesized. Binding affinity at 5-HT<sub>3</sub> receptors has been evaluated for several of the abovementioned synthesized compounds. Compounds **28**, **33** and **65** were found to lack affinity at 5-HT<sub>3</sub> receptors; that is,  $K_i > 10,000$  nM. These preliminary binding affinity results indicate that the ring-nitrogen atoms are important for 5-HT<sub>3</sub> receptor binding. 5-HT<sub>3</sub> receptor binding affinity results of the remaining synthesized

compounds will further evaluate the role of the nitrogen atoms and the chloro substituent in MD-354 (**21**) and conformationally-constrained analogs of MD-354 (**21**) in 5-HT<sub>3</sub> receptor binding.

### C. Molecular modeling

Although MD-354 (**21**) shows no antinociceptive effects when administered alone, it potentiates the antinociceptive actions of the clinically used analgesic clonidine (**7**; non-subtype selective  $\alpha_2$ -AR agonist) in a synergistic manner in the mouse tail-flick assay due to an  $\alpha_2$ -AR mechanism (Table 8).<sup>31,34</sup> Mechanisms underlying the analgesia-potentiating effect are thought to involve at least an  $\alpha_{2A}$ -AR component.<sup>31</sup> Radioligand binding assays indicate that MD-354 (**21**) binds at both low-affinity states (antagonist [ethyl-<sup>3</sup>H]RS-79948-197) and high-affinity states (agonist [<sup>125</sup>I]clonidine) of the three  $\alpha_2$ -AR subtypes (Table 5).<sup>31,34</sup> Furthermore, functional assays show that MD-354 (**21**) is a weak partial agonist at  $\alpha_{2A}$ -ARs, but an antagonist at  $\alpha_{2B/2C}$ -ARs.<sup>31</sup> In an attempt to explain the binding affinity and functional activity of MD-354 (**21**), molecular models were constructed to allow an examination of its binding modes to low- and high-affinity states of  $\alpha_{2A}$ -,  $\alpha_{2B}$ -, and  $\alpha_{2C}$ -ARs.

The  $\alpha_2$ -ARs are G protein-coupled receptors (GPCRs) which are integral membrane proteins that are structurally characterized by 7 transmembrane-spanning (TM) helices connected by intra- and extracellular loops, an amino-terminal (Nt) extracellular domain and a carboxyl-terminal (Ct) intracellular domain (Figures 3, 4 and 54). Interaction with agonists induces a conformational change in the receptor that



allows the receptor to associate with G proteins and initiates a signaling cascade that produces an effect. Due to this conformational change in the receptor, it was necessary to model the “inactive” (or low-affinity) and “active” (or high-affinity) state of  $\alpha_{2A}$ -,  $\alpha_{2B}$ -, and  $\alpha_{2C}$ - ARs.

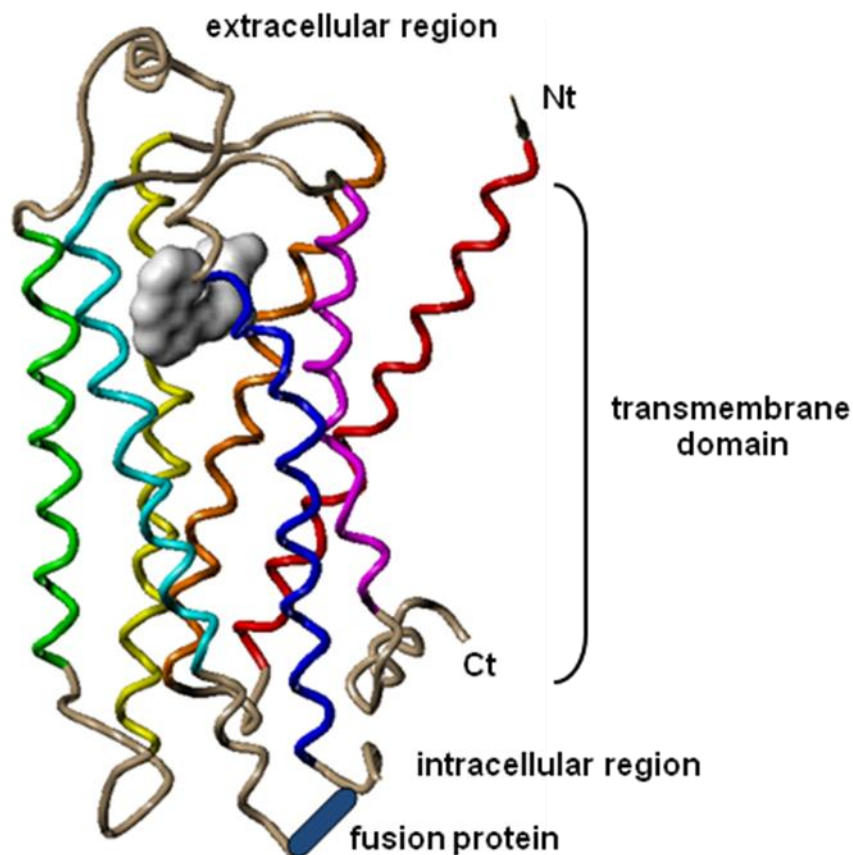


**Figure 54.** X-Ray crystal structure of the  $\beta_2$ -AR (2RH1): TM1 (red), TM2 (orange), TM3 (yellow), TM4 (green), TM5 (cyan), TM6 (blue), TM7 (magenta), intra- and extra-cellular loops (tan) bound to the inverse agonist (carazolol; gray).<sup>57</sup>

There are no high resolution structures of  $\alpha_{2A}$ -,  $\alpha_{2B}$ -, or  $\alpha_{2C}$ -ARs. Among the known GPCR crystal structures, the  $\beta_2$ -AR X-ray crystal structure (pdb = 2RH1; 2.4-Å resolution; Figure 54) has the greatest sequence similarity to the three subtypes of  $\alpha_2$ -

ARs.<sup>57</sup> Therefore, this crystal structure, which is in the low-affinity state, was used as a template to generate homology models of  $\alpha_2$ -ARs. This  $\beta_2$ -AR X-ray crystal structure mimics the low-affinity state because an inverse agonist (i.e., carazolol) is bound to the receptor (i.e., an inverse agonist binds preferentially to the inactive conformation of the receptor).<sup>57</sup>

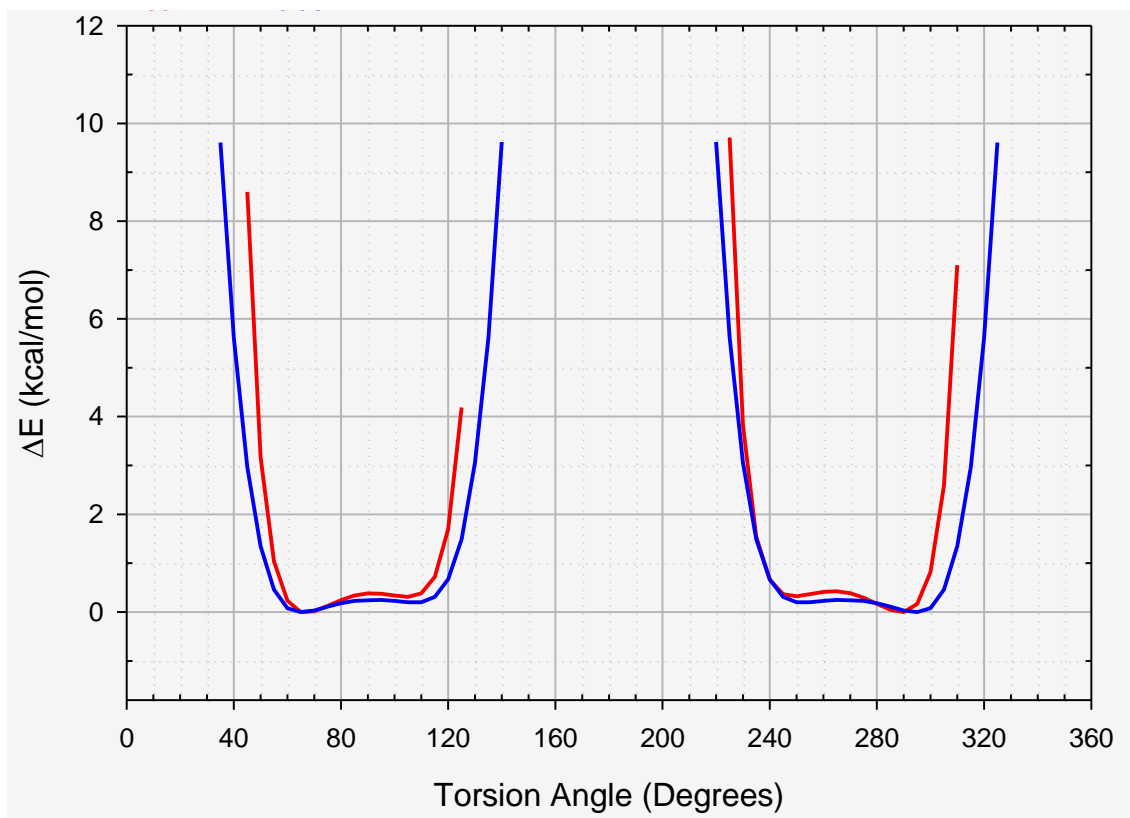
### 1. MD-354 (21) rotamers

MD-354 (21) possesses a rotatable bond (bond between C<sup>1</sup> and the aniline N), and exists as an indefinite number of rotamers (Figure 13). Therefore, it was important to first examine the likely conformations of MD-354 (21). There were two ways of examining the possible conformation(s) of MD-354 (21): (a) a systematic conformation search (SYBYL 8.1) and (b) determination of the conformations of arginine and clonidine in their X-Ray crystal structures, both of which have a guanidine moiety.

A systematic search was conducted on MD-354 (21) to determine its lowest-energy rotamers (Tripos Force Field, AM1; SYBYL 8.1). The systematic search was used to calculate the energy associated with the possible torsion angles of the rotatable bond between C<sup>1</sup> and the aniline N of MD-354 (21; Figure 55a). In general, syn (s) torsion angles are those between 0 and  $\pm 90^\circ$  whereas anti (a) correspond to torsion angles between  $\pm 90$  and  $180^\circ$ . Similarly, stereochemical conformations with a torsion angle between  $\pm 30$  and  $50^\circ$  are called clinal (c) and those between 0 and  $30^\circ$  or  $150$  and  $180^\circ$  are called periplanar (p). When these terms are combined the following ranges of torsion angles are identified: synperiplanar (sp) =  $-30$  to  $30^\circ$ , synclinal ( $\pm sc$ ) =

$\pm 30$  to  $\pm 90^\circ$ , anticlinal ( $\pm ac$ ) =  $\pm 90$  to  $\pm 150^\circ$ , and antiperiplanar ( $ap$ ) =  $\pm 150$  to  $180^\circ$  (Figure 55b).

(a)



(b)

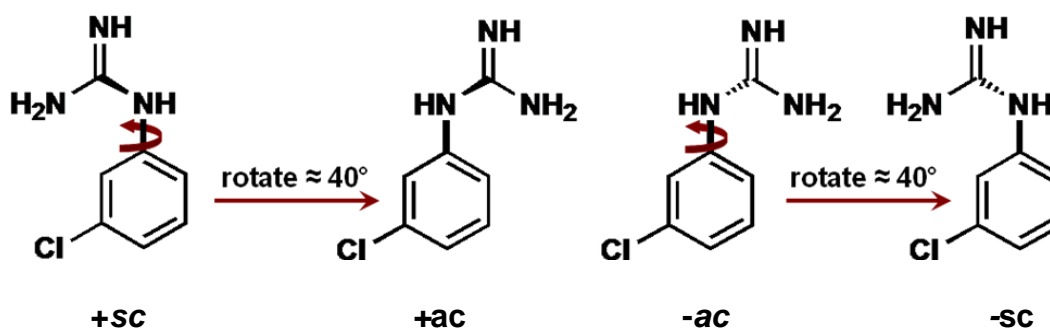


**Figure 55.** (a) Energy associated with the various torsion angles of the rotatable bond in MD-354 (21) (red: TFF; blue: AM1); (b) the four lowest-energy rotamers of MD-354 (21); +/- synclinal (sc) and +/- anticlinal (ac).

Coincidentally, the torsion angle of arginine (from the Cambridge Structural Database) and clonidine crystal structures<sup>212</sup> match one (i.e., the +sc) of the lowest-energy rotamers of MD-354 (**21**). Furthermore, the *m*CPBG crystal structure (57.4 and 301.9° torsion angles) displays similar torsion angles to +sc- and –sc-MD-354 (**21**) (65 and 295° torsion angles).<sup>213</sup> Due to the results from both conformational analyses, the four lowest-energy rotamers of MD-354 (**21**) were employed in the docking studies.

## 2. $\alpha_{2A}$ -Adrenoceptor 3D models

In order to generate the inactive model of  $\alpha_{2A}$ -ARs, the sequences of various GPCRs including the human  $\alpha_{2A}$ -AR and  $\beta_2$ -AR were aligned using ClustalX (other GPCR sequences: human muscarinic ACh M1 receptor, human vasopressin V1a receptor, human dopamine D3 receptor, human  $\delta$ -opioid receptor and bovine rhodopsin) as described by Bissantz et al.<sup>214</sup> This sequence alignment (Figure 56) is, in general, based on aligning the highly conserved amino acids among GPCRs (e.g., D3.32). When comparing the amino acid sequence of the transmembrane regions (TM1-TM7) of  $\alpha_{2A}$ -ARs and  $\beta_2$ -ARs, 41% are identical and 68% are similar (e.g., L and V residues are similar, but not identical). Using the ClustalX alignment, the side chains of amino acids within the transmembrane (TM) helices of the  $\beta_2$ -AR crystal structure (pdb ID: 2RH1) were mutated to mimic the  $\alpha_{2A}$ -AR (Sybyl 8.1). The intra- and extracellular loops of the homology model were based on similar protein loops (Sybyl 8.1).

```

ACM1_HUMAN      -----MNTSAP-----PAVSPNITVLPAGKG-----PWQVAFIGITTTGL
V1AR_HUMAN      MRLSAGPDAGPSGNSSPWNPATGAGNTRSREAEALGEGNGPDRVFNELAKLEIAVLAV
D3DR_HUMAN      -----MASLSQ-----LSSHLYNTTCG--AEN-----STGASQARPHAYYALS YCA
B2AR_HUMAN      MGQPGNGSAFLL-----APNR--SHAPDHDV-----TQQ-RDEVWVWQMGIVMSL
OPRD_HUMAN      MEPAFSAGAEIQPPLFANA--SDAYPSAFPSAGANASGPPG-ARSASSLALAIATLAYS
OPSD_BOVIN      MNGTEGPNFYVP-----FSNKTGVVRS PFEAP-----QYYLAEFWQFSMLAAYMFL
ADA2A_HUMAN      -----MGSLOPDAGNASWNGTEAPGGGARATPYSLQVTLTLVCLAGL

L S L A T V T G N L L V L I S F K V N T E L K T V M N Y F L L S L A C A D L I I G T F S M N L Y T T Y L I M G - H W A L
T F A V A V L G N S S V L L A L H R T P R K T S R N G H L F I R H L S L A D L A V A F F Q V L P Q M C W D I T Y - R F R G
I L L A I V F G N G L V C M A V L K E R A L Q T T N Y L V V S L A V A D L L V A T L V M G W V V Y L E V T G G V M N F
I V L A I V F G N V L V I T A I A K F E R L Q T V T N Y F I T S L A C A D L V M G L A V V F F G A A H I I M K - M W T F
V C A V G L L G N V L V M P G I V R Y T M K T A T N I Y I F N L A L A D A L A T S T L P F Q S A K Y L M E T - W P - F
L I M L G F P I N F L T L Y V T V Q E K L R T P L N Y I L I M L A V A D L F M V F G G F T T T L Y T S L R G - Y V F F
I M L L T V F G N V L V I I A V F T S R A L K A P Q N L F L V S L A S A D I L V A T L V I P F S L A N E V M G - Y W Y F
      . . . . . : : : : :

G T L A C D L N L A L D Y V A S N A S V M N L L L I S F D R Y F S V T R P L S Y R - - - A K R T P R R A A L M I G L A W
P D M L C R V V G H L Q V F G M F A S A Y M L V V M T A D R Y I A V C H P L K T L - - - Q Q - P A R R S R L M I A A A W
S R I C C D V F V T L D V M C T A S I I N L C A I S I D R Y T A V V M P V H Y Q H G T Q Q S S C R R V A L M I T A V W
G N F W C E F W T S I D V L C V T A S I E T L C V I A V D R Y F A I T S P F K Y Q S - L L T - - - I G N Q A R V I I L M W
G E L L C K A V L S I D Y N G M T S I F T L D M S V D R Y I A V C H P V K A L - - - D F R T P A K A K L I N I C I W
G P T Q C N L E G F F A T L G C E I A L W S L V L A I E R Y V V V C K P M S N F - - - R F G - E N H A I M G V A F T W
G R A W C E I Y L A L D V L F C T S S I V H L C A I S L D R Y M S I T Q A I E Y N - - - L S R T P R R I K A I I T V W
      * : : * : : * * : .. : * :

I V S F V L M A P A I L F W Q Y L V G E R T V L A - - - G Q C Y I Q F L S - - - - - Q P I I T F G T A M A A F Y L P V T
V L S F V L S T P Q Y F S M I E V N - - - N - - - V T K A R D C K A T F I Q P W - - - G S R A V Y T W M T G G I F V A F V V
V L A F A V S C P L L F G F N T T - - - G - - - D P - - - T V C S I S - - - - - N P D F V I Y S S V V S F Y L P F G
I V S G L T S F L P I Q M H Y R A T H Q - - - E A - - - I N C Y A N - - - E T C D F F T N Q A Y A I A S S I V S F Y V P L V
V L A S G V G V P I M V - M A V T R P R D - - - G A - - - V V C M L Q F P S P S W Y W - - - D T V T K I C V F L F A F V V P I L
V M A L A C A A P F L V G M S R Y I P E G - - - M Q - - - C S C G I D Y Y T P H E E T N N E S F V I Y M F V V H F I I P L I
V I S A V I S F P P L I S I E K K G G G G P Q P A E P R C E I N - - - - - D Q K W V V I S S C I G S F F A P C L
: : * . . . . .

V M C T L Y N R I Y R E F S L V K E K K A A R T L S A I L L A F I L T W T F Y N I M V L V S T F C K D - C - -
I L G T C Y G F I C Y N S I S R A K I R T V F M T F V I V T A Y I V C W A P F F I I Q M S V W M D P M S V W T
V T V L V Y A R I Y V V G V P L R E K K A T Q M V A I V L G A F I V C W L P F F L T H V L N T H C Q T C H - -
D M V F V Y S R V F Q E K F C L K E H K A L K T L G I D M G T F T L C W L P F F F I V N I V H V I Q D - N L - -
I I T V C Y G I M L L R E K D R S L R R I T R M V L V V G A F V V C W A P I H I F V I V W T L V D I D R R D
V I F F C Y G Q L V F T T T Q K A E K E V T R M V I I M V I A F L I C W L P Y A G V A F Y I P T H Q G S D - -
I M I L V Y V R I Y Q I G R Q N R E K R F T F V L A V V I G V F V V C W F F F F T Y T L T A V G C S V P - -
: * : . . . . .

- V P E T L N E L G Y W L C Y V N S T I N P M C Y A L C N K - - - - -
E S E N P T I T I T A L G S L N S C C N P W I Y M F F S G - - - - -
- V S P E L Y S A T T W L G Y V N S A L N E V I Y T T F N I - - - - -
- I R K E V Y I L L N W I G Y V N S G F N P L I Y I Y C R S - - - - -
P L V V A A L H L C I A L G Y A N S S I N E V L Y A F L D E - - - - -
- F G P I F M T I P A F F A K T S A V Y N E V I Y D Q Q K - - - - -
- - - R T L F K F F F N F G Y C N S S I N E V I Y T I F N H D F R R A F K K I L C R G D
      : . : * *

```

**Figure 56.** Amino acid sequence alignment of 6 GPCRs (human muscarinic acetylcholine receptor M1, human vasopressin V1a receptor, human dopamine D3 receptor, human  $\beta_2$  adrenoceptor, human delta-type opioid receptor and bovine rhodopsin receptor) and human  $\alpha_{2A}$ -AR (ADA2A\_HUMAN); the 7 transmembrane helices are highlighted in yellow and highly conserved amino acids amongst GPCRs are highlighted in cyan.

Protein side chains were optimized using a backbone-dependent rotamer library (SCWRL4), and PROCHECK was performed to examine the stereochemistry of the receptor. Protable (SYBYL 8.1) was utilized to check all amino acid bond angles, bond lengths, and torsion angles.

Once the inactive  $\alpha_{2A}$ -AR homology model was energy minimized (Tripos Force Field; Gasteiger-Hückel charges, distance-dependent dielectric constant = 4.0), modifications to the receptor were made to mimic the active state: (a) rotating TM6 (-30°; R6.29-V6.60), (b) tilting the extracellular portion of TM5 into the binding pocket (6°; K5.36-A5.49), and (c) 'turning on' the toggle switch<sup>63</sup> (i.e., modifying the  $\chi_1$  rotameric state of C6.47, W6.48 and F6.52 to *g+*, *t* and *t*, respectively). These modifications were assumed to simulate an active state because they have been observed in other active-state structures of GPCRs.<sup>61-63</sup> Tilting of TM5 brought residues S5.42 and S5.46 approximately 1 Å closer to D3.32. Rigid rotation of TM6 broke the ionic lock (R3.50–E6.30 C $\alpha$  distance = 12.9 Å) and enlarged the intracellular G protein binding cavity consistent with experimental results.<sup>62</sup> Side chain conformations of residues on TM5 and TM6 were adjusted using SCWRL4, and manually, to optimize side chain–side chain interactions. PROCHECK was performed which resulted in a Ramachandran plot. This plot indicates which amino acid residues are within the most favorable (red), additional allowed (yellow), generously allowed (khaki), and disallowed (white) regions (Figure 57). As depicted in Figure 57, 90.4% of the amino acids were within the most favorable region (red), 8.8% in the allowed regions (yellow or khaki) and only two amino acids (0.8%) showed disallowed stereochemistry (white): E237 and C401. However, both of these latter two amino acids are located outside of the proposed binding pocket

and, therefore, for our purposes, these imperfections were ignored and should not impact the docking studies. More specifically, E237, which was just outside the allowable region (Figure 57), is part of IL-3, whereas C401 is part of EL-3.

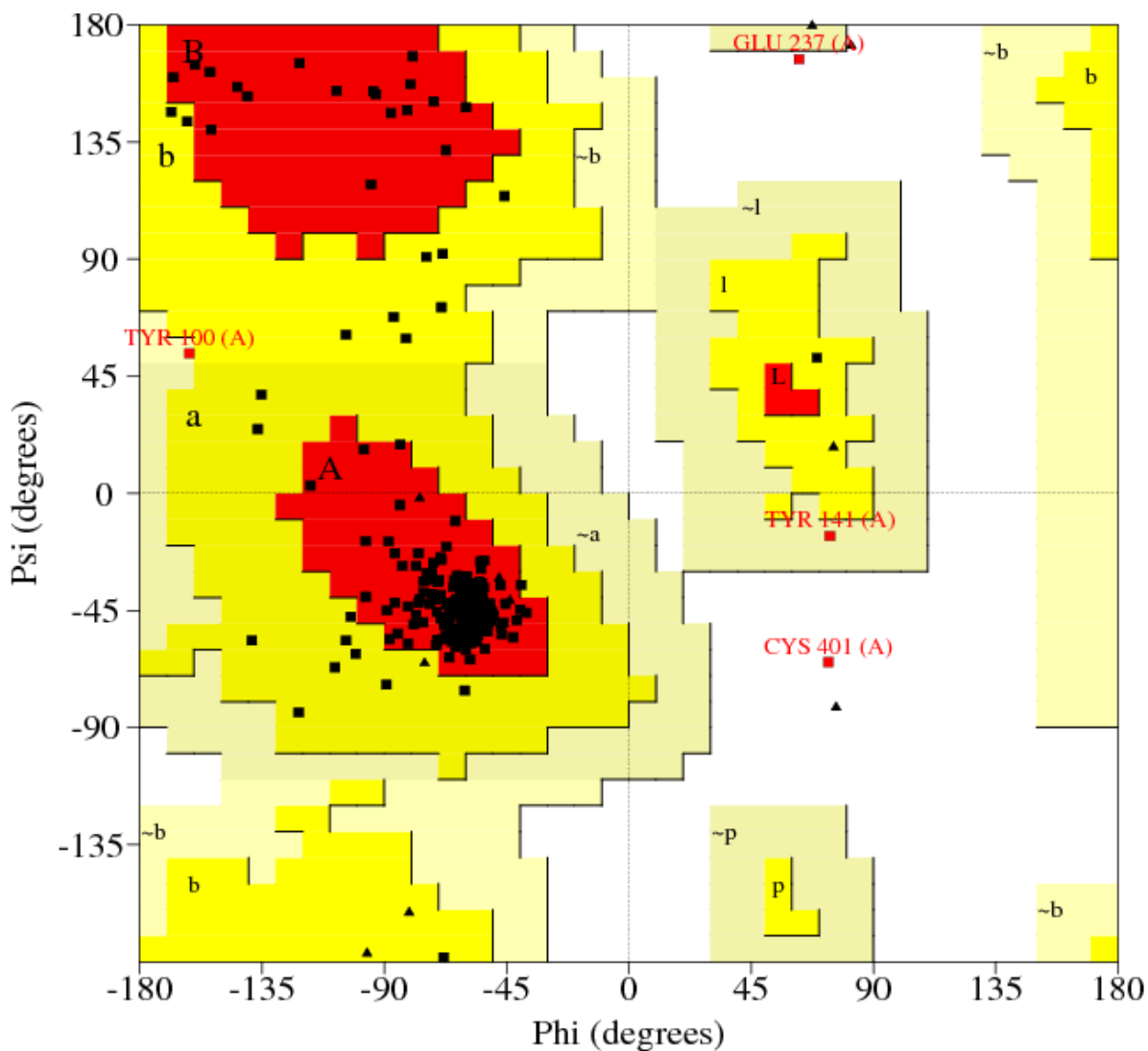


**Figure 57.** A Ramachandran plot of the active  $\alpha_{2A}$ -AR homology model (generated by PROCHECK; Sybyl 8.1).

To validate the energy-minimized active  $\alpha_{2A}$ -AR homology model, the endogenous ligands norepinephrine (NE; **1**) and epinephrine (EPI; **2**) were docked (GOLD 4.0) into the binding pocket (15-18 Å sphere centered around the conserved aspartate in TM3, D3.32). Since both NE (**1**) and EPI (**2**) have a stereocenter, all four isomers were examined in the docking study (NE: (*R*)-**1** and (*S*)-**1**; EPI: (*R*)-**2** and (*S*)-**2**). In the case of both phenylethylamines, the *R*-enantiomers are more active and have higher affinity at  $\alpha_2$ -ARs than those with the *S*-configuration of the  $\beta$ -OH group.<sup>53</sup> Additionally, *N*-methyl-substituted phenylethylamines, such as **2**, have higher binding affinity at  $\alpha_2$ -ARs than unsubstituted analogs, such as **1**.<sup>53</sup> Additional SAFIR studies, including other analogs of **1** and **2**, which were discussed in greater detail in the Background section, have been published in the past two decades (Figure 5 and Table 1).

Due to extensive SAFIR studies, as well as site-directed mutagenesis studies, of phenethylamines, much is known about the binding mode of these agents, which makes phenethylamines a good tool to help validate the homology model. With support from catecholamine molecular modeling studies, the Easson-Stedman hypothesis suggests a three-point interaction between adrenoceptors and catecholamines [e.g., NE (**1**) and EPI (**2**): (a) the protonated aliphatic amine, (b) the catecholic hydroxyl groups, and (c) the  $\beta$ -hydroxyl group (see Table 13 for specific interactions)].<sup>83,84</sup>



**Table 13.** Interactions between  $\alpha_2$ -ARs and catecholamines.<sup>70,85,86</sup>

Chemical interaction	$\alpha_2$ -AR residue	catecholamine moiety
ionic bond	D3.32	charged amine
hydrogen bond	S5.42	<i>meta</i> -hydroxyl
hydrogen bond	S5.46	<i>para</i> -hydroxyl
hydrogen bond	S2.61 or Y6.55	$\beta$ -OH

When necessary, constraints were incorporated into the GOLD dockings of the endogenous ligands: H-bond constraints with the highly conserved D3.32, and distance constraints with S5.42 and S5.46. In general, data from site-directed mutagenesis<sup>85,86,215</sup> and structure-activity relationship (SAR)<sup>215</sup> studies of epinephrine (**2**) and its analogs were used to guide the docked poses into the models. In addition to comparing results to the Easson-Stedman hypothesis (Table 13), various characteristics were analyzed when examining the docking results, such as the GOLDScore (the higher the score, the better the docking result is likely to be based on factors such as H-bonding energy, van der Waals energy and ligand torsion strain), potential “unfavorable” interactions (e.g., the ligand is “too close” to the protein backbone; clashing), and favorable bonding distances (e.g., hydrogen bond  $\approx$  3 Å).

Of the four isomers [i.e., (*R*) and (*S*) isomers of NE (**1**) and EPI (**2**)], (*R*)-EPI (**2**;  $K_i$  = 13 nM) has the highest binding affinity at  $\alpha_{2A}$ -ARs (active state) and, therefore, should display additional and/or stronger interactions with the receptor in comparison to the remaining 3 isomers. As shown in Figure 58, the main ligand–receptor interactions of (*R*)-EPI (**2**) observed in the active  $\alpha_{2A}$ -AR model were: (a) ionic:  $N^+$ —D3.32; (b) HB:  $\beta$ -

OH—D3.32, *m*-OH—S5.42 and *p*-OH—S5.46; (c)  $\pi$ - $\pi$  (edge-to-face): F6.51, Y6.55; CH- $\pi$ : V3.33; (d)  $\pi$ -cation: N<sup>+</sup>—F7.39. The  $\beta$ -OH moiety of (*R*)-EPI (**2**) seems to strongly interact (H-bond) with D3.32 whereas in the docking poses of (*S*)-EPI (**2**), the additional H-bond interaction with D3.32 was absent (i.e., the distance between the oxygen atoms of the  $\beta$ -OH and D3.32 side chain was > 5 Å). This is consistent with the lower binding affinity of (*S*)-EPI (**2**) at  $\alpha_{2A}$ -ARs ( $K_i$  = 687 nM; agonist radioligand).<sup>215</sup>

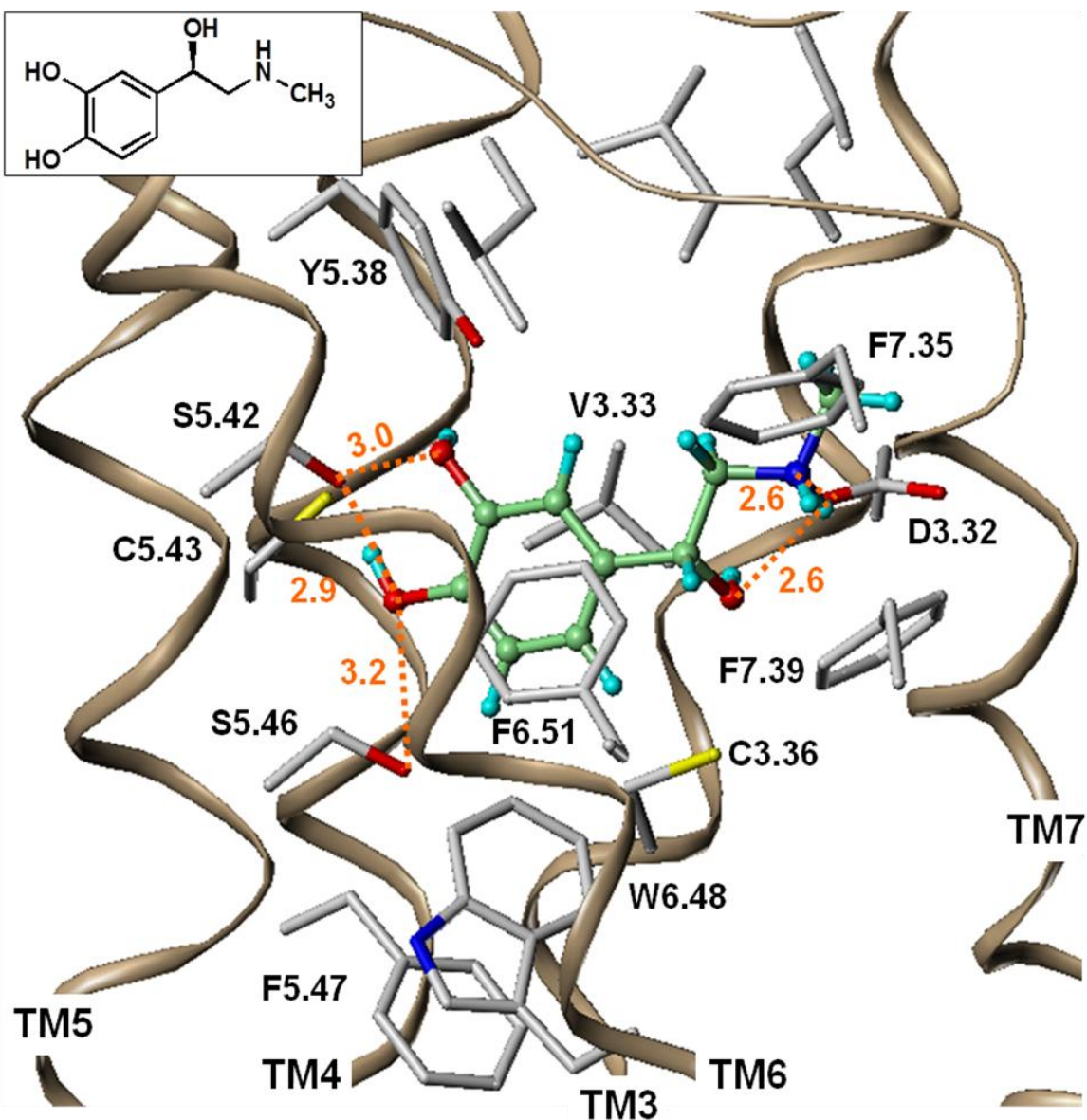


**Figure 58.** Proposed binding mode of (*R*)-epinephrine (**2**) in the active  $\alpha_{2A}$ -AR model. Amino acids within 4 Å are shown as capped sticks (grey) and distances (Å) of favorable ionic and HB interactions are shown in orange.

The docked poses of the norepinephrine (**1**) isomers showed similar results (data not shown). In general, the poses are consistent with binding affinity assay studies of endogenous ligands (and their analogs) that indicate affinity is affected by:  $\beta$ -OH ((*R*)-

isomer > (*S*)-isomers by  $\approx$  20-fold; presence > absence by  $\approx$  8-fold), *m*-OH (presence > absence by  $\approx$  100-fold); *p*-OH (presence > absence by  $\approx$  30-fold).<sup>86</sup> These favorable interactions have been suggested by site-directed mutagenesis studies and are consistent with previous models.<sup>86,215,216</sup>

The four lowest-energy rotamers of MD-354 (**21**), as interpreted from both conformational analyses, were docked in the abovementioned active model of the  $\alpha_{2A}$ -AR (Figure 55). After the MD-354 (**21**) rotamers were docked, energy minimization was implemented in order to optimize the bonding interactions between ligand and receptor. The major bonding interactions observed in the docked poses of MD-354 (**21**) rotamers include: (a) an ionic interaction between both the aniline and terminal nitrogens and D3.32 and (b) hydrogen bonding between the *m*-Cl group and either S5.42 or S5.46, with optimal bond distances (i.e., approximately 3 Å; Figure 59 and Table 14a). There are, also, additional hydrophobic interactions observed in the proposed binding mode of MD-354 (**21**) at the active  $\alpha_{2A}$ -ARs (e.g., V3.33, F6.51, F7.35 and F7.39; Figure 59).

**Table 14.** Distances (Å) of favorable HB and ionic interactions observed in proposed binding mode between ligands and the (a) active and (b) inactive  $\alpha_{2A}$ -ARs.

<b>(a)</b>				
Ligand	D3.32	Y5.38	S5.42	S5.46
<b>(R)-EPI (2)</b>				
terminal N	2.6			
$\beta$ -OH	2.6			
<i>m</i> -OH			3.0	
<i>p</i> -OH			2.9	3.2
<b>+sc-MD-354 (21)</b>				
aniline N	2.8			
terminal N	3.3			
terminal N		3.8		
<i>m</i> -Cl			3.0	
<b>-ac-MD-354 (21)</b>				
aniline N	2.8			
terminal N	3.4			
terminal N		3.9		
<i>m</i> -Cl				3.0
<b>(b)</b>				
Ligand	D3.32	Y6.55	S5.42	
<b>+sc-MD-354 (21)</b>				
aniline N	2.8			
terminal N	3.0			
terminal N		3.1		
<i>m</i> -Cl			3.8	

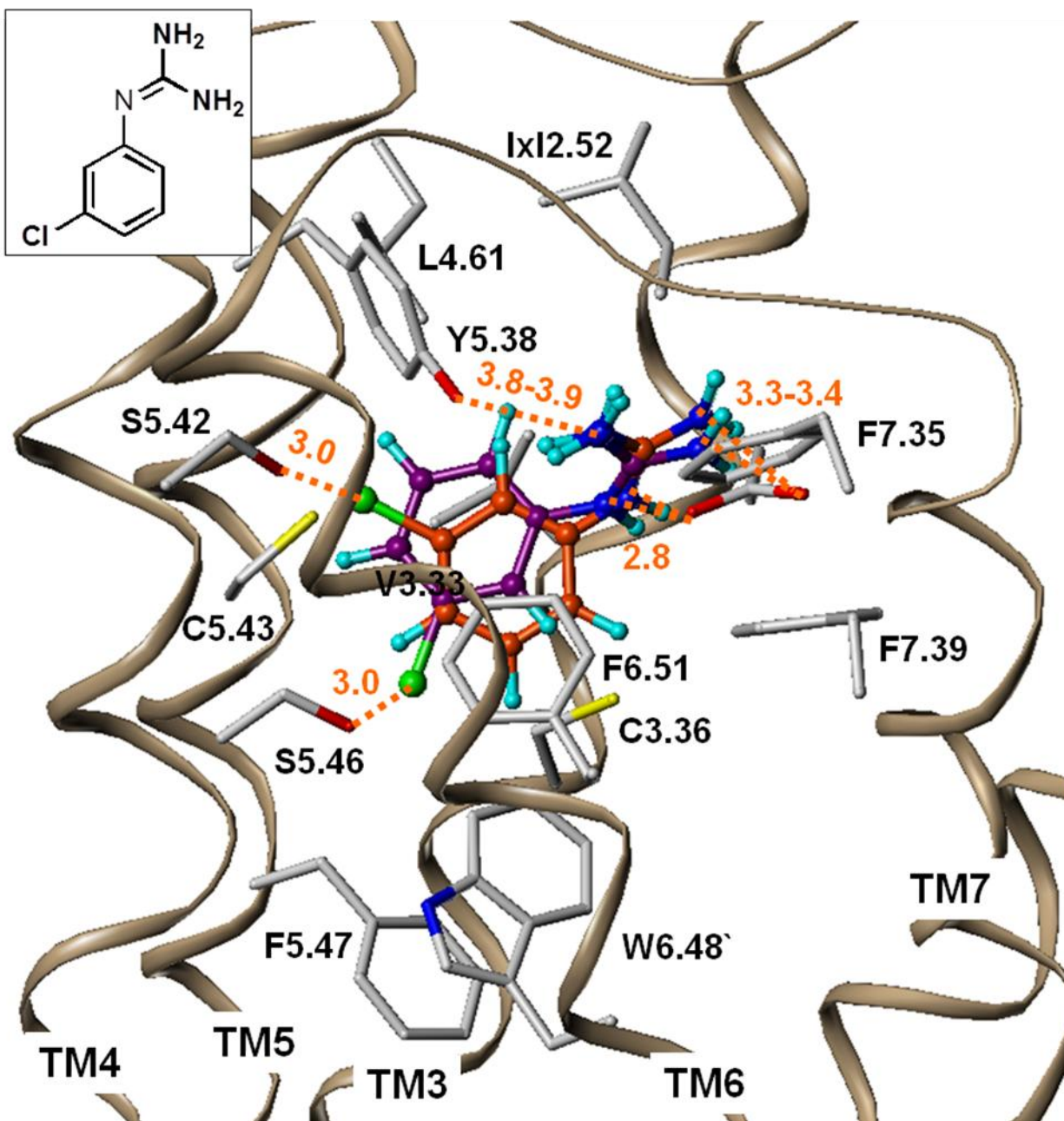


**Figure 59.** Proposed binding mode of  $-ac-$  (magenta) and  $+sc-$  (orange) MD-354 (**21**) in the active  $\alpha_{2A}$ -AR model. Amino acids within 4 Å are shown in capped sticks (grey) and distances (Å) of favorable HB or ionic interactions are shown in orange.

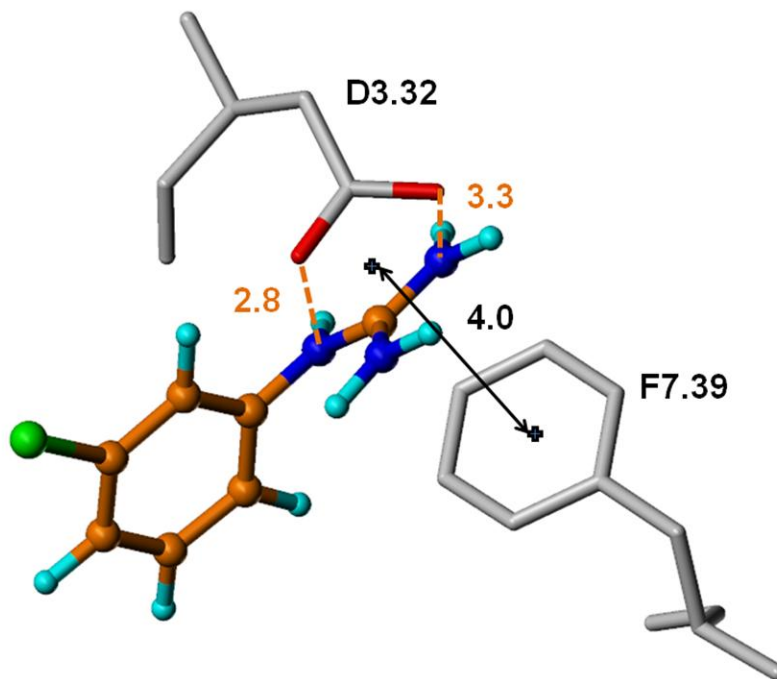


**Figure 60.** Proposed binding mode of +sc-MD-354 (**21**) in the active  $\alpha_{2A}$ -AR model; close-up of the interaction between the guanidinium-D3.32 hydrogen bond network with the aryl ring of F7.39. D3.32 and F7.39 are shown in capped sticks (grey) and distances (Å) of favorable HB interactions are shown in orange whereas the centroid-to-centroid distance between the aryl ring of F7.39 and the 6-membered ring formed between the guanidinium and D3.32 are shown by the black arrow.

In the inactive model of  $\alpha_{2A}$ -ARs, MD-354 (**21**) docked in a similar manner as compared to the active-state docking pose. Although the interaction with the TM5 residues was minimal (i.e., the distance between the *m*-Cl group and the serine residues of TM5 was not optimal for halogen bonding; Table 14b), a more favorable interaction with all three nitrogen atoms of the guanidinium moiety was observed (Figure 61 and Table 14b). Measurements between the heavy atoms indicate a favorable bonding distance between the aniline N and D3.32, the terminal amine and D3.32, and the other terminal amine and Y6.55.

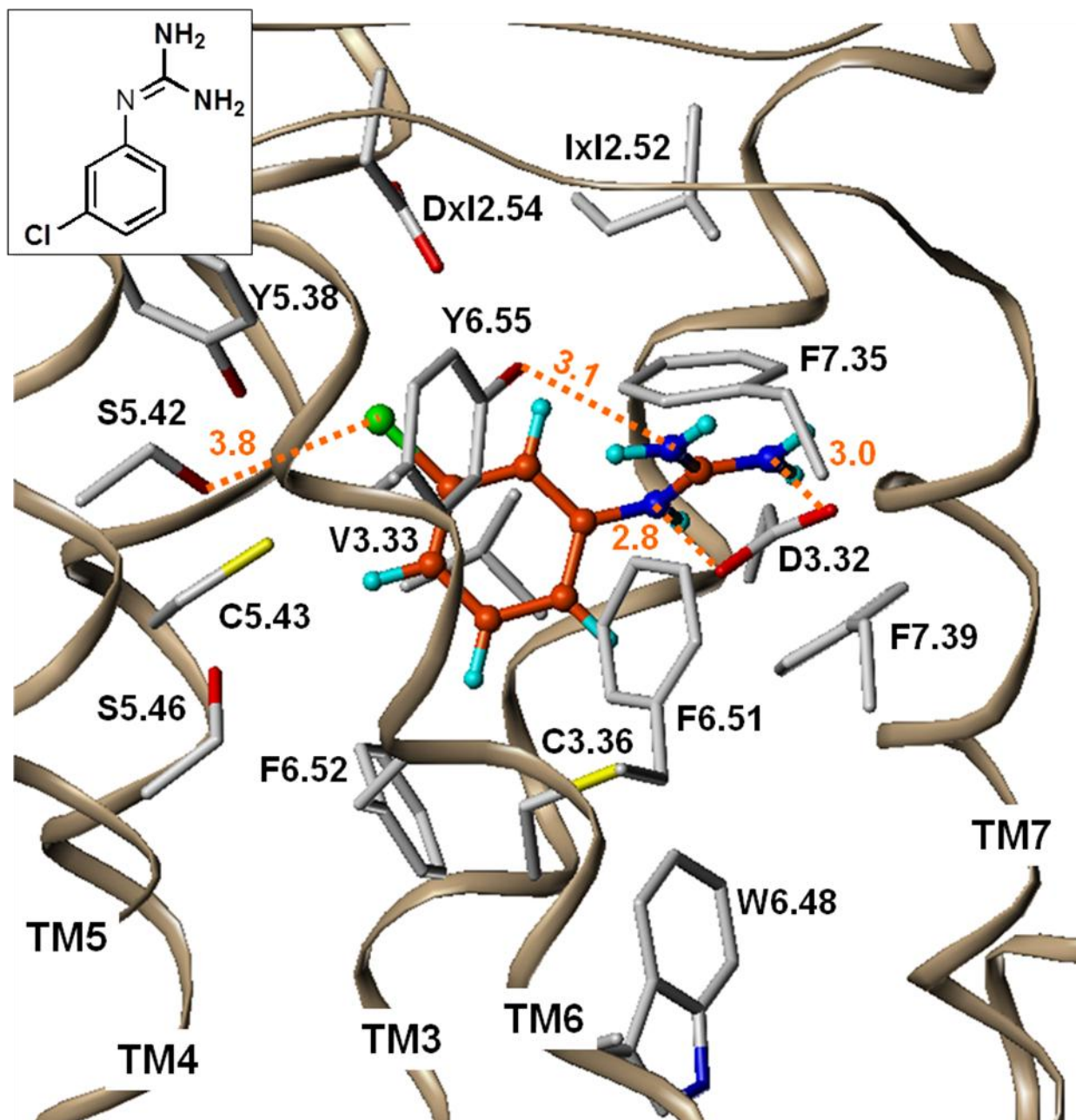


**Figure 61.** Proposed binding mode of +sc-MD-354 (**21**) in the inactive  $\alpha_{2A}$ -AR model. Amino acids within 4 Å are shown in capped sticks (grey) and distances (Å) of favorable HB or ionic interactions are shown in orange.



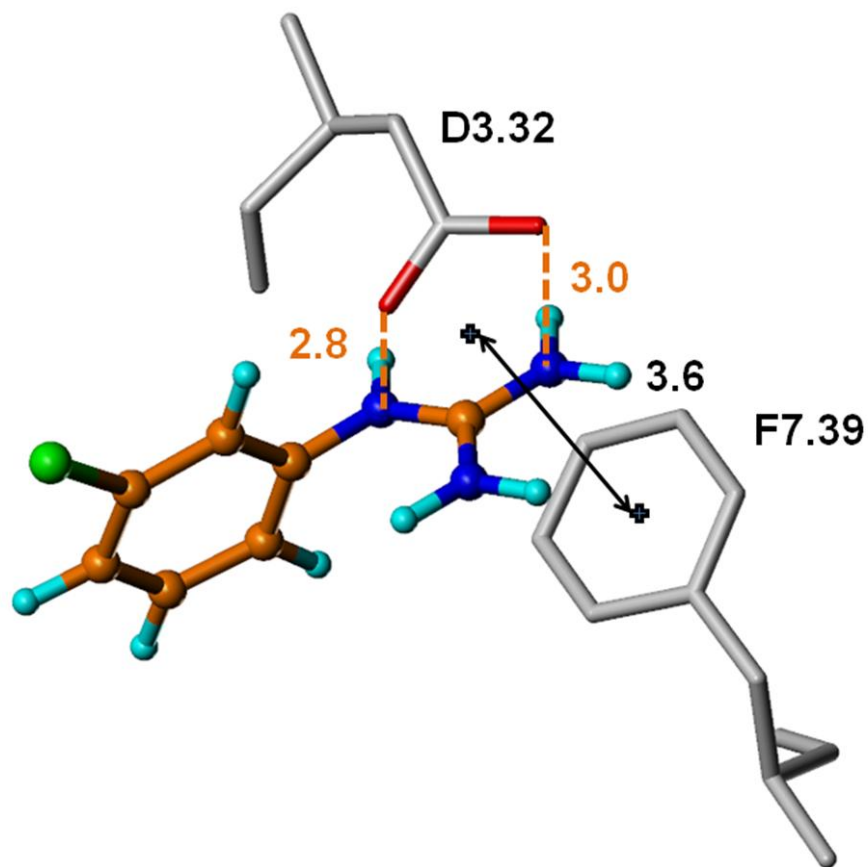


**Figure 62.** Proposed binding mode of +sc-MD-354 (**21**) in the inactive  $\alpha_{2A}$ -AR model; close-up of the interaction between the guanidine-D3.32 hydrogen bond network with the aryl ring of F7.39. D3.32 and F7.39 are shown in capped sticks (grey) and distances ( $\text{\AA}$ ) of favorable HB interactions are shown in orange whereas the centroid-to-centroid distance between the aryl ring of F7.39 and the 6-membered ring formed between the guanidine and D3.32 are shown by the black arrow.

Furthermore, the bonding network between the guanidine moiety of MD-354 (**21**) and the aspartate carboxylate moiety (D3.32) is stacked over the aromatic ring of F7.39 in both the inactive and active  $\alpha_{2A}$ -AR models (Figures 60 and 62). The centroid-to-centroid distance, as shown in these figures, indicates that the 6-membered ring formed by the hydrogen bonding network between the guanidine moiety of MD-354 (**21**) and the carboxylate group of D3.32 has a slightly stronger parallel-stacking interaction with the

aryl ring of F7.39 in the inactive state (3.6 Å) in comparison with the active state (4.0 Å) of the  $\alpha_{2A}$ -AR models.<sup>217</sup>

### 3. $\alpha_{2B}$ -Adrenoceptor 3D models

Since the sequence similarity within the TM regions is greater between  $\alpha_{2A}$ - and  $\alpha_{2B}$ -ARs (94%) compared to  $\alpha_{2B}$ -ARs and  $\beta_2$ -ARs (66%),  $\alpha_{2B}$ -AR homology models were generated based on the previously generated  $\alpha_{2A}$ -AR models. The “active”  $\alpha_{2A}$ -AR model, which was previously supported by simulating the proposed binding mode of the neurotransmitters (i.e., the binding mode based on site-directed mutagenesis results and other homology models), was used as the template for the “active”  $\alpha_{2B}$ -AR model. First, the amino acid side chains among the transmembrane helices were mutated to mimic the  $\alpha_{2B}$ -AR sequence. The intra- and extracellular loops were replaced by protein loops with similar sequences and then the side chains were mutated if necessary (Sybyl 8.1). All protein side chains were optimized using a backbone-dependent rotamer library (SCWRL 4). As a final assessment, PROCHECK was performed to examine the stereochemistry of the receptor and Protable was used to check all amino acid bond angles, bond lengths, and torsion angles (SYBYL 8.1). Protein modifications were manually made when necessary; for example, the  $\chi_1$  torsion angle of S5.42, which has been implicated in neurotransmitter binding, was modified so that the serine side chain pointed into the binding pocket. Protein modifications were followed by energy minimization in order to optimize ligand—receptor interactions.

The two best binding modes of MD-354 (**21**) (i.e., those with the most optimal bonding interactions) at the active  $\alpha_{2B}$ -ARs showed favorable ionic interactions with the conserved D3.32 (bonding distance = 2.7-3.0 Å), as well as hydrogen bonding interaction between the terminal amine of MD-354 (**21**) and Y5.38 (Table 15a and Figure 63). Furthermore, only one MD-354 (**21**) rotamer displayed an interaction with TM5. The proposed binding mode of the *-ac*-MD-354 (**21**) rotamer showed favorable distance (approximately 3 Å) between the *m*-Cl moiety and a serine residue of TM5 (S5.46); that is, a halogen bond interaction was observed between the ligand and receptor (Table 15a and Figure 63).

**Table 15.** Distances (Å) of favorable HB and ionic interactions observed in proposed binding mode between ligands and the (a) active and (b) inactive  $\alpha_{2B}$ -ARs.

<b>(a)</b>			
Ligand	D3.32	Y5.38	S5.46
<b>+sc-MD-354 (21)</b>			
aniline N		2.9	
terminal N	3.0		
terminal N	2.8		
<i>m</i> -Cl			
<b>-ac-MD-354 (21)</b>			
aniline N		2.8	
terminal N	2.9		
terminal N	2.7		
<i>m</i> -Cl			3.2
<b>(b)</b>			
Ligand	D3.32	Y6.55	S5.42
<b>+sc-MD-354 (21)</b>			
aniline N	2.6		
terminal N	2.8		
terminal N			
<i>m</i> -Cl		3.4	
<b>+ac-MD-354 (21)</b>			
aniline N	2.7		
terminal N	2.7		
terminal N			
<i>m</i> -Cl		3.1	3.4
<b>-sc-MD-354 (21)</b>			
aniline N	3.2		
terminal N	3.2		
terminal N	3.0		
<i>m</i> -Cl		2.8	3.9

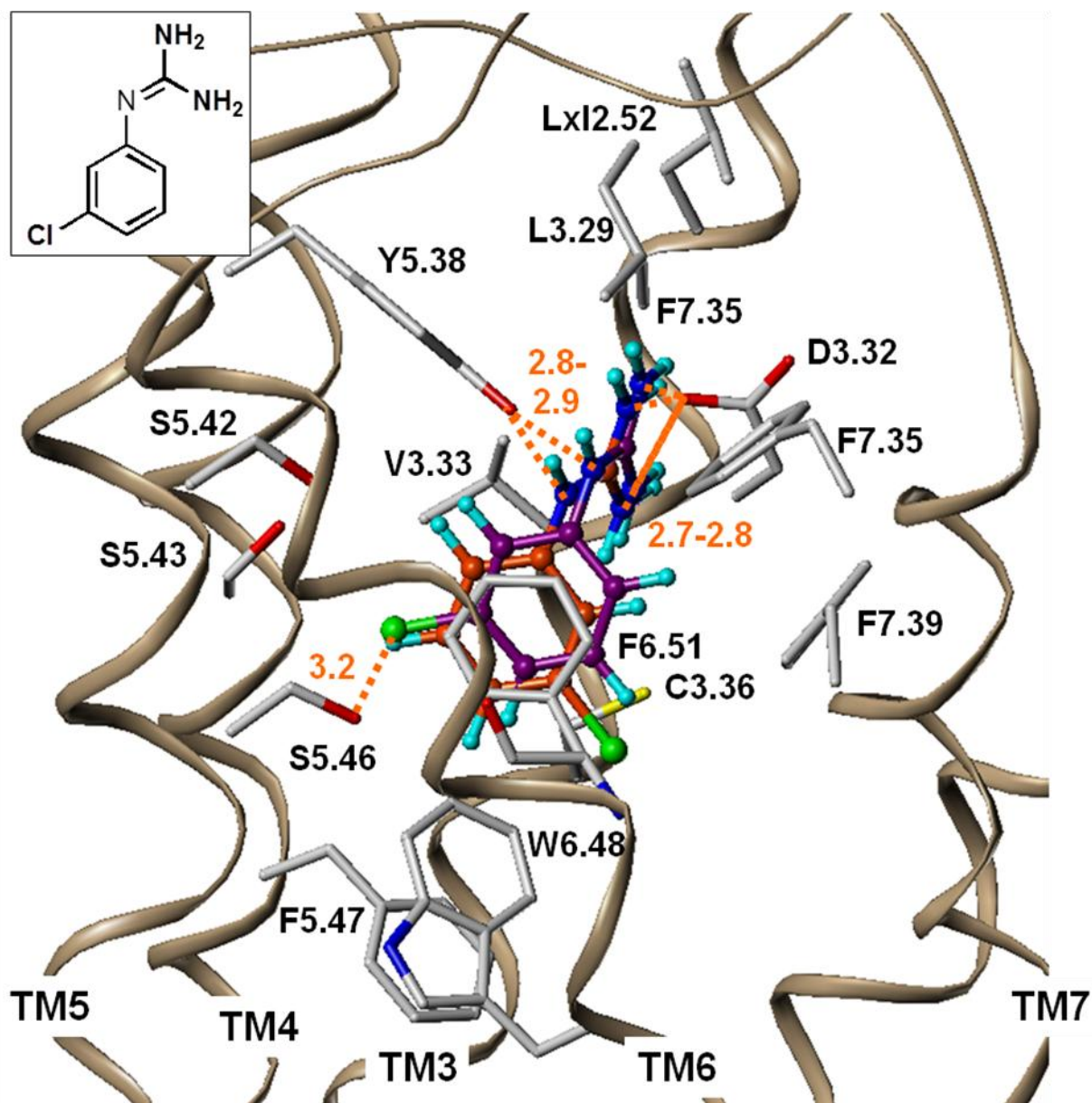


**Figure 63.** Proposed binding mode of  $-ac-$  (magenta) and  $+sc-$  (orange) MD-354 (**21**) in the active  $\alpha_{2B}$ -AR model. Amino acids within 4 Å are shown in capped sticks and distances (Å) of favorable HB or ionic interactions are shown in orange.

In the inactive model of  $\alpha_{2B}$ -ARs, three conformers of MD-354 (**21**) showed good ionic interactions with the conserved aspartate residue (D3.32), as well as, hydrogen

bonding with Y6.55 and either the terminal amine or *m*-Cl group (dependent on the rotamer; Table 15b and Figure 64).

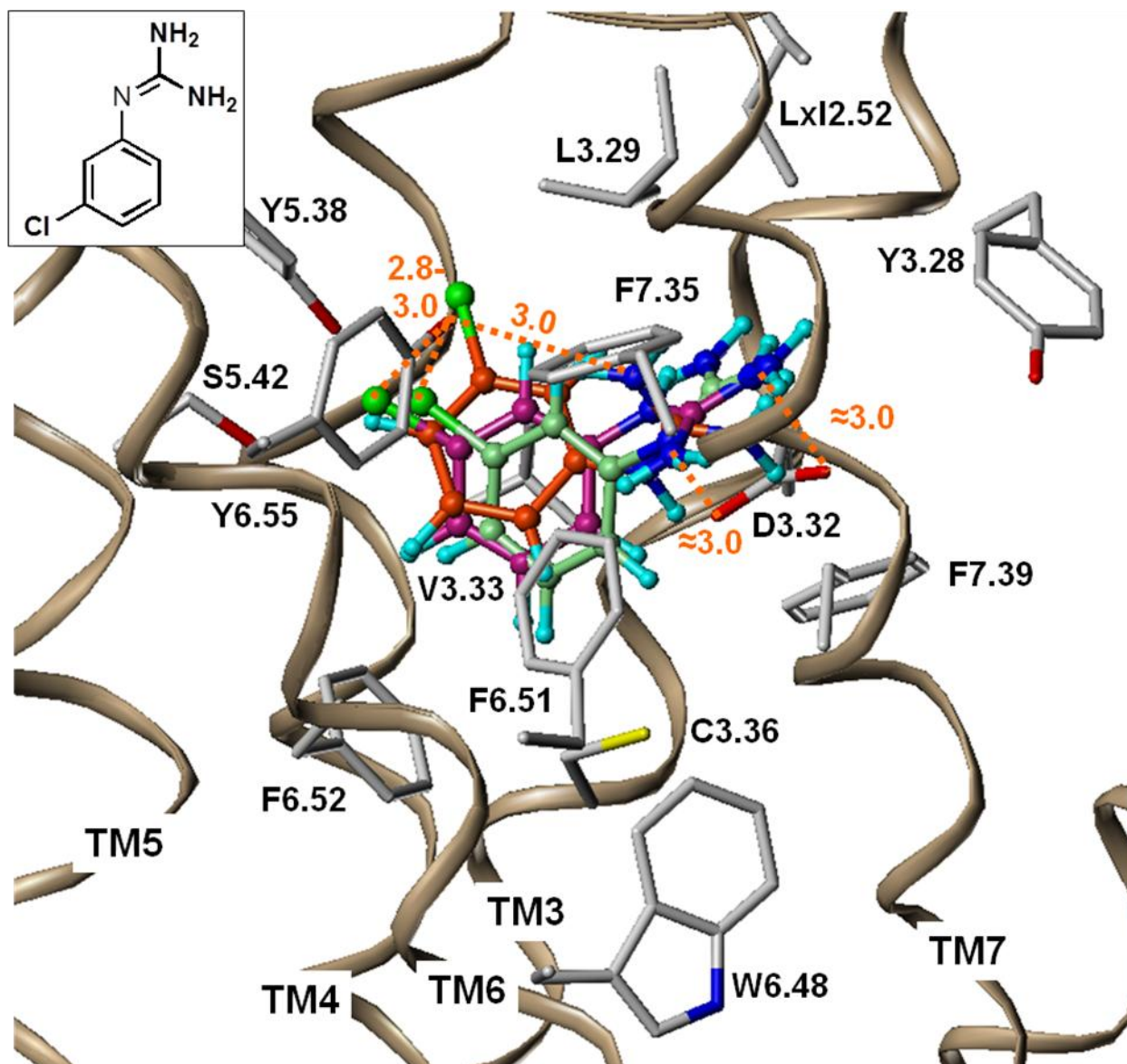


**Figure 64.** Proposed binding mode of *-sc-* (green), *+ac* (magenta), and *+sc-* (orange) MD-354 (**21**) in the inactive  $\alpha_{2B}$ -AR model. Amino acids within 4 Å are shown in capped sticks and distances (Å) of favorable HB or ionic interactions are shown in orange.

As in the active and inactive models of  $\alpha_{2A}$ -ARs, parallel stacking (i.e., a  $\pi$ - $\pi$  interaction) was observed between the bonding network of the amines in MD-354 (**21**) and D3.32 with F7.39 in the inactive model only (i.e., not in the active model) of  $\alpha_{2B}$ -ARs (centroid-to-centroid distance = 3.6 Å; Figure 64).

#### 4. $\alpha_{2C}$ -Adrenoceptor 3D models

The active model of the  $\alpha_{2C}$ -AR was generated in a similar manner to that of the  $\alpha_{2B}$ -ARs. That is, the active  $\alpha_{2A}$ -AR model was mutated to simulate the  $\alpha_{2C}$ -AR sequence, loopsearch was conducted to incorporate possible loop configurations, SCWRL was conducted, protein modifications were made if necessary and the receptor was energy minimized. Next, the NTs [(*R*)- and (*S*)-isomers of NE (**1**) and EPI (**2**)] were docked and the resulting ligand—receptor complex was energy minimized (data not shown). This model (with the ligand removed) was used for subsequent MD-354 (**21**) dockings.

The two best binding modes of MD-354 (**21**) in the active  $\alpha_{2C}$ -AR model showed favorable bonding distances for a halogen bond between the *m*-Cl group of **21** and S5.46 ( $\approx 3.1$  Å), as well as ionic interactions between the amines of **21** and D3.32 and Y5.38 ( $\approx 2.7$ -3.0 Å) (Figure 65).

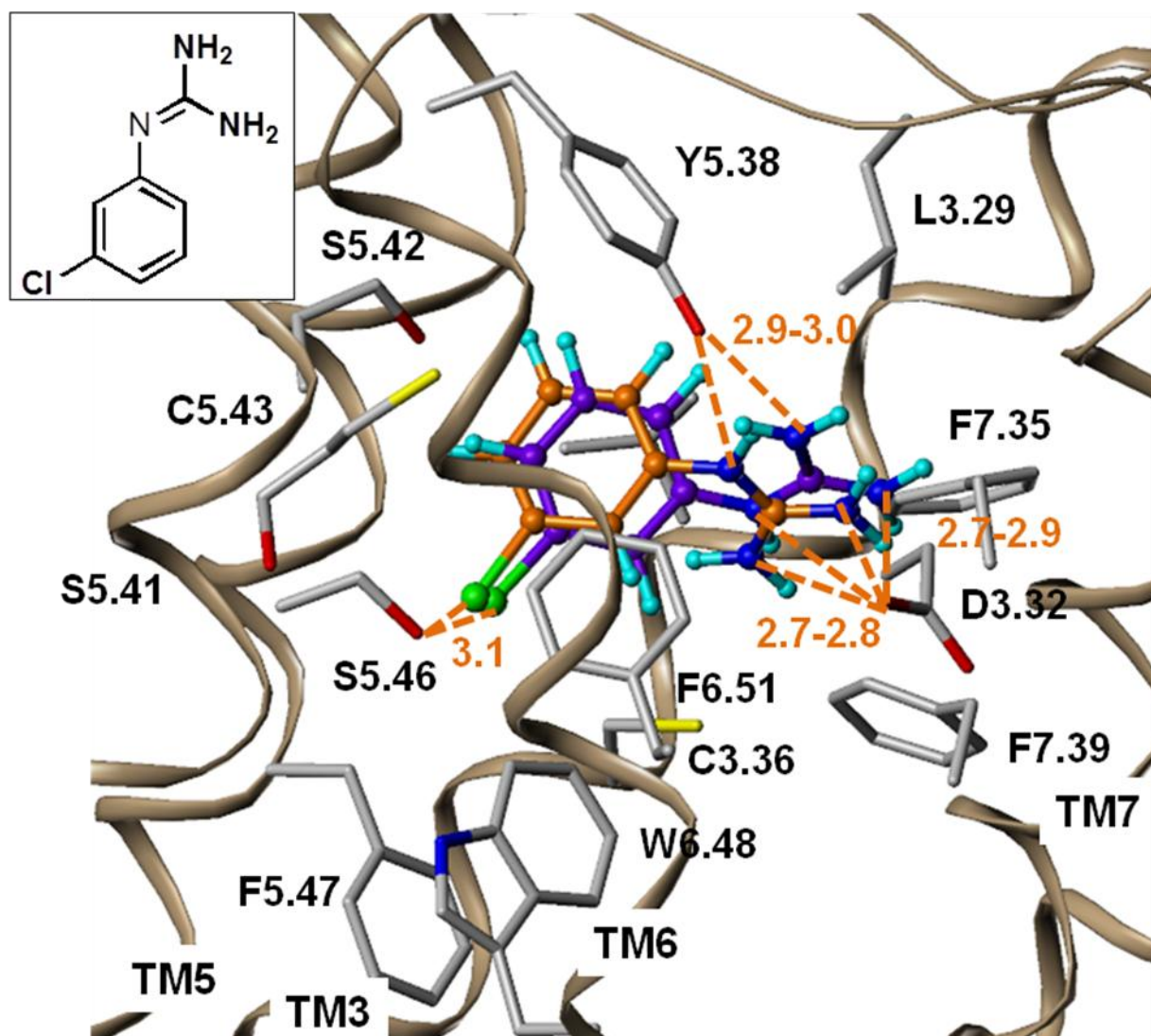


**Figure 65.** Proposed binding mode of  $-ac-$  (purple) and  $+sc-$  (orange) MD-354 (**21**) in the active  $\alpha_{2C}$ -AR model. Amino acids within 4 Å are shown in capped sticks (grey) and distances (Å) of favorable HB or ionic interactions are shown in orange.

MD-354 (**21**) docking studies with the inactive  $\alpha_{2C}$ -AR model proved to be difficult; MD-354 (**21**) did not seem to bind favorably into the binding pocket. That is, MD-354 (**21**) would sometimes interact with the conserved aspartate D3.32, but would never reach the other side of the binding pocket near TM5 regardless of which rotamer of MD-354 (**21**) was utilized in the docking study (data not shown). Unsuccessful



attempts to influence the binding mode of MD-354 (**21**) in the inactive  $\alpha_{2C}$ -AR model were made. Manually docking MD-354 (**21**) closer to TM5, as well as additional binding constraints in GOLD (e.g., distance constraints between the *m*-Cl group of MD-354 (**21**) and the conserved TM5 serines), resulted in unfavorable interactions and therefore, upon energy minimizations, **21** moved away from TM5.

## 5. Discussion

3D molecular modeling studies suggest that MD-354 (**21**) might bind to the “active”  $\alpha_{2A}$ -AR model in a manner similar to that of epinephrine (**2**). More specifically, when superimposing +*sc*-MD-354 (**21**) and (*R*)-EPI (**2**) docked poses, the terminal amines, as well as the *m*-hydroxyl and chloro groups, overlap (Figure 66). In turn, these functional groups appear to interact with the same amino acid residues (i.e., ionic: N<sup>+</sup>—D3.32; HB: *m*-OH—S5.42 or *m*-Cl—S5.42; Figure 66). Although the aromatic moiety and one of the terminal amines of *–ac*-MD-354 (**21**) does overlap with the docked pose of (*R*)-EPI (**2**), the *m*-Cl group does not overlap with the *m*-OH of (*R*)-EPI (**2**) (Figure 66). Alternatively, this *m*-Cl group overlaps with the unsubstituted *m*-position of (*R*)-EPI (**2**). Therefore, the docked pose of *–ac*-MD-354 (**21**) does not display an optimal interaction with S5.42, but may interact with S5.46 (bonding distance = 3.0 Å).

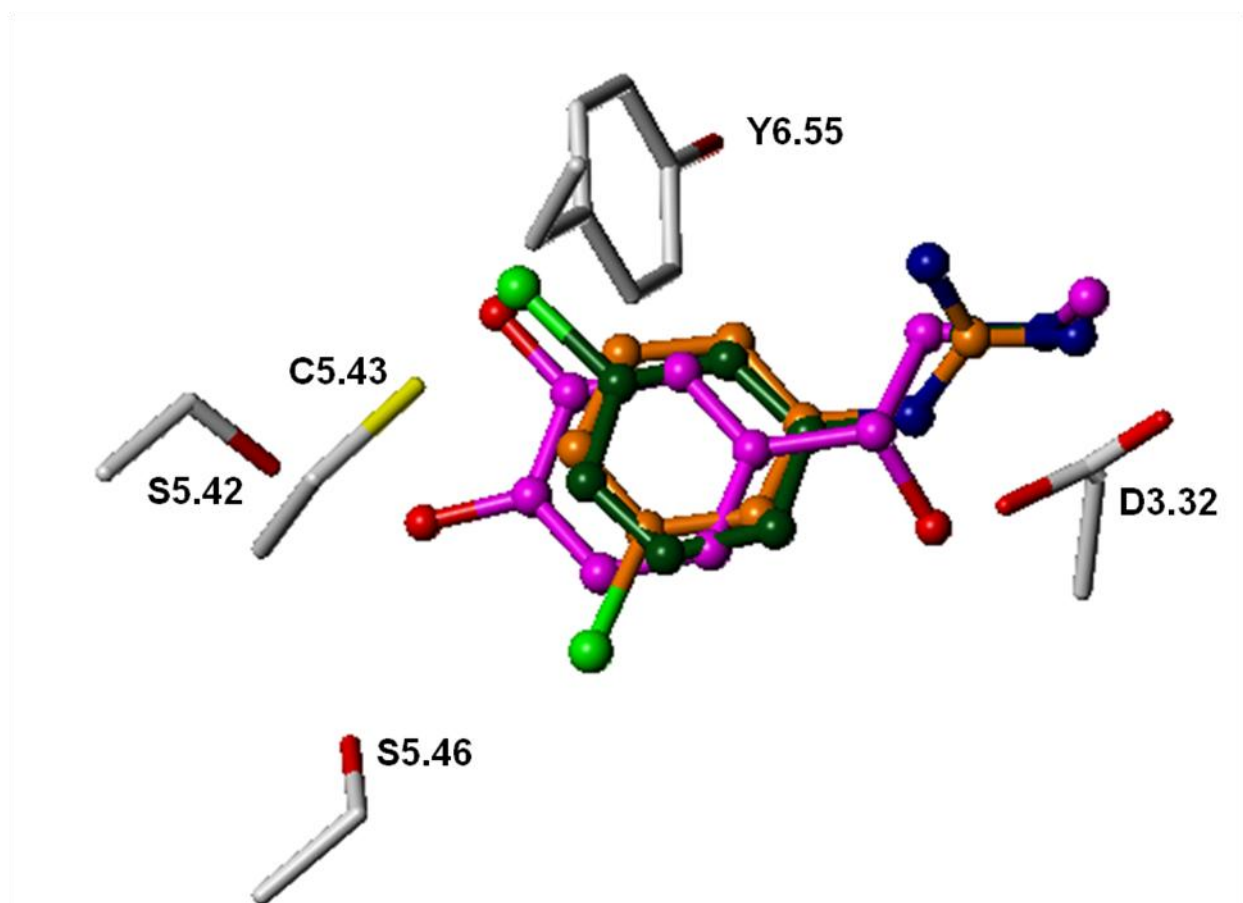


**Figure 66.** Proposed binding mode of (*R*)-Epinephrine (**2**) (magenta), *-ac-* (orange) and *+sc-* (green) MD-354 (**21**) in the active  $\alpha_{2A}$ -AR model. Key amino acids of  $\alpha_{2A}$ -ARs are shown in capped sticks (grey).

Based on the molecular modeling studies, it is possible that MD-354 (**21**) has a greater binding affinity at the low affinity state (i.e., inactive model of  $\alpha_{2A}$ -ARs) in comparison to the high affinity state because of increased interactions with the receptor. In the proposed binding mode of MD-354 (**21**) at the inactive  $\alpha_{2A}$ -ARs, there were three amine—receptor interactions (D3.32 and Y6.55), all of which were in optimal distance from each other (i.e., approximately 3 Å), but no halogen bonding with TM5 (e.g., *m*-Cl—S5.42 or S5.46). When evaluating all docked poses of the four lowest-energy rotamers of MD-354 (**21**) in the inactive  $\alpha_{2A}$ -AR model, the closest measurement

between the *m*-Cl group and the TM5 serine residues was 3.8 Å, which is not optimal for a halogen bond. In general, a halogen bond, which is a short interaction between a carbon-bonded halogen [e.g., the *m*-Cl moiety of MD-354 (**21**)] and a carbonyl, hydroxyl, charged carboxylate, or phosphate group (e.g., S5.42 or S5.46 of  $\alpha_{2A}$ -ARs), is optimally less than 3.3 Å when chlorine is the halogen.<sup>218</sup> In general, the binding mode of MD-354 (**21**) contains three strong amine—receptor interactions in the inactive state, whereas it contains only 2 amine—receptor interactions and a relatively weak halogen bond in the active state. It is hypothesized that this difference in interactions provides support for the MD-354's (**21**) greater binding affinity (less than 10-fold difference between the “active” and “inactive”  $\alpha_{2A}$ -ARs; see Table 5 for  $K_i$  values) at the “inactive” state.

The  $\pi$ - $\pi$  stacking interaction (i.e., the bonding network between the guanidine moiety of MD-354 (**21**) and the aspartate carboxylate moiety (D3.32), which is stacked over the aromatic ring of F7.39) has been previously found between the H-bonding network between R (the guanidinium moiety) and E or D (the carboxylate moiety) and the aromatic moiety of a tyrosine residue.<sup>217</sup> In this particular example, the distance between the center of the hydrogen bonding network and the center of the aromatic residue was 3.7 Å.<sup>217</sup> This additional interaction in the proposed binding mode of MD-354 (**21**) in the inactive state of  $\alpha_{2A}$ -ARs may be one of the factors involved with increased binding affinity as compared to the active state (Figures 60 and 62).

It was not obvious as to how MD-354 (**21**) could behave as a weak partial agonist at  $\alpha_{2A}$ -ARs, while having a greater binding affinity to the low-affinity state of the receptor. However, it is noted, that the docking studies described above do indicate that MD-354

(**21**) only interacts with the conserved TM5 serines (S5.42 or S5.46) when  $\alpha_{2A}$ -AR is in an active conformation. That is, modifications to the inactive  $\alpha_{2A}$ -AR model brought the top portion of TM5 further into the binding pocket, which allowed the *m*-Cl group of MD-354 (**21**) to get close enough to either S5.42 or S5.46 for a favorable halogen bond. As it has been previously proposed that the movement of TM5 is an important conformational change in GPCR activity, the interaction of the ligand and the TM5 residues might be key in keeping a receptor in its active state. Therefore, the agonist activity of MD-354 (**21**) at  $\alpha_{2A}$ -ARs may be due to its halogen bonding with S5.42 or S5.46. Further, it is proposed that MD-354 (**21**) does not produce full agonist activity because halogen bonds are not extremely strong.

When comparing the proposed binding modes of MD-354 (**21**) in the active and inactive  $\alpha_{2B}$ -AR models, one difference is that the four lowest-energy conformers of MD-354 (**21**) do not get close enough to TM5 to have favorable bonding distances between the *m*-Cl group of **21** and the conserved serines, S5.42 and/or S5.46, in the inactive model (Table 15). Secondly, in the active  $\alpha_{2B}$ -AR model, F7.39 was positioned too far away (>5 Å) from the guanidine moiety of MD-354 (**21**) to provide a parallel-stacking interaction. Furthermore, the hydrogen bonding interactions between the guanidine of **21** and the carboxylate group of D3.32 were not optimal; that is, they did not form a 6-membered ring parallel to the aryl ring of F7.39 (as shown in Figure 63). It is possible that the additional parallel stacking interaction of MD-354 (**21**) in the inactive  $\alpha_{2B}$ -AR model with the TM7 phenylalanine (F7.39), prevents the ligand from strongly interacting with the other side of the binding pocket, specifically with the TM5 serines (S5.42 and S5.46).

When comparing the two  $\alpha_{2B}$ -AR models, it is proposed that the approximately 10-fold difference in binding affinity of MD-354 (**21**) at the “active” and “inactive”  $\alpha_{2B}$ -ARs ( $K_i = 25$  and  $220$  nM at agonist [ $^{125}$ I]clonidine and antagonist [ $^3$ H]RX 821002 sites; Table 5) may be due to the halogen bond interaction between the *m*-Cl group and S5.46 observed in the –ac-MD-354 (**21**) binding mode in the active  $\alpha_{2B}$ -AR model (Figure 63). As for the antagonist functional data for MD-354 (**21**) at  $\alpha_{2B}$ -ARs, it is possible that the parallel-stacking interaction (between F7.39 and the hydrogen bonding network of the guanidine moiety of MD-354 (**21**) and the carboxylate group of D3.32) reduces interaction with TM5 and therefore, affects MD-354’s (**21**) activity at  $\alpha_{2B}$ -ARs.

In the docking studies for the active  $\alpha_{2C}$ -AR model, the four lowest-energy conformers of MD-354 (**21**) showed favorable bonding distances to indicate ionic interactions between amines of **21** and D3.32 and Y5.38, as well as halogen bonding interactions between the *m*-Cl group of **21** and S5.46 (Figure 65). On the other hand, the conformers of MD-354 (**21**) did not show optimal interactions when docked to the inactive  $\alpha_{2C}$ -AR model; in fact, MD-354 (**21**) did not always reach the binding pocket (i.e., it did not always interact with the conserved aspartate D3.32). Although not too much can be concluded, these types of results in a docking study are indicative of a relatively low binding affinity.

In summary, the homology modeling results indicate that the difference in binding affinity of MD-354 (**21**) at the low- and high-affinity states of  $\alpha_{2A}$ -ARs may be due to the amine—receptor interactions, which are stronger in the inactive  $\alpha_{2A}$ -AR model than in the active  $\alpha_{2A}$ -AR model, whereas the binding affinity difference of MD-354 (**21**) at the low- and high-affinity states of  $\alpha_{2B}$ -ARs seem to be due to the additional halogen bond

interaction between the *m*-Cl group of **21** and the conserved TM5 serine (S5.46) in the active  $\alpha_{2B}$ -ARs. The inability of the lowest-energy conformer of MD-354 (**21**) to always bind in the binding pocket (i.e., the pocket centered around the conserved D3.32) of the inactive  $\alpha_{2C}$ -AR model correspond to the low binding affinity. Overall the above results are only speculative, and remain to be further investigated (or documented) by mutagenesis studies.

## V. Conclusions

One goal of the current project was to further investigate the mechanism of action of the selective analgesia-potentiating effect of clonidine (**7**) by MD-354 (**21**). As previously reported, co-administration of MD-354 (**21**) and clonidine (**7**) produces a biphasic analgesic effect in the mouse tail-flick assay (Peaks A and B, Figure 12) and mechanistic studies suggested that the analgesic potentiation is due, at least in part, to a 5-HT<sub>3</sub> receptor and an  $\alpha_2$ -AR mechanism.<sup>29,33,34</sup>

In the present investigation, the structurally similar, yet more established, 5-HT<sub>3</sub> receptor agonist *m*CPBG (**20**), also produced saline-like effects when administered alone (Figure 22), but potentiated the antinociceptive effect of an “inactive” dose of clonidine (**7**) in the mouse tail-flick assay (Figure 23a). Similar to the MD-354/clonidine (**21/7**) mechanistic studies,<sup>31,34</sup> attenuation of the antinociceptive effect of the *m*CPBG/clonidine (**20/7**) combination by the 5-HT<sub>3</sub> receptor antagonist tropisetron (**25**; Figure 25), as well as the non-selective  $\alpha_2$ -AR antagonist yohimbine (**11**; Figure 27), indicated that 5-HT<sub>3</sub> receptors and at least some subtypes of the  $\alpha_2$ -AR are involved in *m*CPBG's (**20**) potentiating effect in the mouse tail-flick assay. Furthermore, since the 5-HT<sub>3</sub> receptor antagonist tropisetron methiodide, that does not readily cross the BBB,<sup>116</sup> failed to block the analgesic effect produced by the *m*CPBG/clonidine (**20/7**) combination (Figure 26), it seems that the role of 5-HT<sub>3</sub> receptors in the potentiating mechanism may be centrally-mediated. Similar to the MD-354 (**21**) results presented in

previous investigations,<sup>29,33</sup> *m*CPBG's (**20**) potentiation of the antinociceptive effects of clonidine (**7**) is a selective effect; that is, a dose combination of *m*CPBG (**20**, 6.0 mg/kg) and clonidine (**7**; 0.25 mg/kg), which produce a statistically significant increase in antinociceptive effects (% MPE = 68.0) in the tail-flick assay, did not affect the locomotor effects of clonidine (Figure 30).

Unlike the potentiation effect observed in the mouse tail-flick assay, *m*CPBG (**20**) attenuated clonidine's (**7**) antinociceptive effect in the mouse hot-plate assay (Figure 29). This result was also observed when the structurally similar 5-HT<sub>3</sub> receptor agonist MD-354 (**21**) is co-administered with clonidine (**7**) in the mouse hot-plate assay.<sup>33</sup>

The previous MD-354 (**21**)<sup>34</sup> and current *m*CPBG (**20**) studies both indicate that 5-HT<sub>3</sub> receptors play a role in the analgesia-potentiating effect of clonidine (**7**). Furthermore, the tropisetron (**25**) and tropisetron methiodide mechanistic studies suggest that *m*CPBG (**20**) potentiates the antinociceptive effects of clonidine (**7**), at least in part, due to a central 5-HT<sub>3</sub> receptor mechanism. Therefore, SR57227A (**22**), a known centrally-acting 5-HT<sub>3</sub> receptor agonist, was selected as a pharmacological tool to evaluate central versus peripheral activity. When SR57227A (**22**; 0.3-10 mg/kg doses) was administered alone, saline-like effects were observed in the mouse tail-flick (Figure 31) and hot-plate (Figure 36) assays. In fact, in a modified tail-flick assay wherein radiant heat is adjusted, dose-dependent hyperalgesic effects were produced in SR57227A (**22**)-treated mice (Figure 33). At higher doses, SR57227A (**22**; 30 mg/kg) produced antinociceptive effects in the mouse tail-flick (Figure 31) and hot-plate (Figure 36) assays. However, locomotor activity results indicated that this high dose also, produces significant hypolocomotor actions in comparison to saline (Figure 38), which



can misleadingly suggest that a high dose of SR57227A (**22**; 30 mg/kg) produces antinociceptive effects.

Unlike the other 5-HT<sub>3</sub> receptor ligands studied [MD-354 (**21**) and *m*CPBG (**20**)], SR57227A (**22**) did not attenuate or potentiate the antinociceptive actions of an “inactive” dose (Figure 34) or an ED<sub>50</sub> dose (Figure 35) of clonidine (**7**). SR57227A (**22**), also, had no effect on the antinociceptive effects of clonidine (**7**) in the mouse hot-plate assay (Figure 36). Because it has been previously shown that SR57227A (**22**) behaves as an agonist at central 5-HT<sub>3</sub> receptors<sup>115</sup> and the abovementioned results indicate that SR57227A (**22**) does not alter the antinociceptive effects of clonidine (**7**), it might be speculated that MD-354 (**21**) potentiates the analgesic actions of clonidine (**7**) via a peripheral 5-HT<sub>3</sub> receptor mechanism, but this is highly unlikely as already described above and in the Discussion.

Since previous mechanistic studies of the analgesia-potentiating effect of clonidine (**7**) by MD-354 (**21**) also suggest a role for  $\alpha_2$ -ARs (e.g., an  $\alpha_2$ -AR agonist mechanism in Peak A),<sup>31</sup> TDIQ (**6**), a non-selective  $\alpha_2$ -AR agonist devoid of 5-HT<sub>3</sub> receptor activity, was selected as a pharmacological tool to examine the potential  $\alpha_2$ -AR mechanism. In both antinociceptive assays, TDIQ (**6**) showed saline-like effects when administered alone (tail-flick assay: Figure 39; hot-plate assay: Figure 48). However, studies with co-administration of TDIQ (**6**) and clonidine (**7**; “inactive” dose) in the mouse tail-flick assay indicated potentiation of the antinociceptive effects of clonidine (**7**) in a dose-dependent manner (Figure 40). This is analogous to the MD-354/clonidine (**21/7**) results previously reported.<sup>31</sup>

Furthermore, since both clonidine (**7**) and TDIQ (**6**) are non-selective  $\alpha_{2A/2B/2C}$ -AR agonists, TDIQ's (**6**) potentiation of clonidine (**7**)-induced antinociception might simply be an additive effect of the two agents. However, an isobolographic analysis indicated that TDIQ (**6**) potentiates the analgesic actions of clonidine (**7**) in a synergistic (or super-additive) manner in the mouse tail-flick assay [3:1 and 12:1 fixed ratios for TDIQ (**6**) and clonidine (**7**), Figure 47]; that is, the isobologram suggested that the antinociception produced by the combination of drugs [TDIQ (**6**) and clonidine (**7**)] is greater than the sum of the individual effects of the component drugs.

In order to determine the mechanism of action associated with TDIQ's (**6**) potentiating effect of the antinociceptive actions of an "inactive" dose of clonidine (**7**), various  $\alpha_2$ -AR antagonists were co-administered with the TDIQ/clonidine (**6/7**) combination. Since the selected  $\alpha_2$ -AR antagonists, BRL44408 (**15**; preferentially selective at  $\alpha_{2A}$ -ARs), imiloxan (**12**; preferentially selective at  $\alpha_{2B}$ -ARs) and ARC-239 (**14**; preferentially selective at  $\alpha_{2B/2C}$ -ARs), produced saline-like effects when administered alone, but blocked the antinociceptive effect of the TDIQ/clonidine (**6/7**) combination (Figures 42, 43 and 44), there is support for an  $\alpha_{2A}$ - and  $\alpha_{2B}$ -AR role in the mechanism and, further, a role for  $\alpha_{2C}$ -AR cannot be ruled out. These results support the hypothesis that MD-354 (**21**) could be potentiating the analgesic actions of clonidine (**7**) via an  $\alpha_2$ -AR agonist mechanism.

Thus, potentiation of the analgesic actions of clonidine (**7**) by MD-354 (**21**) might be attributed to its unique 5-HT<sub>3</sub> receptor/ $\alpha_2$ -AR character (Peak A, Figure 12)

As indicative of the abovementioned pharmacological studies, there is support for a 5-HT<sub>3</sub> receptor mechanism in the selective potentiation of the antinociceptive actions

of clonidine (**7**) by MD-354 (**21**), which leads to the next goal of the present investigation: the exploration of conformationally-constrained rotamers of the 5-HT<sub>3</sub> receptor agonist MD-354 (**21**). Preliminary results indicated that when MD-354 (**21**) was constrained into a quinazoline ring to form two MD-354 (**21**) rotamers, 2-amino-7-chloro-3,4-dihydroquinazoline (**26**) and 2-amino-5-chloro-3,4-dihydroquinazoline (**27**), **26** more closely mimics the binding profile of MD-354 (**21**) (Figure 13 and Table 7). Therefore, **26** was used as the parent compound in the present investigation which explored the role of the ring nitrogen atoms and the chloro substituent in binding at 5-HT<sub>3</sub> receptors.

In order to explore the role of the ring nitrogen atoms, procedures to synthesize compounds **28-33** (Figure 14) were developed, but only compound **28**, **29**, **30** and **33** were successfully synthesized (Schemes 2, 7, 9 and 10). Additionally, compound **65** was also synthesized because its precursor was a minor product in the reaction scheme to synthesize **33** (Schemes 11 and 12). Compounds **38** and **39** (Figure 16) were successfully prepared in order to study the role of the chloro substituent (Schemes 13 and 14). Binding affinity at 5-HT<sub>3</sub> receptors have been evaluated for compounds **28**, **33** and **65**, all of which lacked affinity at 5-HT<sub>3</sub> receptors ( $K_i > 10,000$  nM). Due to these preliminary binding results, it is evident that the nitrogen atoms of the conformationally-constrained analogs of MD-354 (**21**) are important for 5-HT<sub>3</sub> receptor binding. The conformationally-constrained MD-354 (**21**) analog **28** is missing one of the two terminal amines of MD-354 (**21**) or when comparing to **26**, it is missing the 3-position amine. Both MD-354 (**21**) and **26** display high affinity at 5-HT<sub>3</sub> receptors ( $K_i = 35$  and  $34$  nM, respectively, Table 7) whereas the des-amino analog **28** lacks 5-HT<sub>3</sub> receptor binding affinity ( $K_i > 10,000$  nM), which suggests that at least one, if not both, of the MD-354

(**21**) terminal amines is necessary for 5-HT<sub>3</sub> receptor binding. Furthermore, no matter which *meta*-position the chloro substituent is in, when the aniline and 3-position nitrogen atoms are missing, 5-HT<sub>3</sub> receptor binding is abolished. For example, when comparing compounds **26** ( $K_i = 34$  nM) with **33** ( $K_i > 10,000$  nM), and **27** ( $K_i = 1021$  nM) with **65** ( $K_i > 10,000$  nM), 5-HT<sub>3</sub> receptor binding affinity is reduced by at least 300- and 10-fold, respectively (Table 7). 5-HT<sub>3</sub> receptor binding affinity results of the remaining synthesized compounds will further evaluate the role of the nitrogen atoms and the chloro substituent in MD-354 (**21**) and conformationally-constrained analogs of MD-354 (**21**) in 5-HT<sub>3</sub> receptor binding.

Just as the present investigation showed that various 5-HT<sub>3</sub> receptor [e.g., *m*CPBG (**20**) and SR57227A (**22**)] and  $\alpha_2$ -AR [e.g., TDIQ (**6**)] ligands potentiated the antinociceptive actions of clonidine (**7**) via 5-HT<sub>3</sub> receptor or  $\alpha_2$ -AR mechanisms, previous pharmacological studies indicated that there was a 5-HT<sub>3</sub> receptor and  $\alpha_2$ -AR mechanism involved in clonidine's (**7**) analgesic potentiation by MD-354 (**21**) in the mouse tail-flick assay. Since MD-354 (**21**) shows varied binding affinities and functional activity at the  $\alpha_2$ -AR subtypes, the final goal of the current studies was to explain these subtype differences via examination of the binding mode of MD-354 (**21**) to graphic receptor models of low- and high-affinity states of  $\alpha_{2A}$ -,  $\alpha_{2B}$ - and  $\alpha_{2C}$ -ARs.

In order to examine the binding mode of MD-354 (**21**) at  $\alpha_{2A}$ -,  $\alpha_{2B}$ - and  $\alpha_{2C}$ -ARs in their inactive and active states, it was first necessary to identify the lowest-energy conformers of MD-354 (**21**) as these conformers should mimic the likely conformations of MD-354 (**21**) in its binding mode. A systematic conformation search conducted in SYBYL identified the four lowest-energy rotamers of MD-354 (**21**; Figure 55), which

coincidentally, matched the torsion angles found in arginine, clonidine (**7**) and *m*CPBG (**20**) crystal structures.

The inactive state of  $\alpha_{2A}$ -ARs was modeled by mutating the  $\beta_2$ -AR crystal structure (pdb ID: 2RH1) and the active state of  $\alpha_{2A}$ -ARs was modeled by modifying the inactive  $\alpha_{2A}$ -AR homology model in a manner observed in other active-state structures of GPCRs. Due to extensive SAFIR studies and site-directed mutagenesis studies of phenethylamines, endogenous ligands including NE (**1**) and EPI (**2**), were docked into the binding pocket to help validate the active  $\alpha_{2A}$ -AR homology model. Similar to the support in the literature, the docking studies indicated ligand—receptor interactions of, for example, (*R*)-EPI (**2**) in the active  $\alpha_{2A}$ -AR model: (a) ionic:  $N^+$ —D3.32; (b) HB:  $\beta$ -OH—D3.32, *m*-OH—S5.42 and *p*-OH—S5.46; (c)  $\pi$ - $\pi$  (edge-to-face): F6.51, Y6.55; CH- $\pi$ : V3.33; (d)  $\pi$ -cation:  $N^+$ —F7.39 (Figure 58). The lower binding affinity of (*S*)-EPI (**2**) in comparison to (*R*)-EPI (**2**) may be due to the decreased ligand—receptor interactions such as the H-bond interaction between the conserved D3.32 and the  $\beta$ -OH moiety of (*S*)-EPI (**2**).

Upon docking the four lowest-energy rotamers of MD-354 (**21**) based on the conformational analyses in the active model of  $\alpha_{2A}$ -AR, the major bonding interactions observed included: (a) an ionic interaction between both the aniline and terminal nitrogens and D3.32; (b) hydrogen bonding between the *m*-Cl group and either S5.42 or S5.46; (c) hydrophobic interactions with V3.33, F6.51, F7.35 and F7.39 (Figure 59 and Table 14a). In general, these docking studies suggest that MD-354 (**21**) might bind to the active  $\alpha_{2A}$ -AR model in a manner similar to that of EPI (**2**) (Figure 66).

Furthermore, when comparing the proposed binding modes of MD-354 (**21**) at the inactive and active  $\alpha_{2A}$ -ARs, it is possible that MD-354 (**21**) has a greater binding affinity at the low-affinity state because of increased interactions with the receptor. Specifically, the binding mode of MD-354 (**21**) contains three strong amine—receptor interactions in the inactive state, whereas it contains only 2 amine—receptor interactions and a relatively weak halogen bond in the active state.

Upon a comparison between the proposed binding modes of MD-354 (**21**) at the inactive and active  $\alpha_{2B}$ -AR models, it is proposed that the approximately 10-fold difference in binding affinity of MD-354 (**21**) at the low- and high-affinity state  $\alpha_{2B}$ -ARs ( $K_i = 25$  and  $220$  nM, respectively; Table 5) may be due to the halogen bond interaction between the *m*-Cl group and S5.46 observed in the *-ac*-MD-354 (**21**) binding mode in the active  $\alpha_{2B}$ -AR model (Figure 63). With regards to the antagonist functional data for MD-354 (**21**), it is possible that the additional parallel-stacking interaction (between F7.39 and the hydrogen bonding network of the guanidine moiety of MD-354 (**21**) and the carboxylate group of the conserved D3.32) diminishes the interaction with TM5 residues and therefore, affects MD-354's (**21**) ability to “hold” the  $\alpha_{2B}$ -AR in an active state.

As the lowest-energy conformers of MD-354 (**21**) did not show optimal interactions in the inactive  $\alpha_{2C}$ -AR model, low binding affinity is not surprising. Similar to proposed binding mode of MD-354 (**21**) at active  $\alpha_{2A}$ -AR models, favorable bonding distances for a halogen bond between the *m*-Cl group of **21** and S5.46, as well as ionic interactions between the amines of **21** and D3.32 and Y5.38 was observed in the active  $\alpha_{2C}$ -AR docking results.

To conclude, the pharmacological studies indicated that arylguanidines represent a novel class of analgesic adjuvants with a dual mechanism of action (i.e., the mechanism involves both 5-HT<sub>3</sub> receptors and  $\alpha_2$ -adrenoceptors). The proposed docking modes of MD-354 (**21**) at high-affinity states of  $\alpha_{2A}$ - and  $\alpha_{2B}$ -AR models display a halogen bond interaction between the chloro group of MD-354 (**21**) and conserved TM5 serines. Since the tilting of TM5 into the binding pocket has been implicated in the GPCR activation process, it seems possible that this halogen bond interaction observed in the  $\alpha_{2A}$ - and  $\alpha_{2B}$ -AR models might account for its partial agonist activity. Furthermore, on the basis of available binding affinity data of conformationally-constrained MD-354 (**21**) analogs, the nitrogen atoms seem to be necessary for 5-HT<sub>3</sub> receptor binding affinity.

## VI. Experimental

### A. Pharmacological studies

#### 1. Animals

Male ICR mice (Harlan Laboratories; Indianapolis, IN; 19-30 g) were housed in groups of 5-6, with free access to food and water. The housing rooms were under a temperature- (22 °C) and humidity- (≈50%) controlled environment and a standard 12:12 h light/dark cycle starting at 7:00 a.m. The experiments were conducted in accordance to protocols set by the Institutional Animal Care and Use Committee (IACUC) of Virginia Commonwealth University (IACUC protocol # AM10339). On the experiment day, mice were first acclimated to the testing environment for at least one hour and weighed prior to any treatment.

#### 2. Drugs

The hydrochloride salts of MD-354 (**21**; *meta*-chlorophenylguanidine) and *m*CPBG (**20**) were synthesized in our laboratory. Ondansetron hydrochloride (Zofran®, Lot CO99723; GlaxoSmithKline) was purchased from the MCVH-Pharmacy (Richmond, VA). Imiloxan hydrochloride (**12**), ARC-239 (**14**; 2-[2-(4-(2-Methoxyphenyl)piperazin-



1-yl)ethyl]-4,4-dimethyl-1,3-(2*H*,4*H*)-isoquinolindione dihydrochloride), BRL44408 (**15**; 2-[(4,5-dihydro-1*H*-imidazol-2-yl)methyl]-2,3-dihydro-1-methyl-1*H*-isoindole), SR57227A hydrochloride (**22**; 1-(6-chloro-2-pyridyl)-4-piperidinylamine) and Zacopride (**24**) were purchased from Tocris (Ballwin, MO). TDIQ (**6**; 5,6,7,8-tetrahydro-1,3-dioxolo[4,5-*g*]isoquinoline) hydrochloride was synthesized in our laboratory. Clonidine (**7**), tropisetron (**25**) and yohimbine (**11**) were purchased from Sigma-Aldrich Chemicals (Milwaukee, WI). Tropisetron methiodide was purchased from RBI (Research Biochemicals Inc; Natick, MA). Drug solutions were prepared daily; all drugs were dissolved in 0.9% saline and administered to mice in a total volume of 10 mL/kg body weight by subcutaneous (s.c.) or intraperitoneal (i.p.) injections. Each dose of drug (or combination of drugs) was studied in at least 8 mice (i.e.,  $n \geq 8$  mice/treatment).

### **3. Behavioral assays**

#### **a) Tail-Flick assay**

Antinociception was assessed by the tail-flick method of D'Armour and Smith<sup>219</sup> as modified by Dewey et al.<sup>220</sup> using a Columbus Tail-Flick Analgesia Meter (Columbus Instruments, Columbus, Ohio). Determination of qualifying mice was conducted by screening each mouse before the treatment (qualifying control response time between 1.7 and 4.0 s; in hyperalgesic studies: radiant heat was modified so that qualifying control response time was between 5 and 7 s). Test latency was determined after drug administration. In order to minimize tissue damage, a maximum latency of 10 s was

imposed. The antinociceptive response was calculated as percent maximum possible effect (%MPE), where  $\%MPE = [(test\ latency - control\ latency)/(cutoff\ time - control\ latency)] \times 100$ .

The experimental protocol for testing the antinociceptive effects of drugs was as follows: 15 min prior to s.c. administration of drugs, baseline tail-flick latency was determined for each mouse. Drugs were administered either alone or in combination with other drugs with the following pre-injection times (i.e., injection time prior to test): TDIQ (**6**; 45 minutes), clonidine (**7**; 20 minutes), yohimbine (**11**; 60 minutes), imiloxan (**12**; 55 minutes), ARC-239 (**14**; 50 minutes), BRL-44408 (**15**; 50 minutes), *m*CPBG (**20**; 45 minutes), MD-354 (**21**; 45 minutes), SR57227A (**22**; 45 minutes), ondansetron (**23**; 50 minutes) and tropisetron/tropisetron methiodide (**25**; 50 minutes).

#### **b) Hot-Plate assay**

The hot-plate method is a modification of that described by Eddy and Leimbeck<sup>221</sup> and Atwell and Jacobson.<sup>222</sup> Mice were placed onto a hot-plate (Columbus Hot-plate Analgesia Meter) and covered with a 10 cm-wide glass cylinder, wherein the temperature was maintained at 55 °C. Determination of qualifying mice was conducted by screening each mouse before the treatment (qualifying mouse displays a control response time between 6 and 10 s). Test latency was determined after drug administration. In order to prevent any paw damage, 30 s was used as the cutoff time. The antinociceptive response was calculated as percent maximum possible effect

(%MPE), where %MPE = [(test latency – control latency)/(cutoff time – control latency)] x 100.

The experimental protocol for testing the antinociceptive effects of drugs was as follows: 15 min prior to s.c. administration of drugs, baseline latency was determined for each mouse. Drugs were administered either alone or in combination with other drugs with the following pre-injection times (i.e., injection time prior to test): TDIQ (**6**; 45 minutes), clonidine (**7**; 30 minutes), *m*CPBG (**20**; 45 minutes) and SR57227A (**22**; 45 minutes).

### **c) Locomotor activity assay**

Mice were placed into individual Tru Scan Infrared Locomotor Activity System (Coulbourn Instruments, Allentown, PA) photocell activity cages (40 cm cube) after s.c. (or i.p.) administration of drugs or combination of drugs (mice were only tested once). Ambulatory movement was measured by the number of times the animal interrupted the infrared beams traversing the cage for a period of 15 minutes; measurements were taken 15, 30 and 45 minutes following the start of the assay. The behavioral analysis examined nine measures of activity: movement episodes, movement time (s), movement distance (cm), vertical entries, margin distance (cm), margin time (s), center distance (cm), center time (s) and center entries.

Drugs were administered either alone or in combination with other drugs with the following pre-injection times (i.e., injection time prior to test): TDIQ (**6**; 30 minutes), clonidine (**7**; 5 minutes), *m*CPBG (**20**; 30 minutes) and SR57227A (**22**; 0 minutes).

#### 4. Statistical analysis

Data were analyzed statistically by an analysis of variance (ANOVA) followed by the Dunnett's post-hoc test. A measure of significant difference between two groups was analyzed using a Student's t-test. The null hypothesis was rejected at the 0.05 level.

#### 5. Isobolographic analysis

Synergism was assessed by the isobolographic analysis method described by Tallarida.<sup>223</sup> In order to assess if a biological effect produced by a combination of drugs is greater than, equal to, or smaller than the sum of the individual effects of the component drugs, an isobolographic analysis was performed. The representative graph, an isobologram, compares the experimental  $ED_{50}$  of the combination of drugs ( $ED_{50mix}$ ) to the theoretical additive combination ( $ED_{50add}$ ).  $ED_{50add}$  is based on the individual potencies of the components (e.g. drug 1 and 2) in the combination. If only drug 2 is active when administered alone then, the  $ED_{50add}$  is based on the  $ED_{50}$  of drug 2 and its proportion in the combination. To evaluate synergism, the experimental  $ED_{50mix}$  of a fixed-ratio of TDIQ (6) and clonidine (7) is compared to the theoretical  $ED_{50add}$  of a simply additive mixture having the same proportions, wherein  $ED_{50add} = (ED_{50clonidine}) / P_{clonidine}$  ( $P = \text{proportion}$ ).  $ED_{50mix}$  and  $ED_{50clonidine}$  were obtained from the regression analysis of the % MPE against log total dose. The difference between the two  $ED_{50}$  values with its corresponding standard error was statistically tested with a

Student's t-test. Evaluation of results: a super-additive effect (exaggerated effect) occurs when  $ED_{50mix} < ED_{50add}$ , an additive effect (theoretical effect) occurs when  $ED_{50mix} = ED_{50add}$  and a sub-additive effect (attenuated effect) occurs when  $ED_{50mix} > ED_{50add}$ .

## B. Synthesis

Reactions were monitored by thin layer chromatography (tlc) on silica gel GHLF plates (250  $\mu$ , 2.5 x 10 cm, Analtech Inc.). Some compounds were purified via column chromatography (silica gel 62, 60-200 mesh, Sigma-Aldrich) or flash chromatography (CombiFlash Companion/TS, Teledyne Isco Inc.). All solid products were characterized by melting point on a Thomas-Hoover mp apparatus (and are uncorrected).  $^1H$  NMR spectra were obtained on either a Varian 300 MHz spectrometer or a Bruker 400 MHz spectrometer with tetramethylsilane as internal standard. Nicolet Avatar 360 FT-IR or Nicolet 52DX FT-IR spectrophotometers were used to obtain IR spectra for all compounds. Combustion analysis of carbon, hydrogen, and nitrogen was conducted by Atlantic Microlab Inc. (Norcross, GA) on all unknown target compounds. Calculated values were +/- 0.4 % of the theoretical values.

***m*-Chlorophenylbiguanide Hydrochloride (20).** Compound **20** was prepared according to a literature procedure for a similar compound.<sup>179</sup> Compound **41** (6.83 g, 41.64 mmol) was added to a stirred mixture of cyanoguanidine (3.50 g, 41.64 mmol) in H<sub>2</sub>O (10 mL) and heated at reflux for 4 h. The reaction mixture was allowed to cool to 10 °C for 24 h. The precipitated salt was collected by filtration, washed with Et<sub>2</sub>O (6 x 5

mL), and recrystallized from H<sub>2</sub>O (2 x) to afford 4.46 g (22%) of **20** as white crystals: mp 195.5-196.5 °C (lit.<sup>181</sup> mp 197-198 °C); <sup>1</sup>H NMR (DMSO-*d*<sub>6</sub>) δ 7.00-7.15 (m, 3H, ArH and NH, D<sub>2</sub>O ex), 7.22-7.30 (m, 2H, ArH and NH, D<sub>2</sub>O ex), 7.32 (t, 1H, ArH), 7.44 (br s, 3H, NH, D<sub>2</sub>O ex), 7.59 (s, 1H, ArH), 9.92 (br s, 1H, NH<sup>+</sup>, D<sub>2</sub>O ex); IR (diamond, cm<sup>-1</sup>) 3303, 3129, 2962, 1629, 1596.

**2-Amino-7-chloroquinoline Hydrochloride (28).** Compound **28** was prepared according to a literature procedure for a similar compound.<sup>224</sup> A solution of **45** (1.54 g, 7.40 mmol) and SnCl<sub>2</sub>·2H<sub>2</sub>O (16.66 g, 7.40 mmol) in absolute EtOH (100 mL) was heated at reflux for 2.5 h. The reaction mixture was allowed to cool to room temperature and poured into ice-water (75 mL). The solution was made slightly basic (pH ≈ 8-9) by the addition of saturated NaHCO<sub>3</sub> solution. Solid NaCl (≈ 2-3 g) was added to the solution, and the solution extracted with EtOAc (5 x 200 mL). The combined organic extract was dried (Na<sub>2</sub>SO<sub>4</sub>) and the solvent was removed under reduced pressure. The mixture of products (R<sub>f</sub> = 0.5 and 0.9; CH<sub>2</sub>Cl<sub>2</sub>/MeOH/NH<sub>4</sub>OH; 9:1:0.1) was purified by column chromatography (silica gel; CH<sub>2</sub>Cl<sub>2</sub>/MeOH/NH<sub>4</sub>OH; 9:1:0.1) to afford the free base (R<sub>f</sub> = 0.5) of **28** as an off-white solid (0.20 g; 15%): mp 237-240 °C; <sup>1</sup>H NMR (DMSO-*d*<sub>6</sub>) δ 7.11 (d, 1H, ArH), 7.40 (dd, 1H, ArH), 7.51 (br s, 2H, NH<sub>2</sub>, D<sub>2</sub>O ex); IR (diamond, cm<sup>-1</sup>) 3300, 3075, 2915, 1645, 1608.

A saturated solution of HCl (g)/Et<sub>2</sub>O was added to a methanolic solution of the above free base (0.15 g). The resulting salt was collected via filtration and purified by recrystallization from EtOH/Et<sub>2</sub>O to yield 0.08 g (42%) of **28** as a white solid: mp 268-270 °C; <sup>1</sup>H NMR (DMSO-*d*<sub>6</sub>) δ 3.44 (br s, 3H, NH<sub>3</sub><sup>+</sup>, D<sub>2</sub>O ex), 7.27 (d, 1H, ArH), 7.62 (d,

1H, ArH), 8.00 (s, 1H, ArH), 8.04 (d, 1H, ArH), 8.30 (d, 1H, ArH), 9.35 (br s, 1H, NH<sup>+</sup>, D<sub>2</sub>O ex); IR (diamond, cm<sup>-1</sup>) 3263, 3069, 1649. Anal. Calcd (C<sub>9</sub>H<sub>7</sub>N<sub>2</sub>Cl·1.5 HCl) C, 46.33; H, 3.67; N, 12.01. Found: C, 46.67; H, 3.47; N, 11.99.

**3-Amino-6-chloroisoquinoline (29).** Compound **29** was prepared according to a literature procedure for a similar compound.<sup>194</sup> A 2.5 M solution of *n*-BuLi in hexanes (3.7 mL, 9.32 mmol) was added to a stirred solution of **53** (2.0 g, 7.77 mmol) in anhydrous THF (50 mL) at -70 °C under a N<sub>2</sub> atmosphere and allowed to stir for 30 min. The reaction was quenched with absolute EtOH (50 mL) and then allowed to warm to room temperature. The solvent was removed under reduced pressure and the resulting residue was dissolved in CH<sub>2</sub>Cl<sub>2</sub> (100 mL). The solution was washed successively with H<sub>2</sub>O (100 mL) and saturated NH<sub>4</sub>Cl solution (100 mL). The organic extract was dried (Na<sub>2</sub>SO<sub>4</sub>) and concentrated under reduced pressure. The crude product was purified via column chromatography (silica gel; 1<sup>st</sup> column: CH<sub>2</sub>Cl<sub>2</sub>/MeOH; 40:1 to 20:1; 2<sup>nd</sup> column: hexanes/EtOAc = 10:1) and then subsequently recrystallized from benzene to yield 74 mg of **29** (5%) as a yellow solid: mp 228-230 °C (dec.); <sup>1</sup>H NMR (CDCl<sub>3</sub>) δ 4.53 (br s, 2H, NH<sub>2</sub>), 6.65 (s, 1H, ArH), 7.18-7.21 (dd, 1H, ArH), 7.53 (s, 1H, ArH), 7.72-7.74 (d, 1H, ArH), 8.84 (s, 1H, ArH); IR (diamond, cm<sup>-1</sup>) 3428, 3300, 3159, 1647; Anal. Calcd (C<sub>9</sub>H<sub>7</sub>N<sub>2</sub>Cl·0.125 CH<sub>2</sub>Cl<sub>2</sub>) C, 57.92; H, 3.86; N, 14.80, Found: C, 58.12; H, 3.87; N, 14.50.

**2-Amino-7-chloronaphthalene Hydrochloride (30).** Absolute EtOH (5 mL) and platinum oxide (2 mg, 5% w/w) were added to **60** (0.03 g, 0.17 mmol) and the mixture

was allowed to stir at room temperature under a N<sub>2</sub> atmosphere for 15 min. A H<sub>2</sub> balloon was added and the reaction mixture was allowed to stir for 6.5 h. The reaction mixture was filtered over Celite and the solid material was washed with absolute EtOH (35 mL). The filtrate was evaporated under reduced pressure and the resulting beige solid was dried under reduced pressure for 5 h to afford the crude free base of **30** (0.02 g). Hydrogen chloride gas was bubbled slowly through an ethanolic solution (≈3 mL) of the crude free base for 10 min at 0 °C (ice-bath). The solvent was removed under reduced pressure and the crude product as a hydrochloride salt was purified via recrystallization from acetone to yield 0.01 g (34%) product as a brown solid: mp 262-264 °C (lit.<sup>205</sup> mp 261-263 °C).

**2-Amino-7-chlorotetralin Hydrochloride (33).** Compound **33** was prepared according to a literature procedure for a similar compound.<sup>206</sup> Sodium cyanoborohydride (0.08 g, 1.33 mmol) was added to a solution of **63** (0.20 g, 1.11 mmol) and NH<sub>4</sub>OAc (0.85 g, 11.07 mmol) in MeOH (15 mL) at room temperature. The resulting yellow/green solution was allowed to stir for 23 h. The reaction mixture was acidified with 10% HCl to pH ≈ 2, concentrated under reduced pressure, and then extracted with CH<sub>2</sub>Cl<sub>2</sub> (2 x 75 mL). The aqueous portion was basified with 6 N NaOH to pH ≈ 10 and extracted with CH<sub>2</sub>Cl<sub>2</sub> (3 x 75 mL). The combined organic extract was dried (Na<sub>2</sub>SO<sub>4</sub>), concentrated, and the product was dried under reduced pressure for 2 h to yield 0.03 g (16%) of the free base of **33** as a yellow/green oil: <sup>1</sup>H NMR (CDCl<sub>3</sub>) δ 1.50-1.56 (m, 1H, CH), 1.89-1.94 (m, 1H, CH), 2.42-2.49 (m, 1H, CH), 2.67-2.91 (m, 3H, CH), 3.07-3.14 (m, 1H, CH), 6.92-7.00 (m, 3H, ArH); IR (diamond, cm<sup>-1</sup>) 2920, 2849, 2658, 1573.



The free base was converted to the HCl salt by dissolving the oil in absolute EtOH (8 mL); a saturated solution of HCl (g) in EtOH (4 mL) was added at 0 °C (ice-bath) and the mixture was allowed to stir for 30 min. The reaction mixture was concentrated under reduced pressure and washed with anhydrous Et<sub>2</sub>O (10 mL). The resulting solid was recrystallized from EtOH/Et<sub>2</sub>O to yield 0.02 g (50%) of **33** as a pink solid: mp >260 °C; <sup>1</sup>H NMR (DMSO-*d*<sub>6</sub>) δ 1.68-1.78 (m, 1H, CH), 2.09-2.13 (m, 1H, CH), 2.75-2.85 (m, 3H, CH), 3.06-3.11 (m, 1H, CH), 3.43-3.46 (m, 1H, CH), 7.13-7.26 (m, 3H, ArH), 8.12 (br s, 3H, NH<sub>3</sub><sup>+</sup>, D<sub>2</sub>O ex); IR (diamond, cm<sup>-1</sup>) 2920, 2719, 2627, 2556, 2037, 1621, 1599. Anal. Calcd (C<sub>10</sub>H<sub>12</sub>NCl·HCl·0.25 H<sub>2</sub>O) C, 53.95; H, 6.11; N, 6.29. Found: C, 54.26; H, 5.71; N, 6.08.

**2-Amino-5,7-dichloro-3,4-dihydroquinazoline Hydrochloride (38).** Compound **38** was prepared according to a literature procedure for a similar compound.<sup>210</sup> A solution of BH<sub>3</sub>·THF complex (2.9 mL, 1 M) was added in a dropwise manner to 2-amino-5,7-dichloroquinazolin-4(3*H*)-one (**68**) under a N<sub>2</sub> atmosphere. The green reaction mixture was heated at reflux for 1 h. A solution of 6 N HCl (1 mL) was added in a dropwise manner at 0 °C (ice-bath) to hydrolyze the borate complex and excess reagent. The dark-blue suspension was basified with 6 N NaOH (1.5 mL). The reaction mixture was concentrated under reduced pressure and the resulting residue was extracted with hot CHCl<sub>3</sub> (2 x 15 mL). Crude product precipitated when the combined organic extract cooled to room temperature. The combined organic extract was filtered. The filtrate was evaporated to dryness and the product was recrystallized from CHCl<sub>3</sub>. The combined solid was dried in an Abderhalden over toluene heated at reflux for 8 h to

yield 0.09 g (59%) of the free base of **38** as an off-white solid: mp 207-208 °C; <sup>1</sup>H NMR (DMSO-*d*<sub>6</sub>) δ 4.34 (s, 2H, CH<sub>2</sub>), 5.87 (br s, 2H, NH<sub>2</sub>, D<sub>2</sub>O ex), 6.41 (br s, 1H, NH, D<sub>2</sub>O ex), 6.48 (d, 1H, ArH), 6.78 (d, 1H, ArH); IR (diamond, cm<sup>-1</sup>) 3466, 3309, 3162, 1648, 1607.

2-Amino-5,7-dichloro-3,4-dihydroquinazoline (0.04 g, 0.20 mmol) was dissolved in absolute EtOH (5 mL) at 0 °C (ice-bath). A saturated solution of HCl (g) in EtOH (5 mL) was added and allowed to stir for 30 min. The solvent was removed under reduced pressure and the resulting off-white residue was recrystallized from absolute EtOH, washed with cold anhydrous Et<sub>2</sub>O, and dried in an Abderhalden over toluene heated at reflux for 4 d to yield 0.04 g (68%) of **38** as an off-white solid: mp 272-273 °C; <sup>1</sup>H NMR (DMSO-*d*<sub>6</sub>) δ 4.48 (s, 2H, CH<sub>2</sub>), 7.03 (d, 1H, ArH), 7.36 (d, 1H, ArH), 7.85 (br s, 2H, NH<sub>2</sub>, D<sub>2</sub>O ex), 8.69 (br s, 1H, NH, D<sub>2</sub>O ex), 11.22 (br s, 1H, NH<sup>+</sup>, D<sub>2</sub>O ex); IR (diamond, cm<sup>-1</sup>) 3251, 3026, 2972, 2915, 2837, 1662, 1618. Anal. Calcd (C<sub>8</sub>H<sub>7</sub>Cl<sub>2</sub>N<sub>3</sub> HCl·0.25 EtOH·0.25 H<sub>2</sub>O) C, 38.02; H, 3.75; N, 15.65. Found: C, 38.07; H, 3.76; N, 15.57.

**2-Amino-3,4-dihydroquinazoline Hydrochloride (39).** Compound **39** was prepared according to a literature procedure for a similar compound.<sup>210</sup> A solution of BH<sub>3</sub>·THF complex (12 mL, 1 M) was added in a dropwise manner to a solution of **70** (0.50 g, 3.10 mmol) in anhydrous THF (6 mL) under a N<sub>2</sub> atmosphere at 0 °C (ice-bath). The reaction mixture was heated at reflux for 5 h and then allowed to stir at room temperature for 72 h. A solution of 6 N HCl (10 mL) was added in a dropwise manner at 0 °C (ice-bath) to hydrolyze the borate complex and excess reagent. The reaction mixture was heated at reflux without a condenser to remove the solvent. The

suspension was basified with 15% NaOH and extracted with hot CHCl<sub>3</sub> (25 mL). The product precipitated when the combined organic extract cooled to room temperature. The suspension was filtered and the solid was dried in a desiccator over NaOH pellets to yield 0.23 g (49%) of the free base of **39** as an off-white solid: mp 228 °C (lit.<sup>211</sup> mp 214-216 °C); <sup>1</sup>H NMR (DMSO-*d*<sub>6</sub>) δ 4.27 (s, 2H, CH<sub>2</sub>), 6.51 (d, 1H, ArH), 6.63 (t, 1H, ArH), 6.79 (d, 1H, ArH), 6.93 (t, 1H, ArH); IR (diamond, cm<sup>-1</sup>) 3390, 3307, 3108, 2819, 1653.

2-Amino-3,4-dihydroquinazoline (0.10 g, 0.07 mmol) was dissolved in absolute EtOH (5 mL) and allowed to stir at 0 °C (ice-water). A saturated solution of HCl (g) in absolute EtOH (5 mL) was added and the reaction mixture was allowed to stir for 30 min. The solvent was removed under reduced pressure and the resulting off-white residue was dissolved in hot absolute EtOH. The suspension was filtered and the filtrate was concentrated under reduced pressure. The residue was recrystallized from absolute EtOH and then dried in an Abderhalden over toluene heated at reflux for 12 h to yield 0.09 g (74%) of **39** as an off-white solid: mp 158-160 °C (lit.<sup>210</sup> ·HI mp 199-200 °C); <sup>1</sup>H NMR (DMSO-*d*<sub>6</sub>) δ 4.49 (s, 2H, CH<sub>2</sub>), 6.97 (d, 1H, ArH), 7.09 (t, 1H, ArH), 7.18 (d, 1H, ArH), 7.26 (t, 1H, ArH), 7.63 (br s, 2H, NH<sub>2</sub>, D<sub>2</sub>O ex), 8.51 (br s, 1H, NH, D<sub>2</sub>O ex), 10.83 (br s, 1H, NH<sup>+</sup>, D<sub>2</sub>O ex); IR (diamond, cm<sup>-1</sup>) 3261, 3088, 2963, 2870, 1671, 1626. Anal. Calcd (C<sub>8</sub>H<sub>9</sub>N<sub>3</sub>·HCl·0.25 EtOH·0.25 H<sub>2</sub>O) C, 51.13; H, 6.06; N, 21.05. Found: C, 51.23; H, 5.66; N, 20.92.

**meta-Chloroaniline Hydrochloride (41).** A 35 M HCl/Et<sub>2</sub>O solution (22.5 mL, 78.75 mmol) was added in a dropwise manner to a solution of *m*-chloroaniline (**40**; 10.00 g,

78.39 mmol) in absolute EtOH (100 mL) at -10 °C. The precipitated HCl salt was collected by filtration, recrystallized three times from acetone, and dried (KOH) to yield 3.59 g (28%) of **41** as a white powder: mp 218-219 °C (lit.<sup>180</sup> mp 221.5-222.5 °C).

**[2-(4-Chloro-2-nitrophenyl)vinyl]dimethylamine (43)**. Compound **43** was prepared according to a literature procedure for a similar compound.<sup>225</sup> Dimethylformamide dimethylacetal (11.6 mL, 87 mmol) and pyrrolidine (3.6 mL, 44 mmol) were added to a solution of 4-chloro-2-nitrotoluene (**42**; 5.00 g, 29 mmol) in DMF (25 mL) at 110 °C under a N<sub>2</sub> atmosphere. The reaction mixture was allowed to stir for 1 h, diluted with Et<sub>2</sub>O (200 mL), and washed with H<sub>2</sub>O (150 mL). Solid NaCl (≈ 3-4 g) was added to the suspension and the organic portion was dried (MgSO<sub>4</sub>). The solvent was removed under reduced pressure to afford 7.60 g (100%) of **43** as a dark-violet crude substance: mp 43-45 °C (lit.<sup>226</sup> mp 44-46 °C); <sup>1</sup>H NMR (CDCl<sub>3</sub>) δ 2.92 (s, 6H, CH<sub>3</sub>), 5.82 (d, 1H, CH), 6.94 (d, 1H, CH), 7.21-7.29 (m, 1H, ArH), 7.38 (d, 1H, ArH), 7.85 (s, 1H, ArH); IR (diamond, cm<sup>-1</sup>) 2976, 2930, 2853, 1691, 1596.

**4-Chloro-2-nitrobenzaldehyde (44)**. Compound **44** was prepared according to a literature procedure for a similar compound.<sup>227</sup> Compound **43** (0.64 g, 2.80 mmol) in DMF (2.5 mL) was added in a dropwise manner to a solution of NaIO<sub>4</sub> (1.80 g, 8.50 mmol) in H<sub>2</sub>O (5 mL) at room temperature. The reaction mixture was allowed to stir for 1.5 h. The crude reaction mixture was filtered and the solid was washed with toluene (50 mL). The organic portion of the filtrate was washed with H<sub>2</sub>O (3 x 25 mL) and concentrated under reduced pressure. The oily residue was purified by column

chromatography (silica gel; hexanes/EtOAc; 5:1) to afford 0.32 g (61%) of **44** as a pale-yellow solid: mp 66-68 °C (lit.<sup>228</sup> mp 67-68 °C, Et<sub>2</sub>O); <sup>1</sup>H NMR (CDCl<sub>3</sub>) δ 7.76 (dd, 1H, ArH), 7.94 (d, 1H, ArH), 8.10 (s, 1H, ArH), 10.39 (s, 1H, CHO); IR (diamond, cm<sup>-1</sup>) 3368, 3087, 2926, 1691, 1597.

**3-(4-Chloro-2-nitrophenyl)acrylonitrile (45).** Compound **45** was prepared according to a literature procedure for a similar compound.<sup>229</sup> Sodium hydride (0.55 g, 13.80 mmol) was added portionwise to a stirred solution of diethyl cyanomethylphosphonate (2.45 g, 13.80 mmol) in anhydrous DMF (100 mL) at 0 °C (ice-bath). A solution of **44** (2.57 g, 13.80 mmol) in anhydrous DMF (25 mL) was added to the reaction mixture in a dropwise manner (over 10 min). After another 5 min, the reaction mixture was poured into ice-water and extracted with Et<sub>2</sub>O (100 mL). The organic portion was dried (MgSO<sub>4</sub>) and concentrated under reduced pressure. The residue was purified by column chromatography (silica gel; hexanes/EtOAc; 1:1) to afford 1.55 g (54%) of **45** as a dark-purple oil: <sup>1</sup>H NMR (CDCl<sub>3</sub>) δ 5.73 (d, 1H, CH), 5.85 (d, 1H, CH), 7.51-8.21 (m, 3H, ArH); IR (nujol, cm<sup>-1</sup>) 2958, 2905, 2844, 2344, 2215, 1514.

**(E)-3-(2-Amino-4-chlorophenyl)acrylonitrile (46).** The second product from the previous reaction was isolated by column chromatography (silica gel; CH<sub>2</sub>Cl<sub>2</sub>/MeOH/NH<sub>4</sub>OH; 9:1:0.1) and recrystallized from benzene to afford the free base (R<sub>f</sub> = 0.9) of **46** as a light-brown solid (0.33 g, 25%): mp 159-160 °C; <sup>1</sup>H NMR (DMSO-*d*<sub>6</sub>) δ 6.03 (br s, 2H, NH<sub>2</sub>, D<sub>2</sub>O ex), 6.18 (d, 1H, CH), 6.55 (d, 1H, ArH), 6.73 (d, 1H, CH),

7.44 (d, 1H, ArH), 7.76 (d, 1H, ArH); IR (diamond,  $\text{cm}^{-1}$ ) 3461, 3374, 3230, 3057, 2214, 1635, 1598.

**7-Chloro-2-acetamidoquinoline (49).** Compound **49** was prepared according to a literature procedure for a similar compound.<sup>230</sup> Acetic acid (0.1 mL, 1.70 mmol) was added in a dropwise manner to acetic anhydride (0.14 mL, 1.51 mmol) at 0 °C (ice-bath) and allowed to stir for 2 h at room temperature. The reaction mixture was added to a solution of **28** (free base; 135 mg, 0.76 mmol) in anhydrous THF (25 mL) under a  $\text{N}_2$  atmosphere and allowed to stir for 30 min. The solvent was removed under reduced pressure. Methanol (20 mL) was added, the reaction mixture was allowed to stir for 30 min and the solvent was removed under reduced pressure. Diethyl ether (20 mL) was added, the reaction mixture was allowed to stir for 1 h and subsequently filtered. The precipitate was dried in an Abderhalden over toluene heated at reflux for 12 h to yield 120 mg (72%) of **49** as an off-white solid: mp 209-210 °C;  $^1\text{H}$  NMR ( $\text{CDCl}_3$ )  $\delta$  2.31 (s, 3H,  $\text{CH}_3$ ), 7.44-7.47 (dd, 1H, ArH), 7.69-7.72 (m, 2H, ArH), 8.53-8.55 (d, 1H, ArH), 8.59-8.60 (d, 1H, ArH), 10.24 (br s, 1H, NH); IR (diamond,  $\text{cm}^{-1}$ ) 3138, 1696, 1607.

**4-Chloro-2-cyanomethylbenzotrile (52).** Compound **52** was prepared according to a literature procedure for a similar compound.<sup>199</sup> Ethyl cyanoacetate (6.81 mL, 64 mmol) was added over 10 min to a suspension of NaH (2.56 g, 64 mmol, 60% dispersion in mineral oil) in DMSO (25 mL) at 0 °C (ice-bath). The yellow reaction mixture was allowed to stir at room temperature for 30 min. Compound **51** (5.0 g, 32 mmol) was added as a solution in DMSO (25 mL) and the resulting peach-colored

solution was allowed to stir at 90 °C for 9 h. Water (25 mL) was added and the reaction mixture was heated at reflux for 8 h. The bright-yellow reaction mixture was allowed to cool to 5 °C over 30 min. A 0.15 N HCl solution (20 mL) was added and the reaction mixture was allowed to stir for an additional 30 min. The resulting precipitate was filtered, washed successively with H<sub>2</sub>O (25 mL), 0.1 M NaOH solution (2 x 75 mL) and brine (50 mL), and dried (Na<sub>2</sub>SO<sub>4</sub>) to yield 4.70 g of **52** (83%) as a pale-yellow powder: mp 116-117 °C (lit.<sup>191</sup> mp 119-120 °C); <sup>1</sup>H NMR (CDCl<sub>3</sub>) δ 3.92 (s, 2H, CH<sub>2</sub>), 7.40-7.42 (dd, 1H, ArH), 7.57-7.59 (d, 1H, ArH), 7.61-7.62 (d, 1H, ArH); IR (diamond, cm<sup>-1</sup>) 3083, 2991, 2226, 1592.

**3-Amino-1-bromo-6-chloroisoquinoline (53).** Compound **53** was prepared according to a literature procedure for a similar compound.<sup>231</sup> Compound **52** (4.7 g, 27 mmol) and a solution of HBr (g) in AcOH (25 mL, 30%) were allowed to stir for 1 h at room temperature. Diethyl ether (50 mL) was added, and the reaction mixture was allowed to stir for 30 min. The resulting yellow/orange precipitate was filtered, washed with Et<sub>2</sub>O (2 x 25 mL), suspended in EtOAc (150 mL), and neutralized with saturated aq NaHCO<sub>3</sub> solution (100 mL). The organic extract was dried (Na<sub>2</sub>SO<sub>4</sub>) and concentrated under reduced pressure. The crude product was washed with cold Et<sub>2</sub>O (2 x 50 mL) to yield 2.01 g of **53** (29%) as an orange solid: mp 175-177 °C; <sup>1</sup>H NMR (CDCl<sub>3</sub>) δ 7.39-7.42 (dd, 1H, ArH), 7.72-7.73 (d, 1H, ArH), 7.87 (br s, 2H, NH<sub>2</sub>), 8.03-8.06 (d, 1H, ArH), 8.36 (s, 1H, ArH); IR (diamond, cm<sup>-1</sup>) 3222, 3183, 3045, 1664, 1552.

**3,6-Dinitro-1,8-naphthalic anhydride (57).** Compound **57** was prepared according to a literature procedure.<sup>195</sup> 1,8-Naphthalic anhydride (**56**; 10.0 g, 50.0 mmol) was added to concentrated H<sub>2</sub>SO<sub>4</sub> (40.4 mL) and the resulting green solution was cooled to 5 °C. While avoiding a rise in temperature above 20 °C, concentrated HNO<sub>3</sub> (9.3 mL) was added in a dropwise manner to the solution. The yellow solution was heated to 60 °C for 1.5 h and then allowed to cool to room temperature. The reaction mixture was added to ice-water (100 mL) in a dropwise manner and the resulting precipitate was filtered and washed with H<sub>2</sub>O (3 x 75 mL). The crude product was recrystallized from glacial AcOH, washed with H<sub>2</sub>O (3 x 50 mL), and dried in an Abderhalden over toluene heated at reflux for 12 h to yield 8.7 g (60%) of **57** as a yellow solid: mp 199-200 °C (lit.<sup>195</sup> mp 208-210 °C, glacial AcOH); <sup>1</sup>H NMR (CDCl<sub>3</sub>) δ 9.50 (d, 2H, ArH), 9.56 (d, 2H, ArH); IR (diamond, cm<sup>-1</sup>) 3071, 1782, 1741, 1597.

**2,7-Dinitronaphthalene (58).** Compound **58** was prepared according to a literature procedure.<sup>196</sup> Compound **57** (7.6 g, 26.37 mmol) was added over 4 min to a suspension of copper powder (1.9 g) in boiling quinoline (previously distilled, 15.6 mL) and then more copper powder (1.9 g) was added. After 1 h, the reaction mixture was allowed to cool to room temperature and Et<sub>2</sub>O (250 mL) was added. The resulting dark-brown reaction mixture was filtered and the filtrate was washed with H<sub>2</sub>O (2 x 100 mL). The organic extract was washed successively with 15% HCl solution (2 x 75 mL), cold saturated NaHCO<sub>3</sub> solution (100 mL), and H<sub>2</sub>O (100 mL). The organic portion was dried (MgSO<sub>4</sub>) and the solvent was removed under reduced pressure. The crude product was purified via column chromatography (silica gel; hexanes/EtOAc; 2:1 to 1:1) and



dried in an Abderhalden over toluene heated at reflux for 5 h to yield 0.8 g (13%) of **58** as an orange solid: mp 225-228 °C (lit.<sup>196</sup> mp 234 °C, glacial AcOH); <sup>1</sup>H NMR (CDCl<sub>3</sub>) δ 8.17 (d, 2H, ArH), 8.50 (dd, 2H, ArH), 9.04 (s, 2H, ArH); IR (diamond, cm<sup>-1</sup>) 3081, 1628, 1514.

**2-Amino-7-nitronaphthalene (59).** Compound **59** was prepared according to a literature procedure.<sup>197</sup> A solution of NaSH (0.07 g, 1.27 mmol) in MeOH (2 mL) was added over 15 min to a solution of **58** (0.19 g, 0.85 mmol) in MeOH (3 mL) and H<sub>2</sub>O (6 mL) heated at reflux. The dark-purple reaction mixture was heated for 3 h and then poured into ice-water (50 mL). The resulting orange precipitate was filtered and washed with boiling 10% aq HCl solution (25 mL). The filtrate was basified with 10% NaOH solution and extracted with EtOAc (50 mL). The organic extract was dried (MgSO<sub>4</sub>) and the solvent was removed under reduced pressure to afford **59** (0.10 g, 64%) as an orange solid: mp 159-162 °C (lit.<sup>196</sup> mp 184.5 °C, EtOH); <sup>1</sup>H NMR (CDCl<sub>3</sub>) δ 4.14 (br s, 2H, NH<sub>2</sub>, D<sub>2</sub>O ex), 7.13-7.17 (m, 2H, ArH), 7.76-7.83 (m, 2H, ArH), 7.99 (dd, 1H, ArH), 8.56 (d, 1H, ArH); IR (diamond, cm<sup>-1</sup>) 3486, 3383, 2920, 1631, 1518.

**7-Chloro-2-nitronaphthalene (60).** Compound **60** was prepared according to a literature procedure for a similar compound.<sup>198</sup> Acetic acid (0.4 mL) and **59** (0.09 g, 0.48 mmol) were added to a stirred solution of NaNO<sub>2</sub> (0.07 g, 1.06 mmol) in concentrated H<sub>2</sub>SO<sub>4</sub> (0.4 mL) at 0 °C (ice-bath). The resulting solution was added in a dropwise manner to a suspension of CuCl (0.17 g, 1.72 mmol) in concentrated HCl solution (0.7 mL) at 0 °C (ice-bath) and the mixture was allowed to stir for 2 h. The

black reaction mixture was poured into ice-water (50 mL) and the aqueous layer was extracted with CH<sub>2</sub>Cl<sub>2</sub> (50 mL). The organic extract was dried (Na<sub>2</sub>SO<sub>4</sub>) and the solvent was removed under reduced pressure. The crude product was purified via column chromatography (silica gel; hexanes/EtOAc; 20:1) to yield 0.02 g of **60** (19%) as a yellow needle-like solid: mp 137-139 °C (lit.<sup>229</sup> mp 139-140 °C, EtOH); <sup>1</sup>H NMR (CDCl<sub>3</sub>) δ 7.65-7.74 (m, 2H, ArH), 7.92-8.06 (m, 2H, ArH), 8.28 (dd, 1H, ArH), 8.80 (dd, 1H, ArH); IR (diamond, cm<sup>-1</sup>) 2917, 2845, 1731, 1586, 1514.

**3-Chlorophenylacetyl chloride (62).** Compound **62** was prepared according to a literature procedure for a similar compound.<sup>203</sup> Thionyl chloride (3.2 mL, 43.96 mmol) was added to a stirred solution of 3-chlorophenylacetic acid (**61**; 5.00 g, 29.31 mmol) in CH<sub>2</sub>Cl<sub>2</sub> (12 mL) at room temperature. The yellow, translucent reaction mixture was heated at reflux for 24 h and then allowed to cool to room temperature. The orange reaction mixture was concentrated under reduced pressure. The product was purified via Kuger-rohr distillation (0.5 Torr, bp 97-103 °C; lit.<sup>233</sup> 1 Torr, bp 77.5-78 °C) and dried under reduced pressure for 2 h to yield 3.69 g (67%) of **62** as a yellow liquid: <sup>1</sup>H NMR (CDCl<sub>3</sub>) δ 4.05 (s, 2H, CH<sub>2</sub>), 7.08-7.10 (m, 1H, ArH), 7.19-7.25 (m, 3H, ArH); IR (diamond, cm<sup>-1</sup>) 3358, 3065, 2912, 1790, 1599.

**7-Chloro-β-tetralone (63) and 5-Chloro-β-tetralone (64).** Compounds **63** and **64** were prepared according to a literature procedure.<sup>204</sup> Compound **62** (2.49 g, 13.17 mmol) was dissolved in CH<sub>2</sub>Cl<sub>2</sub> (25 mL) and added via an addition funnel over 20 min to a white suspension of AlCl<sub>3</sub> (previously sublimed; 3.86 g, 28.98 mmol) in CH<sub>2</sub>Cl<sub>2</sub> (125

mL) stirring at -10 to 0 °C (cooling bath with CO<sub>2</sub>). Ethylene gas was bubbled into the yellow mixture for 30 min, causing the temperature to rise to 5 °C, and then drop back down to -5 °C. Ethylene gas was allowed to bubble slowly through the mixture for an additional 1.75 h. Ice-water (100 mL) was added to the pale-yellow reaction mixture. The organic layer was separated and washed successively with 10% HCl (100 mL), saturated aq Na<sub>2</sub>CO<sub>3</sub> (100 mL), and then dried (Na<sub>2</sub>SO<sub>4</sub>). The solvent was removed under reduced pressure and the product was isolated via column chromatography (silica gel; hexanes/EtOAc; 9:1) to yield 0.36 g (15%) of **64** as a yellow oil and 0.24 g (10%) of **63** as a pale-yellow solid: mp 37-38 °C (lit.<sup>234</sup> mp 38-39 °C). Both products were dried under reduced pressure for 1 h and stored at -80 °C. **63**: <sup>1</sup>H NMR (CDCl<sub>3</sub>) δ 2.48 (t, 2H, CH<sub>2</sub>), 2.97 (t, 2H, CH<sub>2</sub>), 3.49 (s, 2H, CH<sub>2</sub>), 7.10 (m, 3H, ArH); IR (diamond, cm<sup>-1</sup>) 3022, 2964, 2763, 1686, 1598. **64**: <sup>1</sup>H NMR (CDCl<sub>3</sub>) δ 2.50 (t, 2H, CH<sub>2</sub>), 3.17 (t, 2H, CH<sub>2</sub>), 3.53 (s, 2H, CH<sub>2</sub>), 6.96 (d, 1H, ArH), 7.09 (t, 1H, ArH), 7.23 (d, 1H, ArH); IR (diamond, cm<sup>-1</sup>) 3064, 2916, 2849, 1817, 1715.

**2-Amino-5-chlorotetralin Hydrochloride (65).** Compound **65** was prepared according to a literature procedure for a similar compound.<sup>206</sup> Sodium cyanoborohydride (0.04 g; 0.62 mmol) was added to a solution of **64** (0.09 g; 0.52 mmol) and NH<sub>4</sub>OAc (0.40 g; 5.20 mmol) in MeOH (10 mL) at room temperature. The resulting pale-yellow/brown solution was allowed to stir for 18 h. The reaction mixture was acidified with 10% HCl solution (pH ≈ 2.0), concentrated under reduced pressure, and then extracted with CH<sub>2</sub>Cl<sub>2</sub> (2 x 50 mL). The aqueous portion was basified with 6 N NaOH (pH ≈ 10) and extracted with CH<sub>2</sub>Cl<sub>2</sub> (3 x 50 mL). The combined organic extract was dried (Na<sub>2</sub>SO<sub>4</sub>)

and concentrated under reduced pressure. The resulting yellow oil was dried under reduced pressure for 2 h to yield 0.03 g (32%) of the free base of **65**:  $^1\text{H NMR}$  ( $\text{CDCl}_3$ )  $\delta$  1.52-1.59 (m, 1H, CH), 1.95-2.01 (m, 1H, CH), 2.45-2.54 (m, 1H, CH), 2.63-2.71 (m, 1H, CH), 2.89-2.97 (m, 2H, CH), 3.07-3.14 (m, 1H, CH), 6.90-7.13 (m, 3H, ArH); IR (diamond,  $\text{cm}^{-1}$ ) 3340, 3276, 3060, 2927, 2855, 1568.

The free base was converted to the HCl salt by dissolving the oil in absolute EtOH (5 mL). A saturated solution of HCl (g) in EtOH (4 mL) was added at 0 °C (ice-bath) and allowed to stir for 30 min at 0 °C (ice-bath). The reaction mixture was concentrated under reduced pressure and washed with Et<sub>2</sub>O (10 mL). The resulting crude solid was recrystallized from EtOH/Et<sub>2</sub>O to yield 0.02 g (18%) of **65** as a pink solid: mp 280-282 °C (dec);  $^1\text{H NMR}$  ( $\text{DMSO}-d_6$ )  $\delta$  1.61-1.71 (m, 1H, CH), 2.02-2.05 (m, 1H, CH), 2.67-2.78 (m, 3H, CH), 2.99-3.04 (m, 1H, CH), 3.34-3.38 (m, 1H, CH), 7.06-7.18 (m, 3H, ArH), 8.04 (br s, 3H,  $\text{NH}_3^+$ ,  $\text{D}_2\text{O}$  ex); IR (diamond,  $\text{cm}^{-1}$ ) 2921, 2718, 2627, 2556, 2037, 1620, 1599. Anal. Calcd ( $\text{C}_{10}\text{H}_{12}\text{NCl}\cdot\text{HCl}$ ) C, 55.06; H, 6.01; N, 6.42. Found: C, 55.03; H, 5.95; N, 6.32.

#### **4,6-Dichloroisatoic anhydride (67).**

Method A. Compound **67** was prepared according to a literature procedure.<sup>208</sup> Chromium trioxide (0.33 g, 3.30 mmol) was added portionwise at 90 °C to a stirred suspension of 4,6-dichloroisatin (**66**; 0.72 g, 3.31 mmol) in glacial AcOH (4 mL) and acetic anhydride (4 mL). The reaction mixture was allowed to stir at 90 °C for 1.5 h. Water (20 mL) was added to the green reaction mixture and the crude product precipitated. The crude solid was collected by filtration, washed with H<sub>2</sub>O (15 mL), and

dried under reduced pressure for 1 h to yield 0.55 g of crude product (and starting material) as a yellow solid. It was determined by  $^1\text{H}$  NMR that the crude solid was a mixture of 4,6-dichloroisatin (**66**; 45%) and **67** (55%). This crude product was used in the next step without purification.

Method B. Compound **67** was prepared according to a literature procedure for a similar compound.<sup>232</sup> A suspension of 4,6-dichloroisatin (**66**; 0.50 g, 2.32 mmol) in glacial AcOH (2.5 mL) and concentrated  $\text{H}_2\text{SO}_4$  (2 drops) was heated to 30 °C. The reaction mixture was allowed to stir for 15 min and then an aqueous solution of  $\text{H}_2\text{O}_2$  (0.3 mL; 30%) was added in a dropwise manner. The reaction mixture was slowly heated to 65 °C and after 5 h the reaction mixture was allowed to cool to room temperature. The resulting precipitate was collected by filtration, washed with  $\text{H}_2\text{O}$  (3 x 5 mL), and dried under reduced pressure for 8 h to yield 0.32 g of crude product (and starting material) as a yellow solid. It was determined by  $^1\text{H}$  NMR that the crude solid was a mixture of 4,6-dichloroisatin (**66**; 56%) and **67** (44%). This crude product was used in the next step without purification.

**2-Amino-5,7-dichloroquinazolin-4(3H)-one (68).** Compound **68** was prepared according to a literature procedure for a similar compound.<sup>209</sup> S-Methylthioisourea sulfate (0.30 g, 1.07 mmol) and  $\text{Na}_2\text{CO}_3$  (0.11 g, 1.07 mmol) were added to a solution of 4,6-dichloroisatoic anhydride (**67**; 0.25 g, 1.07 mmol) and 4,6-dichloroisatin (**66**; 0.30 g, 1.37 mmol) dissolved in aq MeCN (11 mL, 80%). The resulting solution was heated at reflux for 23 h. The reaction mixture was allowed to cool to room temperature over a

period of 30 min, H<sub>2</sub>O (20 mL) was added, and the reaction mixture was allowed to stir for 2 h. The reaction mixture was filtered and the precipitate was washed with aq MeCN (3 x 15 mL; 80%). The solid was dried in an Abderhalden over toluene heated at reflux for 24 h to yield 0.17 g (70%) of **68** as a beige solid: mp >300 °C; <sup>1</sup>H NMR (DMSO-*d*<sub>6</sub>) δ 6.64 (br s, 2H, NH<sub>2</sub>, D<sub>2</sub>O ex), 7.13-7.15 (m, 2H, ArH), 11.10 (br s, 1H, NH, D<sub>2</sub>O ex); IR (diamond, cm<sup>-1</sup>) 3385, 2925, 2257, 2130, 1652.

To recover the isatin starting material, the filtrate was concentrated under reduced pressure, dissolved in EtOAc (100 mL), and washed with 15% HCl solution (50 mL). The aqueous layer was basified with 10% NaOH and extracted with EtOAc (2 x 50 mL). The combined organic portion was dried (MgSO<sub>4</sub>) and the solvent was removed under reduced pressure.

**2-Aminoquinazolin-4(3H)-one (70).** Compound **70** was prepared according to a literature procedure for a similar compound.<sup>209</sup> S-Methylthioisourea sulfate (5.56 g, 20.00 mmol) and Na<sub>2</sub>CO<sub>3</sub> (3.20 g, 30.00 mmol) were added to a solution of isatoic anhydride (**69**; 3.26 g, 20.00 mmol) in aq MeCN (100 mL, 80%) and the resulting dark-brown solution was heated at reflux for 23 h. The light-yellow reaction mixture was allowed to cool to room temperature over a period of 30 min. The resulting precipitate was collected by filtration and washed successively with aq MeCN (3 x 25 mL; 80%) and H<sub>2</sub>O (75 mL). The solid was dried under reduced pressure and recrystallized from absolute EtOH to yield 1.14 g (35%) of **70** as a white solid: mp >300 °C (lit.<sup>214</sup> mp >250 °C); <sup>1</sup>H NMR (DMSO-*d*<sub>6</sub>) δ 6.40 (br s, 2H, NH<sub>2</sub>, D<sub>2</sub>O ex), 7.10 (t, 1H, ArH), 7.20 (d, 1H,

ArH), 7.55 (t, 1H, ArH), 7.88 (d, 1H, ArH), 11.03 (br s, 1H, NH, D<sub>2</sub>O ex); IR (KBr, cm<sup>-1</sup>) 3404, 3144, 3061, 1684, 1656, 1606.

### C. Molecular modeling

All ligands and models were built in Sybyl (version 8.1; Tripos Associates, St. Louis, MO) on a Silicon Graphics workstation and given AM1 charges and geometries based on MOPAC. A conformation search of MD-354 (**21**), in order to identify the lowest-energy conformers, was conducted using Sybyl (Tripos Force Field, AM1).

In order to generate homology models of the inactive and active state of  $\alpha_{2A}$ ,  $\alpha_{2B}$ - and  $\alpha_{2C}$ -ARs, first, a sequence alignment of the  $\alpha_2$ -ARs and other GPCRs was created. Mimicking Bissantz et al.,<sup>214</sup> an alignment profile of several GPCRs including the primary sequences of human muscarinic cholinergic M<sub>1</sub> (P11229), human vasopressin V<sub>1a</sub> (P37288), human dopamine D<sub>3</sub> (P35462), human adrenergic  $\beta_2$  (P07550), human  $\delta$ -opioid (P41143) and bovine rhodopsin (P02699), all of which were retrieved from the ExPASy Proteomics Server (<http://www.expasy.org/>) at the Swiss Institute of Bioinformatics, was generated and further aligned to the human  $\alpha_{2A}$ -AR (P08913) sequence using the ClustalX program (BLOSUM matrix series; gap opening: 15.0). Two alignments were generated as described above: (1) included amino acid residues from the *N*-terminus to the IL-3 and (2) included amino acid residues from the IL-3 to the *C*-terminus.<sup>236</sup> Previously identified highly conserved amino acid residues within GPCRs<sup>237,238</sup> are aligned and there are no insertions or deletions in the transmembrane regions.

This alignment was used to generate the model of the  $\alpha_{2A}$ -AR based on its homology to human  $\beta_2$ -AR (chain A of PDB entry = 2RH1; RCSB Protein Data Bank, <http://www.rcsb.org>). The  $\alpha_{2A}$ -AR model was used as a template for  $\alpha_{2B}$ - and  $\alpha_{2C}$ -ARs, which means sequence alignments of  $\alpha_{2B}$ -AR and  $\alpha_{2A}$ -AR, as well as  $\alpha_{2C}$ -AR and  $\alpha_{2A}$ -AR, were first generated followed by mutating amino acid residues in the  $\alpha_{2A}$ -AR model to mimic the  $\alpha_{2B}$ -AR and  $\alpha_{2C}$ -AR. Ligand docking in these models was performed via GOLD (Version 4.0; 10 genetic algorithm runs/15 Å sphere around conserved D3.32).



## References

1. American Cancer Society. Cancer facts and statistics 2010. Atlanta: American Cancer Society: **2010**.
2. Christo, P. J.; Mazloomdoost, D. Cancer pain and analgesia. *Ann. N.Y. Acad. Sci.* **2008**, *1138*, 278-298.
3. World Health Organization. Cancer pain relief. 2<sup>nd</sup> ed. World Health Organization: **1996**.
4. Droney, J.; Riley, J. Recent advances in the use of opioids for cancer pain. *J. Pain Res.* **2009**, *2*, 135-155.
5. Pharo, G. H.; Zhou, L. Pharmacologic management of cancer pain. *J. Am. Osteopath. Assoc.* **2005**, *105*, S21-S28.
6. Pharo, G. H.; Zhou, L. Controlling cancer pain with pharmacotherapy. *J. Am. Osteopath. Assoc.* **2007**, *107*, ES22-ES32.
7. McNicol, E.; Strassels, S.; Goudas, L.; Lau, J.; Carr, D. Nonsteroidal anti-inflammatory drugs, alone or combined with opioids, for cancer pain: a systematic review. *J. Clin. Oncol.* **2004**, *22*, 1975-1992.
8. Passik, S. D. Issues in long-term opioid therapy: unmet needs, risks, and solutions. *Mayo Clin. Proc.* **2009**, *84*, 593-601.

9. Eisenach, J. C.; Du Pen, S.; Dubois, M.; Miguel, R.; Allin, D. Epidural clonidine analgesia for intractable cancer pain. The epidural clonidine study group. *Pain* **1995**, *61*, 391-399.
10. Eisenach, J. C.; De Kock, M.; Klimscha, W.  $\alpha_2$ -Adrenergic agonists for regional anesthesia – a clinical review of clonidine, 1984-1995. *Anesthesiology* **1996**, *85*, 655-674.
11. Honore, P.; Chapman, V.; Burtova, J.; Besson, J. M. To what extent do spinal interactions between an  $\alpha_2$  adrenoceptor agonist and a  $\mu$ -opioid agonist influence noxiously evoked c-fos expression in the rat? A pharmacological study. *J. Pharmacol. Exp. Ther.* **1996**, *278*, 393-403.
12. Millan, M. J. The role of descending noradrenergic and serotonergic pathways in the modulation of nociception: focus on receptor multiplicity. In *The Pharmacology of Pain, Handbook of Experimental Pharmacology*, Dickenson, A.; Besson, J. M., Eds.; Springer: Berlin, **1997**; *130*, pp 385-446.
13. Shinomura, T.; Nakao, S. I.; Adachi, T.; Shigu, K. Clonidine inhibits and phorbol acetate activates glutamate release from rat spinal synaptoneurosomes. *Anesth. Analg.* **1999**, *88*, 1401-1405.
14. Supowit, S. C.; Hallman, D. M.; Zhao, H.; DiPette, D. J.  $\alpha_2$ -Adrenergic receptor activation inhibits calcitonin gene-related peptide expression in cultured dorsal horn root ganglia neurons. *Brain Res.* **1998**, *782*, 184-193.
15. Yaksh, T. L. Pharmacology of spinal adrenergic systems which modulate spinal nociceptive processing. *Pharmacol. Biochem. Behav.* **1985**, *22*, 845-858.
16. Millan, M. J. Descending control of pain. *Prog. Neurobiol.* **2002**, *66*, 355-474.

17. MacDonald, E.; Kobilka, B. K.; Scheinin, M. Gene targeting – homing in on alpha2-adrenoceptor-subtype function. *Trends Pharmacol. Sci.* **1997**, *18*, 211-219.
18. Lahdesmaki, J.; Sallinen, J.; MacDonald, E.; Kobilka, B. K.; Fagerholm, V.; Scheinin, M. Behavioral and neurochemical characterization of  $\alpha_{2A}$ -adrenergic receptor knockout mice. *Neuroscience* **2002**, *113*, 289-299.
19. Millan, M. J. Serotonin (5-HT) and pain: a reappraisal of its role in the light of receptor multiplicity. *Semin. Neurosci.* **1995**, *7*, 409-419.
20. Millan, M. J. The role of descending noradrenergic and serotonergic pathways in the modulation of nociception: Focus on receptor multiplicity. In *The Pharmacology of Pain: Handbook of Experimental Pharmacology*, Vol. 130, Dickenson, A.; Besson, J. M., Eds.; Springer: Berlin, **1997**; pp 385-446.
21. Hanna, M. C.; Davies, P. A.; Hales, T. G.; Kirkness, E. F. Evidence for expression of heteromeric serotonin 5-HT<sub>3</sub> receptors in rodents. *J. Neurochem.* **2000**, *75*, 240-247.
22. Barnes, N. M.; Sharp, T. A review of central 5-HT receptors and their function. *Neuropharmacology* **1999**, *38*, 1083-1152.
23. Van Hooft, J. A.; Vijverberg, H. P. M. 5-HT<sub>3</sub> receptors and neurotransmitter release in the CNS: a nerve ending story? *Trends Neurosci.* **2000**, *23*, 605-610.
24. Morales, M. A.; McCollum, N.; Kirkness, E. F. 5-HT<sub>3</sub>-receptor subunits A and B are co-expressed in neurons of the dorsal root ganglion. *J. Comp. Neurol.* **2001**, *438*, 163-172.

25. Crisp, T.; Stafinsky, J. L.; Spanos, L. J.; Uram, M.; Perni, V. C.; Donepudi, H. B. Analgesic effects of serotonin and receptor-selective serotonin agonists in the rat spinal cord. *Gen. Pharmacol.* **1991**, *22*, 247-251.
26. Ali, Z.; Wu, G.; Kozlov, A.; Barasi, S. The role of 5HT<sub>3</sub> in nociceptive processing in the rat spinal cord: from behavioural and electrophysiological studies. *Neurosci. Lett.* **1996**, *208*, 203-207.
27. Alhaider, A. A. Effect of systemically administered SR 57227A on the tail-flick latency in mice. *Pharmacologist* **1997**, *39*, 108.
28. Alhaider, A. A.; Lei, S.; Kitto, K. F.; Wilcox, G. L. Behavioral and electrophysiological studies of 5-HT<sub>3</sub> receptor-mediated spinal antinociception. *Eur. J. Pharmacol.* **1990**, *183*, 1671.
29. Dukat, M.; Wesolowska, A. Antinociception: Mechanistic studies on the action of MD-354 and clonidine. Part I. The 5-HT<sub>3</sub> component. *Eur. J. Pharmacol.* **2005**, *528*, 59-64.
30. Glaum, S. R.; Proudfit, H. K.; Anderson, E. G. Reversal of the antinociceptive effects of intrathecally administered serotonin in the rat by a selective antagonist. *Neurosci. Lett.* **1988**, *95*, 313-317.
31. Young, S.; Vainio, M.; Scheinin, M.; Dukat, M. Antinociceptive synergism of MD-354 and clonidine. Part II. The  $\alpha_2$ -adrenoceptor component. *Basic Clin. Pharmacol. Toxicol.* **2010**, *107*, 690-697.
32. Dukat, M.; Abdel-Rahman, A. A.; Ismaiel, A. M.; Ingher, S.; Teitler, M.; Gyermek, L.; Glennon, R. A. Structure-activity relationships for the binding of arylpiperazines and arylbiguanides at 5-HT<sub>3</sub> serotonin receptors. *J. Med. Chem.* **1996**, *39*, 4017-4026.

33. Wesolowska, A.; Young, S.; Dukat, M. MD-354 potentiates the antinociceptive effect of clonidine in the mouse tail-flick but not hot-plate assay. *Eur. J. Pharmacol.* **2004**, *495*, 129-136.
34. Dukat, M.; Glennon, R. A.; Young, S. MD-354: What is it good for? *CNS Drug Rev.* **2007**, *13*, 1-20.
35. Guindon, J.; Walczak, J.-S.; Beaulieu, P. Recent advances in the pharmacological management of pain. *Drugs* **2007**, *67*, 2121-2133.
36. Vardeh, D.; Wang, D.; Costigan, M.; Lazarus, M.; Saper, C. B.; Woolf, C. J.; Fitzgerald, G. A.; Samad, T. A. COX2 in CNS neural cells mediates mechanical inflammatory pain hypersensitivity in mice. *J. Clin. Invest.* **2009**, *119*, 287-294.
37. Knotkova, H.; Pappagallo, M. Adjuvant analgesics. *Anesthesiol. Clin.* **2007**, *25*, 775-786.
38. Descartes, R. *L'Homme*. Paris, **1664**.
39. Descartes, R. *Treatise of Man*. Hall, T. S., Translator; Harvard University Press: Cambridge, MA, **1972**.
40. DeLeo, J. A. Basic science of pain. *J. Bone Joint Surg.* **2006**, *88*, 58-62.
41. Fields, H.; Heinricher, M.; Mason, P. Neurotransmitters in nociceptive modulatory circuits. *Annu. Rev. Neurosci.* **1991**, *14*, 219-245.
42. Bymaster, F.; Leed, T.; Knadler, M.; Detke, M.; Iyengar, S. The dual transporter inhibitor duloxetine: a review of its preclinical pharmacology, pharmacokinetic profile, and clinical results in depression. *Curr. Pharm. Des.* **2005**, *11*, 1475-1493.
43. Hein, L. Adrenoceptors and signal transduction in neurons. *Cell Tissue Res* **2006**, *326*, 541-551.

44. Alquist, R. P. A study of the adrenotropic receptors. *Am. J. Physiol.* **1948**, *153*, 586-600.
45. Langer, S. Z. Presynaptic regulation of catecholamine release. *Biochem. Pharmacol.* **1974**, *23*, 1793-1800.
46. Berthelsen, S.; Pettinger, W. A. A functional basis for classification of  $\alpha$ -adrenergic receptors. *Life Sci.* **1977**, *21*, 595-606.
47. Morrow, A. L.; Creese, I. Characterization of  $\alpha_1$ -adrenergic subtypes in rat brain: a reevaluation of [ $^3$ H]WB4101 and [ $^3$ H]prazosin binding. *Mol. Pharmacol.* **1986**, *29*, 321-330.
48. Murphy, T. J.; Bylund, D. B. Characterization of alpha-2 adrenergic receptors in the OK cell, an opossum kidney cell line. *J. Pharmacol. Exp. Ther.* **1988**, *244*, 571-578.
49. Cotecchia, S.; Schwinn, D. A.; Randall, R. R.; Lefkowitz, R. J.; Caron, M. G.; Kobilka, B. K. Molecular cloning and expression of the cDNA for the hamster  $\alpha_1$ -adrenergic receptor. *Proc. Natl. Acad. Sci. U.S.A.* **1988**, *85*, 7159-7163.
50. Schwinn, D. A.; Lomasney, J. W.; Lorenz, W.; Szklut, P. J.; Fremeau, R. T., Jr.; Yang-Feng, T. L.; Caron, M. G.; Lefkowitz, R. J.; Cotecchia, S. Molecular cloning and expression of the cDNA for a novel  $\alpha_1$ -adrenergic receptor subtype. *J. Biol. Chem.* **1990**, *265*, 8183-8189.
51. Lomasney, J. W.; Cotecchia, S.; Lorenz, W.; Leung, W. Y.; Schwinn, D. A.; Yang-Feng, T. L.; Brownstein, M.; Lefkowitz, R. J.; Caron, M. G. Molecular cloning and expression of the cDNA for the  $\alpha_{1A}$ -adrenergic receptor. The gene for which is located on human chromosome 5. *J. Biol. Chem.* **1991**, *266*, 6365-6369.

52. Kobilka, B. K.; Kobilka, T. S.; Yang-Feng, T. L.; Francke, U.; Caron, M. G.; Lefkowitz, R. J.; Regan, J. W. Cloning, sequencing and expression of the gene encoding for the human platelet  $\alpha_2$ -adrenergic receptor. *Science* **1987**, *238*, 650-656.
53. Griffith, R. K. Adrenergic receptors and drugs affecting adrenergic neurotransmission. In *Foye's Principles of Medicinal Chemistry*, 6<sup>th</sup> ed., Lemke, T. L.; Williams, D. A., Eds.; Lippincott Williams & Wilkins: Baltimore, **2008**; pp 392-416.
54. Bylund, D. B.; Eikenberg, D. C.; Hieble, J. P.; Langer, S. Z.; Lefkowitz, R. J.; Minneman, K. P.; Ruffolo, R. R., Jr.; Trendelenburg, U. International union of pharmacology nomenclature of adrenoceptors. *Pharmacol. Rev.* **1994**, *46*, 121-136.
55. Palczewski, K.; Kumasaka, T.; Hori, T.; Behnke, C. A.; Motoshima, H.; Fox, B. A.; LeTrong, I.; Teller, D. C.; Okada, T.; Stenkamp, R. E.; Yamamoto, M.; Miyano, M. Crystal structure of rhodopsin: A G protein-coupled receptor. *Science* **2000**, *289*, 733-734.
56. Rasmussen, S. G. F.; Choi, H.-E.; Rosenbaum, D. M.; Kobilka, T. S.; Thian, F. S.; Edwards, P. C.; Burghammer, M.; Ratnala, V. R. P.; Sanishvilli, R.; Fischetti, R. F.; Schertler, G. F. X.; Weis, W. I.; Kobilka, B. K. Crystal structure of the human  $\beta_2$  adrenergic G-protein-coupled receptor. *Nature* **2007**, *450*, 383-387.
57. Cherezov, V.; Rosenbaum, D. M.; Hanson, M. A.; Rasmussen, S. G. F.; Thian, F. S.; Kobilka, T. S.; Choi, H.-J.; Kuhn, P.; Weis, W. I.; Kobilka, B. K.; Stevens, R. C.

- High-resolution crystal structure of an engineered human  $\beta_2$ -adrenergic G protein-coupled receptor. *Science* **2007**, *318*, 1258-1265.
58. Warne, T.; Serrano-Vega, M. J.; Baker, J. G.; Moukhametsianov, R.; Edwards, P. C.; Henderson, R.; Leslie, A. G. W.; Tate, C. G.; Schertler, G. F. X. Structure of a  $\beta_1$ -adrenergic G-protein-coupled receptor. *Nature* **2008**, *454*, 486-491.
59. Jaakola, V.-P.; Griffith, M. T.; Hanson, M. A.; Cherezov, V.; Chien, E. Y. T.; Lane, J. R.; IJzerman, A. P.; Stevens, R. C. The 2.6 angstrom crystal structure of a human  $A_{2A}$  adenosine receptor bound to an antagonist. *Science* **2008**, *322*, 1211-1217.
60. Schneider, E. H.; Schnell, D.; Strasser, A.; Dove, S.; Seifert, R. Impact of the DRY motif and the missing "ionic lock" on constitutive activity and G-protein-coupling of the human histamine  $H_4$  receptor. *J. Pharmacol. Exp. Ther.* **2010**, *333*, 382-392.
61. Nygaard, R.; Frimurer, T. M.; Holst, B.; Rosenkilde, M. M.; Schwartz, T. W. Ligand binding and micro-switches in 7TM receptor structures. *Trends Pharmacol. Sci.* **2009**, *30*, 249-259.
62. Crocker, E.; Eilers, M.; Ahuja, S.; Hornak, V.; Hirshfeld, A.; Sheves, M.; Smith, S. O. Location of Trp265 in metarhodopsin II: Implications for the activation mechanism of the visual receptor rhodopsin. *J. Mol. Biol.* **2006**, *357*, 163-172.
63. Shi, L.; Liapakis, G.; Xu, R.; Guarnieri, F.; Ballesteros, J. A.; Javitch, J. A.  $\beta_2$  adrenergic receptor activation: Modulation of the proline kink in transmembrane 6 by a rotamer toggle switch. *J. Biol. Chem.* **2002**, *277*, 40989-40996.
64. Holst, B.; Nygaard, R.; Valentin-Hansen, L.; Back, A.; Engelstoft, M. S.; Petersen, P. S.; Frimurer, T.; Schwartz, T. W. A conserved aromatic lock for the tryptophan



- rotameric switch in TM-VI of seven-transmembrane receptors. *J. Biol. Chem.* **2010**, *285*, 3973-3985.
65. Gyires, K.; Zádori, Z. S.; Török, T.; Mátyus, P.  $\alpha_2$ -Adrenoceptor subtypes – mediated physiological, pharmacological actions. *Neurochem. Int.* **2009**, *55*, 447-453.
66. MacDonald, E.; Scheinin, M. Distribution and pharmacology of alpha 2-adrenoceptors in the central nervous system. *J. Physiol. Pharmacol.* **1995**, *46*, 241–258.
67. Scheinin, M.; Lomasney, J. W.; Hayden-Hixson, D. M.; Schambra, U. B.; Caron, M. G.; Lefkowitz, R. J.; Fremeau, R. T., Jr. Distribution of alpha 2-adrenergic receptor subtype gene expression in rat brain. *Mol. Brain Res.* **1994**, *21*, 133-149.
68. Guyenet, P. G.; Stornetta, R. L.; Riley, T.; Norton, F. R.; Rosin, D. L.; Lynch, K. R. Alpha<sub>2A</sub>-adrenergic receptors are present in lower brainstem catecholaminergic and serotonergic neurons innervating spinal cord. *Brain Res.* **1994**, *638*, 285–294.
69. Wozniak, M.; Schramm, N. L.; Limbird, L. E. The noradrenergic receptor subtypes. In *Neuropsychopharmacology: The Fourth Generation of Progress*, Bloom, F. E., Kupfer, D. J., Eds.; Raven Press: New York, **2000**.
70. Gentili, F.; Pignini, M.; Peirgentili, A.; Giannella, M. Agonists and antagonists targeting the different  $\alpha_2$ -adrenoceptor subtypes. *Curr. Top. Med. Chem.* **2007**, *7*, 163-186.
71. Kable, J. W.; Murrin, L. C.; Bylund, D. B. In vivo gene modification elucidates subtype-specific functions of  $\alpha_2$ -adrenergic receptors. *J. Pharmacol. Exp. Ther.* **2000**, *293*, 1-7.

72. Glennon, R. A.; Young, R.; Rangisetty, J. B. Further characterization of the stimulus properties of 5,6,7,8-tetrahydro-1,3-dioxolo[4,5-g]isoquinoline. *Pharmacol., Biochem. Behav.* **2002**, *72*, 379-387.
73. Eisenach, J. C.; Lysak, S. Z.; Viscomi, C. M. Epidural clonidine analgesia following surgery: Phase I. *Anesthesiology* **1989**, *71*, 640-646.
74. Eisenach, J. C.; Rauck, R. L.; Buzzanell, C.; Lysak, S. Z. Epidural clonidine analgesia for intractable cancer pain: Phase I. *Anesthesiology* **1989**, *71*, 647-652.
75. Bousquet, P.; Feldman, J.; Schwartz, J. Central cardiovascular effects of alpha-adrenergic drugs: differences between catecholamines and imidazolines. *J. Pharmacol. Exp. Ther.* **1984**, *230*, 232-236.
76. Audinot, V.; Fabry, N.; Nicolas, J.-P.; Beauverger, P.; Newman-Tandredi, A.; Millan, M. J.; Try, A.; Bornancin, F.; Canet, E.; Boutin, J. A. Ligand modulation of [<sup>35</sup>S]GTPγS binding at human α<sub>2A</sub>, α<sub>2B</sub> and α<sub>2C</sub> adrenoceptors. *Cell. Sign.* **2002**, *14*, 829-837.
77. Holmes, B.; Brogden, R. N.; Heel, R. C.; Speight, T. M.; Avery, G. S. Guanabenz. A review of its pharmacodynamic properties and therapeutic efficacy in hypertension. *Drugs* **1983**, *26*, 212-229.
78. Reeves, G.; Schweitzer, J. Pharmacological management of attention-deficit hyperactivity disorder. *Expert Opin. Pharmacother.* **2004**, *5*, 1313-1320.
79. Vitezic, D.; Pelcic, J. M. Erectile dysfunction: oral pharmacotherapy options. *Int. J. Clin. Pharmacol. Ther.* **2002**, *40*, 393-403.

80. Crassous, P.-A.; Denis, C.; Paris, H.; Senard, J. M. Interest of  $\alpha_2$ -adrenergic agonists and antagonists in clinical practice: Background, facts and perspectives. *Curr. Top. Med. Chem.* **2007**, *7*, 187-194.
81. Millan, M. J.; Newman-Tancredi, A.; Audinot, V.; Cussac, D.; Lejeune, F.; Nicolas, J. P.; Cogé, F.; Galizzi, J. P.; Boutin, J. A.; Rivet, J. M.; Dekeyne, A.; Gobert, A. Agonist and antagonist actions of yohimbine as compared to fluparoxan at alpha(2)-adrenergic receptors (AR)s, serotonin (5-HT)(1A), 5-HT(1B), 5-HT(1D) and dopamine D(2) and D(3) receptors. Significance for the modulation of frontocortical monoaminergic transmission and depressive states. *Synapse* **2000**, *35*, 79-95.
82. Uhlén, S.; Porter, A. C.; Neubig, R. R. The novel alpha-2 adrenergic radioligand [3H]-MK912 is alpha-2C selective among human alpha-2A, alpha-2B and alpha-2C adrenoceptors. *J. Pharmacol. Exp. Ther.* **1994**, *271*, 1558-1565.
83. Easson, L. H.; Stedman, E. Studies on the relationship between chemical constitution and physiological action. *Biochem. J.* **1933**, *27*, 1257-1266.
84. Ruffolo, R. R., Jr.; Rice, P. J.; Patil, P. N.; Hamada, A.; Miller, D. D. Differences in the applicability of the Easson-Stedman hypothesis to the  $\alpha_1$ - and  $\alpha_2$ -adrenergic effects of phenethylamines and imidazolines. *Eur. J. Pharmacol.* **1983**, *86*, 471-475.
85. Wang, C.-D.; Buck, M. A.; Fraser, C. M. Site-directed mutagenesis of  $\alpha_2A$ -adrenergic receptors: Identification of amino acids involved in ligand binding and receptor activation by agonists. *Mol. Pharmacol.* **1991**, *40*, 168-179.
86. Peltonen, J. M.; Nyronen, T.; Wurster, S.; Pihlavisto, M.; Hoffren, A.-M.; Marjamaki, A.; Xhaard, H.; Kanerva, L.; Savola, J.-M.; Johnson, M. S.; Scheinin, M. Molecular

- mechanisms of ligand-receptor interactions in transmembrane domain V of the  $\alpha_{2A}$ -adrenoceptor. *Br. J. Pharmacol.* **2003**, *140*, 347-358.
87. Ballesteros, J. A.; Weinstein, H. Integrated methods for modeling G-protein coupled receptors. *Methods Neurosci.* **1995**, *25*, 366-428.
88. Yaksh, T. L. Central pharmacology of nociceptive transmission. In *Textbook of Pain*, 4<sup>th</sup> ed., Wall, P. D.; Melzack, R., Eds.; Churchill Livingstone: Edinburgh, **1999**; pp 253-308.
89. Sawamura, S.; Kingery, W. S.; Davies, M. F.; Agashe, G. S.; Clark, J. D.; Kobilka, B. K.; Hashimoto, T.; Maze, M. Antinociceptive actions of nitrous oxide is mediated by stimulation of noradrenergic neurons in the brainstem and activation of  $\alpha_{2B}$  adrenoceptors. *J. Neurosci.* **2000**, *20*, 9242-9251.
90. Glennon, R. A.; Dukat, M.; Westkaemper, R. B. Serotonin receptor subtypes and ligands. In *Neuropsychopharmacology: The Fourth Generation of Progress*, Bloom, F. E., Kupfer, D. J., Eds.; Raven Press: New York, 1995; pp 415-429.
91. Hoyer, D.; Hannon, J. P.; Martin, G. R. Molecular, pharmacological and functional diversity of 5-HT receptors. *Pharmacol., Biochem. Behav.* **2002**, *71*, 533-554.
92. Hartig, P.R. Molecular biology of 5-HT receptors. *Trends Pharmacol. Sci.* **1989**, *10*, 64-69.
93. Glennon, R. A.; Dukat, M. Serotonin receptors and drugs affecting serotonergic neurotransmission. In *Foye's Principles of Medicinal Chemistry*, 6<sup>th</sup> ed., Lemke, T. L.; Williams, D. A., Eds.; Lippincott Williams & Wilkins: Baltimore, **2008**; pp 417-443.

94. Andrade, R.; Barnes, N. M.; Baxter, G.; Bockaert, J.; Branchek, T.; Cohen, M. L.; Dumuis, A.; Eglen, R. M.; Göthert, M.; Hamblin, M.; Hamon, M.; Hartig, P. R.; Hen, R.; Herrick-Davis, K.; Hills, R.; Hoyer, D.; Humphrey, P. P. A.; Latté, K. P.; Maroteaux, L.; Martin, G. R.; Middlemiss, D. N.; Mylecharane, E.; Peroutka, S. J.; Saxena, P. R.; Sleight, A.; Villalon, C. M.; Yocca, F. 5-Hydroxytryptamine receptors. Last modified on 2010-08-11. Accessed on 2010-09-08. IUPHAR database (IUPHAR-DB), <http://www.iuphar-db.org/DATABASE/FamilyMenuForward?familyId=1>.
95. Peters, J. A.; Lummis, S. C. R.; Barnes, N. M.; Hales, T. G.; Niesler, B. 5-HT<sub>3</sub> receptors. Last modified on 2010-03-29. Accessed on 2010-06-22. IUPHAR database (IUPHAR-DB), <http://www.iuphar-db.org/DATABASE/FamilyMenuForward?familyId=68>.
96. Barnes, N. M.; Hales, T. G.; Lummis, S. C. R.; Peters, J. A. The 5-HT<sub>3</sub> receptor – the relationship between structure and function. *Neuropharmacology* **2009**, *56*, 273-284.
97. Davies, P. A.; Pistis, M.; Hanna, M. C.; Peters, J. A.; Lambert, J. J.; Hales, T. G.; Kirkness, E. F. The 5-HT<sub>3B</sub> subunit is a major determinant of serotonin receptor function. *Nature* **1999**, *397*, 359-363.
98. Dubin, A. E.; Huvar, R.; D'Andrea, M. R.; Pyati, J.; Zhu, J. Y.; Joy, K. C.; Wilson, S. J.; Galindo, J. E.; Glass, C. A.; Luo, L.; Jackson, M. R.; Lovenberg, T. W.; Erlander, M. G. The pharmacological and functional characteristics of the serotonin 5-HT<sub>3A</sub> receptor are specifically modified by a 5-HT<sub>3B</sub> receptor subunit. *J. Biol. Chem.* **1999**, *274*, 30799-30810.

99. Boyd, G. W.; Low, P. B.; Dunlop, J. I.; Robertson, L. A.; Vardy, A.; Lambert, J. J.; Peters, J. A.; Connolly, C. N. Assembly and cell surface expression of homomeric and heteromeric 5-HT<sub>3</sub> receptors: the role of oligomerization and chaperone proteins. *Mol. Cell. Neurosci.* **2002**, *21*, 38-50.
100. Reeves, D. C.; Lummis, S. C. R. Detection of human and rodent 5-HT<sub>3B</sub> receptor subunits by anti-peptide polyclonal antibodies. *BMC Neurosci.* **2006**, *7*, 27.
101. Barrera, N. P.; Herbert, P.; Henderson, R. M.; Martin, I. L.; Edwardson, J. M. Atomic force microscopy reveals the stoichiometry and subunit arrangement of 5-HT<sub>3</sub> receptors. *Proc. Natl. Acad. Sci. U.S.A.* **2005**, *102*, 12595-12600.
102. Brown, A. M.; Hope, A. G.; Lambert, J. J.; Peters, J. A. Ion permeation and conduction in a human recombinant 5-HT<sub>3</sub> receptor subunit (h5-HT<sub>3A</sub>). *J. Physiol.* **1998**, *507*, 653-665.
103. Livesay, M. R.; Cooper, M. A.; Deeb, T. Z.; Carland, J. E.; Kozuska, J.; Hales, T. G.; Lambert, J. J.; Peters, J. A. Structural determinants of Ca<sup>2+</sup> permeability and conduction in the human 5-HT<sub>3A</sub> receptor. *J. Biol. Chem.* **2008**, *282*, 6172-6182.
104. Yang, J. Ion permeation through 5-hydroxytryptamine-gated channels in neuroblastoma N18 cells. *J. Gen. Physiol.* **1990**, *96*, 1177-1198.
105. Chameau, P.; van Hooft, J. A. Serotonin 5-HT<sub>3</sub> receptors in the central nervous system. *Cell Tissue Res.* **2006**, *326*, 573-581.
106. Gaddum, J. H.; Picarelli, Z. P. Two kinds of tryptamine receptors. *Br. J. Pharmacol. Chemother.* **1957**, *12*, 323-328.
107. Pratt, G. D.; Bowery, N. G.; Kilpatrick, G. J.; Leslie, R. A.; Barnes, N. M.; Naylor, R. J.; Jones, B. J.; Nelson, D. R.; Palacios, J. M.; Slater, P.; Reynolds, D. J. M.

- Consensus meeting agrees distribution of 5-HT<sub>3</sub> receptors in mammalian hindbrain. *Trends Pharmacol. Sci.* **1990**, *11*, 135-137.
108. Doucet, E.; Miquel, M. C.; Nosjean, A.; Vergé, D.; Hamon, M.; Emerit, M. B. Immunolabeling of the rat central nervous system with antibodies partially selective of the short form of the 5-HT<sub>3</sub> receptor. *Neuroscience* **2000**, *95*, 881-892.
109. Barnes, N. M.; Sharp, T. A review of central 5-HT receptors and their function. *Neuropharmacology* **1999**, *38*, 1083-1152.
110. Richardson, B. P.; Engel, G.; Donatsch, P.; Stadler, P. A. Identification of serotonin M-receptor subtypes and their specific blockade by a new class of drugs. *Nature* **1985**, *316*, 126-131.
111. Dukat, M. 5-HT<sub>3</sub> Serotonin receptor agonists: A pharmacophoric journey. *Curr. Med. Chem. – Central Nervous System Agents* **2004**, *4*, 77-94.
112. Glennon, R. A.; Bondarev, M.; Roth, B. 5-HT<sub>6</sub> serotonin receptor binding of indolealkylamines: A preliminary structure-affinity investigations. *Med. Chem. Res.* **1999**, *9*, 108-117.
113. Dukat, M.; Young, R.; Darmani, N. N.; Ahmed, B.; Glennon, R. A. The 5-HT<sub>3</sub> agent *N*-(3-chlorophenyl)guanidine (MD-354) serves as a discriminative stimulus in rats and displays partial agonist character in a shrew emesis assay. *Psychopharmacology (Berlin)* **2000**, *150*, 200-207.
114. Dukat, M.; Choi, Y. N.; Teitler, M.; Du Pre, A.; Herrick-Davis, K.; Smith, C.; Glennon, R. A. The binding of arylguanidines at 5-HT<sub>3</sub> serotonin receptors: a structure-affinity investigation. *Bioorg. Med. Chem. Lett.* **2001**, *11*, 1599-1603.

115. Bachy, A.; Heaulme, M.; Giudice, A.; Michaud, J.-C.; Lefevre, I. A.; Souilhac, J.; Manara, L.; Emerit, M. B.; Gozlan, H.; Hamon, M.; Keane, P. E.; Soubrie, P.; LeFure, G. SR 57227A: A potent and selective agonist at central and peripheral 5-HT<sub>3</sub> receptors *in vitro* and *in vivo*. *Eur. J. Pharmacol.* **1993**, *237*, 299-309.
116. Maksay, G.; Bikadi, Z.; Simonyi, M. Binding interactions of antagonists with 5-hydroxytryptamine<sub>3A</sub> receptor models. *J. Recept. Signal Transduct. Res.* **2003**, *23*, 255-270.
117. Reeves, D. C.; Sayed, M. F.; Chau, P. L.; Price, K. L.; Lummis, S. C. R. Prediction of 5-HT<sub>3</sub> receptor agonist-binding residues using homology modeling. *Biophys. J.* **2003**, *84*, 2338-2344.
118. Alix, K. E. Novel analogs of *m*-chlorophenylguanidine as 5-HT<sub>3</sub> receptor -ligands. M.S. Thesis, Virginia Commonwealth University, Richmond, VA, 2009.
119. Beene, D. L.; Price, K. L.; Lester, H. A.; Dougherty, D. A.; Lummis, S. C. R. Tyrosine residues that control binding and gating in the 5-hydroxytryptamine<sub>3</sub> receptor revealed by unnatural amino acid mutagenesis. *J. Neurosci.* **2004**, *24*, 9097-9104.
120. Boess, F. G.; Steward, L. J.; Steele, J. A.; Liu, D.; Reid, J.; Glencorse, T. A.; Martin, I. L. Analysis of the ligand binding site of the 5-HT<sub>3</sub> receptor using site directed mutagenesis: importance of glutamate 106. *Neuropharmacology* **1997**, *36*, 637-647.
121. Faerber, L.; Drechsler, S.; Ladenburger, S.; Gschaidmeier, H.; Fischer, W. The neuronal 5-HT<sub>3</sub> receptor network after 20 years of research – Evolving concepts in management of pain and inflammation. *Eur. J. Pharmacol.* **2007**, *560*, 1-8.



122. Fozard, J. R.; Mobarok Ali, A. T. M.; Newgrosh, G. Blockade of serotonin receptors on autonomic neurones by (-)-cocaine and some related compounds. *Eur. J. Pharmacol.* **1979**, *59*, 195-210.
123. Fozard, J. R. MDL 72222: A potent and highly selective antagonist at neuronal 5-hydroxytryptamine receptors. *Naunyn-Schmiedeberg's Arch. Pharmacol.* **1984**, *326*, 36-44.
124. Thompson, A. J.; Lummis, S. C. R. 5-HT<sub>3</sub> receptors. *Curr. Pharm. Des.* **2006**, *12*, 3615-3630.
125. Nelson, D. R.; Thomas, D. R. [<sup>3</sup>H]-BRL 43694 (granisetron), a specific ligand for 5-HT<sub>3</sub> binding sites in rat brain cortical membranes. *Biochem. Pharmacol.* **1989**, *38*, 1693-1695.
126. Dumuis, A.; Gozlan, H.; Sebben, M.; Ansanay, H.; Rizzi, C. A.; Turcone, M.; Monferini, E.; Giraldo, E.; Schiantarelli, P.; Ladinsky, H.; Bockaert, J. Characterization of a novel 5-HT<sub>4</sub> receptor antagonist of the azabicycloalkyl benzimidazolone class: DAU 6285. *Naunyn-Schmiedeberg's Arch. Pharmacol.* **1992**, *345*, 264-269.
127. Bardin, L.; Lavarenne, J.; Eschalier, A. Serotonin receptor subtypes involved in the spinal antinociceptive effect of 5-HT in rats. *Pain* **2000**, *86*, 11-18.
128. Bardin, L.; Jourdan, D.; Alloui, A.; Lavarenne, J.; Eschalier, A. Differential influence of two serotonin 5-HT<sub>3</sub> receptor antagonists on spinal serotonin-induced analgesia in rats. *Brain Res.* **1997**, *765*, 267-272.
129. Giordano, J.; Dyche, J. Differential analgesic actions of serotonin 5-HT<sub>3</sub> receptor antagonists in the mouse. *Neuropharmacology* **1989**, *28*, 423-427.

130. Giordano, J. Analgesic profile of centrally administered 2-methyl serotonin against acute pain in rats. *Eur. J. Pharmacol.* **1991**, *199*, 233-236.
131. Libert, F.; Bonnefont, J.; Bourinet, E.; Doucet, E.; Alloui, A.; Hamon, M.; Nargeot, J.; Eschalier, A. Acetaminophen: A central analgesic drug that involves a spinal tropisetron-sensitive, non-5-HT<sub>3</sub> receptor-mediated effect. *Mol. Pharmacol.* **2004**, *66*, 728-734.
132. Belcheva, S.; Petkov, V. D.; Konstantinova, E.; Petkov, V. V.; Boyanova, E. Effects on nociception of the Ca<sup>2+</sup> and 5-HT antagonist dotarizine and other 5-HT receptor agonists and antagonists. *Acta Physiol. Pharmacol. Bulg.* **1995**, *21*, 93-98.
133. Yoon, M. H.; Bae, H. B.; Choi, J. I.; Kim, S. J.; Chung, S. T.; Kim, C. M. Lack of reciprocity between opioid and 5-HT<sub>3</sub> receptors for antinociception in rat spinal cord. *Pharmacology* **2006**, *77*, 195-202.
134. Odagaki, Y.; Toyoshima, R. Pharmacological characterization of  $\alpha_{2D}$ -adrenergic receptor-mediated [<sup>35</sup>S]GTP $\gamma$ S binding in rat cerebral cortical membranes. *Pharmacol. Res.* **2008**, *57*, 435-444.
135. Dukat, M.; Wesolowska, A.; Young, R.; Glennon, R. A. The 5-HT<sub>3</sub> receptor partial agonist MD-354 (meta-chlorophenylguanidine) enhances the discriminative stimulus actions of (+) amphetamine in rats. *Pharmacol., Biochem. Behav.* **2007**, *87*, 203-207.
136. Devedjian, J. C.; Esclapez, F.; Denis-Pouxviel, C.; Paris, H. Further characterization of human alpha 2-adrenoceptor subtypes: [<sup>3</sup>H]RX821002 binding and definition of additional selective drugs. *Eur. J. Pharmacol.* **1994**, *252*, 43-49.

137. Jasper, J. R.; Lesnick, J. D.; Chang, L. K.; Yamanishi, S. S.; Chang, T. K.; Hsu, S. A.; Daunt, D. A.; Bonhaus, D. W.; Eglén, R. M. Ligand efficacy and potency at recombinant  $\alpha_2$  adrenergic receptors. *Biochem. Pharmacol.* **1998**, *55*, 1035-1043.
138. Steward, L. J.; West, K. E.; Kilpatrick, G. J.; Barnes, N. M. Labelling of 5-HT<sub>3</sub> receptor recognition sites in the rat brain using the agonist radioligands [<sup>3</sup>H]meta-chlorophenylbiguanide. *Eur. J. Pharmacol.* **1993**, *243*, 13-18.
139. Kilpatrick, G. J.; Butler, A.; Burridge, J.; Oxford, A. W. 1-(*m*-Chlorophenyl)-biguanide, a potent high affinity 5-HT<sub>3</sub> receptor agonist. *Eur. J. Pharmacol.* **1990**, *182*, 193-197.
140. Rahman, A. A.; Daoud, M. K.; Dukat, M.; Herrick-Davis, K.; Purohit, A.; Teitler, M.; Taveres do Amaral, A.; Malvezzi, A.; Glennon, R. A. Conformationally-restricted analogues and partition coefficients of the 5-HT<sub>3</sub> serotonin receptor ligands meta-chlorophenylbiguanide (*m*CPBG) and meta-chlorophenylguanidine (*m*CPG). *Bioorg. Med. Chem. Lett.* **2003**, *13*, 1119-1123.
141. Hansch, C.; Björkroth, J. P.; Leo, A. Hydrophobicity and central nervous system agents: On the principle of minimal hydrophobicity in drug design. *J. Pharm. Sci.* **1987**, *76*, 663-687.
142. Naumenko, V. S.; Kondaurova, E. M.; Popova, N. K. Central 5-HT<sub>3</sub> receptor-induced hypothermia in mice: Interstrain differences and comparison with hypothermia mediated via 5-HT<sub>1A</sub> receptor. *Neurosci. Lett.* **2009**, *465*, 50-54.
143. Le Bars, D.; Gozariu, M.; Cadden, S. W. Animal models of nociception. *Pharmacol. Rev.* **2001**, *53*, 597-652.

144. Bannon, A. W.; Gunther, K. L.; Decker, M. W. Is epibatidine really analgesic? Dissociation of the activity, temperature, and analgesic effects of ( $\pm$ )-epibatidine. *Pharmacol., Biochem. Behav.* **1995**, *51*, 693-698.
145. Roth, B. L., PDSP. In National Institute of Mental Health's Psychoactive Drug Screening Program: 2009.
146. Tehan, B. G.; Lloyd, E. J.; Wong, M. G.; Pitt, W. R.; Gancia, E.; Manallack, D. T. Estimation of  $pK_a$  using semiempirical molecular orbital methods. Part 2: Application to amines, anilines and various nitrogen containing heterocyclic compounds. *Quant. Struct.-Act. Relat.* **2002**, *21*, 473-485.
147. Spaulding, T. C.; Fielding, S.; Venafro, J. J.; Lal, H. Antinociceptive activity of clonidine and its potentiation of morphine analgesia. *Eur. J. Pharmacol.* **1979**, *58*, 19-25.
148. Kameyama, T.; Nabeshima, T.; Matsuno, K.; Sugimoto, A. A comparison of  $\alpha$ -adrenoceptor involvement in the antinociceptive action of tizanidine and clonidine in the mouse. *Eur. J. Pharmacol.* **1986**, *125*, 257-264.
149. Schlicker, E.; Kathmann, M.; Exner, H. J.; Detzner, M.; Göthert, M. The 5-HT<sub>3</sub> receptor agonist 1-(m-chlorophenyl)-biguanide facilitates noradrenaline release by blockade of  $\alpha_2$ -adrenoceptors in the mouse brain cortex. *Naunyn-Schmiedeberg's Arch. Pharmacol.* **1994**, *349*, 20-24.
150. Young, S. E. Dual mechanism analgesia-enhancing agents. M.S. Thesis, Virginia Commonwealth University, Richmond, VA, 2005.

151. Sirles, G. W.; Worsham, J.; Dukat, M. Antinociceptive actions of TDIQ – an isobolographic analysis. *Proceedings of the 86<sup>th</sup> Annual Virginia Academy of Science Meeting*, Hampton, VA, May 22, 2008.
152. Odagagi, Y.; Toyoshima, R. Pharmacological characterization of  $\alpha_{2D}$ -adrenergic receptor-mediated [<sup>35</sup>S]GTP $\gamma$ S binding in rat cortical cerebral cortical membranes. *Pharmacol. Res.* **2008**, *57*, 435-444.
153. Brookshire, B. R.; Jones, S. R. Direct and indirect 5-HT receptor agonists produce gender-specific effects on locomotor and vertical activity in C57 BL/6J mice. *Pharmacol. Biochem. Behav.* **2009**, *94*, 194-203.
154. Poncelet, M.; Péro, A.; Simiand, J.; Gout, G.; Soubrié, P.; Le Fur, G. Antidepressant-like effects of SR 57227A, a 5-HT<sub>3</sub> receptor agonist, in rodents. *J. Neural Transm.* **1995**, *102*, 83-90.
155. Worsham, J. N. 5-HT<sub>3</sub> receptor ligands and their effect on psychomotor stimulants. M.S. Thesis, Virginia Commonwealth University, Richmond, VA, 2008.
156. Mazzola-Pomietto, P.; Aulakh, C. S.; Murphy, D. L. Temperature, food intake, and locomotor activity effects of a 5-HT<sub>3</sub> receptor agonist and two 5-HT<sub>3</sub> receptor antagonists in rats. *Psychopharmacology* (Berlin) **1995**, *121*, 488-493.
157. Higgins, G. A.; Joharchi, N.; Sellers, E. M. Behavioral effects of the 5-hydroxytryptamine<sub>3</sub> receptor agonists 1-phenylbiguanide and m-chlorophenylbiguanide in rats. *J. Pharmacol. Exp. Ther.* **1993**, *264*, 1440-1449.
158. Morain, P.; Abraham, C.; Bernard, P.; De Nanteuil, G. Biguanide derivatives: Agonist pharmacology at 5-hydroxytryptamine type 3 receptors *in vitro*. *Mol. Pharmacol.* **1994**, *46*, 732-742.

159. Miyake, A.; Mochizuki, S.; Takemoto, Y.; Akuzawa, S. Molecular cloning of human 5-hydroxytryptamine<sub>3</sub> receptor: Heterogeneity in distribution and function among species. *Mol. Pharmacol.* **1995**, *48*, 407-416.
160. Mochizuki, S.; Watanabe, T.; Miyake, A.; Saito, M.; Furuichi, K. Cloning, expression, and characterization of ferret 5-HT<sub>3</sub> receptor subunit. *Eur. J. Pharmacol.* **2000**, *399*, 97-106.
161. Niemeyer, M.-I.; Lummis, S. C. R. Different efficacy of specific agonists at 5-HT<sub>3</sub> receptor splice variants: The role of the extra six amino acid segment. *Br. J. Pharmacol.* **1998**, *123*, 661-666.
162. Mair, I. D.; Lambert, J. J.; Yang, J.; Dempster, J.; Peters, J. A. Pharmacological characterization of a rat 5-hydroxytryptamine type<sub>3</sub> receptor subunit (r5-HT<sub>3A(b)</sub>) expressed in *Xenopus laevis* oocytes. *Br. J. Pharmacol.* **1998**, *124*, 1667-1674.
163. Boess, F. G.; Sepúlveda, M.-I.; Lummis, S. C. R.; Martin, I. L. 5-HT<sub>3</sub> Receptors in NG108-15 neuroblastoma x glioma cells: Effect of the novel agonist 1-(*m*-chlorophenyl)-biguanide. *Neuropharmacology* **1992**, *31*, 561-564.
164. Sepúlveda, M.-I.; Lummis, S. C. R.; Martin, I. L. The agonist properties of *m*-chlorophenylbiguanide and 2-methyl-5-hydroxytryptamine on 5-HT<sub>3</sub> receptors in N1E-115 neuroblastoma cells. *Br. J. Pharmacol.* **1991**, *104*, 536-540.
165. Ito, H.; Kiso, T.; Miyata, K.; Kamato, T.; Yuki, H.; Akuzawa, S.; Nagakura, Y.; Yamano, M.; Suzuki, M.; Naitoh, Y.; Sakai, H.; Iwaoka, K.; Yamaguchi, T. Pharmacological profile of YM-31636, a novel 5-HT<sub>3</sub> receptor agonist, in vitro. *Eur. J. Pharmacol.* **2000**, *409*, 195-201.

166. Costall, B.; Naylor, R. J. The psychopharmacology of 5-HT<sub>3</sub> receptors. *Pharmacol. Toxicol.* **1992**, *71*, 401-415.
167. King, G. R.; Xiong, Z.; Ellinwood, E. H., Jr. Blockade of cocaine sensitization and tolerance by the co-administration of ondansetron, a 5-HT<sub>3</sub> receptor antagonist, and cocaine. *Psychopharmacology* **1997**, *130*, 159-165.
168. Pitsikas, N.; Borsini, F. Different effects of tropisetron and ondansetron in learning and memory paradigms. *Pharmacol., Biochem. Behav.* **1997**, *56*, 571-574.
169. Hashimoto, K.; Fujita, Y.; Ishima, T.; Hagiwara, H.; Iyo, M. Phencyclidine-induced cognitive deficits in mice are improved by subsequent subchronic administration of tropisetron: Role of  $\alpha 7$  nicotinic receptors. *Eur. J. Pharmacol.* **2006**, *553*, 191-195.
170. Ginawi, O. T.; Al-Majed, A. A.; Al-Suwailem, A. K.; El-Hadiyah, T. M. H.; Al-Shabanah, O. A. Involvement of some 5-HT receptors in methamphetamine-induced locomotor activity in mice. *J. Physiol. Pharmacol.* **2004**, *55*, 357-369.
171. Pakulska, W.; Czarnecka, E. The effect of gabapentin on antinociceptive action of analgesics. *Acta Pol. Pharm.* **2004**, *61*, 393-400.
172. Bender, T. S.; Abdel-Rahman, A. A.  $\alpha 2A$ -Adrenergic receptor signaling underlies synergistic enhancement of ethanol-induced behavioral impairment by clonidine. *Alcohol Clin. Exp. Res.* **2009**, *33*, 408-418.
173. Ozdogan, U. K.; Lähdesmäki, J.; Hakala, K.; Scheinin, M. The involvement of alpha 2A-adrenoceptors in morphine analgesia, tolerance and withdrawal in mice. *Eur. J. Pharmacol.* **2004**, *497*, 161-171.

174. Vučković, S. M.; Tomić, M. A.; Stepanović-Petrović, R. M.; Ugresšić, N.; Prostran, M. Š.; Bošković, B. The effects of  $\alpha_2$ -adrenoceptor agents on anti-hyperalgesic effects of carbamazepine and oxcarbazepine in a rat model of inflammatory pain. *Pain* **2006**, *125*, 10-19.
175. Miranda, H. F.; Sierralta, F.; Pinardi, G. An isobolographic analysis of the adrenergic modulation of diclofenac antinociception. *Anesth Analg.* **2001**, *93*, 430-435.
176. Fairbanks, C. A.; Kitto, K. F.; Nguyen, H. O.; Stone, L. S.; Wilcox, G. L. Clonidine and dexmedetomidine produce antinociceptive synergy in mouse spinal cord. *Anesthesiology* **2009**, *110*, 638-647.
177. Chan, J. Y. H.; Chan, S. H. H. Interactions between guanabenz and clonidine in their antinociceptive effects in the rat. *Exp. Neurol.* **1987**, *96*, 233-236.
178. Huong, N. T. T.; Matsumoto, K.; Yamasaki, K.; Watanabe, H. Involvement of supraspinal GABA receptors in majonoside-R2 suppression of clonidine-induced antinociception in mice. *Life Sci.* **1997**, *6*, 427-436.
179. Curd, F. H. S.; Rose, F. L. Synthetic antimalarials. Part IV. 2-Phenylguanidino-4-aminoalkylamino-6-methylpyrimidines. *J. Chem. Soc.* **1946**, 362-366.
180. Bamberger, E. Die einwirkung von halogenwasserstoffsäuren (auch schwefelsäure) auf arylhydroxylamine. *Justus Liebigs Ann. Chem.* **1925**, *441*, 297-318.
181. King, H.; Tonkin, I. M. Antiplasmodial action and chemical constitution. Part VIII. Guanidines and diguanides. *J. Chem. Soc.* **1946**, 1063-1069.



182. Okamoto, K.; Akiyama, R.; Yoshida, H.; Yoshida, T.; Kobayashi, S. Formation of nanoarchitectures including subnanometer palladium clusters and their use as highly active catalysts. *J. Am. Chem. Soc.* **2005**, *127*, 2125-2135.
183. Lunn, G.; Sansone, E. B. Facile reduction of pyridines with nickel-aluminum alloy. *J. Org. Chem.* **1986**, *51*, 513-517.
184. Léger, B.; Nowicki, A.; Roucoux, A.; Rolland, J.-P. Competitive hydrogenation/dehalogenation of halogenoarenes with surfactant-stabilized aqueous suspensions of rhodium and palladium colloids: A major effect of the metal nature. *J. Mol. Catal.* **2007**, *266*, 221-225.
185. Cárdenas-Lizana, F.; Gómez-Quero, S.; Keane, M. A. Clean production of chloroanilines by selective gas phase hydrogenation over supported Ni catalysts. *Appl. Catal., A* **2008**, *334*, 199-206.
186. Ishikawa, H.; Tabusa, F.; Miyamoto, H.; Kano, M.; Vedo, H.; Tamaoka, H.; Nakagawa, K. *Chem. Pharm. Bull.* **1989**, *37*, 2103-2108.
187. Barbaro, P.; Bianchini, C.; Meli, A.; Moreno, M.; Vizza, F. Hydrogenation of indole by phosphine-modified rhodium and ruthenium catalysts. *Organometallics* **2002**, *21*, 1430-1437.
188. Fache, F. Solvent dependent regioselective hydrogenation of substituted quinolines. *Synlett* **2004**, *15*, 2827-2829.
189. Srikrishna, A.; Reddy, T. J.; Viswajanani, R. Reduction of quinolines to 1,2,3,4-tetrahydro derivatives employing a combination of NaCNBH<sub>3</sub> and BH<sub>3</sub>-OEt<sub>2</sub>. *Tetrahedron* **1996**, *52*, 1631-1636.

190. Moon, M. W.; Hsi, R. S. P. Synthesis of (*R*)-5-(di[2,3-<sup>3</sup>H<sub>2</sub>]propylamino)-5,6-dihydro-4*H*-imidazo[4,5,1-*ij*]quinolin-2(1*H*)-one ([<sup>3</sup>H]U-86170) and (*R*)-5-([2,3-<sup>3</sup>H<sub>2</sub>]propylamino)-5,6-dihydro-4*H*-imidazo[4,5,1-*ij*]quinolin-2(1*H*)-one ([<sup>3</sup>H]U-91356). *J. Labelled Compd. Radiopharm.* **1992**, *31*, 933-943.
191. Ando, K.; Tokoroyama, T.; Kubota, T. Cyclization reactions of 2,3-bis(2-cyanophenyl)propionitriles. III. Substituent effect on the carboanion reactivities of the propionitriles and tautomerism of 5-acetamido-11-cyanoindeno[1,2-*c*]isoquinolines. *Bull. Chem. Soc. Jpn.* **1980**, *53*, 2885-2890.
192. Zeng, Q.; Zhang, D.; Yao, G.; Wohlhieter, G. E.; Wang, X.; Rider, J.; Reichelt, A.; Monenschein, H.; Hong, F.-T.; Falsey, J. R.; Dominguez, C.; Bourbeau, M. P.; Allen, J. G. Heterocyclic Modulators of PKB. US Patent Application Publication 2009/0275592, Nov. 5, 2009.
193. Han, B. H.; Boudjouk, P. Organic Sonochemistry. Ultrasonic acceleration of the reduction of simple and deactivated aryl halides using lithium aluminum hydride. *Tetrahedron Lett.* **1982**, *23*, 1643-1646.
194. Muchowski, J. M. 1-Methylthio-3-lithioisoquinoline. The first simple isoquinoline lithiated at the 3-position. *ARKIVOC* (Gainesville, FL, U.S.) **2005**, *6*, 470-479.
195. Girouard, S.; Houle, M.-H.; Grandbois, A.; Keillor, J. W.; Michnick, S. W. Synthesis and characterization of dimaleimide fluorogens designed for specific labeling of proteins. *J. Am. Chem. Soc.* **2005**, *127*, 559-566.

196. Hodgson, H. H.; Ward, E. R. The preparation of 7-nitro-2-naphthylamine and of 3,6-dinitronaphthalic anhydride. *J. Chem. Soc.* **1945**, 590-591.
197. Fujimoto, R. A.; Mcquire, L. W.; Monovich, L. G.; Mugrage, B. B.; Parker, D. T.; Van Duzer, J. H.; Wattanasin, S. Substituted amino phenylacetic acids, derivatives thereof, their preparation and their use as cyclooxygenase 2 (COX-2) inhibitors. WO 2004/048314, June 10, 2004.
198. Buettelmann, B.; Heitz Neidhart, M.-P.; Jaeschke, G.; Pinard, E. Substituted imidazol-pyridazine derivatives. WO 03/097637, Nov. 27, 2003.
199. Frohn, M.; Buerli, R. W.; Riahi, B.; Hungate, R. W. An efficient synthesis of 1,6- and 1,7-dibromo-3-aminoisoquinolines: versatile templates for the preparation of functionalized isoquinolines. *Tetrahedron Lett.* **2007**, *48*, 487-489.
200. Shepard, A. F.; Winslow, N. R.; Johnson, J. R. The simple halogen derivatives of furan. *J. Am. Chem. Soc.* **1930**, *52*, 2083-2094.
201. Lisitsyn, A. S. 2,2'-Bipyridine and related *N*-chelants as very effective promoters for Cu catalysts in the decarboxylation. *Appl. Catal., A* **2007**, *332*, 166-170.
202. Fieser, L. F.; Fieser, M. Reagents for Organic Chemistry, John Wiley and Sons, Inc.: New York, 1967; Vol. 1, pp. 157-158.
203. Nakamura, I.; Sato, Y.; Terada, M. Platinum-catalyzed dehydroalkoxylation-cyclization cascade via N-O bond cleavage. *J. Am. Chem. Soc.* **2009**, *131*, 4198-4199.
204. Youngman, M. A.; Willard, N. M.; Dax, S. L.; McNally, J. J. The synthesis of novel *cis*- $\alpha$ -substituted- $\beta$ -aminotetralins. *Synth. Commun.* **2003**, *33*, 2215-2227.

205. Rosowsky, A.; Battaglia, J.; Chen, K. K. N.; Papathanasopoulos, N.; Modest, E. J. Synthesis of some heteronuclear mono- and di-chloro-2-naphthylamines. *J. Chem. Soc. C* **1969**, *10*, 1376-1378.
206. Hu, X. E. Melanin concentrating hormone antagonists. U. S. Patent 7,304,065, April 7, 2005.
207. Burckhalter, J. H.; Campbell, J. R. Ethylene and phenylacetyl chloride in the Friedel-Crafts Reaction. Novel synthesis of 2-tetralones and benzofuranones. *J. Org. Chem.* **1961**, *26*, 4232-4235.
208. Colotta, V.; Catarzi, D.; Varano, F.; Cecchi, L.; Filacchioni, G.; Galli, A.; Costagli, C. Synthesis and biological evaluation of a series of quinazoline-2-carboxylic acids and quinazoline-2,4-diones as glycine-NMDA antagonists: a pharmacophore model based approach. *Arch. Pharm. Pharm. Med. Chem.* **1997**, *330*, 129-134.
209. Grosso, J. A.; Nichols, D. E.; Kohli, J. D.; Glock, D. Synthesis of 2-(alkylamino)-5,6- and -6,7-dihydroxy-3,4-dihydroquinazolines and evaluation as potential dopamine agonists. *J. Med. Chem.* **1982**, *25*, 703-708.
210. Grosso, J. A.; Nichols, D. E. Synthesis and adrenergic blocking effects of 2-(alkylamino)-3,4-dihydroquinazolines. *J. Med. Chem.* **1980**, *23*, 1261-1264.
211. Ishikawa, F.; Watunabe, Y.; Saegusa, J. Cyclic guanidines. IX. Synthesis of 2-amino-3,4-dihydroquinazoline as blood platelet aggregation inhibitors. *Chem. Pharm. Bull.* **1980**, *28*, 1357-1364.
212. Cody, V.; DeTitta, G. T. The molecular conformation of clonidine hydrochloride, an  $\alpha$ -adrenergic agonist. *J. Chem. Crystallogr.* **1979**, *9*, 33-43.

213. López-Olvera, G.; Soriano-García, M. Crystal structure of 1-(*m*-chlorophenyl)biguanide hydrochloride. *Anal. Sci.* **2004**, *20*, x151-x152.
214. Garratt, P. J.; Hobbs, C. J.; Wrigglesworth, R. One-carbon compounds as synthetic intermediates. The synthesis of hydroypyrimidines and hydroquinazolines by sequential nucleophilic addition to diphenyl cyanocarbonimidate with concomitant cyclization. *J. Org. Chem.* **1989**, *54*, 1062-1069.
215. Hieble, J. P.; Hehr, A.; Li, Y.-O.; Ruffolo, R. R. Molecular basis for the stereoselective interactions of catecholamines with  $\alpha$ -adrenoceptors. *Proc. West. Pharmacol. Soc.* **1998**, *41*, 225-228.
216. Balogh, B.; Szilágyi, A.; Gyires, K.; Bylund, D. B.; Mátyus, P. Molecular modelling of subtypes ( $\alpha_{2A}$ ,  $\alpha_{2B}$ , and  $\alpha_{2C}$ ) of  $\alpha_2$ -adrenoceptors: A comparative study. *Neurochem. Int.* **2009**, *55*, 355-361.
217. Meyer, E. A.; Castellano, R. K.; Diederich, F. Interactions with aromatic rings in chemical and biological recognition. *Angew. Chem. Int. Ed.* **2003**, *42*, 1210-1250.
218. Auffinger, P.; Hays, F. A.; Westhof, W.; Ho, P. S. Halogen bonds in biological molecules. *Proc. Natl. Acad. Sci. U.S.A.* **2004**, *101*, 16789-16794.
219. D'Amour, F.; Smith, D. A method of determining loss of pain sensation. *J. Pharmacol.* **1941**, *72*, 74-79.
220. Dewey, W.; Harris, L.; Howes, J.; Nuite, J. The effect of various neurohormonal modulations on the activity of morphine and the narcotic antagonists in tail-flick and phenylquinone test. *J. Pharmacol. Exp. Ther.* **1970**, *175*, 435-442.
221. Eddy, N.; Leimbach, D. Synthetic analgesic: 11. Dithienylbutenyl and benzomorphans. *J. Pharmacol. Exp. Ther.* **1953**, *107*, 385-439.

222. Atwell, L.; Jacobson, A. The search for less harmful analgesics. *Lab. Anim.* **1978**, *7*, 42-47.
223. Tallarida, R. Statistical analysis of drug combinations for synergism. *Pain* **1992**, *49*, 93-97.
224. Bellamy, F.D.; Ou, K. Selective reduction of aromatic nitro compounds with stannous chloride in nonacidic and nonaqueous medium. *Tetrahedron Lett.* **1984**, *25*, 839-842.
225. Konda-Yomada, Y.; Okada, C.; Yoshida, K.; Umeda, Y.; Arima, S.; Sato, N.; Kai, T.; Takayanagi, H.; Harigaya, Y. Convenient synthesis of 7' and 6'-bromo-D-tryptophan and their derivatives by enzymatic optical resolution using D-aminoacylase. *Tetrahedron* **2002**, *58*, 7851-7861.
226. Batcho, A.D.; Leimgruber, W. Intermediates for indoles. US Patent 3976639, Aug 24, 1976.
227. Caron, S.; Vazquez, E. Efficient synthesis of [6-chloro-2-(4-chlorobenzoyl)-1H-indol-3-yl]-acetic acid, a novel COX-2 inhibitor. *J. Org. Chem.* **2003**, *68*, 4104-4107.
228. Spalding, D.P.; Moersch, G.W.; Mosher, H.S.; Whitmore, F.C. Heterocyclic basic compounds. IX. 3,6-Dichloro-9-(1-methyl-4-diethylaminobutyl)-amino-acridine. *J. Am. Chem. Soc.* **1946**, *68*, 1596-1598.
229. Garanti, L.; Zecchi, G. Thermochemical behavior of o-azidocinnamitriles. *J. Org. Chem.* **1980**, *45*, 4767-4769.
230. Moon, M. W.; Morris, J. K.; Heier, R. F.; Chidester, C. G.; Hoffmann, W. E.; Piercey, M. F.; Althaus, J. S.; VonVoigtlander, P. F.; Evans, D. L. Dopaminergic

- and serotonergic activities of imidazoquinolinones and related compounds. *J. Med. Chem.* **1992**, *35*, 1076–1092.
231. Sommer, M. B.; Begtrup, M.; Boegesoe, K. P. Application of (2-cyanoaryl)arylacetonitriles in cyclization and annulation reactions. Preparation of 3-arylidans, 4-aryl-3,4-dihydronaphthalenes, 4-arylisoquinolines, 1-aminonaphthalenes, and heterocyclic analogues. *J. Org. Chem.* **1990**, *55*, 4822-4827.
232. James, P. M.; Woodcock, D. Synthesis of plant growth regulators. Part I. Substituted  $\beta$ -naphthyloxyacetic acids. *J. Chem. Soc.* **1951**, 3418-3421.
233. Norris, J. F.; Young, H. H., Jr. The reactivity of atoms and groups in organic compounds. XVII. The effect of the change in reactant and of the temperature on the relative reactivities of certain substitution products of benzoyl chloride. *J. Am. Chem. Soc.* **1935**, *57*, 1420-1424.
234. Nevy, J. B.; Hawkinson, D. C.; Blotny, G.; Yao, X.; Pollack, R. M. Transition state imbalance in the deprotonation of substituted 2-tetralones by hydroxide ion. *J. Am. Chem. Soc.* **1997**, *119*, 12722-12726.
235. Reissenweber, G.; Mangold, D. Oxidation of isatins to isatoic anhydrides and 2,3-dioxo-1,4-benzoxazines. *Angew. Chem. Int. Ed. Engl.* **1980**, *19*, 222-223.
236. Bissantz, C.; Bernard, P.; Hibert, M.; Rognan, D. Protein-based virtual screening of chemical databases. II. Are homology models of G-Protein Coupled Receptors suitable targets? *Proteins* **2003**, *50*, 5-25.
237. Baldwin, J. M. The probable arrangement of the helices in G protein-coupled receptors. *EMBO J.* **1993**, *12*, 1693-1703.

238. Baldwin, J. M.; Schertler, G. F. X.; Unger, V. M. An alpha-carbon template for the transmembrane helices in the rhodopsin family of G protein-coupled receptors.

*J. Mol. Biol.* **1997**, *272*, 144-164.



## **Vita**

Genevieve Sirles Alley was born on July 16, 1981 in Richmond, Virginia to the parents Scott and Louisa Sirles. She received a Bachelor of Science degree in Biology from Virginia Commonwealth University in August 2005 and subsequently enrolled in Virginia Commonwealth University's School of Pharmacy, Pharmaceutical Sciences graduate program with a concentration in Medicinal Chemistry.